# VLOGA AVTOFAGINOV IN UBIKVITINU PODOBNEGA KONJUGACIJSKEGA SISTEMA ATG8 V PARAZITU *TRYPANOSOMA CRUZI* IN SESALCIH

Jelena Rajković

**Doktorska disertacija**
**Mednarodna podiplomska šola Jožefa Stefana**
**Ljubljana, Slovenija, november 2015**

**Komisija za oceno doktorske disertacije**:

*prof. dr. Veronika Stoka, predsednica, Institut »Jožef Stefan«, Jamova c. 39, 1000 Ljubljana*

*doc. dr. Marko Fonović, član, Institut »Jožef Stefan«, Jamova c. 39, 1000 Ljubljana*

*prof. dr. Ana Plemenitaš, članica, Medicinska fakulteta, Univerza v Ljubljani, Vrazov trg 2, 1104 Ljubljana*

MEDNARODNA PODIPLOMSKA ŠOLA JOŽEFA STEFANA
JOŽEF STEFAN INTERNATIONAL POSTGRADUATE SCHOOL




Jelena Rajković

# VLOGA AVTOFAGINOV IN UBIKVITINU PODOBNEGA KONJUGACIJSKEGA SISTEMA ATG8 V PARAZITU *TRYPANOSOMA CRUZI* IN SESALCIH

**Doktorska disertacija**

# THE ROLE OF AUTOPHAGINS AND ATG8 UBIQUITIN-LIKE CONJUGATION SYSTEM IN THE PARASITE *TRYPANOSOMA CRUZI* AND MAMMALS

**Doctoral Dissertation**

*Mentor*: prof. ddr. Boris Turk

Ljubljana, Slovenija, november 2015

# Kazalo

**Povzetek** ..... **VII**

**Abstract** ..... **IX**

**Seznam kratic** ..... **XI**

**1 Uvod** ..... **1**
1.1 Avtofagija ..... 1
1.1.1 Potek avtofagije ..... 3
1.1.2 Avtofagini ..... 5
1.1.2.1 Tridimenzionalna struktura človeškega Atg4B ..... 5
1.1.3 Naravni substrati avtofaginov proteini Atg8 ..... 7
1.1.3.1 Tridimenzionalna struktura homologov Atg8 ..... 7
1.1.4 Fiziološke vloge avtofagije ..... 8
1.1.5 Patofiziološke vloge avtofagije ..... 9
1.1.5.1 Trypanosoma cruzi ..... 10
1.1.5.2 Chagasova bolezen ..... 11
1.1.5.3 Vloga avtofagije pri razvoju raka ..... 12
1.1.5.3.1 Cisteinski katepsini in njihovi endogeni inhibitorji pri raku ..... 13
1.1.5.3.2 Mišji model raka mlečne žleze MMTV-PyMT ..... 14
1.2 Sintetični substrati, inhibitorji in pametne aktivnostne sonde ..... 14

**2 Namen dela** ..... **17**

**3 Materiali in metode** ..... **19**
3.1 Materiali ..... 19
3.1.1 Kemikalije ..... 19
3.1.2 Encimi in proteini ..... 19
3.1.3 Gojišča ..... 19
3.1.4 Gostiteljske bakterijske kulture ..... 20
3.1.5 Vektorji ..... 20
3.1.6 Kompleti reagentov ..... 20
3.1.7 Pufri ..... 20
3.1.8 Laboratorijska oprema ..... 21
3.2 Delo z DNA ..... 21
3.2.1 Priprava mutant TcAtg4.2 ..... 21
3.2.2 Priprava mutant TcAtg8.2 ..... 23
3.3 Delo z rekombinantnimi proteini ..... 24
*3.3.1* Izražanje in izolacija rekombinantnih proteinov v bakteriji *Escherichia coli* ..... 24
3.3.2 Cirkularni dikroizem (CD) spektroskopija ..... 25
3.3.3 Cepitve TcAtg8 s TcAtg4.2 ..... 25

3.3.4 Vpliv pH na aktivnost TcAtg4.2 ..... 25
3.3.5 Vpliv kozmotropnih soli na aktivnost TcAtg4.2 ..... 25
3.3.6 Določanje substratne specifičnosti TcAtg4.2 z uporabo fluorogene kombinatorne tetrapeptidne knjižnice ..... 26
3.3.7 Iskanje specifičnih substratov za TcAtg4.2 ..... 27
3.3.8 Določanje selektivnosti optimalnih substratov za TcAtg4.2 ..... 28
3.3.9 Inhibicija s pametno aktivnostno sondo MP001 ..... 29
3.4 Delo z mišjimi primarnimi tumorskimi celicami MMTV-PyMT ..... 29
3.4.1 Priprava celičnih lizatov za imunološko detekcijo LC3 ..... 29
3.4.2 Prenos proteinov po Westernu ..... 30
3.4.3 Pretočna citometrija ..... 30
3.4.4 Statistične analize ..... 30

**4 Rezultati ..... 31**
4.1 Analiza očiščenih rekombinantnih proteinov ..... 31
4.2 Cys 91 je odgovoren za katalitično aktivnost TcAtg4.2 ..... 31
4.3 TcAtg4.2 cepi substrat TcAtg8.1 hitreje kakor TcAtg8.2 ..... 32
4.4 Biokemijska karakterizacija TcAtg4.2 ..... 32
4.5 Funkcijske študije TcAtg4.2 ..... 35
4.6 Določanje substratne specifičnosti TcAtg4.2 ..... 41
4.7 Iskanje optimalnega tetrapeptidnega substrata za TcAtg4.2 ..... 43
4.8 Določanje selektivnosti optimalnih substratov za TcAtg4.2 ..... 44
4.9 Inhibicija TcAtg4.2 s pametno aktivnostno sondo MP-001 ..... 46
4.10 Določanje selektivnosti pametne aktivnostne sonde MP001 ..... 47
4.11 Imunološka detekcija LC3 v lizatih tumorskih celic MMTV-PyMT ..... 48
4.12 Vpliv regulacije avtofagije na preživetje tumorskih celic MMTV-PyMT ..... 49

**5 Razprava ..... 51**

**6 Zaključki ..... 57**

**Zahvale ..... 59**

**Literatura in viri ..... 61**

**Kazalo slik ..... 75**

**Priloge ..... 81**

# Povzetek

Chagasovo bolezen, ki na področju Latinske Amerike predstavlja poglaviten zdravstveni problem, povzroča znotrajcelični protozojni parazit *Trypanosoma cruzi*. V genomu parazita se nahajata zapisa za dve kopiji z avtofagijo povezanih cisteinskih proteaz, Atg4.1 in Atg4.2. TcAtg4.2 je glavni nosilec proteolitične aktivnosti in je odgovoren za procesiranje Atg8 proteinov blizu njihovega karboksilnega (C-) konca. Po proteolitični cepitvi v Atg8 se izpostavi C-končni glicin, ki omogoči nadaljnji potek avtofagije in diferenciacijo parazita ter uspešno kolonizacijo človeškega gostitelja. Za uspešno spremljanje in zdravljenje Chagasove bolezni je nujen razvoj orodij, ki bi omogočala selektivno spremljanje proteolitične aktivnosti parazitskega TcAtg4.2 brez vpliva na človeške Atg4 proteaze. Mehanizem vezave substrata in njegove katalize se je skozi evolucijo dobro ohranil, kar smo pokazali tudi z mutacijo ohranjenega glicina 244, ki se nahaja tik pred regulatorno zanko in omogoča njeno fleksibilnost, ter z delecijo regulatorne zanke. Obe mutaciji sta povzročili popolno izgubo katalitične aktivnosti encima. Z uporabo kombinatorne substratne knjižnice (PS-SCL) smo določili substratno specifičnost TcAtg4.2. Podobno kakor človeški HsAtg4B tudi TcAtg4.2 na pozicijah P4 in P3 sprejema širok spekter aminokislinskih preostankov. Na pozicijah P2 in P1 oba encima kažeta izključno preferenco do aromatskih aminokislinskih preostankov na P2 in glicina na P1, ki so prisotni tudi v vseh naravnih substratih in so se evolucijsko popolnoma ohranili. Z uporabo razširjene podknjižnice P2, ki poleg naravnih aminokislinskih preostankov vsebuje tudi nenaravne derivate fenilalanina, smo sintetizirali izjemno selektivna tetrapeptidna substrata za TcAtg4.2, acetil-Lys-Lys-Cha-Gly-AFC (Ac-KKChaG-AFC) in acetil-Lys-Thr-Cha-Gly-AFC (Ac-KTChaG-AFC). Pri obeh se na poziciji P2 nahaja nenaravni aminokislinski preostanek cikloheksilalanin. Človeškemu HsAtg4B ter človeškim funkcijsko podobnim proteazam SENP1, SENP2 in UCH-L3, udeleženim v ubikvitin-proteasomski poti, pa cikloheksilalanin ne ustreza, zato teh substratov ne morejo cepiti. Cisteinski katepsini, ki v zaključni fazi avtofagije razgrajujejo zajete komponente, vključno s proteini Atg8, oba omenjena sintetična substrata cepijo zelo dobro, zaradi česar nista primerna za uporabo *in vivo*. Kljub temu oba substrata predstavljata dobro orodje za spremljanje katalitične aktivnosti TcAtg4.2 v pogojih *in vitro*.

Avtofagija ima poleg ključne vloge pri preživetju parazita *T. cruzi* znotraj človeškega gostitelja pomembno vlogo tudi pri preživetju in razvoju tumorjev. V notranjosti nekaterih vrst tumorjev, kjer prevladujejo acidoza, hipoksija in pomanjkanje nutrientov, ki jih spremlja tudi povišan nivo reaktivnih kisikovih spojin (ROS), znanih induktorjev avtofagije, omogoča njihovo rast in napredovanje. Tumorske celice mišjega modela raka mlečne žleze MMTV-PyMT z izbitim genom za *stefin B* (PyMT;StfB-/-) imajo v primerjavi s tumorskimi celicami divjega tipa (PyMT;WT) povišan nivo ROS ter kakor pričakovano tudi zvišano količino LC3, markerja avtofagije. Dokazali smo, da obe skupini za preživetje nujno potrebujeta nespremenjeno avtofagijo. Kljub povišani avtofagiji v PyMT:StfB-/- sta bili obe skupini tumorskih celic v pogojih stradanja z inhibicijo avtofagije podvrženi apoptozi brez statistično značilnih razlik.

# Abstract

The protozoan parasite *Trypanosoma cruzi* is the causative agent of Chagas' disease, a prevalent health problem in Latin America. The genome of the parasite encodes two copies of autophagy-related cysteine proteases, Atg4.1 and Atg4.2. TcAtg4.2 carries the majority of proteolytic activity and is responsible for the processing of Atg8 proteins near the carboxy-terminus, exposing a conserved glycine. This enables the progression of autophagy and differentiation of the parasite which is required for a successful colonization of humans. Successful monitoring and treatment of Chagas' disease would largely benefit from a development of tools for specific monitoring of the activity of TcAtg4.2 from the parasite without affecting human Atg4 proteases. The mechanism of substrate binding and catalysis by Atg4 was found to be highly conserved among the species as demonstrated by critical mutations in the TcAtg4.2, including mutation of the conserved Gly244 residue in the hinge region, responsible for the flexibility of the regulatory loop, and the deletion of the regulatory loop and the N-terminal tail domain, which resulted in a complete lack of activity of the mutants. Using a Positional scanning-substrate combinatorial library (PS-SCL) we determined that TcAtg4.2 tolerates a broad spectrum of amino acids in the P4 and P3 positions, similar to the human orthologue HsAtg4B. In contrast, both human and trypanosome Atg4 orthologues exhibited exclusive preference for aromatic amino acid residues in the P2 position, and for Gly in the P1 position, which is absolutely conserved in the natural Atg8 substrates. Using an extended P2 substrate library, which also included unnatural amino acid derivatives of Phe, we generated highly selective tetrapeptide substrates acetyl-Lys-Lys-Cha-Gly-AFC (Ac-KKChaG-AFC) and acetyl-Lys-Thr-Cha-Gly-AFC (Ac-KTChaG-AFC) with unnatural cyclohexylalanine (Cha), which were recognized exclusively by TcAtg4.2, but not by HsAtg4B nor by the structurally related human proteases SENP1, SENP2 and UCH-L3, involved in the SUMOylation and ubiquitin-proteasome pathway. However, cysteine cathepsins that are involved in the final stages of autophagy and recycle the engulfed material, including the Atg8 proteins, were found to effectively cleave synthetic fluorogenic substrates designed for TcAtg4.2, making them less suitable for *in vivo* work. Nevertheless, tetrapeptide substrates in the present form could be used for monitoring TcAtg4.2 activity *in vitro*.

Intact autophagy enables survival of the parasite *T. cruzi* and its successful colonization of the human host. It is also critical for the survival of the tumor cells in harsh hypoxic, acidic and nutrient deprived environment, accompanied by elevated reactive oxygen species (ROS). The latter are well known inducers of autophagy. Mouse stefin B-deficient breast cancer cells (PyMT;StfB-/-) have, as compared with wild type tumor cells (PyMT;WT), elevated levels of intracellular ROS as well as LC3, an established autophagy marker. Intact autophagy enables survival of both groups. Despite an elevated expression of LC3 in PyMT;StfB-/- no significant difference in survival between these groups was detected when autophagy was blocked.

# Seznam kratic

| | | |
|---|---|---|
| Ac- | = | acetil- |
| ACC | = | 7-amino-4-karbamoilmetil kumarin |
| AMC | = | 7-amino-4-metil kumarin |
| AFC | = | 7-amino-4-trifluorometil kumarin |
| AGE | = | agarozna gelska elektroforeza |
| Atg | = | z avtofagijo povezani proteini (angl. *autophagy-related protein*) |
| ATP | = | adenozin-5'-trifosfat |
| DMSO | = | dimetil sulfoksid |
| DNA | = | deoksiribonukleinska kislina |
| DTT | = | ditiotreitol |
| DUB | = | deubikvitinirajoči encim (angl. *deubiquitinating enzyme*) |
| FPLC | = | tekočinska kromatografija za hitro ločevanje proteinov (angl. *fast protein liquid chromatography*) |
| GABARAP | = | protein, povezan z γ-aminobutirično kislinskim receptorjem (angl. *γ-aminobutyric acid receptor-associated protein*) |
| GATE-16 | = | z Golgijem povezan ojačevalec ATPaze z velikostjo 16 kDa (angl. *Golgi-associated ATPase enhancer-16*) |
| IPTG | = | izopropil tiogalaktopiranozid |
| LB | = | Luria-Bertani |
| MAP1A/B/LC3 | = | z mikrotubuli povezan protein 1 A/B / lahka veriga 3 (angl. *microtubule-associated proteins 1 A/B light chain 3*) |
| NaDS PAGE | = | poliakrilamidna gelska elektroforeza v prisotnosti natrijevega dodecil sulfata |
| PAS | = | mesto nastanka fagofora (angl. *phagophore assembly site*) |
| PBS | = | fosfatni pufer (angl. *phosphate buffered saline*) |
| PCR | = | verižna reakcija s polimerazo |
| PE | = | fosfatidiletanolamin |
| PS-SCL | = | kombinatorna substratna knjižnica (angl. *positional scanning-substrate combinatorial library*) |
| RFU | = | relativne fluorescenčne enote (angl. *relative fluorescence unit*) |
| ROS | = | reaktivne kisikove spojine (angl. *reactive oxygen species*) |
| Rpm | = | vrtljaji na minuto (angl. *revolutions per minute*) |
| SENP | = | proteaza, specifična za sentrin/SUMO (angl. *sentrin/SUMO-specific protease*) |
| TEMED | = | N,N,N',N'-tetrametilendiamin |
| Tris | = | tris (hidroksimetil) aminometan-hidroklorid |

**Okrajšave aminokislin:**

| | | |
|---|---|---|
| Ala, A | = | alanin |
| Arg, R | = | arginin |
| Asn, N | = | asparagin |

| | | |
|---|---|---|
| Asp, D | = | aspartat |
| Cys, C | = | cistein |
| Gln, Q | = | glutamin |
| Glu, E | = | glutamat |
| Gly, G | = | glicin |
| Cha | = | cikloheksilalanin (analog fenilalanina) |
| hPhe | = | homofenilalanin (analog fenilalaina) |
| His, H | = | histidin |
| Ile, I | = | izolevcin |
| Leu, L | = | levcin |
| Met, M | = | metionin |
| O | = | nor-levcin (analog levcina) |
| Phe, F | = | fenilalanin |
| Pro, P | = | prolin |
| Ser, S | = | serin |
| Thr, T | = | treonin |
| Trp, W | = | triptofan |
| Tyr, Y | = | tirozin |
| Val, V | = | valin |

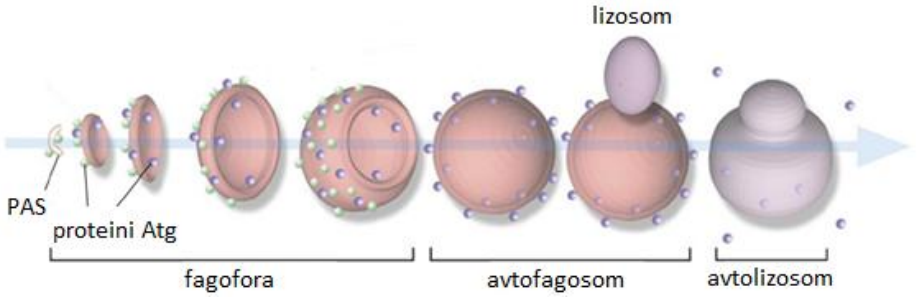
# 1 Uvod

## 1.1 Avtofagija

V evkariontskih celicah razgradnja celičnih komponent poteka preko dveh glavnih poti; proteasoma in avtofagije. Proteasom razgrajuje kratkoživeče ter nepravilno zvite proteine [1], z avtofagijo pa se odstranjujejo tudi komponente, ki so za proteasom prevelike.

Avtofagija je katabolni proces, pri katerem celice razgrajujejo oziroma reciklirajo svoje lastne makromolekule. S pomočjo avtofagije se razgrajujejo dolgoživeči proteini, proteinski agregati, komponente citoplazme ter organeli [2]. V vseh celicah organizma poteka na nizkem, bazalnem nivoju ter s svojim delovanjem ohranja homeostazo celic in celotnega organizma. Nivo avtofagije se močno poveča kot odgovor na znotrajcelični stres (kopičenje odvečnih in poškodovanih citosolnih proteinov in agregatov [3], organelov [4,5], oksidativni stres [6], okužbe s patogeni [7,8]) kot tudi zunajcelični stres (pomanjkanje rastnih faktorjev in hranil v celičnem okolju [9-11], hipoksija [12-14]). Ob stradanju, ko celicam primanjkuje hranil, s pomočjo avtofagije poteka razgradnja beljakovin in lipidov na osnovne gradnike. Slednji se ponovno uporabijo za sintezo s stresom povezanih makromolekul ali pa s pomočjo Krebsovega cikla (beljakovine) oz. β-oksidacije (maščobne kisline) celice oskrbujejo s celično energijo (ATP). Poleg zagotavljanja hitrejše prilagoditve celic na stresne pogoje je avtofagija zelo pomembna tudi pri embriogenezi [15], razvoju [16,17], diferenciaciji [18,19], remodeliranju tkiv [20,21], zaščiti organizmov pred razvojem tumorjev [22,23] in pripravo antigenskih peptidov, ki jih prepoznavajo celice imunskega sistema [24]. Nepravilnosti v delovanju avtofagije vodijo v razvoj številnih humanih bolezni kot so rak [22,23,25], nevrodegenerativne bolezni [26], srčno-žilne bolezni [27] ter okužbe s patogeni [7,8,24,28].

Proces avtofagije se začne z nastankom ukrivljene membrane, fagofore, na mestu njegovega nastajanja, imenovanega PAS (angl. *phagophore assembly site*). Je struktura, sestavljena iz fosfolipidnega dvosloja. Njeno rast in širitev omogočajo z avtofagijo povezani (angl. *Atg; Autophagy related*) proteini, ki so pripeti nanjo. Fagofora se širi v vse smeri ter zaobjame tarčo znotraj celice. Nastane vezikel imenovan avtofagosom [29]. S površine avtofagosoma se pred fuzijo z lizosomom sprostijo vsi proteini Atg razen proteinov Atg8 v lumnu avtofagosoma in omogočijo fuzijo obeh veziklov (Slika 1).



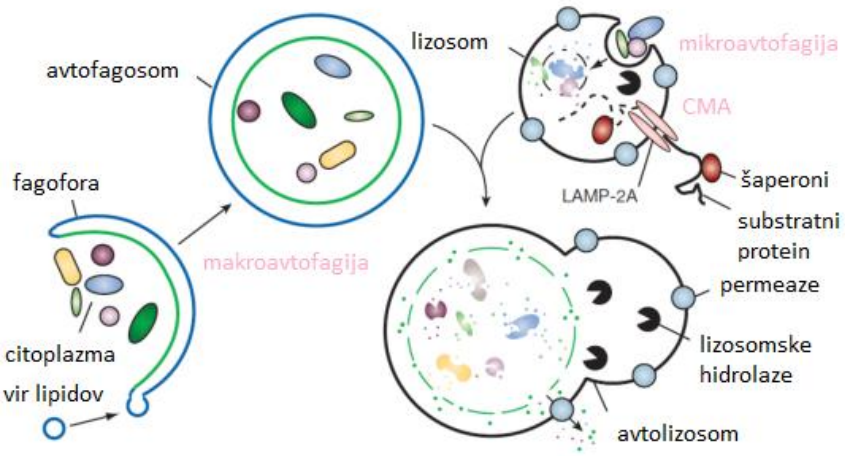

Slika 1: *Potek nastajanja avtofagosoma* (povzeto po [29]). PAS (angl. *phagophore assembly site*) predstavlja mesto nastanka fagofore. Slednja s pomočjo proteinov Atg raste in zaobjame celične komponente. Nastane vezikel, imenovan avtofagosom. Le-ta se združi z lizosomom v avtolizosom, kjer poteče razgradnja zajete vsebine.

Pojem avtofagije zajema več različnih procesov (Slika 2) [30]:

1.) Makroavtofagija je prevladujoča oblika avtofagije. Zanjo je značilen nastanek avtofagosoma, ki se v fazi zorenja združi z lizosomom, kjer se zajete makromolekule razgradijo na osnovne gradnike in reciklirajo nazaj v citosol. V literaturi se pojem »avtofagija« v večini primerov nanaša na proces makroavtofagije.

2.) Mikroavtofagija se nanaša na proces direktne invaginacije lizosomske membrane, ki v lumen lizosoma zajema dele citoplazme.

3.) Od šaperonov odvisna avtofagija (angl. *CMA - chaperone-mediated autophagy*) predstavlja direkten prenos proteinov preko lizosomske membrane s pomočjo šaperonov. Citosolni proteini s pentapeptidnim motivom KFERQ ali funkcijsko podobnim zaporedjem se premestijo na membrano lizosoma, kjer se s pomočjo adaptorskih proteinov razvijejo in prenesejo v lumen lizosoma [31]. CMA je značilna le za višje evkariontske organizme in je pri kvasovkah ne zasledimo.

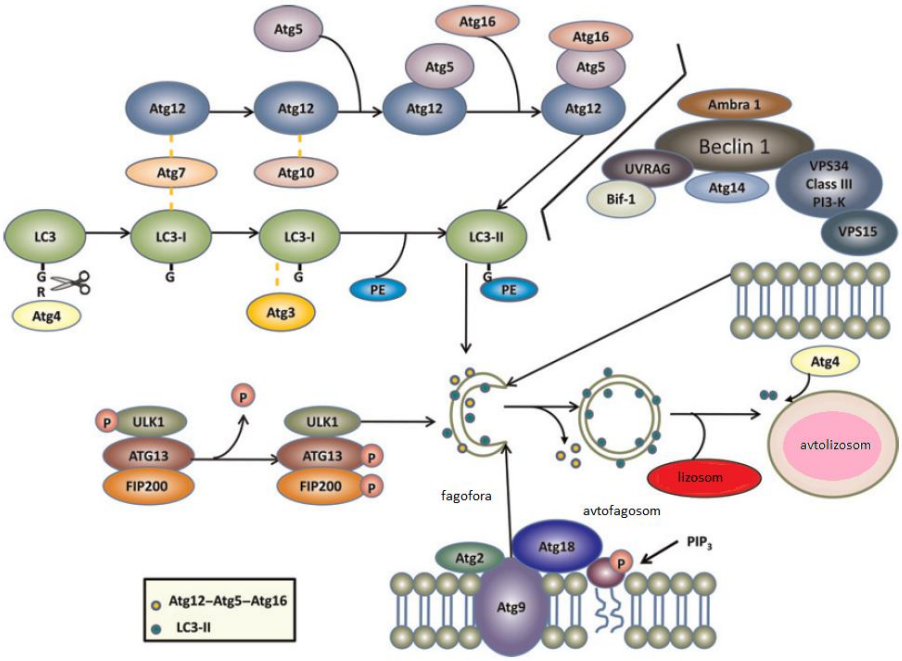



Slika 2: *Oblike avtofagije* (povzeto po [32]). Pojem avtofagije zajema tri različne procese razgradnje celičnih komponent: makroavtofagijo, mikroavtofagijo in od šaperonov odvisno avtofagijo (CMA).

Z analizami genetskih mutant kvasovk *Saccharomyces cerevisiae*, ki danes predstavlja modelni organizem za preučevanje avtofagije ter metilotrofnih kvasovk *Pichia pastoris* in *Hansenula polymorpha* so identificirali več kot 30 z avtofagijo povezanih (ATG) genov. Zaradi dobre evolucijske ohranjenosti ortologov Atg v višjih evkariontih se kot modelni organizmi za določanje vloge izbranih proteinov pri avtofagiji danes uporabljajo kvasne

mutante z izbitimi geni za proteine Atg.

Proteini Atg se združujejo v vsaj štiri proteinske komplekse in sodelujejo v vseh stopnjah avtofagnega procesa (iniciacija, ekspanzija fagofore, prepoznavanje in selekcija tarče, tvorba vezikla in razgradnja) ter s svojim delovanjem omogočajo normalen potek avtofagije (Slika 3).




Slika 3: *Kompleksi Atg, ki omogočajo nastanek avtofagosoma* (povzeto po [33]). Za avtofagijo je značilen nastanek avtofagosoma. Pri njegovem nastajanju sodelujejo vsaj štirje med seboj natančno usklajeni kompleksi Atg: (1) Kompleks ULK1-Atg13-FIP200 je odgovoren za iniciacijo avtofagije. (2) Kompleks Vps34-Beklin 1 (PI3-kinaza razreda III) sodeluje pri nukleaciji. (3) Kompleks Atg9-Atg2-Atg18 na PAS prinaša lipide in omogoča rast in širitev fagofore. (4) Konjugacijska sistema, Atg5-Atg12-Atg16 ter sesalski homolog Atg8, LC3, uravnavata podaljšanje membrane avtofagosoma.

### 1.1.1 Potek avtofagije

Glede na selektivnost avtofagijo delimo na neselektivno in selektivno obliko. Pri neselektivni avtofagiji so v avtofagosomu zajete različne komponente citoplazme, ki predvsem v času stradanja in drugih oblikah stresa celice oskrbujejo z osnovnimi gradniki in energijo. Selektivne oziroma specializirane oblike avtofagije pa naj bi opravljale homeostatsko in biosintetsko funkcijo. Pri specializiranih oblikah avtofagije so v avtofagosomu selektivno zajeti odvečni ali poškodovani organeli (mitohondriji, endoplazmatski retikulum) in znotrajcelični patogeni, ki v citosolu lahko predstavljajo tarčo avtofagije. V kvasovkah predstavlja selektivno obliko avtofagije Cvt metabolna pot (angl. *cytosol to vacuole targeting*), ki v prebavne vakuole dostavlja številne prekurzorske oblike hidrolaz, tudi proaminopeptidazo 1 (proApeI), kjer se aktivirajo in omogočajo normalno delovanje kvasovk [34]. V večceličnih organizmih eno izmed selektivnih oblik avtofagije predstavlja odstranjevanje ubikvitiniranih substratov in agregatov [3].

Proces avtofagije lahko razdelimo na naslednje stopnje: iniciacija, rast in širitev avtofagosoma, fuzija avtofagosoma z endosomom ali lizosomom, razgradnja tarče in

recikliranje osnovnih gradnikov nazaj v citosol.

Pri uravnavanju nivoja avtofagije ima osrednjo vlogo inhibitor avtofagije serinska/treoninska (Ser/Thr) kinaza TOR (angl. *target of rapamycin*). Je evolucijsko ohranjena in prisotna v vseh evkariontih, od kvasovk (TOR) do sesalcev (mTOR), ter predstavlja osrednji senzor številnih transdukcijskih signalnih poti. TOR je v svoji aktivni obliki pripet na kompleks Atg1/ULK1-Atg13-FIP200, ki je odgovoren za indukcijo avtofagije, in ga s fosforilacijo ohranja v neaktivni obliki. Pri stradanju ali uporabi inhibitorja TOR, rapamicina, kompleks TOR/mTOR-Atg1/ULK1-Atg13-FIP200 razpade. Protein Atg1 se aktivira. Sledi indukcija avtofagije in začetek nastajanja avtofagosoma [35].

V začetnih stopnjah nastajanja fagofore je ključna aktivnost fosfatidilinozitol 3-kinaznega kompleksa (kompleks PI3K) razreda III (Vps34; angl. *vacuolar protein sorting 34*), miristoilirana Ser/Thr kinaza Vps15 (v sesalcih p150), Atg14 (v sesalcih Bakor/mAtg14) ter Atg6/Vps30 (v sesalcih beklin 1) [36-38]. Pri stradanju kompleks PI3K proizvaja fosfatidilinozitol 3-fosfat ($PIP_3$), ki se veže na številne proteine Atg (v kvasovkah Atg18, Atg20, Atg21 in Atg24) [39,40]. Le-ti se nato povežejo s kompleksom Atg1-Atg13-Atg17 in omogočijo iniciacijo avtofagije.

Kompleks Atg9-Atg2-Atg18 omogoča širitev fagofore. V kvasovkah kroži med mestom nastanka fagofore, PAS, in perifernimi strukturami ter prenaša lipidne molekule iz vira v nastajajoči avtofagosom. Podobno kot v kvasovkah sesalski Atg9 (mAtg9) kroži med trans-Golgijevim mrežjem in poznimi endosomi. Vir lipidnih molekul za izgradnjo avtofagosoma naj bi bili endoplazmatski retikulum (ER) [41], Golgijev kompleks [42] in mitohondriji [43,44].

Rast, širitev in ukrivljanje fagofore okoli tarče uravnavata dva ubikvitinu podobna konjugacijska sistema, sistem Atg12-Atg5-Atg16 ter sistem Atg8 [45]. Oba ubikvitinu podobna proteina, Atg12 in Atg8, sta podvržena procesu konjugacije, ki je podoben konjugaciji ubikvitina, in sta odgovorna nastanek avtofagosoma. V konjugacijskem sistemu Atg12 se Atg7 veže na Atg12 in ga aktivira. Aktiviran Atg12 se nato prenese na Atg10, temu pa sledi nastanek izopeptidne vezi z Atg5. V nasprotju z ubikvitinacijo je konjugacija Atg12-Agt5 konstitutivna in ireverzibilna. Pri procesu najverjetneje ne sodeluje nobena ligaza E3 (povzeto v [46]). Konjugat Atg12-Atg15 interagira z Atg16. Nastali kompleks Atg12-Atg5-Atg16 se poveže v tetramer in pritrdi na membrano fagofore [47]. V konjugacijskem sistemu Atg8 cisteinska proteaza Atg4 procesira Atg8 blizu karboksilnega (C-) konca. Izpostavi se C-končni glicin, preko katerega se Atg7 veže na Atg8 in ga aktivira. Sledi prenos na Atg3 in tvorba amidne vezi s fosfatidiletanolaminom (PE) na membrani fagofore. Konjugacijo Atg8 s PE pospešuje konjugat Atg12-Atg5, ki deluje podobno kot ligaza E3, vendar njegovo delovanje ni nujno za konjugacijo Atg8 s PE. Atg8-PE najverjetneje preko ukrivljenosti membrane določa velikost avtofagosoma [48].

Po tvorbi avtofagosoma se vsi proteini Atg, z izjemo Atg8, ki se nahaja na notranji strani lipidnega dvosloja, sprostijo nazaj v citosol. Fuzija avtofagosoma in lizosoma se izvrši preko proteinskih kompleksov, ki omogočajo tudi homotipično fuzijo veziklov. V sesalskih celicah fuzijo omogočata lizosomski transmembranski protein LAMP-2 in mala GTPaza Rab7 [27,49].

Proteaza Atg4, ki procesira substrat Atg8 in s svojim delovanjem omogoča rast in širitev fagofore, je tudi edina proteaza, udeležena v celotnem procesu avtofagije. Je ključena in nepogrešljiva komponenta, brez katere je avtofagija onemogočena.

Glede na katalitski mehanizem v aktivnem mestu encima jo uvrščamo med cisteinske proteaze, glede na mesto cepitve pa med endopeptidaze, saj peptidno vez cepi znotraj polipeptidne verige substratne molekule Atg8.

## 1.1.2 Avtofagini

Kirisako in sod. so leta 2000 v kvasovki *S. cerevisiae* odkrili novo proteazo in jo poimenovali Apg4/Aut2/Atg4 [50]. Danes predstavnike te družine imenujemo tudi avtofagini in so nujno potrebni za nemoten potek avtofagije.

Po klasifikaciji MEROPS avtofagine uvrščamo v klan CA in družino C54. Vsi predstavniki te družine so endopeptidaze z značilno substratno specifičnostjo. Katalizirajo razpad peptidne vezi v molekulah Atg8 samo v primeru, kadar se na poziciji P1 nahaja glicin [50-52]. Po cepitvi Atg8 se izpostavi C-končni glicin, preko katerega se Atg8 kovalentno poveže s fosfatidiletanolaminom (PE) v membrani fagofore. Poleg endopeptidazne aktivnosti imajo avtofagini tudi izopeptidazno aktivnost. Ko fagofora zaobjame tovor, nastane avtofagosom. Atg4 z zrelega avtofagosoma odceplja Atg8. Po odstranitvi Atg8 s površine avtofagosoma se le-ta lahko zlije z lizosomom, v katerem se tovor razgradi na osnovne makromolekule. Nepogrešljivost obeh funkcij proteina Atg4 pri procesu avtofagije je dokazana na kvasnih mutantah z izbitim genom za *atg4* (*atg4Δ*) [50,53].

Za razliko od kvasovk z enim predstavnikom Atg4, ki ima tako endopeptidazno kot tudi izopeptidazno aktivnost, v genomu kinetoplastidov, med katere sodijo tudi paraziti *Typanosoma cruzi*, najdemo zapisa za dva homologa Atg4, Atg4.1 in Atg4.2.

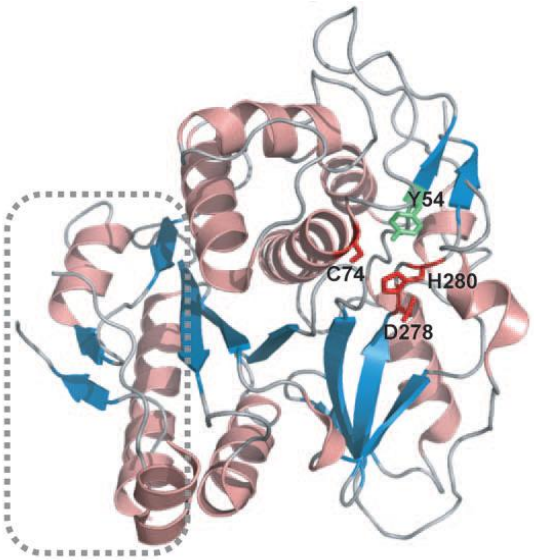
V kvasnih mutantah z izbitim genom za *ATG4* lahko oba avtofagina iz *T. cruzi*, TcAtg4.1 in TcAtg4.2, komplementirata kvasno Cvt metabolno pot, kar kaže na funkcijsko ohranjenost obeh homologov s kvasnim Atg4. TcAtg4.2 ima vlogo endopeptidaze, ki naravna substrata proTcAtg8.1 in proTcAtg8.2 procesira s ~10,000 × višjo katalitično aktivnostjo kakor TcAtg4.1. Funkcija TcAtg4.1 še ni znana [18].

V višje razvitih večceličnih organizmih najdemo večje število homologov Atg4, ki zaradi različne tkivne distribucije znotraj organizma/tkiv najverjetneje sodelujejo pri različnih tkivno specifičnih procesih. Pri sesalcih najdemo štiri homologe Atg4 (avtofagin-1/Atg4B, avtofagin-2/Atg4A, avtofagin-3/Atg4C in avtofagin-4/Atg4D), vendar vloge nekaterih še niso popolnoma razjasnjene [53].

V pogojih *in vitro* sta katalitično aktivna le HsAtg4A in HsAtg4B. HsAtg4A najbolje cepi homologe Atg8, ki spadajo v poddružino GABARAP, medtem ko LC3B predstavnika poddružine MAP1/LC3 ne cepi. Atg4B, ki je glavni nosilec avtofagije pri sesalcih, cepi predstavnike obeh poddružin s skoraj enako afiniteto. HsAtg4C in HsAtg4D ne kažeta afinitete do nobenega izmed človeških homologov Atg8 [54].

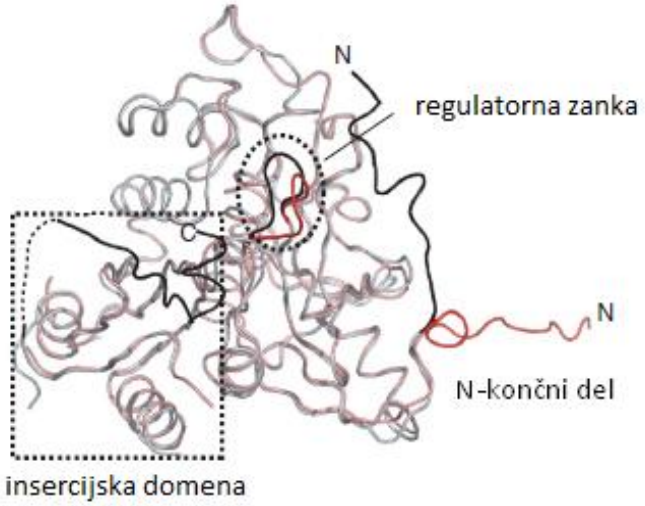
### *1.1.2.1 Tridimenzionalna struktura človeškega Atg4B*

Sugawara in sod. so določili kristalno strukturo človeškega HsAtg4B z resolucijo 1.9 Å [51]. HsAtg4B ima α/β zvitje, sestavljeno iz devetih α-vijačnic in 13 β-trakov. Centralna antiparalelna ploskev je sestavljena iz trakov β6, β7, β8, β9, β11 in β12. Štiri α-vijačnice (F-I) ter dva β-trakova (β5 in β13) se nahajajo na eni strani centralne β-ploskve, pet α-vijačnic (A-E) ter dva β-trakova (β3 in β10) pa na drugi strani centralne regije. Zvitje HsAtg4B je strukturno zelo podobno zvitju papainske družine cisteinskih proteaz, vključno z deubikvitinirajočimi encimi DUB-i (angl. *deubiquitinating enzymes*). Strukturna posebnost HsAtg4B je majhna insercijska domena, sestavljena iz α-vijačnic F, H in I ter β-trakov β5 in β13, na katero se veže njegov substrat LC3 (Slika 4).




Slika 4: *Tridimenzionalna struktura človeškega Atg4B* (povzeto po [55]). Človeški Atg4B (koda PDB: 2CY7) ima papainu podobno zvitje, sestavljeno iz devetih α-vijačnic (roza) in 13 β-trakov (modra). Aminokislinski preostanki katalitične triade so prikazani z rdečo, z zeleno je prikazan aminokislinski preostanek, ki gradi oksaanionsko luknjo. V kvadratu, ki ga omejuje prekinjena črta, je prikazana insercijska regija, ki predstavlja strukturno posebnost avtofaginov.

V neaktivni konformaciji je HsAtg4B avtoinhibiran z regulatorno zanko, ki pokriva režo aktivnega mesta s katalitičnim Cys 74. Prost dostop do reže aktivnega mesta poleg regulatorne zanke onemogoča tudi N-končni del encima. Ob vezavi substrata ti dve področji spremenita konformacijo iz »zaprte« v »odprto« in omogočita hidrolizo peptidne vezi v substratni molekuli (Slika 5).




Slika 5: *Konformacijske spremembe HsAtg4B ob vezavi substrata* (povzeto po [56]). Ob nastanku kompleksa HsAtg4B-LC3 regulatorna zanka in N-končni del encima spremenita konformacijo in omogočita procesiranje substratne molekule. S črno je označena »zaprta«, neaktivna konformacija avtofagina, z rdečo pa »odprta«, aktivna konformacija encima. S kvadratom, obdanim s prekinjeno črto, je označena insercijska regija, na katero se veže substratna molekula.

### 1.1.3 Naravni substrati avtofaginov proteini Atg8

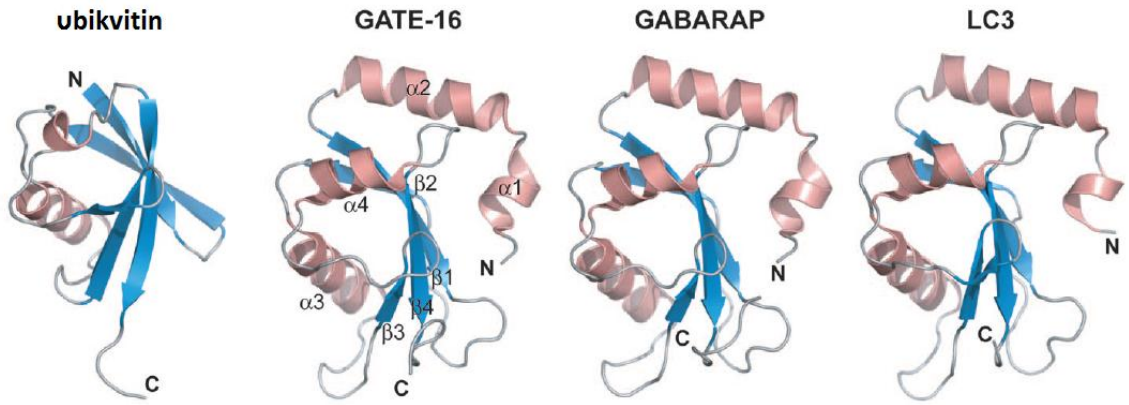
V konjugacijskem sistemu Atg8 sodelujejo številni proteini, ki strukturno in funkcijsko spominjajo na proteine, udeležene v ubikvitin-proteasomski poti. Osrednji protein avtofagnega konjugacijskega sistema Atg8 je ubikvitinu podoben protein Atg8. Genom kvasovke *S. cerevisiae* nosi zapis le za enega predstavnika *atg8*, pri sesalcih najdemo vsaj šest homologov Atg8, v kintetoplastidnih protozojih, kamor spada tudi *Trypanosoma cruzi*, pa se število Atg8 glede na organizem spreminja. V genomu *T. cruzi* najdemo zapisa za dva predstavnika Atg8, TcAtg8.1 in TcAtg8.2. Imed njiju le TcAtg8.1 uspešno komplementira Cvt metabolno pot v kvasnih mutantah z izbitim genom za *ATG8*. Tudi študije, narejene na *T. cruzi* epimastigotih, transficiranih s TcAtg8.1 oz. TcAtg8.2, ki so bili izpostavljeni stradanju, so pokazale, da le pri TcAtg8.1 pride do spremembe celične lokalizacije iz enakomerno razporejene citosolne lokalizacije v prerazporeditev na membrane avtofagosomov, zaradi česar je TcAtg8.1 resnični kvasni homolog Atg8. Fiziološka vloga TcAtg8.2 do danes še ni poznana [18].

Genom *T. brucei* nosi zapise za tri predstavnike, TbAtg8.1, TbAtg8.2 in TbAtg8.3, kjer TbAtg8.1 in TbAtg8.2 komplementirata Cvt metabolno pot v kvasnih mutantah z izbitim genom za *ATG8*. Prav tako se v citoplazmi parazita v pogojih stradanja oba prerazporedita na membrane avtofagosomov, kjer omogočata potek avtofagije. TbAtg8.3 lahko le delno komplementira Cvt metabolno pot v kvasnih mutantah z izbitim genom za *ATG12* [57].

Sesalski homologi Atg8 se delijo na dve poddružini; prva je MAP1A/B / LC3 poddružina: z mikrotubuli povezani proteini 1 A/B / lahka veriga 3 (MAP1A/B / LC3; angl. *macrotubule-associated proteins 1A/B / light chain 3*) s tremi predstavniki MAP1LC3A (LC3A), MAP1LC3B (LC3B) in MAP1LC3C (LC3C) ter poddružina proteinov, povezanih z γ-aminobutirično kislinskim receptorjem (GABARAP; angl. *γ-aminobutiric acid receptor-associated protein*) s tremi predstavniki: GABARAP, GABARAPL1/ATG8L, GABARAPL2/GATE-16 (angl. *Golgi-associated ATPase enhancer of 16 kDa*) [58]. Ob stradanju se homologi Atg8 prerazporedijo na membrane avtofagosomov, kjer omogočajo normalen potek avtofagije [59,60]. GABARAP je poleg avtofagije udeležen tudi pri proliferaciji in diferenciaciji celic, programirani celični smrti ter tumorigenezi [61-64].

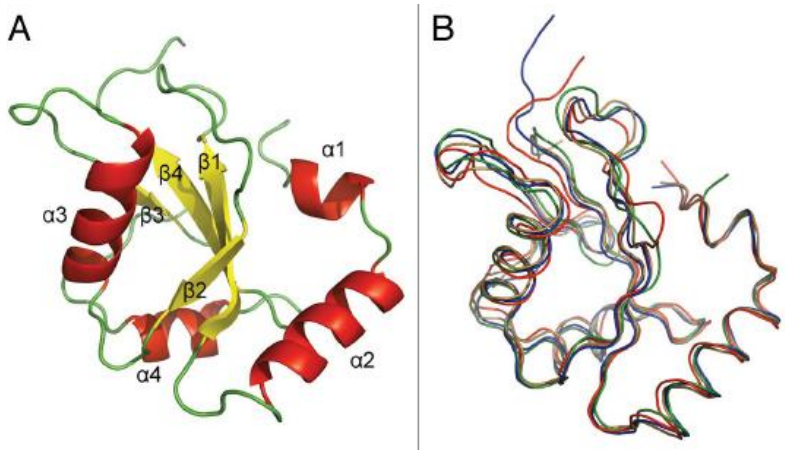
#### *1.1.3.1 Tridimenzionalna struktura homologov Atg8*

Strukturne študije Atg8 so bile narejene na kvasnem Atg8 ter sesalskih homologih (Slika 6). Tridimenzionalno strukturo večine homologov Atg8 so določili tako s kristalografijo [65] kot tudi z NMR [66]. Vse strukture imajo izjemno podobno tridimenzionalno strukturo z dobro ohranjenimi aminokislinskimi preostanki, ki so pomembni za funkcijo proteinov Atg8. LC3, najverjetneje pa tudi vsi ostali homologi Atg8, so na PE pritrjeni podobno kakor kvasni homolog Atg8 [67-69]. Sestavljeni so iz N-končne helične domene in C-končne ubikvitinu podobne domene. C-končno ubikvitinu podobno domeno sestavljajo štiri centralne β-ploskve (β1−β4) in štiri α-vijačnice. α3 se nahaja med β2 in β3, α4 pa med β3 in β4. N-končna helična domena je sestavljena iz dveh α-vijačnic, α1 in α2. Delno prekriva C-končno domeno in v proteinih Atg8, ki spadajo v superdružino proteinov z ubikvitinu-podobnim zvitjem, predstavlja posebnost. Zanimivost N-helične domene v LC3 in najverjetneje tudi ostalih homologov Atg8 je tudi površinski elektrostatski potencial α-vijačnic α1 (močno bazičen) in α2 (kisel), kar nakazuje na posebno fiziološko funkcijo N-končne domene. Tako so študije *in vitro* pokazale vlogo N-končne domene LC3 pri vezavi tubulina in mikrotubulov [66].




Slika 6: *Struktura ubikvitina in človeških homologov Atg8* (povzeto po [55]). Vse molekule so predstavljene v enaki orientaciji. α-vijačnice so predstavljene z roza barvo, β-ploskve z modro. Posebna značilnost homologov Atg8 sta α-vijačnici α1 in α2, ki tvorita N-končno helično domeno. LC3 se v pogojih *in vitro* preko te domene veže na tubulin in mikrotubule. Kode PDB: ubikvitin – 1UB1, GATE-16 – 1EO6, GABARAP – 1GNU, LC3 – 1UGM.

Koopmann in sod. so s pomočjo kristalografije določili tudi prvo tridimenzionalno strukturo proteina Atg8 iz družine kinetoplastidnih parazitov, in sicer iz parazita *Trypanosoma brucei* (Slika 7). Tako kot pri ostalih homologih Atg8 ima tudi TbAtg8.2 karakteristično strukturo, sestavljeno iz N-končne helične domene in C-končne ubikvitinu podobne domene, ki je izjemno podobna kvasnemu in sesalskim homologom, kar nakazuje na evolucijsko ohranjenost proteinov in najverjetneje tudi na ohranjenost mehanizma delovanja [70].




Slika 7: *Tridimenzionalna struktura TbAtg8.2 in superpozicija homologov Atg8* [70]. (A) Kristalna struktura *Trypanosoma brucei* Atg8.2. (B) Superpozicija homologov Atg8: rdeča – TbAtg8B, modra – GATE-16 (*Bos taurus*, koda PDB: Ieo6), zelena – LC3 (*Rattus norvegicus*, koda PDB: Iugm), rjava – GABARAP (*Rattus norvegicus*, koda PDB: Ikjt).

### 1.1.4 Fiziološke vloge avtofagije

V normalnih pogojih avtofagija poteka na nizkem bazalnem nivoju. Odstranjuje poškodovane organele in proteine, preprečuje akumulacijo proteinskih agregatov in odstranjuje znotrajcelične patogene. S svojim delovanjem ohranja homeostazo celic ter

zavira nastanek raka, nevrodegenerativnih bolezni in infekcij ter upočasnjuje staranje organizma. Avtofagija se aktivira ob različnih oblikah metabolnega stresa, kot so pomanjkanje nutrientov, rastnih faktorjev in hipoksija. Razgradnja s pomočjo avtofagije generira aminokisline in proste maščobne kisline, ki se s pomočjo permeaz, ki se nahajajo v membrani lizosomov/prebavnih vakuol, reciklirajo nazaj v citosol. Reciklirane makromolekule so na voljo za *de novo* sintezo s stresom povezanih proteinov, ki omogočajo učinkovito prilagoditev organizma na stres. Prav tako lahko reciklirane molekule vstopijo v Krebsov cikel ter so na voljo za proizvodnjo celične energije v obliki ATP [71].

Med apoptozo se z avtofagijo pospešeno odstranjujejo odvečne celične komponente, hkrati pa se proizvaja tudi energija, ki je nujna za nemoteno eliminacijo celic [72].
Med embriogenezo mišjih zarodkov je bazalni nivo avtofagije nizek. V neonatalnem obdobju, ko se materina oskrba s hranili prekine, se nivo avtofagije v miših divjega tipa močno poveča in mladičem omogoči preživetje v prvih dneh življenja. Mladiči miši z izbitim genom *atg5* umrejo že po prvem dnevu. Prav tako imajo v primerjavi z mišmi divjega tipa močno zmanjšano koncentracijo tkivnih aminokislin in ATP molekul [73].
Tudi maščobe se reciklirajo s pomočjo avtofagije. Stopnja recikliranja maščob se z načinom prehrane spreminja. V miših se Atg proteini med stradanjem razvrstijo v bližino lipidnih kapljic, kjer lipidni dvosloj zaobjema majhne količine lipidnih molekul. Tvorijo se avtolipofagosomi, ki se združijo z lizosomi. Ob podaljšanem prehranjevanju miši s hrano, ki vsebuje visok odstotek maščob, se avtofagija okvari. Maščobe se začnejo kopičiti znotraj jetrnih celic, kar vodi v zamaščenost jeter (angl. *fatty-liver disease*). Takšno kopičenje lipidov znotraj hepatocit najdemo tudi pri debelih ljudeh in alkoholikih [74].

Študije na imortaliziranih epitelijskih celičnih linijah z izbitimi *atg* geni so pokazale pomembno vlogo avtofagije pri ohranjanju kromosomske stabilnosti in omejevanju poškodb DNA, zaradi česar se zmanjša verjetnost za nastanek in napredovanje tumorjev ter razvoj nevrodegenerativnih bolezni. Mehanizem ohranjanja genomske stabilnosti še ni povsem razjasnjen. Neuspešna kontrola popravljanja napak ob celičnem podvojevanju, deregulirano recikliranje centrosomov, nezadostne količine ATP za uspešno podvojevanje DNA in povečana količina reaktivnih kisikovih spojin (*ROS* angl. - *reactive oxygen species*), ki nastajajo zaradi nepravilnega odstranjevanja poškodovanih mitohondrijev, predstavljajo potencialne mehanizme, ki pospešujejo genomsko nestabilnost v celicah z okvarjeno avtofagijo [71].

### 1.1.5 Patofiziološke vloge avtofagije

Bazalni nivo avtofagije se med različnimi tkivi spreminja. Povišan nivo bazalne avtofagije najdemo v jetrih, ki so zaradi svoje prečiščevalne funkcije izpostavljene številnim toksičnim substancam, ter v nevronskih celicah in miocitah, ki se po diferenciaciji ne delijo več. Pri ohranjanju zdravja teh celic ima avtofagija še posebej pomembno vlogo. Nepogrešljiva pa je tudi v vseh ostalih celicah in tkivih, kjer je bazalni nivo avtofagije nižji. Številni dokazi povezujejo spremenjen nivo avtofagije z razvojem številnih humanih bolezni, vključno z boleznimi jeter in srca, nevrodegenerativnimi boleznimi, rakom in okužbami s patogeni [32].

Zaradi številnih zdravstvenih in ekonomskih težav v nerazvitih in razvijajočih se državah tropskega in subtropskega pasu, se v zadnjem času vedno več pozornosti usmerja v preučevanje avtofagije v človeških in živalskih parazitih, ki spadajo v družino tripanosomatidov in povzročajo številne bolezni, kot sta Chagasova bolezen v Južni Ameriki in spalna bolezen v Afriki.

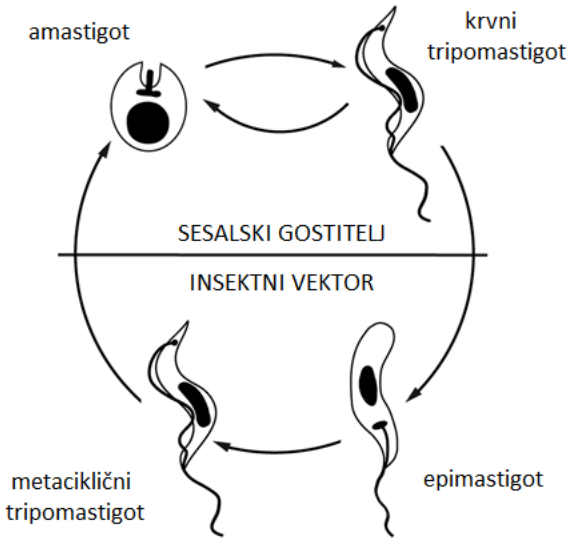
V začetnih fazah raziskav so se pri *in silico* analizi genomov kot matrice uporabljala

aminokislinska zaporedja proteinov Atg iz kvasovke *S. cerevisiae*, kasneje pa so se zaradi prevelike evolucijske oddaljenosti tarčnih organizmov in posledično slabše ohranjenosti proteinskih zaporedij namesto kvasnih aminokislinskih zaporedij začele uporabljati tudi živalske ali rastlinske matrice, ki so razkrile prisotnost številnih novih ortologov Atg [75].

### *1.1.5.1 Trypanosoma cruzi*

*Trypanosoma cruzi* je obligatorni znotrajcelični parazit, značilen za Centralno in Južno Ameriko. Pri ljudeh povzroča Chagasovo bolezen, ki zaradi svoje razširjenosti na področju Latinske Amerike predstavlja poglavitni zdravstveni probem. Parazit ima dvofazen življenjski cikel z vmesnimi, krvosesnimi insektnimi gostitelji, ki sodijo v družino Reduviidae in poddružino Triatominae, ter glavnimi gostitelji, vretenčarji.

Življenjski cikel *T. cruzi* vključuje štiri razvojne faze; dve replikativni in dve infektivni fazi (Slika 8). Replikativni obliki parazita sta epimastigot, ki ga najdemo v prebavilih insektnega vektorja, ter amastigot, ki se nahaja v sesalskih celicah. Infektivni obliki pa sta metaciklični tripomastigot v insektih in krvni tripomastigot v sesalcih. Prenos parazita med gostitelji ter njegovo diferenciacijo iz ene oblike v drugo spremljajo obsežne metabolne in morfološke spremembe [76,77].



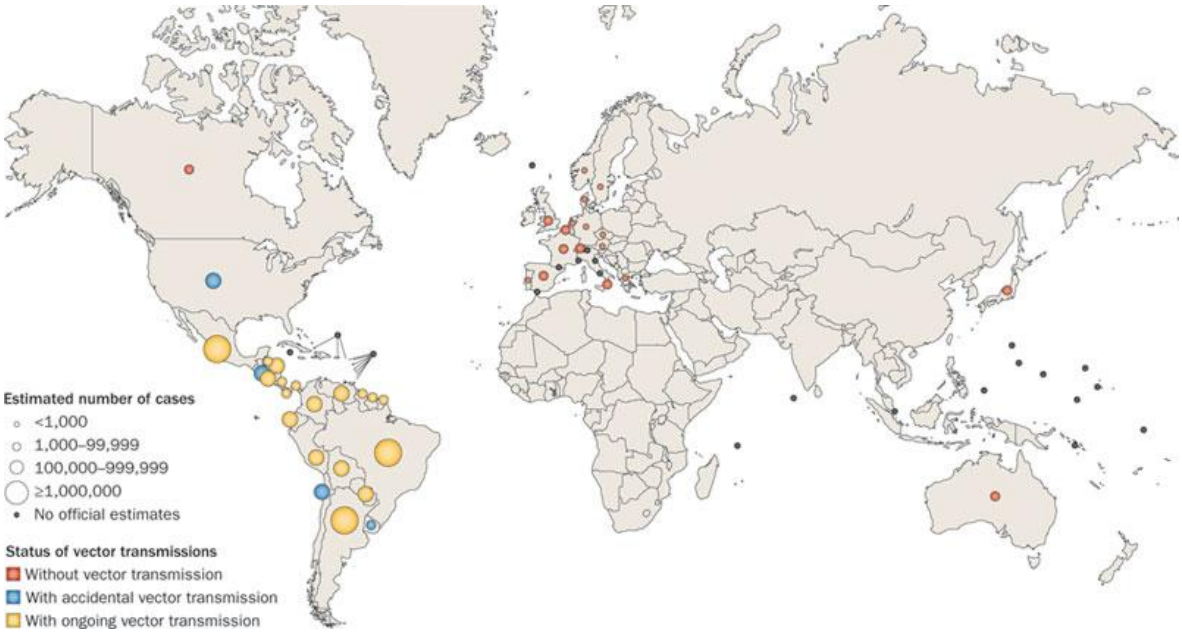

Slika 8: *Življenjski cikel parazita Trypanosoma cruzi* [78]. Življenjski cikel *T. cruzi* vključuje štiri razvojne stopnje. Replikativni obliki sta epimastigot v insektnem vektorju in amastigot v sesalskih gostiteljih ter infektivni obliki metaciklični in krvni tripomastigot pri insektih in sesalcih.

Parazit v sesalske celice lahko vstopa s pomočjo fagocitnega mehanizma [79] ali od kaveolina-, klatrina- ter od flotilina-odvisne endocitoze. Poleg endocitotskih poti vnosa parazita v gostiteljske celice pa *T. cruzi* lahko v gostiteljske celice vstopa tudi z aktivno penetracijo skozi gostiteljevo membrano [80]. Infektivni tripomastigot se ob vstopu v sesalske celice za kratek čas skrije v vezikle, imenovane parazitoforne membrane, iz katerih se nato vrne nazaj v citosol, kjer se spremeni v replikativno obliko parazita, amastigot, se namnoži in spremeni nazaj v infektivno obliko, krvni tripomastigot. Slednji zapusti celico in se po krvi raznese po celotnem organizmu gostitelja.

### *1.1.5.2 Chagasova bolezen*

Chagasovo bolezen je leta 1909 prvi okarakteriziral brazilski infektolog Carlos Chagas, ki je v prebavnem traktu krvosesnih insektov iz družine Teduviidae odkril novo vrsto bičkaste praživali iz rodu *Trypanosoma*. Eksperimentalno je dokazal prenos parazita iz okuženega insekta na opice. Novo vrsto parazita je poimenoval *Trypanosoma cruzi* v čast brazilskemu epidemologu Oswaldu Cruzu, ki se je v začetku 20. stoletja trudil omejiti epidemije vodenih koz, rumene mrzlice in bubonske kuge v Riu de Janeiru.

Chagasova bolezen ali južnoameriška tripanosomioza predstavlja poglavitni zdravstveni problem v državah Južne Amerike. Z globalizacijo in preseljevanjem se je bolezen začela širiti po vsem svetu (Slika 9). S parazitom *Trypanosoma cruzi* naj bi bilo okuženih med 7 in 8 milijoni prebivalcev Južne Amerike [81], 75 do 90 milijonov pa je izpostavljenih možnosti okužbe vsak dan [82].




Slika 9: *Geografska porazdelitev ljudi, okuženih s T. cruzi v letu 2012* [83]. Največ ljudi, okuženih s *T. cruzi*, živi na področju Latinske Amerike, z migracijami latinskoameriških prebivalcev se je bolezen razširila tudi na ostale predele sveta.

Pri prenosu *T. cruzi* s pomočjo triatomidov se na mestu vstopa parazita skozi kožo mnogokrat razvije vnetje in oteklina, poznana kot šagom. Makrofagi sesalskega gostitelja s fagocitozo poskušajo preprečiti okužbo gostitelja, a ravno s svojim delovanjem omogočijo uspešen vstop parazita v celice. Po zaključenem ciklu podvojevanja in diferenciacije se krvni tripomastigoti naselijo v gostiteljeve organe, grajene predvsem iz gladkih mišic (srce, prebavni trakt), lahko pa kolonizirajo tudi druge organe v telesu (skeletne mišice, živčevje).

Poleg okužbe preko triatomidov se parazit na človeka lahko prenaša tudi s transfuzijo okužene krvi, transplantacijo organov, oralno (s kontaminirano hrano), spolno, preko placente oz. porodnega kanala ter pri rokovanju z okuženimi živalmi [82].

Za Chagasovo bolezen sta značilni dve fazi razvoja bolezni: akutna in kronična faza. Akutna faza je največkrat asimptomatična in brez zdravljenja preide v kronično. Skoraj 70 % pacientov je asimptomatičnih, dobrih 30 % pacientov pa razvije neozdravljive bolezni srca (27 %), prebavnega trakta (6 %) in perifernega živčnega sistema (3 %) [84]. Zdravljenje pacientov, okuženih s *T. cruzi*, je zelo problematično zaradi odpornosti

parazita na večino testiranih zdravil, vključno s terapijami, ki so se izkazale kot uspešne v boju z afriškimi tripanosomami in ostalimi protozoji [85]. Na voljo sta nifurtimox (Lampit; Bayer 2502) ter benznidazol (Radamil; Roche 7-1051), ki zelo uspešno zdravita akutne infekcije s *T. cruzi*, vendar nista uspešna pri zdravljenju kronične Chagasove bolezni. Poleg neuspešnosti zdravljenja pa je obe zdravili potrebno uporabljati daljše časovno obdobje, kar privede do neželenih stranskih učinkov. Nifurtimox deluje toksično na centralno in periferno živčevje ter prebavila, benznidazol pa poleg stranskih učinkov, omenjenih pri nifurtimoxu, povzroča preveliko občutljivost kože, ki se nadalje razvije v dermalne lezije.

Med procesom diferenciacije parazita se avtofagija močno poveča in je ključnega pomena za uspešno kolonizacijo gostiteljskega organizma [78]. Za nemoten potek avtofagije ter uspešno diferenciacijo parazita so nepogrešljivi tudi encimi, ki se nahajajo znotraj lizosomov in/ali prebavnih vakuol, s pomočjo katerih poteka masovna proteoliza odpadnih in odvečnih celičnih komponent, ki nastajajo pri procesu diferenciacije. Z inhibicijo lizosomskih cisteinskih proteaz se avtofagija ustavi. Posledično je inhibirana tudi diferenciacija epimastigotov v metaciklične tripomastigote [86,87]. V kokulturi sesalskih celic Vero in *T. cruzi* se ob inhibiciji lizosomskih cisteinskih proteaz močno zmanjša tudi infektivni potencial parazita [88]. Uporaba inhibitorja K777, ki inhibira poglavitno cisteinsko proteazo v lizosomih *T. cruzi*, cruzipain, je znatno upočasnila napredovanje infekcije psov, okuženih s *T. cruzi*, in razvoj Chagasove bolezni, a le-te ni pozdravila v celoti [89]. Za razvoj uspešnih antiparazitskih učinkovin bo najverjetneje potrebno uporabiti kombinirani pristop, ki bo ciljal več kot le eno tarčo.

### *1.1.5.3 Vloga avtofagije pri razvoju raka*

Rak je ena prvih bolezni, pri kateri so dokazali okvaro avtofagije na genetskem nivoju. Monoalelno delecijo *ATG* gena *beklin 1* najdemo pri 40–70 % primerih humanega raka dojke [90], prostate [91] in ovarijev [92]. *Beklin 1* heterozigotne miši imajo zmanjšan bazalni nivo avtofagije in so nagnjene k spontanemu nastajanju limfomov ter pljučnih in hepatocelularnih karcinomov. Močno tumorigene so tudi imortalizirane ledvične in epitelijske celice raka dojke, pridobljene iz *beklin 1* heterozigotnih miši [25]. Pri prekomerni ekspresiji beklina 1 v celični liniji raka dojke MCF-7 se nivo avtofagije poviša. Posledično sta se zmanjšali tako celična proliferacija kot tudi tumorigenost celične linije [93]. Poleg proteina beklin 1 naj bi imeli tumor-supresorsko funkcijo tudi drugi Atg proteini. Miši z izbitim genom za *avtofagin-3*, *atg4c*, ki predstavlja del Atg8 konjugacijskega sistema, poleg znižanega nivoja avtofagije v pogojih stradanja kažejo povečano dovzetnost za razvoj kemijsko induciranih fibrosarkomov [94]. Znižanje oz. inhibicija avtofagije se kaže kot kopičenje nepravilno zvitih proteinov ter poškodovanih organelov, predvsem mitohondrijev, ki generirajo ROS in druge proste radikale. Le-ti povzročajo poškodbe proteinov in lipidov ter omogočajo mutacije DNA in s tem povečujejo genomsko nestabilnost, ki je gonilo razvoja tumorskih celic [95,96]. V takšnih primerih bi indukcija avtofagije lahko predstavljala primerno obliko antitumorskega zdravljenja [97]. V poznih fazah raka črevesja [98] in dojke [99] ter melanoma [100], hepatoma [101] in malignega glioma [102] se avtofagija, kot odgovor na celični stres zaradi pomanjkanja kisika in nutrientov, močno poveča. Prav tako se avtofagija v tumorskih celicah močno poveča tudi kot odgovor na antitumorske terapije [103] in omogoča preživetje ter prilagoditev oz. rezistenco tumorskih celic na konvencionalne antitumorske terapije. Zaradi pomembnosti avtofagije pri razvoju rezistence tumorskih celic na antitumorska zdravljenja se v zadnjem času vse več pozornosti usmerja v kombinirane antitumorske terapije. Le-te naj bi z regulacijo avtofagije tumorske celice naredile bolj dovzetne na reagente, ki povzročajo različne oblike celičnega stresa, kot so genotoksični stres, proizvodnjo ROS v kombinaciji z radiacijsko terapijo, okvare v

metabolizmu in inhibicijo signalizacije s pomočjo rastnih faktorjev, ki vodijo v celično smrt. Pri uporabi regulatorjev avtofagije je tako za pravilno izbiro regulatorja potrebno podrobno proučiti vrsto tumorja, določiti njegovo fazo rasti in fiziološki odziv celic na spremenjen nivo avtofagije kot tudi dopolnilno antitumorsko zdravilo, ki naj bi s pomočjo apoptoze eliminiralo senzitizirane tumorske celice [104].

#### 1.1.5.3.1 Cisteinski katepsini in njihovi endogeni inhibitorji pri raku

Cisteinski katepsini so lizosomske proteaze z optimalno aktivnostjo v rahlo reducirajočem, kislem okolju. Človeški genom nosi zapise za 11 predstavnikov: katepsine B, C, F, H, K, L, O, S, V, X in W [105]. Glede na terciarno strukturo spadajo v klan CA in družino C1A, kamor sodijo papainu podobni encimi. Sintetizirajo se kot preproencimi, ki se v kislem pH-ju endolizosomov aktivirajo v zrelo obliko. Sprva je veljalo, da skupaj z aspartatnimi (katepsina D in E) in serinskimi katepsini (A in G) sodelujejo le pri masovni proteolizi znotraj endosomov/lizosomov. Zaradi naraščajočega števila dokazov danes velja, da so katepsini poleg masovne proteolize nepogrešljivi pri natančni regulaciji signalnih poti, kjer z omejenim/reguliranim procesiranjem substratnih molekul ohranjajo homeostazo celic in celotnega organizma [106,107].

Katalitična aktivnost cisteinskih katepsinov se poleg kompartmentizacije, aktivacije proencimov, pH-ja in regulacije njihove aktivnosti z majhnimi molekulskimi inhibitorji uravnavava tudi endogenimi proteinskimi inhibitorji, cistatini, tiropini, serpini in drugimi [108]. Vsi endogeni proteinski inhibitorji so kompetitivni, reverzibilni inhibitorji z močno vezavo, ki katepsine inhibirajo v pM- do μM-območju.

Predstavnike cistatinov glede na število cistatinskih domen in disulfidnih mostičkov delimo na štiri različne tipe: stefine (cistatini tipa I), cistatine (cistatini tipa II), kininogene (cistatini tipa III) in neinhibirajoče cistatinske homologe [109].

Stefini so enoverižni proteinski inhibitorji, zgrajeni iz ~100 aminokislinskih preostankov. Sintetizirajo se brez propeptida. Prav tako nimajo disulfidnih mostičkov in glikozilacijskih mest. Primarno se nahajajo znotraj celic, zasledimo pa jih lahko tudi v telesnih tekočinah [110]. Znotraj te družine pri sesalcih najdemo dva predstavnika, stefina A in B.

Pri raku porušena celična homeostaza je mnogokrat povezana tako katepsini kot tudi z njihovimi endogenimi proteinskimi inhibitorji. Številne študije so vlogo katepsinov, še posebej katepsina B, z razvojem raka povezale že pred 30 leti [111]. Danes vemo, tudi na podlagi kliničnih rezultatov ter študij na mišjih modelih, da imajo zelo pomembno vlogo pri nastanku in razvoju raka kot tudi pri invaziji in metastaziranju rakavih celic [112,113]. Zvišan nivo izražanja in/ali zvišana aktivnost katepsinov ter znižan nivo izražanja njihovih endogenih proteinskih inhibitorjev sovpada s slabimi napovedmi za preživetje pacientov z rakom [114,115], zvišan nivo izražanja inhibitorjev pa sovpada z boljšimi prognostičnimi napovedmi [116,117]. Poleg spremenjenega izražanja katepsinov je mnogokrat spremenjena tudi njihova celična lokalizacija, pri kateri se prerazporedijo na površino celic in/ali se izločajo v medcelični prostor. V medceličnini razgrajujejo komponente zunajceličnega matriksa ter s svojim delovanjem omogočajo hitrejšo in bolj invazivno migracijo in metastaziranje tumorskih celic (povzeto v [106]). Pri ~ 50 % tumorjev je poleg prisotnosti zunajceličnih katepsinov znižan še nivo zunajceličnega inhibitorja cistatina C. Zaradi tega je zunajcelična proteoliza dodatno povečana, kar omogoča hitrejše in bolj invazivno metastaziranje rakavih celic [118].

Razvoj tehnologije tkivno specifičnega in/ali sistemskega izbitja genov je omogočil preučevanje tkivne oz. sistemske vloge posameznih katepsinov pri razvoju raka v

številnih živalskih modelih. Neodvisni študiji, narejeni na dveh različnih mišjih modelih z izbitim genom za *katepsinB* (*CtsB-/-*), RIP12-Tag2 mišjem modelu raka pankreasa ter MMTV-PYMT mišjem modelu raka dojke, sta pokazali pomembno vlogo katepsina B pri nastanku, napredovanju in metastaziranju tumorskih celic. V primerjavi z mišmi divjega tipa je izbitje gena za *katepsin B* v obeh modelih sovpadalo z izrazito upočasnjenim nastankom ter znatno zmanjšanimi tumorji [119,120]. V nasprotju z protumorigeno funkcijo katepsina B pri razvoju raka pa vpliv znotrajceličnih inhibitorjev stefina A in B na razvoj in invazijo tumorskih celic zaradi številnih nasprotujočih si študij še ni povsem razjasnjen [116,121-123]. Zato bodo potrebne dodatne študije, ki bodo razjasnile vlogo stefinov pri nastanku in napredovanju rakavih obolenj.

#### 1.1.5.3.2 Mišji model raka mlečne žleze MMTV-PyMT

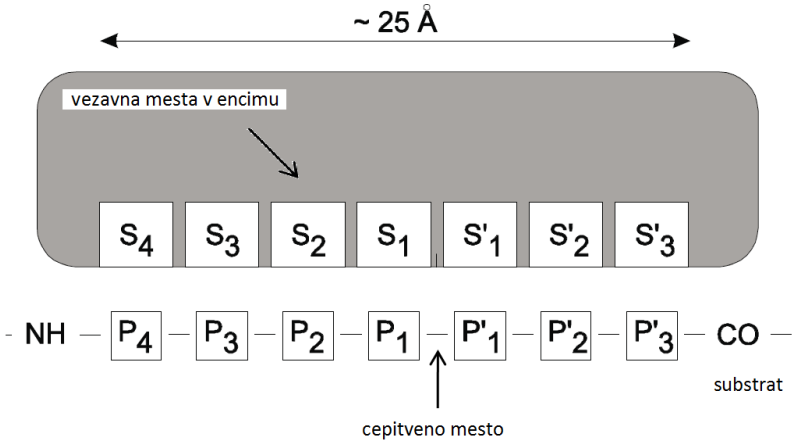
Transgene miši modela raka mlečne žleze MMTV-PyMT razvijejo tumorje na vseh desetih mlečnih žlezah. Mlečno žlezno hipertenzijo, ki nastane zaradi izražanja onkoproteina *Polyoma virus middle-T* (PyMT), ki je pod kontrolo promotorja MMTV, je možno opaziti že v četrtem tednu starosti. Pri 14 tednih pa miši na mlečnih žlezah razvijejo tumorje, ki metastazirajo tudi v pljuča in delno v limfne vozle. Onkoprotein PyMT vpliva na transdukcijo številnih signalnih poti, kot so *Src*, *Ras*, *c-myc* in PI3 kinazna pot, ki so spremenjene tudi pri ljudeh, obolelih za rakom dojke. Tudi razvoj normalnega tkiva v tumor poteka pri človeku in miši podobno, zato te miši predstavljajo dober model za različne študije *in vivo* [124].

## 1.2 Sintetični substrati, inhibitorji in pametne aktivnostne sonde

Proteaze poleg razgradnje substratov sodelujejo pri sprožanju in prenosu signalov številnih signalnih kaskad in v normalnih pogojih ohranjajo homeostazo celic. Njihovo spremenjeno delovanje, kot sta prekomerno ali nezadostno izražanje ter spremenjena lokalizacija, pa pomembno prispeva k razvoju številnih humanih bolezni, od kardiovaskularnih bolezni do raka. Zato proteaze predstavljajo pomembne tarče pri razvoju zdravilnih učinkovin (povzeto v [125]).

Za razvoj selektivnih zdravilnih učinkovin je potrebno dobro poznavanje mehanizma delovanja tarče ter njenih strukturno-funkcijskih lastnosti. Najbolj direktna metoda opazovanja proteolitične aktivnosti je spremljanje hidrolize substrata. Pri cepitvah naravnih substratov spremljamo potek cepitve na NaDS-PAGE, z imunodetekcijo s protitelesi ali z masno spektrometrijo. Proteolitično aktivnost pa lahko spremljamo tudi z uporabo sintetičnih substratov.

Zaradi vedno večjega števila študij določanja encimskih specifičnosti proteaz sta Schechter in Berger leta 1967 uvedla univerzalen način poimenovanja vezavnih mest v proteazah kot tudi pripadajoče pozicije v substratnih molekulah (Slika 10) [126]. Vezavna mesta v encimu imajo oznake S, pripadajoči aminokislinski preostanki v substratu pa P. Aminokislinski preostanki v substratu so z N-konca proti C-koncu označeni -NH-P3-P2-P1-P1’-P2’-P3’-CO-. Cepitveno mesto se nahaja med aminokislinskima preostankoma P1 in P1’. Pripadajoča vezavna mesta v encimu imajo namesto oznak P oznake S in so oštevilčena enako kakor mesta na substratu.




Slika 10: *Schechterjeva in Bergerjeva nomenklatura* (povzeto po [126]). Poimenovanje aminokislinskih preostankov okoli cepitvenega mesta v substratu in v vezavnem žepu encima.

Aminokislinska zaporedja sintetičnih substratov so največkrat identična ali podobna zaporedjem naravnih substratov ali pa so sintetizirana na osnovi poznane substratne specifičnosti proteaze, dobljene s cepitvami substratnih knjižnic. V obeh primerih so aminokislinska zaporedja sintetičnih substratov pripeta na fluorofor, ki v substratni molekuli zaseda pozicijo P1'. Ob cepitvi se fluorofor sprosti in začne oddajati fluorescenčni signal. Takšni substrati na čistih proteinskih vzorcih delujejo dobro, vendar so njihova glavna slabost nespecifične cepitve pri uporabi v kompleksnejših vzorcih.

Za izboljšanje selektivnosti substratov so se v zadnjem času začele uporabljati kombinatorne substratne knjižnice (angl. *PS-SCL - positional scanning-substrate combinatorial library*), ki omogočajo med seboj neodvisno mapiranje vezavnih mest v reži aktivnega mesta encima [127]. Tako dobimo informacijo o vezavni afiniteti vsakega posameznega vezavnega žepa v reži aktivnega mesta. Pri uporabi preferenčnih aminokislinskih preostankov, ki vključujejo tako naravne aminokisline kot tudi njihove nenaravne izoforme, pa lahko razvijemo izjemno selektivne sintetične substrate, ki so primerni za študije *in vitro* tako v čistih kot tudi v kompleksnejših proteinskih vzorcih ter za spremljanje encimske aktivnosti *ex vivo* in/ali *in vivo* [128]. Vendar imajo tudi izjemno selektivni sintetični substrati svoje pomanjkljivosti. Glavna slabost peptidnih substratov je difuzija peptida od tarčne proteaze po končani cepitvi, kar onemogoča identifikacijo vseh proteaz, udeleženih pri cepitvah izbranega sintetičnega substrata. Prav zaradi te slabosti se je vzporedno z optimizacijo selektivnih sintetičnih substratov in inhibitorjev razvoj usmeril tudi v sintezo selektivnih pametnih aktivnostnih sond (*ABP* angl. *activity based probe*). ABP so v osnovi sintetični substrati oz. inhibitorji, ki se ob proteolitični aktivnosti kovalentno vežejo na proteazo. Reporterski skupini sta največkrat fluorofor, ki omogoča spremljanje proteolitične aktivnosti *in vitro* ter lokalizacijo tarče *ex vivo* in/ali *in vivo* ali afinitetni priveski, ki omogočajo analitične študije, kot so detekcija tarč na SDS PAGE ali izolacija in identifikacija tarč s pomočjo masne spektrometrije. Zaradi svoje kovalentne vezave na tarčo so aktivnostne sonde izjemno močno orodje, saj poleg sledenja in uravnavanja proteolitične aktivnosti tarčne proteaze omogočajo tudi identifikacijo proteaz, ki se nespecifično vežejo na sondo. V primeru cisteinskih proteaz lahko z uporabo različnih elektrofilov, ki so gonilo kovalentne vezave med nukleofilom in elektrofilom, pomembno vplivamo na razmerje med ravnotežnostno konstanto $K_D$ ter konstanto afinitete $K_m$ ter tako še dodatno izboljšamo selektivnost aktivnostne sonde, kar predstavlja še dodatno prednost ABP-jev pred sintetičnimi peptidnimi substrati (povzeto v [129]).

# 2 Namen dela

Avtofagija je evolucijsko ohranjen katabolni proces, pri katerem poteka recikliranje celici lastnih makromolekul. Pri avtofagiji poleg številnih z avtofagijo povezanih proteinov Atg sodelujejo tudi proteaze Atg4 (avtofagini), ki so tudi edine proteaze, udeležene v celotnem procesu. Procesirajo substrat Atg8, ki se po cepitvi lahko pripne na membrano avtofagosoma in omogoči nadaljnjo razgradnjo komponent. Avtofagini so nepogrešljivi za nemoten potek avtofagije, zato bi natančna biokemijska karakterizacija avtofagina-2 iz parazita *T. cruzi*, TcAtg4.2, povzročitelja Chagasove bolezni v Latinski Ameriki, ter natančno mapiranje posameznih vezavnih mest v reži aktivnega mesta encima lahko predstavljalo osnovo za razvoj selektivnih sintetičnih substratov in inhibitorjev, ki bi omogočali spremljanje in uravnavanje proteolitične aktivnosti omenjenega encima.

Avtofagija je ključna tudi pri preživetju tumorskih celic. Primerjava mišjih modelov raka mlečne žleze MMTV-PyMT divjega tipa (*PyMT;WT*) in miši z izbitim genom za *stefin B* (*PyMT;StfB-/-*) je pokazala, da odsotnost stefina B v tumorskih celicah PyMT poviša nivo oksidativnih kisikovih spojin (ROS), znanih induktorjev avtofagije. Zanimalo nas je, ali imajo tumorske celice *PyMT;StfB-/-* v primerjavi z divjim tipom *PyMT;WT* spremenjen nivo avtofagije in ali bi z uravnavanjem avtofagije z indukcijo ali inhibicijo lahko zaznali razlike v preživetju med tumorskimi celicami *PyMT;WT* in *PyMT;StfB-/-*.

Delovne hipoteze so bile:

1. Avtofagin-2 iz parazita *T. cruzi* (TcAtg4.2) lahko procesira male fluorogene substrate.
2. Substratni specifičnosti avtofagina-2 iz parazita *T. cruzi* (TcAtg4.2) in človeškega avtofagina-1 (HsAtg4B), ki sta evolucijsko ohranjena ortologa, sta podobni.
3. Z uporabo nenaravnih aminokislinskih preostankov je možno sintetizirati specifične substrate za TcAtg4.2, ki jih HsAtg4B ne bo cepil.
4. Na osnovi optimalnih substratov za TcAtg4.2 je možno sintetizirati pametne aktivnostne sonde, ki bi selektivno inhibirale le TcAtg4.2, brez vpliva na aktivnost HsAtg4B.
5. Tumorske celice z izbitim genom za *stefin B* (*PyMT;StfB-/-*) imajo v primerjavi s celicami divjega tipa (*PyMT;WT*) povišan nivo avtofagije.
6. Inhibicija avtofagije povzroči pospešeno programirano celično smrt tumorskih celic *PyMT;StfB-/-*.

Da bi preverili, ali TcAtg4.2 lahko cepi male fluorogene substrate, nameravamo cepitve substratov spremljati v odsotnosti in prisotnosti različnih kozmotropnih soli ter poiskati pogoje, pri katerih bomo zaznali najvišjo katalitično aktivnost encima.

Za potrditev druge, tretje in četrte hipoteze bomo s pomočjo kombinatorne substratne knjižnice določili preferenčne aminokislinske preostanke za TcAtg4.2 na pozicijah P4, P3 in P2 ter na osnovi razlik v substratnih specifičnostih TcAtg4.2 in HsAtg4B sintetizirali optimizirane sintetične substrate in pametne aktivnostne sonde.

Da bi potrdili peto hipotezo, bomo tako *PyMT;WT* kot tudi *PyMT;StfB-/-* gojili pri normalnih pogojih ter v pogojih stradanja. Z imunološko detekcijo LC3, markerja za avtofagijo, bomo določili nivo avtofagije pri obeh modelih.

Za potrditev šeste hipoteze bomo *PyMT;WT* kot tudi *PyMT;StfB-/-* poleg stradanja tretirali tudi z induktorjem avtofagije rapamicinom ter z inhibitorjem avtofagije klorokinom ter s pomočjo pretočne citometrije določili delež umirajočih celic.

# 3 Materiali in metode

## 3.1 Materiali

### 3.1.1 Kemikalije

Kemikalije za PCR (dNTP, $MgCl_2$; MBI Fermentas), oligonukleotidi (Sigma Aldrich), Kod Hot Start DNA polimeraza (Merck Millipore), Taq polimeraza (Thermo Scientific Fermentas), agaroza (Lonza), označevalec velikosti DNA (GeneRuler 1 kb DNA ladder; MBI Fermentas), označevalec velikosti proteinov (PageRuler Prestained Protein Ladder ; MBI Fermentas), TEMED (N,N,N',N'-tetrametiletilendiamid; Merck), DMSO (Sigma Aldrich), DTT (Sigma), Z-Phe-Arg-AMC (Bachem), Z-Phe-Val-Arg-AMC (Bachem), iodoacetamid (IAA, Amersham Biosciences), ampicilin (100 mg/ml) (Sigma Aldrich), primarna protitelesa anti-LC3 (Abcam), sekundarna protitelesa, konjugirana s hrenovo peroksidazo (Sigma Aldrich), barvilo Coomassie Brilliant blue (Sigma Aldrich), reagent ECL (GE Healthcare), Aneksin V-PI (BD Biosciences), DMEM (Gibco, Invitrogen), fetalni goveji serum (FBS, Sigma Aldrich), cikloheksamid (CHX, Sigma Aldrich), glutaMAX$^{TM}$ (Gibco, Invitrogen), TrypleSelect tripsin (Gibco, Invitrogen), PBS (Gibco, Invitrogen), penicilin/steptomicin (Gibco, Invitrogen), primarna protitelesa anti-LC3 (Abcam).

### 3.1.2 Encimi in proteini

*T. cruzi* avtofagin-2 (TcAtg4.2), človeški avtofagin-1 (HsAtg4B), človeški deubikvitinirajoč protein UCH-L3, človeška deSUMOilirajoča proteina SENP-1 in -2, *T. cruzi* Atg8.1 (TcAtg8.1) in Atg8.2 (TcAtg8.2), restrikcijske endonukleaze *Nde*I, *Bam*HI (New England Biolabs), človeški katepsini B [130], K [131], L in S [132].

### 3.1.3 Gojišča

Hranilna gojišča za gojenje bakterijskih sevov:
Gojišče LB: 10 g peptona, 10 g NaCl, 5 g kvasnega ekstrakta, do 1 l $dH_20$

Gojišče LBA: Gojišče LB, ki vsebuje 50 μg/ml ampicilina gojišče.
Gojišče LBK: Gojišče, ki vsebuje 50 μg/ml kanamicina.

Hranilna gojišča za gojenje sesalskih celičnih linij:
Gojišče DMEM, ki vsebuje 10 % FBS (fetalnega govejega seruma), 1 % glutaMAX$^{TM}$, 1 % penicilin/streptomicin.

### 3.1.4 Gostiteljske bakterijske kulture

Bakterijski sev *Escherichia coli* DH5α, bakterijski sev *Escherichia coli* BL21[DE3].

### 3.1.5 Vektorji

pET28a, pET28b in pOPINe, pET23

### 3.1.6 Kompleti reagentov

Komplet reagentov za čiščenje DNA iz agaroznega gela "Wizard SV Gel And PCR Clean-up System" (Promega), Komplet reagentov za mini izolacijo plazmidne DNA "Wizard Plus SV Minipreps DNA Purification System" (Promega).

### 3.1.7 Pufri

Elektroforezni pufer za NaDS-PAGE
20 mM Tris
192 mM *L*-glicin
0,1 % NaDS

Nanašalni pufer za NaDS-PAGE (6×) – za 10 ml
0,363 g Tris (300 mM)
0,3 g NaDS (100 mM)
0,112 g EDTA (40 mM)
1,83 g DTT (1,2 M)
6 ml glicerol (60 % (v/v))
30 mg bromfenol modro

Pufer za barvanje proteinov po NaDS-PAGE
0,025 % barvilo Coomassie Blue R-250
30 % etanol
10 % ocetna kislina

Pufer za razbarvanje proteinov po NaDS-PAGE
10 % ocetna kislina
30 % etanol

Pufer BANA
15 mM $Na_2HPO_4$
88 mM $KH_2PO_4$
1 mM EDTA
0,1 % PEG-6000
pH 6,0

Prenašalni pufer
192 mM glicin
25 mM Tris
20 % (v/v) metanol

Pufer PBS

145 mM NaCl
2,5 mM $NaH_2PO_4 \times 2H_2O$
7,5 mM $Na_2HPO_4 \times 4H_2O$
pH 7,4

Pufer TBST
20 mM Tris
500 mM NaCl
0,5 % (v/v) Tween-20

Pufer za merjenje encimske aktivnosti TcAtg4.2
50 mM Tris-HCl pH 8,0
0,5 M $K_2HPO_4$
5 mM DTT

Pufer za merjenje encimske aktivnosti HsAtg4B, SENP1, -2 in UCH-L3
50 mM Tris-HCl pH 8,0
0,5 M $Na_3C_3H_5O(COO)_3$
5 mM DTT

Pufer za merjenje encimske aktivnosti katepsinov B, K, L in S
15 mM $Na_2HPO_4$ pH 6,0
88 mM $KH_2PO_4$
1 mM EDTA
0,1 % PEG-6000
5 mM DTT

### 3.1.8 Laboratorijska oprema

Aparatura za cirkularni dikroizem 62A DS (Aviv), aparatura za PCR 2720 Thermal cycler (Applied Biosystems), avtomatske pipete 0,1-2,5 µl, 0,5-10 µl, 2-20 µl, 20-200 µl, 100-1000 µl (Eppendorf), centrifuga RC 5C plus (Sorvall), centrifuge Eppendorf 5402, 5410, 5417R, 5415Rm 5810R (Eppendorf), fluorimeter za mikrotitrske plošče Safire (Tecan), kadička za agarozno elektroforezo (Owl Separations Systems), kadička za NaDS-PAGE Mini Protean II (Biorad), kolona HisTrap FF crude za afinitetno kromatografijo 1 ml in 5 ml (GE Healthcare), mikrotitrske plošče s 96 luknjicami (Costar), mikrotitrske plošče s 96 luknjicami (Greiner), pH meter (Metrel), sistem FPLC (angl. *fast protein liquid chromatography*; Äkta), spektrofotometer Lambda 18 (Perkin Elmer), spektrofotometer ND-1000 (Nanodrop), ultrafilter Amicon 3 in 10 kDa (Millipore).

## 3.2 Delo z DNA

### 3.2.1 Priprava mutant TcAtg4.2

Za pripravo N-končno skrajšanih mutant TcAtg4.2 ΔN18 (delecija aminokislin 1 do 18) in ΔN24 (delecija aminokislin 1 do 24) smo uporabili nukleotidno zaporedje TcAtg4.2, ki so ga objavili Alvarez in sod. [18].

Z verižno reakcijo s polimerazo (PCR - angl. *polymerase chain reaction*) smo namnožili nukleotidni zaporedji obeh skrajšanih konstruktov. Pomnoženi nukleotidni zaporedji skrajšanih vključkov ter plazmid pET28a+ (Novagen) smo tretirali z

restrikcijskima endonukleazama *Nde*I in *Bam*HI. Po restrikciji smo oba vključka ligirali v plazmid in ju izrazili v bakteriji *Escherichia coli*. Ustreznost nukleotidnih zaporedij smo preverili z analizo nukleotidnega zaporedja pri komercialnem ponudniku storitev Macrogen (Macrogen Europe, Amsterdam, Nizozemska).

Začetna oligonukleotida, ki se prilegata 5'-koncu DNA sta:

➔ Začetni oligonukleotid TcAtg4.2ΔN18:

*Nde*I
5'-AACATATGTTAGCGATTAAGGCTGTGT-3'

➔ Začetni oligonukleotid TcAtg4.2ΔN24:

*Nde*I
5'-TAACATATGAATTGTATGTTTCGCCTCCGG-3'

Začetni oligonukleotid, ki se prilega 3'-koncu DNA:

➔ Začetni oligonukleotid TcAtg4.2rev:

*Bam*HI
5'-AAGGATCCTACTCCGCCACGTCC-3'

Za pripravo katalitične mutante TcAtg4.2 C91S, mutante z delecijo regulatorne zanke TcAtg4.2 dL (delecija aminokislin 245 do 248) ter mutant TcAtg4.2 W158A, G244H, S246D in S246P smo uporabili metodo QuikChange™ (Stratagene). Pri tej metodi smo uporabili dva mutagena začetna oligonukleotida (smiselnega in protismiselnega), ki se prilegata na isto mesto v kodirajoči regiji. S PCR reakcijo pomnožimo celoten plazmid, vključno s kodirajočo regijo. Po končani PCR reakciji reakcijsko mešanico tretiramo z restrikcijsko endonukleazo *Dpn*I. *Dpn*I razgradi le metilirano DNA, ki ne nosi mutacije.

Mutagena oligonukleotida za pripravo katalitične mutante TcAtg4.2 C91S:

➔ Smiselni oligonukleotid:
5'-ATCTCTTCTGGGGATCCATGATCCGGACAGG-3'

➔ Protismiselni oligonukleotid:
5'-CCTGTCCGGATCATGGATCCCCAGAAGAGAT-3'

Mutagena oligonukleotida za pripravo mutante z delecijo regulatorne zanke TcAtg4.2 dL (delecija aminokislin 245 do 258):

➔ Smiselni oligonukleotid:
5'-CTCGATAGGCATTCTTGGAGGTGCGTTATTCCTCTTT-3'

➔ Protismiselni oligonukleotid:
5'-AAAGAGGAATAACGCACCTCCAAGAATGCCTATCGAG-3'

Mutagena oligonukleotida za pripravo mutante TcAtg4.2 W158A:

➔ Smiselni oligonukleotid:
5'-GTTAACTGCGGTGAGGCGTTTGGGCCAACGCC-3'

➔ Protismiselni oligonukleotid:
5'-GGCGTTGGCCCAAACGCCTCACCGCAGTTAAC-3'

Mutagena oligonukleotida za pripravo mutante TcAtg4.2 G244H:

➔ Smiselni oligonukleotid:

5'-AGCTCGATAGGCATTCTTGGACACAAATCTCGCTCCGCGTTATTC-3'

➔ Protismiselni oligonukleotid:
5'-GAATAACGCGGAGCGAGATTTGTGTCCAAGAATGCCTATCGAGCT-3'

Mutagena oligonukleotida za pripravo mutante TcAtg4.2 S246D:

➔ Smiselni oligonukleotid:
5'-CTCGATAGGCATTCTTGGAGGTAAAGATCGCTCCGCGTTA-3'

➔ Protismiselni oligonukleotid:
5'-TAACGCGGAGCGATCTTTACCTCCAAGAATGCCTATCGAG-3'

Mutagena oligonukleotida za pripravo mutante TcAtg4.2 S246P:

➔ Smiselni oligonukleotid:
5'-CGATAGGCATTCTTGGAGGTAAACCGCGCTCCGCGTTA-3'

➔ Protismiselni oligonukleotid:
5'-tAACGCGGAGCGCGGTTTACCTCCAAGAATGCCTATCG-3'

### 3.2.2 Priprava mutant TcAtg8.2

Za pripravo C-končno skrajšanih mutant TcAtg8.1 ΔC8 (delecija aminokislin 116 do 124) in TcAtg8.2 ΔC14 (delecija aminokislin 125 do 139) smo uporabili nukleotidni zaporedji TcAtg8.1 in TcAtg8.2, ki so jih objavili Alvarez in sod. [18].

Z verižno reakcijo s polimerazo (PCR - angl. *polymerase chain reaction*) smo namnožili nukleotidni zaporedji obeh skrajšanih konstruktov. Pomnoženi nukleotidni zaporedji skrajšanih vključkov ter plazmid pET28a+ (Novagen) smo tretirali z restrikcijskima endonukleazama *Nde*I in *Bam*HI. Po restrikciji smo oba vključka ligirali v plazmid in ju izrazili v bakteriji *Escherichia coli*. Ustreznost nukleotidnih zaporedij smo preverili z analizo nukleotidnega zaporedja pri komercialnem ponudniku storitev Macrogen (Macrogen Europe, Amsterdam, Nizozemska).

Začetna oligonukleotida za pripravo TcAtg8.1 ΔC8 sta:

➔ Začetni oligonukleotid, ki se prilega na 5'-konec DNA:
*Nde*I
5'-ACGTCATATGGCGCCAAAGAAATTGG-3'

➔ Začetni oligonukleotid, ki se prilega na 3'-konec DNA:
*Bam*HI
5'-ACGTGGATCCTCAACCCGAGTACTTTATGTA-3'

Začetna oligonukleotida za pripravo TcAtg8.2 ΔC14 sta:

➔ Začetni oligonukleotid, ki se prilega na 5'-konec DNA:
*Nde*I
5'-ACGTCATATGGCACGCAAATATCGCTAC-3'

➔ Začetni oligonukleotid, ki se prilega na 3'-konec DNA:
*Bam*HI
5'-ACGTGGATCCTCAAATGCTGTATGTCATGTA-3'

Za pripravo mutant TcAtg8.2 S128G, A129H, F130S in G131A smo uporabili metodo QuikChange™ (Stratagene). Pri tej metodi smo uporabili dva mutagena začetna oligonukleotida (smiselnega in protismiselnega), ki se prilegata na isto mesto v kodirajoči regiji. S PCR reakcijo pomnožimo celoten plazmid, vključno s kodirajočo regijo. Po končani PCR reakciji reakcijsko mešanico tretiramo z restrikcijsko endonukleazo *Dpn*I. *Dpn*I razgradi le metilirano DNA, ki ne nosi mutacije.

Mutagena oligonukleotida za pripravo katalitične mutante TcAtg8.2 S128G:
- ➔ Smiselni oligonukleotid:
  5'-GACATACAGCATTGAGGGCGCCTTTGGCGGT-3'
- ➔ Protismiselni oligonukleotid:
  5'-ACCGCCAAAGGCGCCCTCAATGCTGTATGTC-3'

Mutagena oligonukleotida za pripravo katalitične mutante TcAtg8.2 A129H:
- ➔ Smiselni oligonukleotid:
  5'-TACAGCATTGAGAGCCACTTTGGCGGTGCGGC-3'
- ➔ Protismiselni oligonukleotid:
  5'-GCCGCACCGCCAAAGTGGCTCTCAATGCTGTA-3'

Mutagena oligonukleotida za pripravo katalitične mutante TcAtg8.2 F130S:
- ➔ Smiselni oligonukleotid:
  5'-CAGCATTGAGAGCGCCTCTGGCGGTGC-3'
- ➔ Protismiselni oligonukleotid:
  5'-GCACCGCCAGAGGCGCTCTCAATGCTG-3'

Mutagena oligonukleotida za pripravo katalitične mutante TcAtg8.2 G131A:
- ➔ Smiselni oligonukleotid:
  5'-GAGCGCCTTTGCCGGTGCGGCTG-3'
- ➔ Protismiselni oligonukleotid:
  5'-CAGCCGCACCGGCAAAGGCGCTC-3'

## 3.3 Delo z rekombinantnimi proteini

### *3.3.1* Izražanje in izolacija rekombinantnih proteinov v bakteriji *Escherichia coli*

Za izražanje vseh rekombinantnih proteinov smo uporabili bakterijski sev *E. coli* BL21[DE3] (Novagen). Izražanje vseh konstruktov TcAtg8.1 in TcAtg8.2 smo sprožili z dodatkom 0.5 mM IPTG in bakterijsko kulturo inkubirali 4 h pri 28 °C. Izražanje HsAtg4B in vseh konstruktov TcAtg4.2 smo sprožili z dodatkom 0,5 mM IPTG ter bakterijsko kulturo inkubirali 6 h pri 25 °C.

Vse rekombinantne proteine smo izrazili v fuziji s histidinskim priveskom, ki omogoča učinkovito čiščenje rekombinantnih proteinov na $Ni^{2+}$-NTA afinitetni kromatografiji. DeSUMOilirajoče (SENP-e) in deubikvitinirajoče (DUB-e) encime smo izrazili in očistili po že objavljenem protokolu [133,134]. Čistost in relativno molekulsko maso očiščenih rekombinantnih proteinov smo preverili z uporabo poliakrilamidne gelske elektroforeze v prisotnosti NaDS (NaDS-PAGE).

### 3.3.2 Cirkularni dikroizem (CD) spektroskopija

CD spektre smo merili na Aviv model 62 ADS CD spektrometru (Aviv Biomedical, Lakewood Township NJ, USA). Za merjenje daljnega in bližnjega UV CD spektra smo uporabili 0,1 cm in 1 cm celice ter širine pasov 1 nm in 0,5 nm pri 25 °C. Podatke smo odčitavali pri vseh valovnih dolžinah v korakih po 1 nm. Za merjenje daljnega-UV CD spektra (250-195 nm) smo uporabili proteinske koncentracije med $A_{280}$=0,1 in $A_{280}$=0,2, za merjenje bližnjega-CD spektra (320-250 nm) pa med $A_{280}$=1,1 do $A_{280}$=1,6. Izmerjene eliptične vrednosti smo preračunali v povprečno eliptičnost [Q]MRW (deg $cm^2$/dmol) z enačbo

$$[\theta](MRW) = \frac{\theta \times M(MRW)}{10 \times c \times l}$$

kjer je MRW povprečna molska masa aminokislinskega preostanka ( g $mol^{-1}$) (molska masa proteina deljena s številom aminokislin, ki sestavljajo protein), θ je merjena eliptičnost v mili stopinjah (mdeg; angl. *milidegree*), c je proteinska koncentracija (mg $ml^{-1}$), l je dolžina optične poti (cm).

### 3.3.3 Cepitve TcAtg8 s TcAtg4.2

Pri določanju kinetike cepitev naravnih substratov TcAtg8.1, TcAtg8.2 in njunih mutant smo uporabili 1-4 µg TcAtg8 in 0-150 ng TcAtg4.2. Reakcije so potekale v reakcijskem pufru (20 mM Tris-HCl pH 7,5, 150 mM NaCl, 5 mM DTT) s končnim volumnom 20 µl pri 37 °C in različnih časovnih intervalih. Reakcije smo prekinili z dodatkom 6 × nanašalnega pufra in inkubacijo vzorcev 5 min pri 100 °C. Za izračun katalitične učinkovitosti ($k_{cat}/K_{m)}$ TcAtg4.2 in njegovih mutant smo uporabili sledečo enačbo: ln 2/(t × $EC_{50}$). $EC_{50}$ je definiran kot koncentracija encima, potrebna za cepitev 50 % substrata [135].

### 3.3.4 Vpliv pH na aktivnost TcAtg4.2

Optimalni pH za TcAtg4.2 smo določili z inkubacijo 4 µM TcAtg4.2 v reakcijskem pufru, ki je vseboval 50 mM MES (pH 6,0 in 6,5), HEPES (pH 7,0 in 7,5), Tris-HCl (pH 8,0 in 8,5) ali Bis-tris propan (pH 9,0) ter 0,5 M $K_2HPO_4$, 5 mM DTT in 100 µM sintetični substrat Ac-ETFG-AFC. Končni volumen reakcijske mešanice je bil 100 µl.

Katalitično aktivnost TcAtg4.2 smo spremljali s fluorimetrom za mikrotitrske plošče (Safire, Tecan, Švica). Merili smo naraščanje fluorescence sproščenega AFC (7-amino-4-trifluorometil kumarin) fluorofora z vzbujanjem pri λ = 400 nm in emisiji pri λ = 505 nm. Meritve so potekale 30 min pri temperaturi 37 °C. Za izračun hitrosti razgradnje substrata smo uporabili linearni del progresijske krivulje.

### 3.3.5 Vpliv kozmotropnih soli na aktivnost TcAtg4.2

Kozmotropne ali Hofmeisterjeve soli so soli, ki lahko povzročijo izsoljevanje ali vsoljevanje proteinov v vodnem okolju. Glede na svojo ionsko jakost so razporejene v kationsko in anionsko Hofmeisterjevo vrsto:

Kationska Hofmeisterjeva vrsta: $NH_4^+ > K^+ > Na^+ > Li^+ > Mg^{2+} > Ca^{2+}$ > gvanidinij

Anionska Hofmeisterjeva vrsta: F- ≈$SO_4^{2-} > HPO_4^{2-}$ > acetat > $Cl^- > NO_3^- > Br^- > ClO_3^-$ >

$I^- > ClO_4^- > SCN^-$

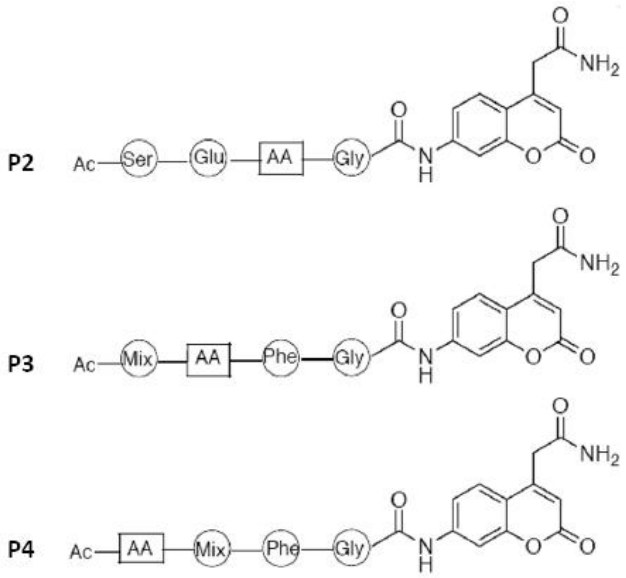
Točen mehanizem delovanja kozmotropnih soli ni povsem razjasnjen. Predvideva se, da vplivajo na stabilizacijo in urejenost vodnih molekul s preferenčnimi interakcijami voda – voda, zaradi česar pride do stabilizacije intramolekularnih interakcij v proteinih ali pa da vplivajo na specifične interakcije med ioni in proteini in/ali med ioni in vodnimi molekulami, ki so v direktnem kontaktu s površino proteinov ter s preurejanjem vode vplivajo na stabilizacijo proteinov [136,137].

Optimalno kozmotropno sol za TcAtg4.2 smo določili z inkubacijo 4 µM TcAtg4.2 v reakcijskem pufru, ki je vseboval 50 mM Tris-HCl pH 8,0, 5 mM DTT, 100 µM Ac-ETFG-AFC ter različne kozmotropne soli s končno koncentracijo 1 M. Končni volumen reakcijske mešanice je bil 100 µl. Spremembe katalitične aktivnosti TcAtg4.2 smo spremljali s fluorimetrom za mikrotitrske plošče (Safire, Tecan, Švica). Merili smo naraščanje fluorescence sproščenega AFC (7-amino-4-trifluorometil kumarin) fluorofora z vzbujanjem pri $\lambda$ = 400 nm in emisiji pri $\lambda$ = 505 nm. Meritve so potekale 30 min pri temperaturi 37 °C. Za izračun hitrosti razgradnje substrata smo uporabili linearni del progresijske krivulje.

### 3.3.6 Določanje substratne specifičnosti TcAtg4.2 z uporabo fluorogene kombinatorne tetrapeptidne knjižnice

S pomočjo fluorogene kombinatorne tetrapeptidne knjižnice smo določili preferenčne aminokislinske preostanke za TcAtg4.2 na pozicijah P2, P3 in P4. Kombinatorno knjižnico sestavljajo tri podknjižnice: P2, P3 in P4. Vsaka omogoča identifikacijo preferenčnih aminokislinskih preostankov na določeni poziciji, neodvisno od ostalih aminokislinskih preostankov v tetrapeptidu. Kot so dokazali že Alvarez in sod., je na poziciji P1 nujen glicin, zato so vsi substrati v kombinatorni knjižnici imeli na poziciji P1 fiksiran glicin [18].

V podknjižnici P2 poleg 19 L-aminokislinskih preostankov najdemo še 3 nenaravne aminokislinske preostanke, in sicer dva analoga fenilalanina homofenilalanin (hPhe) in cikloheksilalanin (Cha) ter analog levcina nor-levcin (O). Podknjižnici P3 in P4 so sestavljali izključno naravni aminokislinski preostanki (Slika 11).



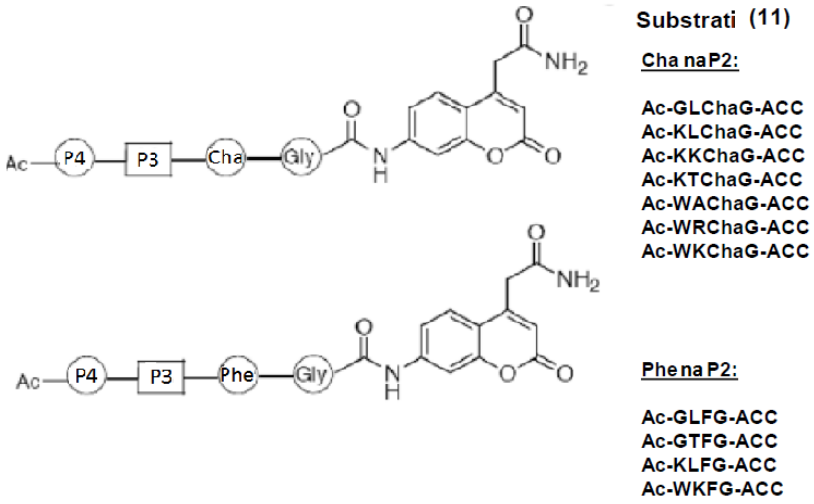

Slika 11: *Zgradba fluorogene kombinatorne tetrapeptidne knjižnice*. Fluorogena kombinatorna tetrapeptidna knjižnica je sestavljena iz treh podknjižnic: P2, P3 in P4. Legenda: Mix – izokinetična mešanica vseh naravnih aminokislinskih preostankov, AA – preučevani aminokislinski preostanki na želeni poziciji (P2, P3 oz. P4), tričrkovna oznaka aminokislin – fiksirani aminokislinski preostanki.

Pri vseh reakcijah določanja substratne specifičnosti TcAtg4.2 smo 4 μM encima predinkubirali v reakcijskem pufru (25 mM Tris-HCl pH 8,0, 0,5 M $K_2HPO_4$, 5 mM DTT) 10 min pri 37 °C. Nato smo po 100 μl reakcijske mešanice z encimom prenesli v luknjice na mikrotitrski plošči s 96 luknjicami, ki so že vsebovale sintetične tetrapeptidne substrate, katerih končna koncentracija je bila 250 μM. Tetrapeptidni substrati iz kombinatorne knjižnice vsebujejo ACC (7-amino-4-karbamoilmetil kumarin) fluorofor, ki po cepitvi začne oddajati fluorescenčni signal, ki ga merimo pri vzbujanju pri λ = 355 nm in emisiji pri λ = 460 nm. Kinetika sproščanja fluorofora omogoča identifikacijo optimalnih preferenčnih aminokislinskih preostankov za vsako vezavno mesto v encimu. Sproščanje ACC fluorofora smo s fluorimetrom za mikrotitrske plošče (Safire, Tecan, Švica) kontinuirno merili 30 min pri 37 °C. V vsaki podknjižnici smo določili najboljši substrat in ga umerili na 100 % ter skladno z njim normirali tudi vse ostale substrate v vsaki podknjižnici. Vsi poskusi so bili ponovljeni vsaj trikrat. Razlike med posameznimi meritvami so bile v vseh primerih manjše od 10 %. Za izračun katalitične učinkovitosti TcAtg4.2 za individualne substrate smo uporabili enačbo: $k_{cat}/K_m$ = naklon/E, kjer je E definiran kot koncentracija encima.

### 3.3.7 Iskanje specifičnih substratov za TcAtg4.2

Pri določanju preferenčnih aminokislinskih preostankov za ortologa Atg4, *T. cruzi* Atg4.2 in človeški Atg4B [135], na pozicijah P2, P3 in P4 je bila uporabljena ista fluorogena tetrapeptidna kombinatorna knjižnica (PS-SCL).
Primerjava substratnih specifičnosti obeh ortologov je razkrila razlike v preferencah do aminokislinskih preostankov na vseh treh pozicijah (P2, P3 in P4). Na osnovi teh razlik smo sintetizirali novo knjižnico z enajstimi tetrapeptidnimi substrati. Sedem substratov ima na poziciji P2 cikloheksilalanin (Cha), ki naj bi ga prepoznaval le TcAtg4.2. Preostale štiri substrate, ki imajo na poziciji P2 Phe, smo uporabili za kontrolo katalitične aktivnosti in selektivnosti HsAtg4B. Nadalje smo na podlagi rezultatov kombinatorne

knjižnice v osmih substratih na poziciji P4 uporabili dva optimalna aminokislinska preostanka za TcAtg4.2, Lys oz. Trp. Prav tako smo sintetizirali še Ac-GLChaG-ACC, ki ima na poziciji P4 Gly in na P3 Leu. Oba sta neoptimalna aminokislinska preostanka za TcAtg4.2. Pri določanju selektivnosti HsAtg4B se je Leu na poziciji P3 izkazal za optimalnega. Ker nas je zanimal tudi njegov vpliv na katalitični aktivnosti TcAtg4.2 in tudi HsAtg4B, smo sintetizirali še Ac-KLChaG-ACC in Ac-KLFG-ACC. Na koncu smo za primerjavo selektivnosti TcAtg4.2 in HsAtg4B sintetizirali še za HsAtg4B optimalna substrata Ac-GLFG-ACC in Ac-GTFG-ACC [135] (Slika 12). Z novo knjižnico smo lahko določili optimalen sintetični tetrapeptidni substrat za TcAtg4.2.




Slika 12: *Zgradba optimizirane substratne knjižnice.* Optimizirana substratna knjižnica je sestavljena iz enajstih substratov.

Pri reakcijah s TcAtg4.2 smo uporabili 4 µM encim in ga predinkubirali v reakcijskem pufru (25 mM Tris-HCl pH7,5, 0,5 M $K_2HPO_4$, 5 mM DTT) 10 min pri 37 °C. Pri reakcijah s HsAtg4B smo uporabili 4 µM encim in ga predinkubirali v reakcijskem pufru (25 mM Tris-HCl pH7,5, 0,5 M $Na_3C_3H_5O(COO)_3$, 5 mM DTT) 10 min pri 37 °C. Nato smo po 100 µl reakcijske mešanice z encimoma prenesli v luknjice na mikrotitrski plošči s 96 luknjicami, ki so že vsebovale novo sintetizirane sintetične tetrapeptidne substrate, katerih končna koncentracija je bila 250 µM. Sproščanje ACC fluorofora smo s fluorimetrom za mikrotitrske plošče (Safire, Tecan, Švica) kontinuirno merili pri 37 °C in vzbujanju pri $\lambda$ = 355 nm ter emisiji pri $\lambda$ = 460 nm 30 min. Na osnovi relativnih RFU smo za vsak encim posebej določili najboljši substrat in ga umerili na 100 % ter skladno z njim normirali tudi vse ostale substrate. Vsi poskusi so bili ponovljeni vsaj trikrat.

### 3.3.8 Določanje selektivnosti optimalnih substratov za TcAtg4.2

Pri testu selektivnosti smo tetrapeptidne fluorogene substrate inkubirali v prisotnosti človeških citosolnih desumoilirajočih encimov SENP1 in -2 in deubikvitinirajočega encima UCH-L3 ter lizosomskih cisteinskih katepsinov B, K, L in S.

Katalitične aktivnosti rekombinantnih proteinov SENP1, -2 in UCH-L3 smo potrdili s cepitvami Ac-QTGG-ACC za oba SENP-a ter Ac-LRGG-ACC za UCH-L3, kot so opisali Drag in sod. [133,134]. Sproščanje ACC fluorofora smo s fluorimetrom za mikrotitrske plošče (Safire, Tecan, Švica) kontinuirno merili pri 37 °C in vzbujanju pri $\lambda$ = 355 nm ter emisiji pri $\lambda$ = 460 nm 30 min. Katalitične aktivnosti cisteinskih katepsinov B, K, L in S smo potrdili s cepitvami rekombinantnih homologov Atg8 človeškega GABARAPL2/GATE-16, TcAtg8.1 in TcAtg8.2 ter sintetičnih fluorogenih substratov z-

FR-AMC in z-FVR-AMC v pufru BANA (15 mM $Na_2HPO_4$, 88 mM $KH_2PO_4$, pH 6,0, 1 mM EDTA, 0,1 % PEG-6000, 5 mM DTT). 2 µg rekombinantnih homologov Atg8 smo inkubirali s 40 ng katepsinov B, K, L in S 1 h pri 37 °C. Reakcijo smo prekinili z dodatkom 6 × nanašalnega pufra in inkubacijo vzorcev 5 min pri 100 °C. Cepitve rekombinantnih homologov Atg8 smo analizirali na NaDS-PAGE. Cepitve fluorogenih substratov (sproščanje AMC fluorofora) smo spremljali 15 min pri 37 °C pri vzbujanju pri $\lambda$ = 370 nm ter emisiji pri $\lambda$ = 460 nm. Končni koncentraciji katepsinov in substratov sta bili 5-20 nM ter 100 µM. Vsi poskusi so bili ponovljeni vsaj trikrat. Za določanje selektivnosti optimalnih substratov za TcAtg4.2 smo sintetizirali nove fluorogene substrate z želenimi tetrapeptidnimi zaporedji in AFC fluoroforom, ki v primerjavi s ACC fluoroforom daje višje signale. Tako ob uporabi AFC reporterske skupine vidimo tudi zelo šibke cepitve, katerih z uporabo ACC fluorofora ne bi zaznali.

### 3.3.9 Inhibicija s pametno aktivnostno sondo MP001

Na podlagi rezultatov, dobljenih z določanjem substratne specifičnosti TcAtg4.2 in testi selektivnosti optimalnih substratov za TcAtg4.2 na človeške proteine HsAtg4B, SENP1, SENP2, UCH-L3 ter cisteinske katepsine B, K, L in S, smo izbrali selektivnejši substrat Ac-KKChaG-AFC ter na podlagi njegove strukture sintetizirali aktivnostno sondo (ABP) MP001. Na C-končni del tetrapeptida smo dodali nukleofilni metilni ester, ki se ob hidrolazi peptidne vezi kovalentno poveže s cisteinom v aktivnem mestu encima ter tako inhibira njegovo delovanje. Na N-koncu tetrapeptida pa smo preko linkerja pripeli biotin, ki omogoča izolacijo aktivnostne sonde ter njenih vezavnih partnerjev iz kompleksnih proteinskih vzorcev ter njihovo identifikacijo.

Pri poskusih inhibicije smo uporabili enake koncentracije encimov in zanje optimalne reakcijske pufre v prisotnosti DTT kakor pri testih encimske aktivnosti, opisanih v poglavju 3.3.7. Encime in različne koncentracije inhibitorja smo v 50 µl reakcijske mešanice predinkubirali 10 min pri 37 °C. Nato smo po 50 µl reakcijske mešanice s substratom prenesli v luknjice na mikrotitrski plošči s 96 luknjicami, ki so že vsebovale encime in pametno aktivnostno sondo MP001. Sproščanje fluorofora smo s fluorimetrom za mikrotitrske plošče (Safire, Tecan, Švica) kontinuirno merili pri 37 °C pri že opisanih valovnih dolžinah vzbujanja in emisije. Za lažjo določitev $IC_{50}$ smo rezultate podali tudi v grafih, ki prikazujejo hitrost cepitve sintetičnega substrata v odvisnosti od naravnega logaritma koncentracije pametne aktivnostne sonde (v g/mol).

## 3.4 Delo z mišjimi primarnimi tumorskimi celicami MMTV-PyMT

### 3.4.1 Priprava celičnih lizatov za imunološko detekcijo LC3

Mišje primarne tumorske celice divjega tipa (*PyMT;WT*) in celice z izbitim genom za *stefin B* (*PyMT;StfB-/-*) smo gojili v 10 cm petrijevki in gojišču DMEM z dodatkom 10 % FBS (fetalnega govejega seruma), 1 % glutaMAX$^{TM}$, 1 % penicilin/steptomicin pri 37 °C in 5 % $CO_2$. Ko so dosegle konfluentnost ~ 90 %, smo jih precepili v plošče z 12 luknjicami in jih gojili, dokler niso prerasle ~ 95 % površine. Za imunološko detekcijo LC3 smo celice gojili pri normalnih pogojih v odsotnosti ali prisotnosti 100 µM klorokina ali smo jih stradali v pufru HBSS (Thermo Fisher Scientific Inc.) v odsotnosti ali prisotnosti 100 µM klorokina 2,5 uri. Totalne proteinske lizate smo pripravili tako, da smo celice sprali s PBS pufrom in jih lizirali z dodatkom pufra RIPA (50 mM Tris-HCl, 150 mM NaCl, 1 % deoksiholat, 5 mM EDTA, 1 % Triton X-100, pH 7,4). S strgalom

smo jih odlepili s površine, jih prenesli v epice in na ledu inkubirali 30 min. Netopne komponente smo odstranili s centrifugiranjem pri 10000 ×g 20 min in 4 °C.

### 3.4.2 Prenos proteinov po Westernu

Proteine v totalnih proteinskih vzorcih smo po velikosti ločili na 12,5 % NaDS-PAGE ter jih s pomočjo električnega toka prenesli na nitrocelulozno membrano. Za prenos smo uporabili prenašalni pufer (192 mM glicin, 25 mM Tris, 20 % (v/v) metanol). Po prenosu proteinov smo nezasedena mesta na nitrocelulozni membrani blokirali z inkubacijo membrane v pufru TBS (pH 7,6), ki je vseboval 5 % (w/v) dehidrogenirano mleko. Sledila je 1,5 h inkubacija membrane v raztopini, ki je vsebovala primarna protitelesa, ki ji je po spiranju sledila inkubacija membrane v raztopini s sekundarnimi protitelesi, konjugiranimi s hrenovo peroksidazo. Za detekcijo proteinskih lis na nitrocelulozni membrani smo uporabili reagent ECL, skladno z navodili proizvajalca. Luminescenčni signal smo vizualizirali z uporabo naprave za razvijanje filmov Konica-Minolta SRX-101A (Marunouchi, Chiyoda, Japonska).

### 3.4.3 Pretočna citometrija

Za analizo vpliva regulacije avtofagije na preživetje tumorskih celic divjega tipa (*PyMT;WT*) in celic z izbitim genom za *stefin B* (*PyMT;StfB-/-*) smo celice 24 h gojili pri normalnih pogojih, v pogojih stradanja ter v prisotnosti obeh regulatorjev avtofagije v prisotnosti inhibitorja avtofagije klorokina oz. induktorja avtofagije rapamicina. Po končani inkubaciji smo po navodilih proizvajalca celice označili z reagentom Annexin V-PEAAD (BD Pharmigen) ter analizirali na pretočnem citometru FACScalibur (Becton Dickinson).

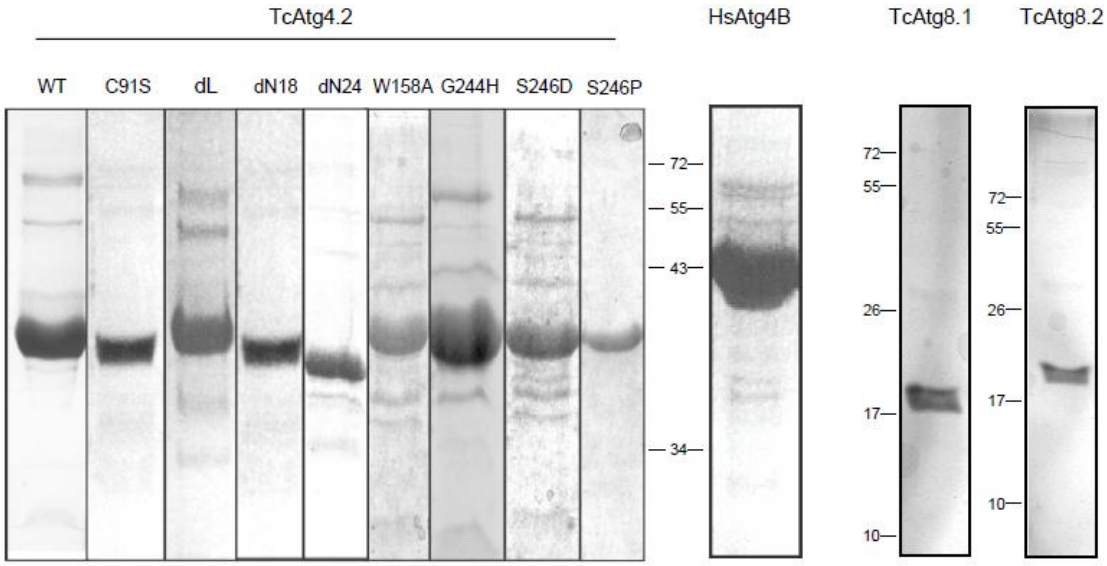
### 3.4.4 Statistične analize

Vsi kvantitativni rezultati so predstavljeni kot srednje vrednosti s standardno napako. Grafi predstavljajo srednje vrednosti vsaj treh med seboj neodvisnih poskusov. Za ugotavljanje statističnih razlik smo uporabili Student's *t* test. Kot statistično značilno razliko smo upoštevali vrednost $p < 0,05$.

# 4 Rezultati

## 4.1 Analiza očiščenih rekombinantnih proteinov

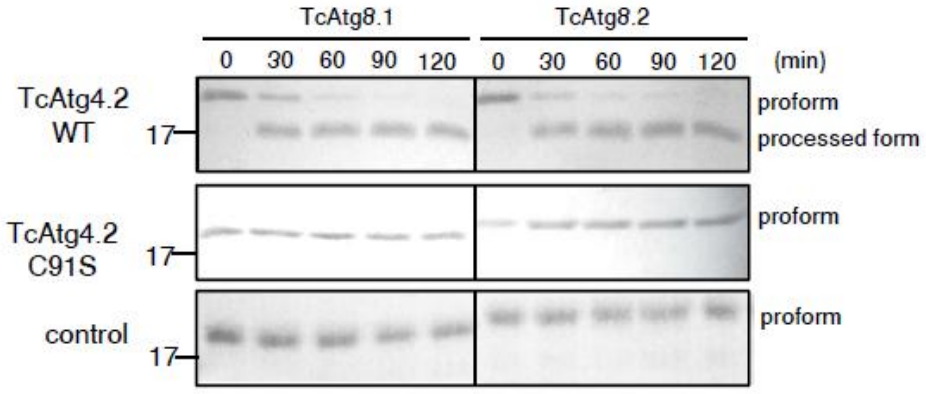
Postopki izražanja in čiščenja vseh rekombinantnih proteinov so podrobneje opisani v poglavju 3.3.1. Po končanem čiščenju smo čistost in relativno molekulsko maso očiščenih rekombinantnih proteinov preverili s poliakrilamidno gelsko elektroforezo v prisotnosti Na (NaDS-PAGE) (Slika 13). Rekombinantni proteini so dobro očiščeni in so primerni za uporabo v nadaljnih eksperimentih. Prav tako relativne molekulske mase očiščenjih rekombinantnih proteinov ustrezajo teoretičnim molekulskim masam.




Slika 13: *Poliakrilamidna gelska elektroforeza v prisotnosti NaDS (12,5 % gel) očiščenih rekombinantnih proteinov*. Relativne molekulske mase očiščenih rekombinantnih proteinov ustrezajo izračunanim relativnim molekulskim masam rekombinantnih proteinov, izraženih v fuziji s histidinskim priveskom.

## 4.2 Cys 91 je odgovoren za katalitično aktivnost TcAtg4.2

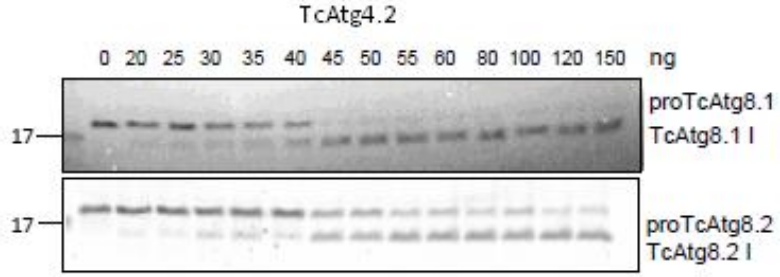
S prileganjem in analizo aminokislinskih zaporedij homologov Atg4 smo predpostavili, da je cistein 91 v TcAtg4.2 odgovoren za katalitično aktivnost encima. Za potrditev hipoteze smo cistein 91 mutirali v serin. Po uspešni izolaciji rekombinantnih proteinov smo s cepitvijo obeh naravnih substratov TcAtg8.1 in TcAtg8.2 smo preverili encimsko aktivnost TcAtg4.2 divjega tipa (WT) in mutante TcAtg4.2 C91S. Ugotovili smo, da mutanta TcAtg4.2 C91S ni bila zmožna procesirati substratov, kar potrjuje hipotezo, da je Cys 91 zares katalitični Cys. V kontrolnem poskusu smo naravna substrata inkubirali v reakcijskem pufru v odsotnosti TcAtg4.2 (Slika 14).




Slika 14: *Poliakrilamidna gelska elektroforeza v prisotnosti NaDS (12,5 %) cepitev TcAtg8.1 in TcAtg8.2 s TcAtg4.2 divjega tipa (WT) in katalitično mutanto TcAtg4.2 C91S.* 50 ng TcAtg4.2 WT oz. TcAtg4.2 C9S in 2 µg TcAtg8.1 oz. TcAtg8.2 smo inkubirali v reakcijskem pufru (20 mM Tris-HCl pH 7,5, 150 mM NaCl, 5 mM DTT) pri 37 °C in stresanju 300 obr./min. Vzorčenje je potekalo v časovnih presledkih 0 min, 30 min, 60 min, 90 min in 120 min. Reakcijo smo prekinili z dodatkom 6 × pufra SDS in inkubacijo alikvotov pri 100 °C 5 min.

## 4.3 TcAtg4.2 cepi substrat TcAtg8.1 hitreje kakor TcAtg8.2

Za izračun encimske učinkovitosti ($k_{cat}/K_m$) TcAtg4.2 WT smo oba substrata (2 µg) inkubirali z različnimi količinami encima (0–150 ng) 1 h pri 37 °C. $k_{cat}/K_m$ smo izračunali z uporabo enačbe: $k_{cat}/K_m = \ln 2/(t \times EC_{50})$, kjer je $EC_{50}$ definiran kot koncentracija encima, potrebna za cepitev 50 % substrata. Ocena encimske učinkovitosti $k_{cat}/K_m$ TcAtg4.2 za TcAtg8.1 je bila $3{,}7 \times 10^3$ $M^{-1}$ $s^{-1}$ in za TcAtg8.2 $3{,}4 \times 10^3$ $M^{-1}$ $s^{-1}$ (Slika 15).

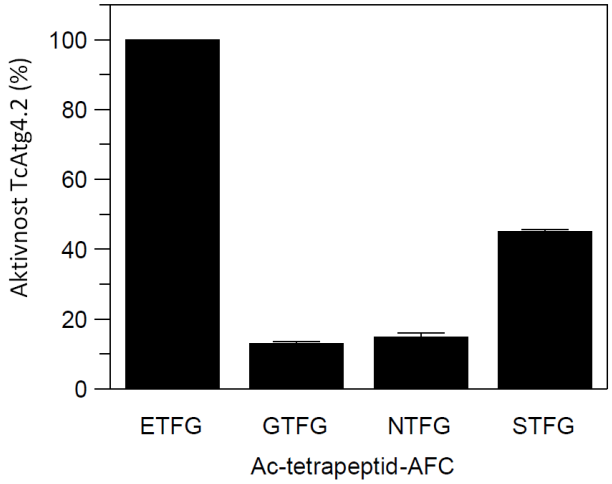



Slika 15:*Poliakrilamidna gelska elektroforeza v prisotnosti NaDS (12,5 %) kinetike cepitev TcAtg8.1 in TcAtg8.2 s TcAtg4.2.* 0-150 ng TcAtg4.2 in 2 µg TcAtg8.1 oz. TcAtg8.2 smo inkubirali v reakcijskem pufru (20 mM Tris-HCl pH 7,5, 150 mM NaCl, 5 mM DTT) pri 37 °C in stresanju 300 obr./min. Reakcijo smo po 60 min prekinili z dodatkom 6 × pufra SDS in inkubacijo vzorcev pri 100 °C 5 min.

## 4.4 Biokemijska karakterizacija TcAtg4.2

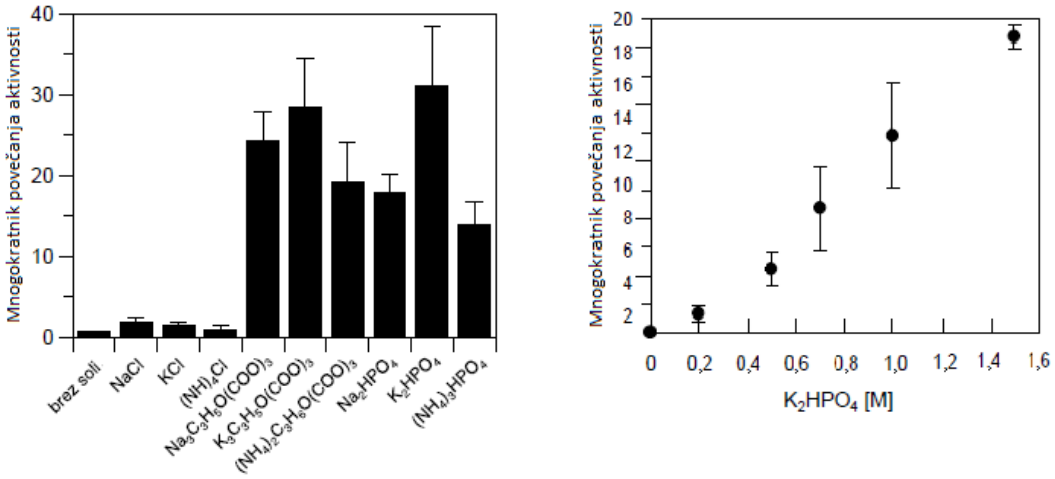
Prednost uporabe sintetičnih fluorogenih substratov pred naravnimi substrati je direktno in hitrejše spremljanje vpliva različnih dejavnikov na proteolitične aktivnosti encimov. Tako kot za veliko število proteaz je bilo tudi za človeški Atg4B pokazano, da lahko cepi male sintetične fluorogene substrate. Zaradi evolucijske ohranjenosti mehanizma delovanja avtofaginov nas je zanimalo, ali jih lahko procesira tudi TcAtg4.2. Uporabili smo štiri fluorogene tetrapeptidne substrate, ki so bili uporabljeni že pri

biokemijski karakterizaciji človeškega Atg4B. Ac-GTFG-AFC in AC-STFG-AFC izhajata iz PS-SCL, narejene na človeškem HsAtg4B, Ac-ETFG-AFC in Ac-NTFG-AFC pa nosita aminokislinski zaporedji človeških homologov Atg8, LC3 in GATE-16 [135]. TcAtg4.2 je procesiral Ac-ETFG-AFC približno 7-, 6- in 2-krat hitreje kakor Ac-STFG-AFC, Ac-NTFG-AFC in Ac-GTFG-AFC (Slika 16), vendar vse z zelo šibko katalitično aktivnostjo. Ac-ETFG-AFC, ki se je izkazal za najboljši substrat, smo uporabili v nadaljnjih študijah biokemijske karakterizacije TcAtg4.2.



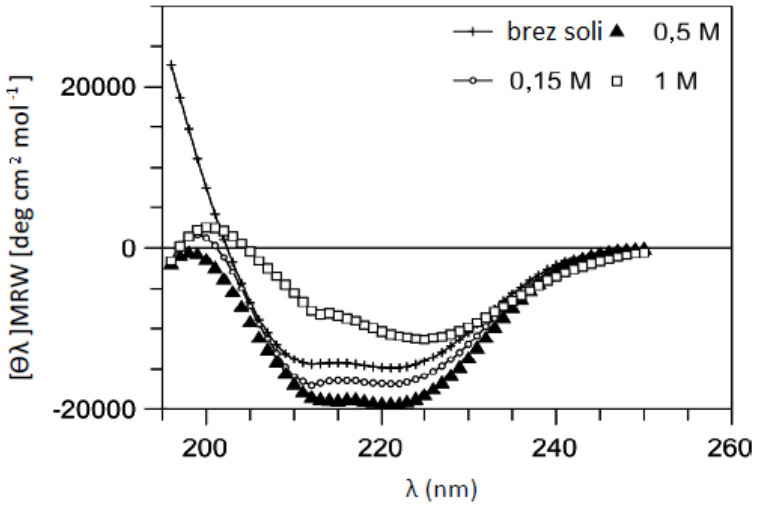

Slika 16: *Vpliv aminokislinskega zaporedja na hitrost cepitve tetrapeptidnih fluorogenih substratov.* 4 µg TcAtg4.2 in 100 µM tetrapeptidnih fluorogenih substratov (Ac-ETFG-AFC, Ac-GTFG-AFC, AC-NTFG-AFC in Ac-STFG-AFC) smo inkubirali v 100 µl reakcijskega pufra (20 mM Tris-HCl pH 7,5, 150 mM NaCl, 5 mM DTT). Cepitve fluorogenih substratov smo spremljali na fluorimetru za mikrotitrske plošče (Safire, Tecan) pri vzbujanju λ = 400 nm in emisiji λ = 505 nm pri 37 °C 30 min.

Šibko afiniteto TcAtg4.2 do malih fluorogenih tetrapeptidnih substratov smo uspešno izboljšali z uporabo kozmotropnih soli. Najvišjo encimsko aktivnost TcAtg4.2 smo zaznali v prisotnosti $K_2HPO_4$. Encimska aktivnost je naraščala sorazmerno z višanjem njegove koncentracije (Slika 17).



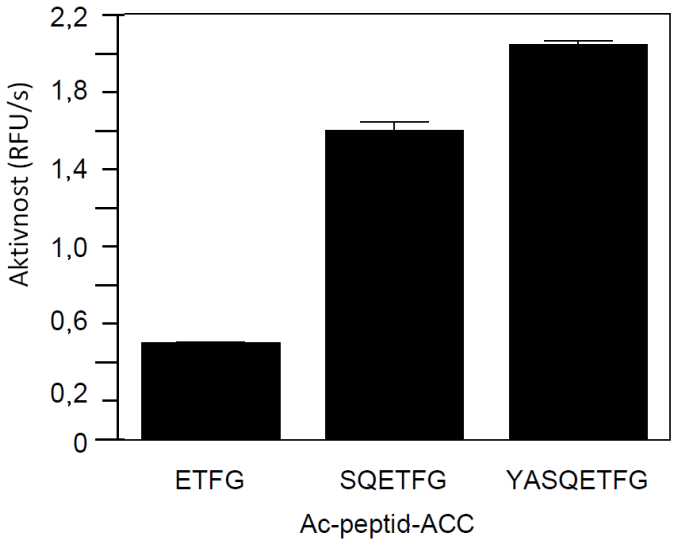
Slika 17: *Vpliv prisotnosti kozmotropnih soli na katalitično aktivnost TcAtg4.2.* Levo: 4 µg TcAtg4.2 in 100 µM Ac-ETFG-AFC smo inkubirali v 100 µl reakcijskega pufra (50 mM Tris-HCl pH 8,0, 1 M kozmotropna sol, 5 mM DTT). Desno: 4 µg TcAtg4.2 in 100 µM Ac-ETFG-AFC smo inkubirali v 100 µl reakcijskega pufra (50 mM Tris-HCl pH 8,0, 0–1,5 M $K_2HPO_4$, 5 mM DTT). Cepitev fluorogenega substrata smo spremljali na fluorimetru za mikrotitrske plošče (Safire, Tecan) pri vzbujanju λ = 400 nm in emisiji λ = 505 nm pri 37 °C 30 min.

CD spekter TcAtg4.2 v daljnem-UV območju je kazal karakteristično α/β sekundarno strukturo z minimumi pri 222, 217 in 208 nm. Analiza CD spektrov z dekonvolucijskim programom Dichroweb [138,139] je pokazala, da prisotnost kozmotropne soli $K_2HPO_4$ v koncentracijskem območju 0–0,5 M ni imela bistvenega vpliva na strukturo encima. Prisotnost 1 M $K_2HPO_4$ pa je povzročila znatno zmanjšanje α-helične strukture s ~ 60 % na ~ 40 % ter tudi β-ploskovne strukture s ~ 10 % na ~ 3 %. Prav tako se je encim začel obarjati, zaradi česar se je zmanjšala aktivna proteinska koncentracija vzorca, kar smo v daljnem-UV CD spektru videli kot zmanjšano eliptičnost vzorca (Slika 18).



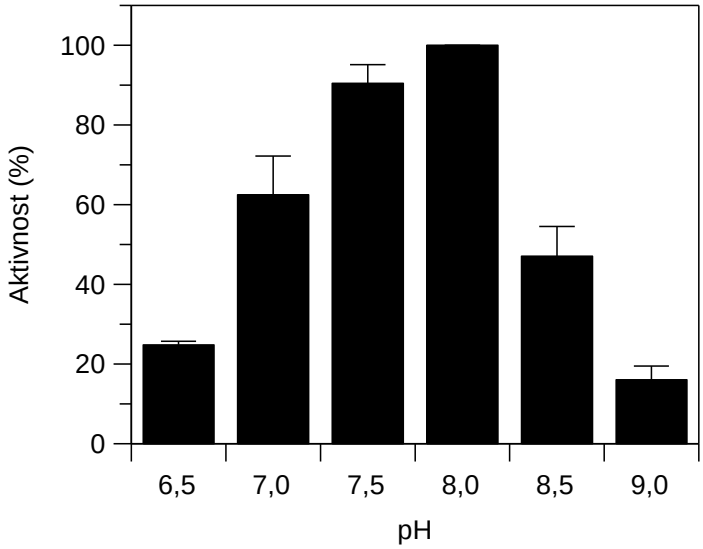

Slika 18: *Vpliv koncentracije $K_2HPO_4$ na urejenost sekundarne strukture TcAtg4.2.* Za merjenje daljnega-UV CD spektra (250–195 nm) smo uporabili proteinsko koncentracijo $A_{280}$ = 0,1. Podatke smo odčitavali v korakih po 1 nm. Izmerjene eliptične vrednosti smo preračunali s pomočjo enačbe, opisane v poglavju 3.3.2.

Poleg prisotnosti kozmotropov smo lahko katalitično aktivnost TcAtg4.2 izboljšali tudi z daljšanjem polipeptidne verige substratov (Slika 19).




Slika 19: *Vpliv dolžine polipeptidne verige na katalitično aktivnost TcAtg4.2*. 4 µg TcAtg4.2 in 100 µM fluorogene tetra-, heksa- in oktapeptide smo inkubirali v 100 µl reakcijskega pufra (50 mM Tris-HCl pH 8, 0,5 M $K_2HPO_4$, 5 mM DTT). Cepitve fluorogenih substratov smo spremljali na fluorimetru za mikrotitrske plošče (Safire, Tecan) pri vzbujanju λ = 355 nm in emisiji λ = 460 nm pri 37 °C 30 min.

Sledilo je določanje pH profila encimske aktivnosti TcAtg4.2. Encim je bil aktiven v pH območju od 6,5 do 9 s pH optimumom okoli 8, nakar je njegova katalitična aktivnost strmo padla (slika 21).

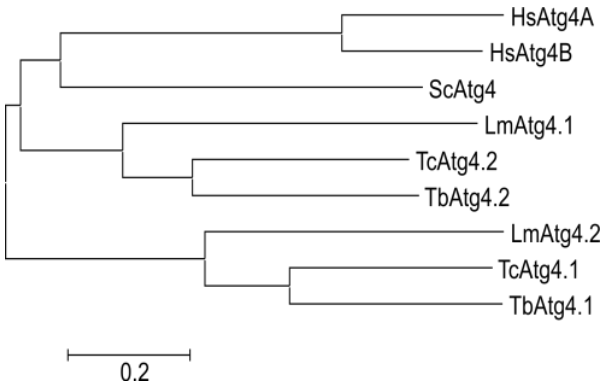



Slika 20: *pH profil encimske aktivnosti TcAtg4.2*. 4 µg TcAtg4.2 in 100 µM Ac-ETFG-AFC smo inkubirali v reakcijskih pufrih z različnimi pH (pH 6,5–9,0, 0,5 M $K_2HPO_4$, 5 mM DTT). Cepitev fluorogenega substrata smo spremljali na fluorimetru za mikrotitrske plošče (Safire, Tecan) pri vzbujanju λ = 400 nm in emisiji λ = 505 nm pri 37 °C 30 min.

## 4.5 Funkcijske študije TcAtg4.2

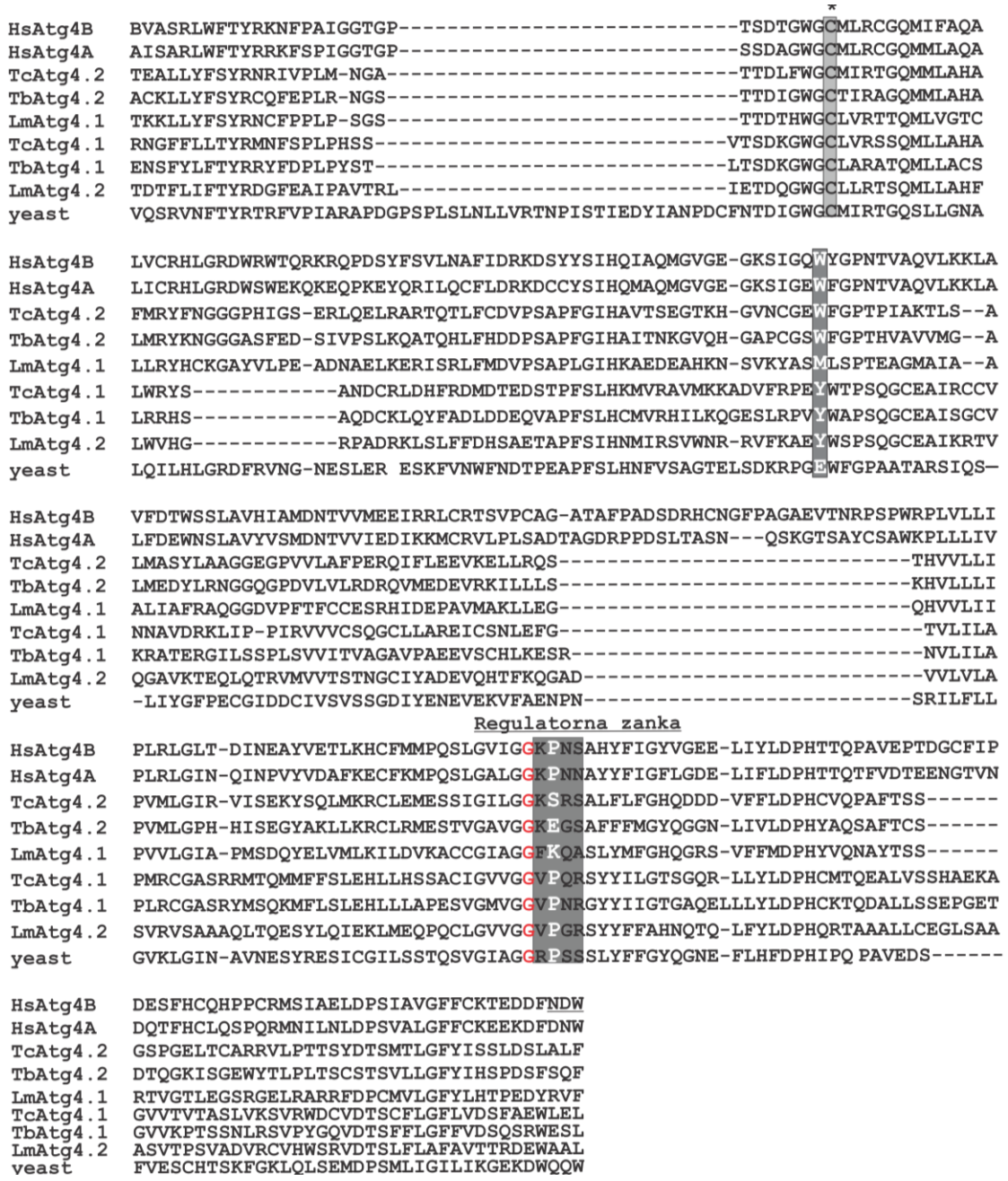
Za podrobnejše razumevanje molekularnega mehanizma substratne hidrolize TcAtg4.2 smo najprej preučili filogenetsko razmerje med Atg4 iz *Trypanosome cruzi* (TcAtg4.1 in TcAtg4.2) in štirimi Atg4 homologi iz človeka (HsAtg4A in HsAtg4B), kvasovke

*Saccharomyces cerevisiae* (ScAtg4) ter dveh kinetoplastidnih parazitov *Trypanosome brucei* (TbAtg4.1 in TbAtg4.2) in *Leishmanie major* (LmAtg4.1 in LmAtg4.2). S programom MEGA 6 smo skonstruirali filogenetsko drevo. V dendogramu je TcAtg4.2 razvrščen blizu TbAtg4.2 in LmAtg4.1, ki si s TcAtg4.2 delita 45 % in 34,5 % ohranjenost aminokislinskega zaporedja ter tako kot TcAtg4.2 oba nosita poglavitno endopeptidazno aktivnost v kinetoplastidnih parazitih (Slika 21).




Slika 21: *Dendogram homologov Atg4.* Za izračun evolucijske oddaljenosti med homologi Atg4 smo uporabili metodo združevanja sosedov. Uporabili smo privzete nastavitve programa MEGA6, ki so se v več študijah izkazale za najoptimalnejše.

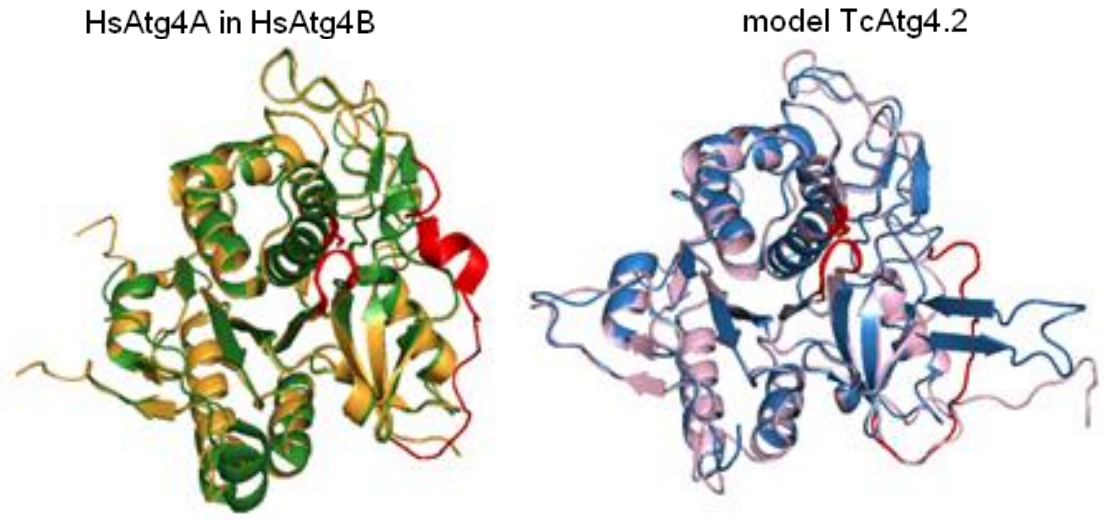
S človeškima HsAtg4A in HsAtg4B si TcAtg4.2 deli 21,3 % in 22,2 % ohranjenost aminokislinskega zaporedja, z višjim odstotkom ohranjenosti v regijah, ki so ključne za katalitično aktivnost avtofaginov (Slika 22).




Slika 22: *Poravnava aminokislinskih zaporedij katalitične domene homologov Atg4.* Prileganje aminokislinskih zaporedij katalitične domene človeških HsAtg4A (Genebank koda: NP_443168.2) in HsAtg4B (NM_013325), *T. cruzi* TcAtg4.1 (DQ768297.1) in TcAtg4.2 (DQ768298), *L major* LmAtg4.1(XM_001685663) in LmAtg4.2 (XM_001684564), *T. brucei* TbAtg4.1 (DQ768297.1) in TbAtg4.2 (XM_824593.1) ter kvasnega Atg4 (NP_014176.2). * – katalitični cisteinski preostanki, temno-siv okvirček – 4 aminokislinski preostanki, ki tvorijo regulatorno zanko, z belo označen S246 znotraj regulatorne zanke tvori van der Waalsove interakcije s Trp158 (z belo označen W v sivem okvirčku), rdeč Gly – omogoča fleksibilnost regulatorne zanke.

Za preučitev ohranjenosti mehanizma delovanja TcAtg4.2 in ostalih avtofaginov, predvsem s človeškim HsAtg4B, smo s pomočjo dveh programov za napovedovanje struktur proteinov, Swiss-Model (Biozentrum, University of Basel, Switzerland) [140] in RaptoX [141], pripravili modela strukture TcAtg4.2. Ker do danes ni rešena še nobena struktura avtofaginov iz družine kinetoplastidnih parazitov, smo za pripravo modelov

TcAtg4.2 uporabili matrici človeških HsAtg4A (koda PDB: 2p82) in HsAtg4B (koda PDB: 2d1i) (Slika 23).



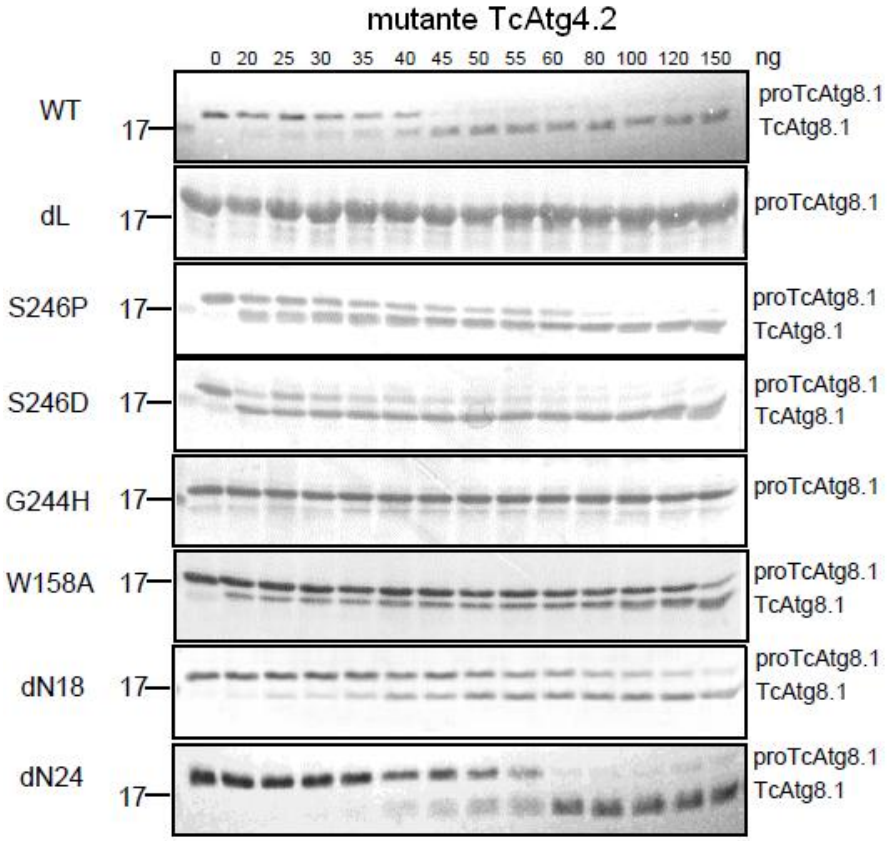

Slika 23: *Superpozicija struktur človeških avtofaginov HsAtg4A in HsAtg4B ter modelov struktur TcAtg4.2.* Modela strukture TcAtg4.2 sta narejena na osnovi človeških HsAtg4A (koda PDB: 2p82) in HsAtg4B (koda PDB: 2d1i). Levo: Superpozicija struktur človeškega HsAtg4A (zelena) in HsAtg4B (rumena). Desno: Superpozicija modelov strukture TcAtg4.2 narejenih s programoma za napovedovanje struktur Swiss-Model (modra) in RaptoX (roza). Slike so narejene v programu PyMOL, verzija 1.3r1 edu (Schrödinger, LLC, USA).

Na osnovi podrobnejše analize obeh modelov TcAtg4.2 in prileganj aminokislinskih zaporedij homologov Atg4 (Slika 22) smo pripravili mutante TcAtg4.2, s pomočjo katerih smo preučili funkcijsko ohranjenost mehanizma delovanja TcAtg4.2.

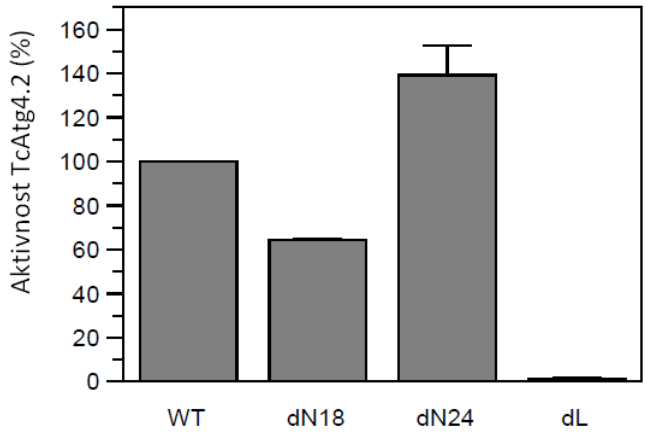
Najprej smo preučili vpliv regulatorne zanke. V človeškem Atg4B (HsAtg4B) jo sestavljajo aminokislinski preostanki 258-263 in je med homologi Atg4 dobro ohranjena. Pri HsAtg4B regulatorna zanka v neaktivni obliki prekriva režo aktivnega mesta s katalitičnim Cys 74 in tako preprečuje nespecifično hidrolizo. Zaprta konformacija regulatorne zanke, značilna za neaktivno obliko HsAtg4B, se vzdržuje s pomočjo van der Waalsovih interakcij med Pro 260, ki se nahaja na regulatorni zanki, in Trp 142, ki se nahaja na zanki med α-vijačnicama D in E. Ob vezavi substrata Phe 119 in Gly 120, ki se nahajata na C-koncu LC3, interagirata s stransko verigo Trp142 v HsAtg4B. Regulatorna zanka se odpre, C-končni del substratne molekule se usede v vezavna mesta v reži aktivnega mesta encima in poteče hidroliza peptidne vezi [51]. V TcAtg4.2 smo pripravili mutanto z delecijo regulatorne zanke TcAtg4.2 dL (delecija aminokislin 243 do 251). Delecija regulatorne zanke je kakor pri HsAtg4B tudi pri TcAtg4.2 povzročila izgubo katalitične aktivnosti encima na naravni kot tudi na sintetični tetrapeptidni substrat. Prav tako nas je zanimala vloga Pro 260 (Ser 246 v TcAtg4.2), ki se nahaja na regulatorni zanki. Najprej smo Ser 246 mutirali v Pro, ki je rahlo izboljšal katalitično aktivnost TcAtg4.2. Mutacija Ser 246 v Asp pa je katalitično aktivnost encima še dodatno izboljšala. Mutacija Ser 246 v Pro bi lahko spremenila konformacijo zanke in tako zmanjšala vpliv okoliških interakcij med stranskimi skupinami aminokislinskih preostankov in/ali zmanjšala jakost interakcij med Trp 142 in Pro 246. Katalitična aktivnost mutante TcAtg4.2 S246D pa se najverjetneje povečala zaradi odbojnih sil med dvema bližnjima negativnima nabojema, ki so se ustvarile med Asp 246 in Glu 141, ki se nahaja tik pred omenjenim Trp 142. V skladu z že objavljenimi rezultati smo pokazali, da kot Pro 260 v HsAtg4B tudi Ser 246 v TcAtg4.2 ni ključen za katalitično aktivnost encima [51].

Fleksibilnost regulatorne zanke ohranjata dva med vsemi homologi Atg4 ohranjena Gly preostanka (Gly 256 in Gly 257 v HsAtg4B), ki se nahajata na N-koncu regulatorne zanke. Mutacija enega izmed obeh Gly (Gly 244 v TcAtg4.2/ Gly257 v HsAtg4B) v His je povzročila popolno izgubo katalitične aktivnosti encima. Dokazali smo, da sta v TcAtg4.2 regulatorna zanka in njena fleksibilnost ključni za katalitično aktivnost encima. Nadalje smo preučili tudi vpliv Trp 158 (Trp 142 v HsAtg4B). Mutacija v Ala je povzročila skoraj popolno izgubo katalitične aktivnosti TcAtg4.2. Tako kot Trp 142 pri HsAtg4B je tudi Trp 158 ključnega pomena za katalitično aktivnost TcAtg4.2.

Druga, za delovanje HsAtg4B pomembna domena, je N-končna domena. V neaktivni obliki prekriva izhod reže aktivnega mesta HsAtg4B [56,135]. Za preučevanje vloge N-končne domene pri TcAtg4.2 smo na osnovi modelne strukture pripravili N-končno skrajšani mutanti TcAtg4.2 ΔN18 (delecija aminokislin 1 do 18) in ΔN24 (delecija aminokislin 1 do 24). V nasprotju z nepogrešljivostjo regulatorne zanke delecija N-končne domene nima bistvenega vpliva na katalitično aktivnost TcAtg4.2. Pri cepitvi naravnega substrata TcAtg8.1 smo katalitično učinkovitost TcAtg4.2 izračunali s pomočjo enačbe, uporabljene v poglavju 4.3. Katalitično učinkovitost TcAtg4.2 WT za TcAtg8.1 smo ocenili na $3{,}7 \times 10^3$ $M^{-1}$ $s^{-1}$, TcAtg4.2 dN18 na $3{,}1 \times 10^3$ $M^{-1}$ $s^{-1}$ z 20 % slabšo katalitično učinkovitostjo ter TcAtg4.2 dN24 na $2{,}8 \times 10^3$ $M^{-1}$ $s^{-1}$ s 30 % slabšo katalitično učinkovitostjo kakor TcAtg4.2 WT (Slika 24). Podobno kakor pri cepitvah naravnega substrata s TcAtg4.2 dN18 in dN24 je tudi pri cepitvi fluorogenega substrata Ac-ETFG-AFC katalitična aktivnost N-končno skrajšanega TcAtg4.2 le rahlo spremenjena (Slika 25).

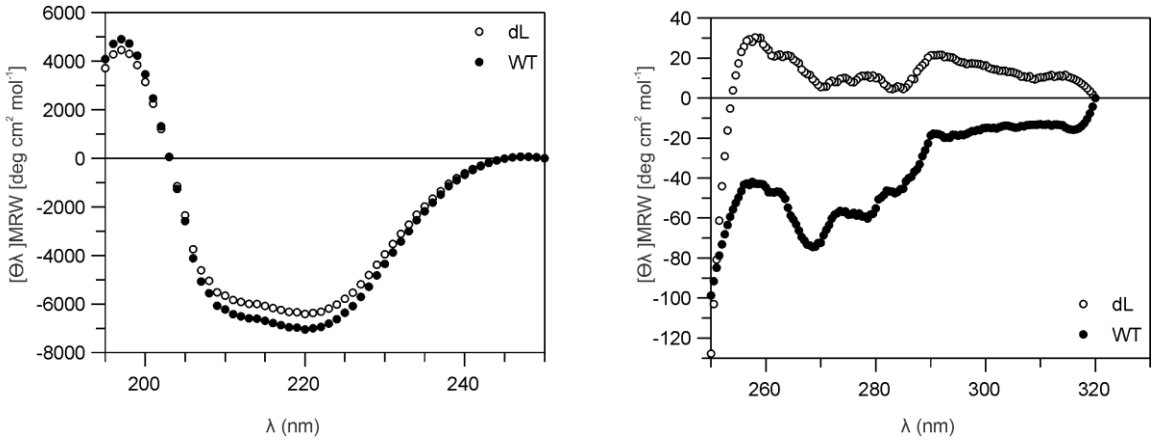



Slika 24: *Vpliv modifikacij TcAtg4.2 na hitrost cepitve naravnega substrata TcAtg8.1.* 0-150 ng TcAtg4.2 WT in mutant TcAtg4.2 dL, W158A, G244H, S246D, S246P, dN18 in dN24 in 2 µg TcAtg8.1 smo inkubirali v reakcijskem pufru (20 mM Tris-HCl pH 7,5, 150 mM NaCl, 5 mM DTT) pri 37 °C in stresanju 300 obr./min. Reakcijo smo po 60 min prekinili z dodatkom 6 × pufra SDS in inkubacijo vzorcev pri 100 °C 5 min.



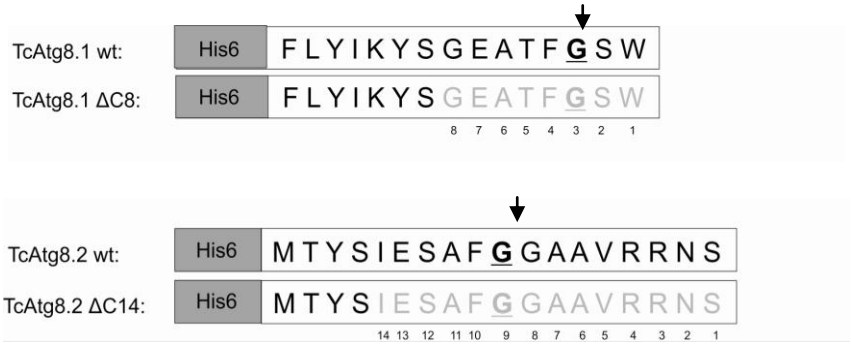

Slika 25: *Primerjava hitrosti cepitev Ac-ETFG-AFC s TcAtg4.2 WT, dN18, dN24 in dL.* 4 µg TcAtg4.2 WT in njegovih mutant TcAtg4.2 dN18, dN24 in dL ter 100 µM tetrapeptidnega fluorogenega substrata Ac-ETFG-AFC smo inkubirali v 100 µl reakcijskega pufra (20 mM Tris-HCl pH 8,0, 0,5 M $K_2HPO_4$, 5 mM DTT). Cepitev fluorogenega substrata smo spremljali na fluorimetru za mikrotitrske plošče (Safire, Tecan) pri vzbujanju λ = 400 nm in emisiji λ = 505 nm pri 37 °C 30 min.

S snemanjem daljnega- in bližnjega-UV CD spektra TcAtg4.2 WT in TcAtg4.2 dL smo preverili, ali je izguba katalitične aktivnosti TcAtg4.2. dL povezana z izgubo sekundarne in terciarne strukture encima. Pri obeh encimih, TcAtg4.2 WT in TcAtg4.2 dL, smo v daljnem-UV CD spektru videli karakteristično α/β sekundarno strukturo z minimumi pri 222, 217 in 208 nm. Prav sta imela oba urejeno tudi terciarno strukturo z značilnimi, za urejeno strukturo karakterističnimi maksimumi pri 290–305 nm za triptofan, 275–282 nm za triozin ter 255–270 nm za fenilalanin, zato izguba katalitične aktivnosti ni bila povezana z nepravilnim zvitjem proteina (Slika 26).



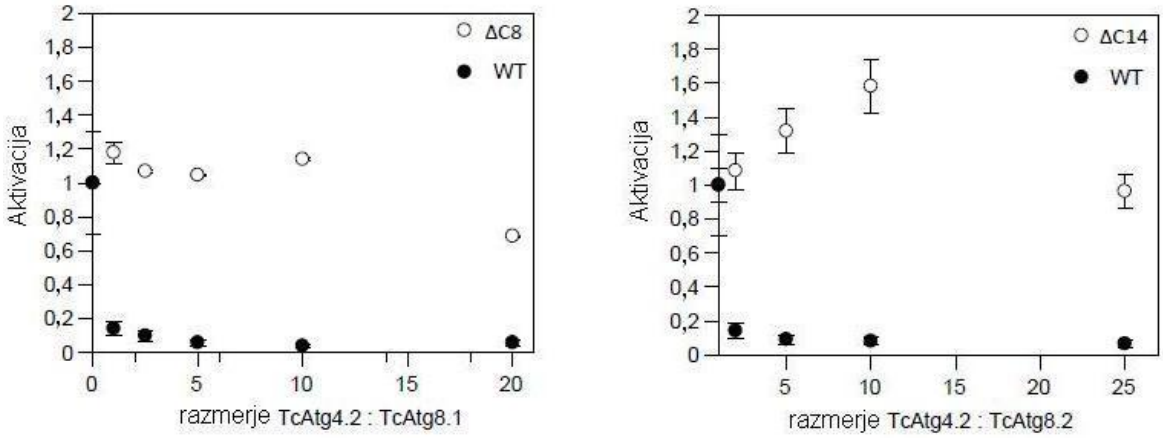

Slika 26: *Primerjava daljnega- in bližnjega-UV CD spektra TcAtg4.2 WT in TcAtg4.2 dL.* Levo: daljni-UV CD spekter. Za merjenje daljnega-UV CD spektra (250–195 nm) smo uporabili proteinsko koncentracijo $A_{280}$ = 0,1. Podatke smo odčitavali v korakih po 1 nm. Desno: bližnji-UV CD spekter. Za merjenje bližnjega-UV CD spektra (320–250 nm) smo uporabili proteinsko koncentracijo med $A_{280}$ = 1,1 in $A_{280}$ = 1,6. Podatke smo odčitavali v korakih po 0,5 nm. Izmerjene eliptične vrednosti smo preračunali s pomočjo enačbe, opisane v poglavju 3.3.2.

Drag in sod. so ob ko-inkubaciji sintetičnega substrata Ac-LRGG-ACC in ubikvitina, naravnega substrata deubikvitinirajočih encimov, ter encima IsoT dosegli 20 × hitrejšo cepitev sintetičnega substrata [133]. Za preizkus te strategije smo uporabili naravna substrata divjega tipa TcAtg8.1 WT in TcAtg8.2 WT ter C-končno skrajšani različici TcAtg8.1 ΔC8 in TcAtg8.2 ΔC14. Slednjima poleg glicina, za katerim poteče cepitev peptidne vezi, manjka še dodatnih pet aminokislin, ki se nahajajo pred omenjenim glicinom (Slika 27).




Slika 27: *Shematski prikaz C-končno skrajšanih konstruktov TcAtg8.1 ΔC8 in TcAtg8.2 ΔC14.* Siva – izbrisani aminokislinski preostanki v skrajšanih Atg8 konstruktih. Puščica – mesto cepitve peptidne verige v substratih divjega tipa (wt).

Koinkubacija C-končno skrajšanih različic TcAtg8.1 ΔC8 oz. TcAtg8.2 ΔC14 in sintetičnega substrata Ac-ETFG-AFC ne izboljša hitrosti cepitve sintetičnega substrata s TcAtg4.2, medtem ko koinkubacija TcAtg8.1 WT oz. TcAtg8.2 WT s sintetičnim substratom prepreči cepitev slednjega, kar nakazuje na direktno kompeticijo obeh substratov za vezavo v režo aktivnega mesta (Slika 28).

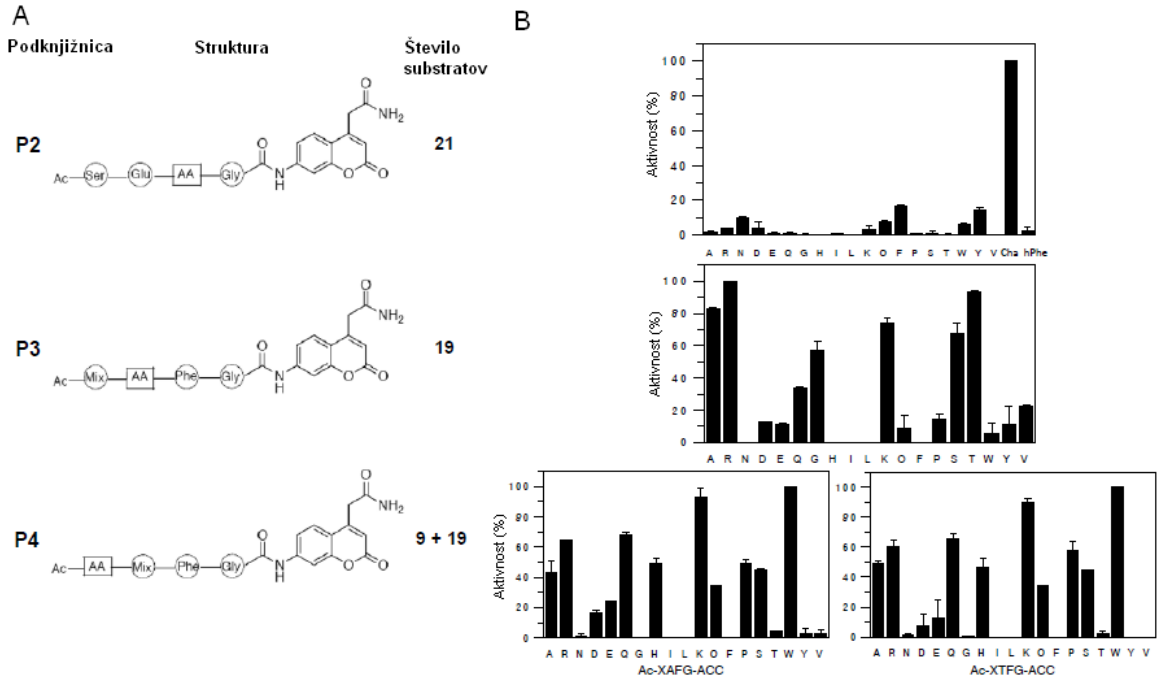



Slika 28: *Vpliv koinkubacije naravnih substratov TcAtg8 in sintetičnega substrata Ac-ETFG-AFC na afiniteto TcAtg4.2 do sintetičnega substrata*. V reakcijskem pufru (20 mM Tris-HCl pH 7,5, 150 mM NaCl, 5 mM DTT) smo TcAtg4.2 in naravna substrata divjega tipa (TcAtg8.1 in TcAtg8.2) ter njuni C-končno skrajšani različici (TcAtg8.1 ΔC8 in TcAtg82 ΔC14) v razmerjih med 0 in 25 koinkubirali z 250 µM tetrapeptidnim fluorogenim substratom Ac-ETFG-AFC. Cepitev fluorogenega substrata smo spremljali na fluorimetru za mikrotitrske plošče (Safire, Tecan) pri vzbujanju $\lambda = 400$ nm in emisiji $\lambda = 505$ nm pri 37 °C 30 min.

## 4.6 Določanje substratne specifičnosti TcAtg4.2

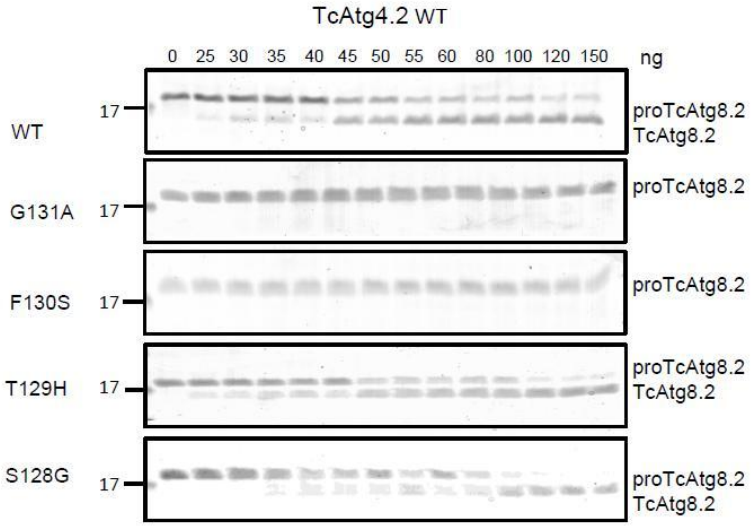
S pomočjo kombinatorne substratne knjižnice (angl. PS-SCL - po*sitional scanning*-

*substrate combinatorial library*) smo določili optimalne aminokislinske preostanke za TcAtg4.2 na pozicijah P2, P3 in P4. Zaradi značilne substratne specifičnosti Atg4, ki na poziciji P1 zahteva Gly, so imeli vsi substrati v kombinatorni knjižnici na poziciji P1 fiksiran Gly [18,52]. Podknjižnica P2 je imela fiksirane Gly na P1, Glu na P3 in Ser na P4. Na poziciji P2 smo poleg 19 naravnih aminokislinskih preostankov vključili tudi tri nenaravne aminokislinske preostanke: analog levcina, norlevcin (O) in dva analoga fenilalanina, cikloheksilalanin (Cha) in homofenilalanin (hPhe). Zaradi visoke afinitete človeškega HsAtg4B do Phe na poziciji P2 smo z vključevanjem nenaravnih aminokislinskih preostankov želeli poiskati selektivne substrate, ki bi razlikovali med substratnima specifičnostma obeh homologov, HsAtg4B in TcAtg4.2. Podknjižnici P3 in P4 sta vključevali le 19 naravnih aminokislinskih preostankov. PS-SCL je vsebovala dve podknjižnici P4. Podknjižnica Ac-XTFG-ACC je nosila aminokislinsko zaporedje naravnega substrata TcAtg8.1, podknjižnica Ac-XAFG-ACC pa aminokislinsko zaporedje naravnega substrata TcAtg8.2. Vsi substrati v PS-SCL so bili pripeti na 7-amino-4-karbamoilmetil kumarin (ACC) fluorofor (Slika 29). Na poziciji P2 je TcAtg4.2 kazal skoraj izključno preferenco do cikloheksilalanina (Cha), nenaravnega analoga fenilalanina (Phe). Na isti poziciji je dopuščal tudi Phe (F) in Tyr (W). Na poziciji P3 je preferiral Arg (R), Thr (T), Ala (A) in Lys (K) ter na poziciji P4 Trp (W) in Lys (K).




Slika 29: *Določanje substratne specifičnosti TcAtg4.2.* (A) Zgradba kombinatorne substratne knjižnice. (B) Pregled substratne specifičnosti TcAtg4.2 na pozicijah P2, P3 in P4.

Za potrditev substratne specifičnosti TcAtg4.2, dobljene s pomočjo PS-SCL, smo pripravili mutante naravnega substrata TcAtg8.2, pri katerih smo na pozicijah P2, P3 in P4 obstoječe aminokislinske preostanke zamenjali z neoptimalnimi aminokislinskimi preostanki, ki smo jih določili s pomočjo PS-SCL, ter spremljali vpliv zamenjave posameznih aminokislinskih preostankov na afiniteto TcAtg4.2 do TcAtg8.2. Pripravili smo P2 mutanto F130S, P3 mutanto T129H in P4 mutanto S128G. Kot pozitivno kontrolo smo pripravili P1 mutanto G131A, za katero je že dokazano, da zamenjava Gly prepreči hidrolizo polipeptidne verige v substratu [18,56]. Tako kot Gly na poziciji P1 je bil tudi Phe na poziciji P2 ključen za hidrolizo peptidne vezi. Aminokislinski preostanki na pozicijah P3 in P4 so imeli na hidrolizo substrata le manjši vpliv (Slika 30).

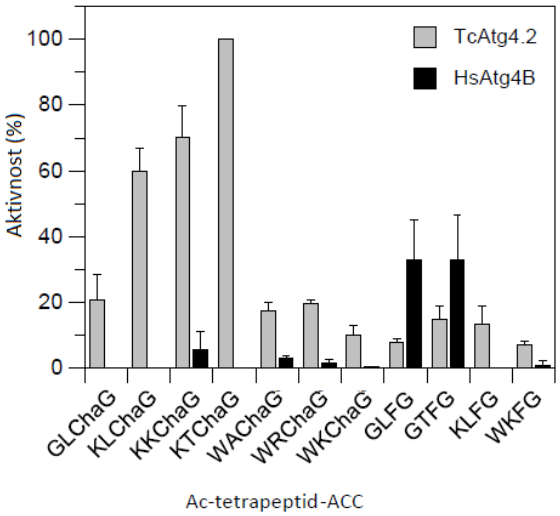



Slika 30: *Vpliv zamenjave aminokislinskih preostankov na pozicijah P1, P2, P3 in P4 na hitrost cepitve TcAtg8.2 s TcAtg4.2*. 0–150 ng TcAtg4.2 in 2 µg TcAtg8.2 WT in njegovih mutant P1 (G131A), P2 (F130S), P3 (T129H) in P4 (S128G) smo inkubirali v reakcijskem pufru (20 mM Tris-HCl pH 7,5, 150 mM NaCl, 5 mM DTT) pri 37 °C in stresanju 300 obr./min. Reakcijo smo po 60 min prekinili z dodatkom 6 × pufra SDS in inkubacijo vzorcev pri 100 °C 5 min.

## 4.7 Iskanje optimalnega tetrapeptidnega substrata za TcAtg4.2

Na osnovi razlik v substratnih specifičnostih med ortologoma *T. cruzi* Atg4.2 (TcAtg4.2) in človeškim Atg4B (HsAtg4B) smo sintetizirali novo substratno knjižnico, sestavljeno iz 11 substratov. Vsi substrati v knjižnici so imeli na poziciji P1 pripet Gly in na C-koncu ACC fluorofor. 7 substratov je imelo na poziciji P2 fiksiran Cha ter na pozicijah P3 in P4 optimalne ter neoptimalne aminokislinske preostanke za TcAtg4.2. 5 substratov, ki so na poziciji P2 imeli Phe ter na pozicijah P3 in P4 za HsAtg4B optimalne aminokislinske preostanke smo uporabili kot pozitivno kontrolo encimske aktivnosti HsAtg4B (Slika 12).

Kot pričakovano je TcAtg4.2 procesiral substrate, ki na poziciji P2 vsebujejo Cha mnogo bolje kakor substrate, ki so na omenjeni poziciji vsebovali Phe. Šibko je procesiral substrat Ac-GLChaG-ACC, ki je na pozicijah P4 in P3 vseboval neoptimalna aminokislinska preostanka za TcAtg4.2. Najvišjo afiniteto je kazal do tetrapeptidnega substrata Ac-KTChaG-ACC, kateremu je tesno sledil še Ac-KKChaG-ACC s $k_{cat}/K_m$ 2,1 ± 0,2 $M^{-1}$ $s^{-1}$ in 3,0 ± 0,2 $M^{-1}$ $s^{-1}$. Rezultati nove knjižnice so potrdili selektivnost TcAtg4.2, določeno s PS-SCL. Prav tako v skladu z že objavljenimi rezultati je HsAtg4B najbolje procesiral Ac-GTFG-ACC in Ac-GLFG-ACC. Do substratov, ki so imeli na poziciji P2 Cha HsAtg4B, ni kazal encimske aktivnosti oz. je bila le-ta zelo šibka (Slika 31).

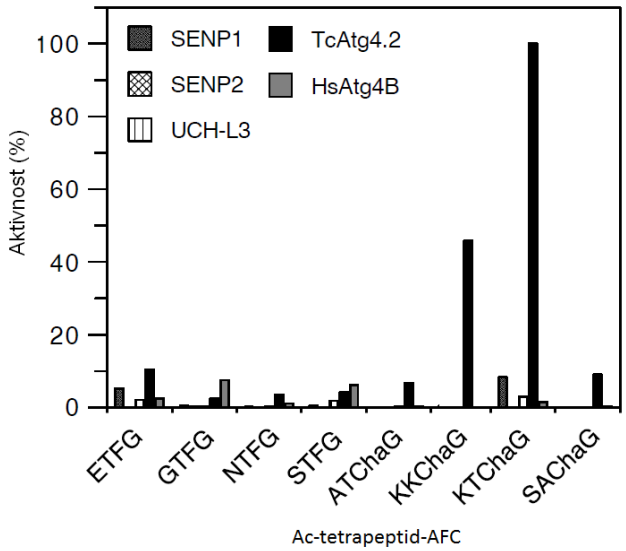



Slika 31*: Spremljanje hitrosti razgradnje substratov v optimizirani substratni tetrapeptidni knjižnici s TcAtg4.2 in HsAtg4B.* 4 µg TcAtg4.2 oz. HsAtg4B smo inkubirali z 250 µM tetrapeptidnimi fluorogenimi substrati v reakcijskem pufru za TcAtg4.2 (25 mM Tris-HCl pH 8,0, 0,5 M $K_2HPO_4$, 5 mMDTT) oz. v reakcijskem pufru za HsAtg4B (25 mM Tris-HCl pH 7,5, 0,5 M $Na_3C_3H_5O(COO)_3$, 5 mMDTT). Hitrost cepitev fluorogenih substratov smo spremljali na fluorimetru za mikrotitrske plošče (Safire, Tecan) pri vzbujanju $\lambda$ = 355 nm in emisiji $\lambda$ = 460 nm pri 37 °C 30 min.

Za izboljšanje katalitične učinkovitosti TcAtg4.2 do tetrapeptidnih substratov smo ACC fluorofor zamenjali s fluoroforom AFC. Izračunani katalitični učinkovitosti $k_{cat}/K_m$ za Ac-KTChaG-AFC in Ac-KKChaG-AFC sta znašali 110 ± 8 $M^{-1}$ $s^{-1}$ in 140 ± 8 $M^{-1}$ $s^{-1}$.

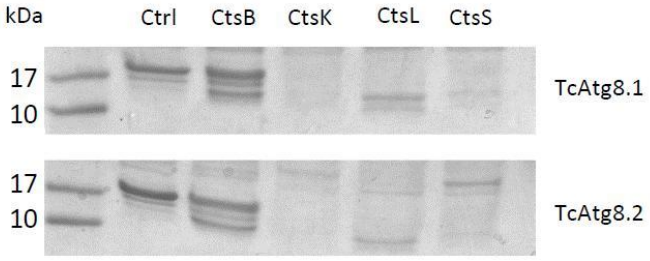
## 4.8 Določanje selektivnosti optimalnih substratov za TcAtg4.2

Avtofagini sodelujejo v ubikvitinu podobni konjugacijski kaskadi. Njihova aktivnost spominja na aktivnost deubikvitinirajočih (DUB) in deSUMOilirajočih (SENP) encimov, ki z endopeptidazno aktivnostjo aktivirajo naravna substrata ubikvitin in proteine SUMO ter jih po opravljeni funkciji tudi dekonjugirajo s tarčnih molekul. Zaradi podobne funkcije smo selektivnost fluorogenih substratov testirali tudi na človeških citosolnih HsAtg4B, deSUMOilirajočih encimih SENP1 in 2 in deubikvitinirajočem encimu UCH-L3. Človeški encimi so kazali zelo šibko katalitično aktivnost do vseh testiranih substratov. TcAtg4.2 smo uporabili kot pozitivno kontrolo (Slika 32).




Slika 32: *Cepitve izbranih tetrapeptidnih substratov s TcAtg4.2 in človeškimi citosolnimi proteini HsAtg4B, SENP1, SENP2 in UCH-L3.* 4 µg TcAtg4.2, HsAtg4B, SENP1, SENP2 oz. UCH-L3 smo inkubirali z 250 µM tetrapeptidnimi fluorogenimi substrati v reakcijskem pufru za TcAtg4.2 (25 mM Tris-HCl pH 8,0, 0,5 M $K_2HPO_4$, 5 mM DTT) oz. v reakcijskem pufru za preostale encime (25 mM Tris-HCl pH 7,5, 0,5 M $Na_3C_3H_5O(COO)_3$, 5 mM DTT). Hitrost cepitev fluorogenih substratov smo spremljali na fluorimetru za mikrotitrske plošče (Safire, Tecan) pri vzbujanju $\lambda$ = 400 nm in emisiji $\lambda$ = 505 nm pri 37 °C 30 min.

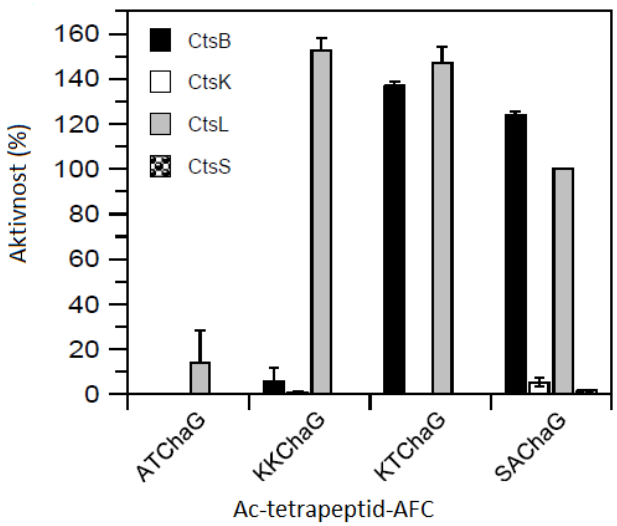
Poleg človeških citosolnih proteinov smo selektivnost izbranih sintetičnih substratov testirali tudi v prisotnosti človeških cisteinskih katepsinov B, K, L in S, ki znotraj lizosomov sodelujejo pri zadnji stopnji avtofagije, tj. razgradnji zaobjetih proteinskih substratov, tudi človeških homologov Atg8 [142,143]. Najprej smo preverili ali rekombinantni katepsini lahko cepijo rekombinantna TcAtg8.1 in TcAtg8.2. Vsi so učinkovito razgrajevali oba substrata (Slika 33).




Slika 33: Cepitve *T. cruzi* homologov, Atg8 TcAtg8.1 in TcAtg8.2 s človeškimi katepsini B, K, L in S. 40 ng rekombinantnih katepsinov B, K, L in S smo v reakcijskem pufru BANA (15 mM $Na_2HPO_4$, 88 mM $KH_2PO_4$ pH 6,0, 1 mM EDTA, 0,1 % PEG-6000, 5 mM DTT) inkubirali z 2 µg TcAtg8.1 oz TcAtg8.2 pri 37 °C. Reakcijo smo po 60 min prekinili z dodatkom 6 × pufra SDS in inkubacijo vzorcev pri 100 °C 5 min.

Ker so katepsini cepili homologe Atg8, smo s katepsini inkubirali tudi sintetične tetrapeptidne substrate Ac-ATChaG-AFC in Ac-SAChaG-AFC z aminokislinskimi zaporedji, ki ustrezajo TcAtg8.1 in TcAtg8.2, in s Cha na poziciji P2 ter optimalna substrata za TcAtg4.2, Ac-KKChaG-AFC in Ac-KTChaG-AFC.
Katepsina B in L sta kazala do Ac-KTChaG-AFC, ki je najoptimalnejši substrat za TcAtg4.2, zelo visoko afiniteto. Ac-KKChaG-AFC je izmed izbranih encimov lahko cepil

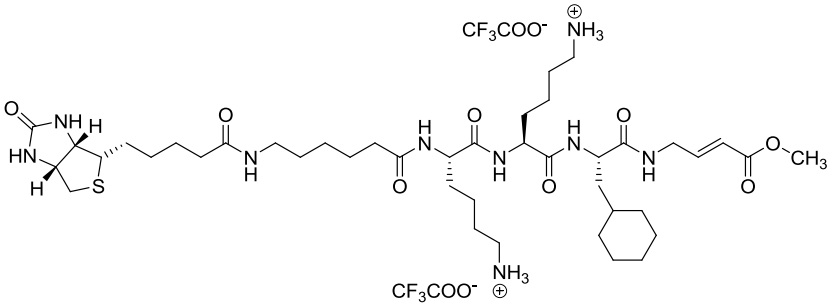
le katepsin L (CtsL) s katalitično učinkovitostjo $k_{cat}/K_m = 5100 \pm 530\ M^{-1}\ s^{-1}$ (Slika 34).




Slika 34: *Cepitve izbranih tetrapeptidnih substratov s človeškimi cisteinskimi katepsini B, K, L in S.* 5 □ 20 nM rekombinantne katepsine B, K, L in S smo v reakcijskem pufru BANA (15 mM $Na_2HPO_4$, 88 mM $KH_2PO_4$ pH 6,0, 1 mM EDTA, 0,1 % PEG-6000, 5 mM DTT) inkubirali s 100 µM tetrapeptidnimi substrati. Hitrosti cepitev fluorogenih substratov smo spremljali na fluorimetru za mikrotitrske plošče (Safire, Tecan) pri vzbujanju λ = 400 nm in emisiji λ = 505 nm pri 37 °C 30 min.

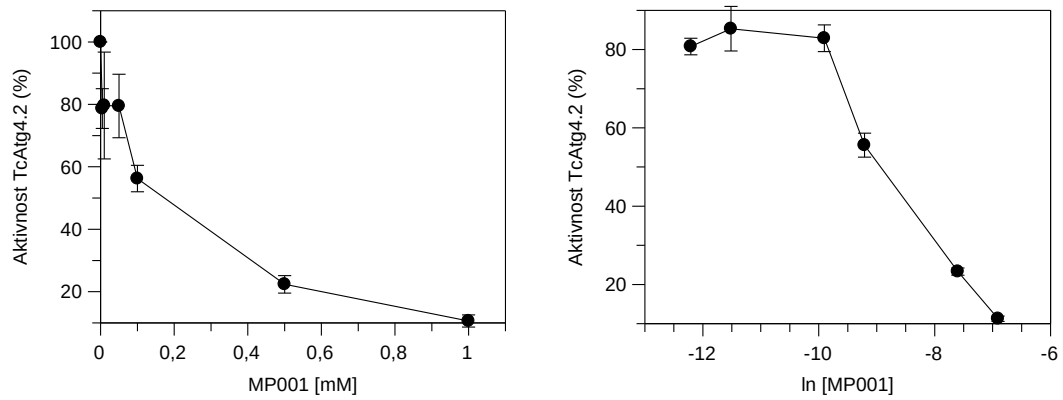
## 4.9 Inhibicija TcAtg4.2 s pametno aktivnostno sondo MP-001

Na podlagi rezultatov, dobljenih z določanjem substratne specifičnosti TcAtg4.2 in testi selektivnosti, smo za sintezo pametne aktivnostne sonde MP001 izbrali tetrapeptidno ogrodje najselektivnejšega substrata, KKChaG (Slika 35).




Slika 35: *Shematski prikaz pametne aktivnostne sonde MP001*. Pametno aktivnostno sondo MP001 smo sintetizirali na osnovi tetrapeptidnega substrata KKChaG. Na N-koncu sonde je preko linkerja pripet biotin, na C-koncu peptida pa je pripet metilni ester, ki se ob hidrolizi peptidne vezi kovalentno poveže s katalitičnim cisteinskim preostankom v reži aktivnega mesta encima.

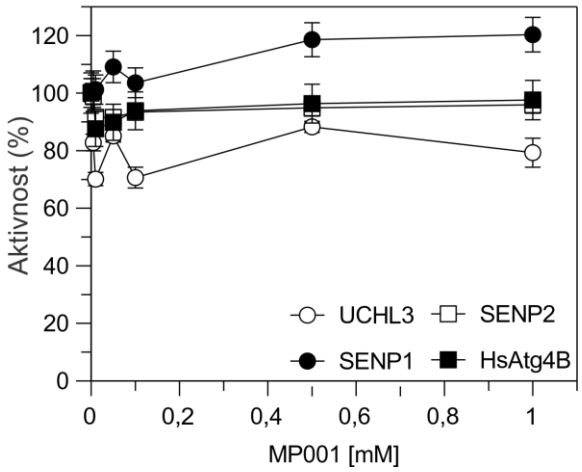
MP001 inhibira TcAtg4.2 z $IC_{50} = 130 \pm 22{,}1$ µM. MP001 (Slika 36).




Slika 36: *Inhibicija TcAtg4.2 s pametno aktivnostno sondo MP001*. Levo: Prikaz aktivnosti TcAtg4.2 (v %) v odvisnosti od naraščajoče koncentracije MP001 (v mM). Desno: Prikaz aktivnosti TcAtg4.2 (v %) v odvisnosti od naravnega logaritma koncentracije MP001 (v M). TcAtg4.2 in MP001 smo v različnih molarnih razmerjih predinkubirali v 50 µl reakcijskega pufra (25 mM Tris-HCl pH 8,0, 0,5 M $K_2HPO_4$, 5 mM DTT) pri 37 °C 10 min. Nato smo k TcAtg4.2 in MP001 dodali še 50 µl reakcijskega pufra, ki je vseboval 100 µM Ac-KKChaG-AFC. Hitrost cepitve smo spremljali na fluorimetru za mikrotitrske plošče (Safire, Tecan) pri vzbujanju λ = 400 nm in emisiji λ = 505 nm pri 37 °C 30 min.

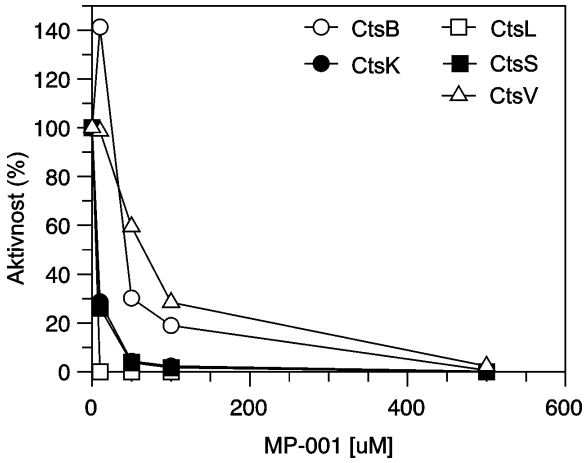
## 4.10 Določanje selektivnosti pametne aktivnostne sonde MP001

Tako kot selektivnost tetrapeptidnih fluorogenih substratov smo testirali tudi selektivnost pametne aktivnostne sonde MP001. V skladu s substratnimi selektivnostnimi testi MP001 ne inhibira človeških citosolnih proteinov HsAtg4B, SENP1, SENP2 ter UCH-LC3 (Slika 37).




Slika 37: *Inhibicija človeških citosolnih cisteinskih proteaz s pametno aktivnostno sondo MP001*. HsAtg4B, SENP1, SENP2 in UCH-3 ter MP001 smo v različnih molarnih razmerjih predinkubirali v 50 µl reakcijskega pufra (25 mM Tris-HCl pH 7,5, 0,5 M $Na_3C_3H_5O(COO)_3$, 5 mM DTT) pri 37 °C 10 min. Nato smo k encimom in MP001 dodali še 50 µl reakcijskega pufra, ki je vseboval 100 µM Ac-KKChaG-AFC. Hitrost cepitve smo spremljali na fluorimetru za mikrotitrske plošče (Safire, Tecan) pri vzbujanju λ = 400 nm in emisiji λ = 505 nm pri 37 °C 30 min.

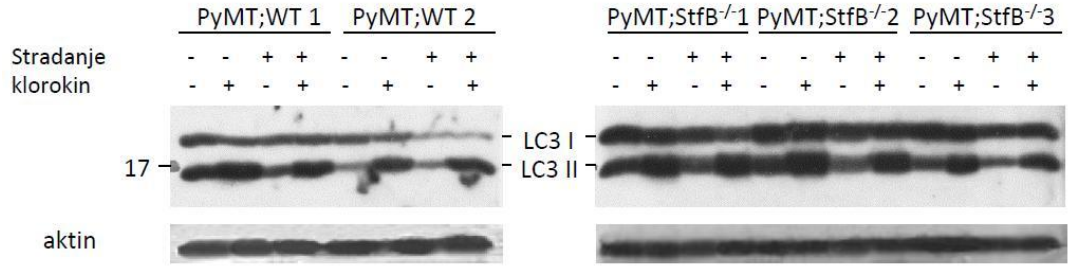
V nasprotju s človeškimi citosolnimi proteini pa pametna aktivnostna sonda MP001 zelo dobro inhibira vse testirane lizosomske cisteinske proteaze katepsin (CtsB, K, L, in S). $IC_{50}$ za katepsin L znaša 0,79 ± 0,02 µM (Slika 38).




Slika 38: *Inhibicija človeških katepsinov B, K, L in S s pametno aktivnostno sondo MP001*. 5 - 20 nM rekombinantnih katepsinov ter MP001 smo v različnih molarnih razmerjih predinkubirali v 50 µl reakcijskega pufra BANA (15 mM $Na_2HPO_4$, 88 mM $KH_2PO_4$ pH 6,0, 1 mM EDTA, 0,1 % PEG-6000, 5 mM DTT). Nato smo k mešanici katepsinov in MP001 dodali še 50 µl reakcijskega pufra, ki je vseboval 100 µM Ac-KKChaG-AFC. Hitrost cepitve smo spremljali na fluorimetru za mikrotitrske plošče (Safire, Tecan) pri vzbujanju $\lambda$ = 400 nm in emisiji $\lambda$ = 505 nm pri 37 °C 30 min.

## 4.11 Imunološka detekcija LC3 v lizatih tumorskih celic MMTV-PyMT

Nivo avtofagije v sesalskih celicah se lahko določa z imunološko detekcijo dobro uveljavljenega markerja avtofagije, sesalskega homologa Atg8 LC3. Določa se njegova količina ter razmerje med citosolno (LC3 I) ter membransko vezano obliko (LC3 II). Slednja direktno sovpada s številom/količino avtofagosomov v celici. S to metodo dobimo informacijo o bazalnem nivoju avtofagije znotraj celice/tkiva. Primerjava razlik v razmerju med LC3 I in LC3 II v odsotnosti in prisotnosti inhibitorjev lizosomskih proteaz (E64d, pepstatin A) ali inhibitorjev protonskih črpalk, ki znotraj lizosomov dvignejo pH in tako preprečijo proteinsko razgradnjo (bafilomicin A, klorokin, hidroksiklorokin, amonijev klorid), pa nam poda še informacijo o avtofagnem fluksu [144]. V totalnih proteinskih lizatih tumorskih celic MMTV-PyMT divjega tipa (PyMT;WT) in celic z izbitim genom za *stefin B* (PyMT;StfB-/-) smo z imunološko detekcijo določili količino LC3 v normalnih pogojih in pogojih stradanja (2,5 h) ter v odsotnosti in prisotnosti inhibitorja avtofagije klorokina. Primerjava količine LC3 v tumorskih celicah PyMT;WT in PyMT;StfB-/- kaže zvišan bazalni nivo avtofagije v tumorskih celicah z izbitim genom za stefin B (Slika 39).

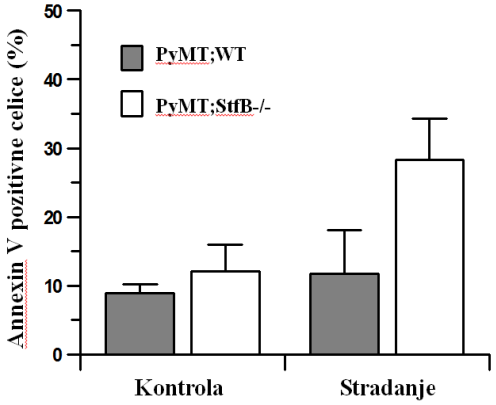


Slika 39: *Imunološka detekcija LC3 v tumorskih celicah PyMT;WT in PyMT;StfB-/-*. Tumorske celice PyMT;WT in PyMT;StfB-/- smo gojili pri normalnih pogojih v gojišču DMEM z dodanimi 10 % FBS, 1 % glutaMAX$^{TM}$ in 1 % penicilin/streptomicinom, v pogojih stradanja v pufru HBSS ter v pogojih stradanja z dodanim 100 µM inhibitorjem avtofagije klorokinom pri 37 °C in 5 % $CO_2$ 2,5 uri.

## 4.12 Vpliv regulacije avtofagije na preživetje tumorskih celic MMTV-PyMT

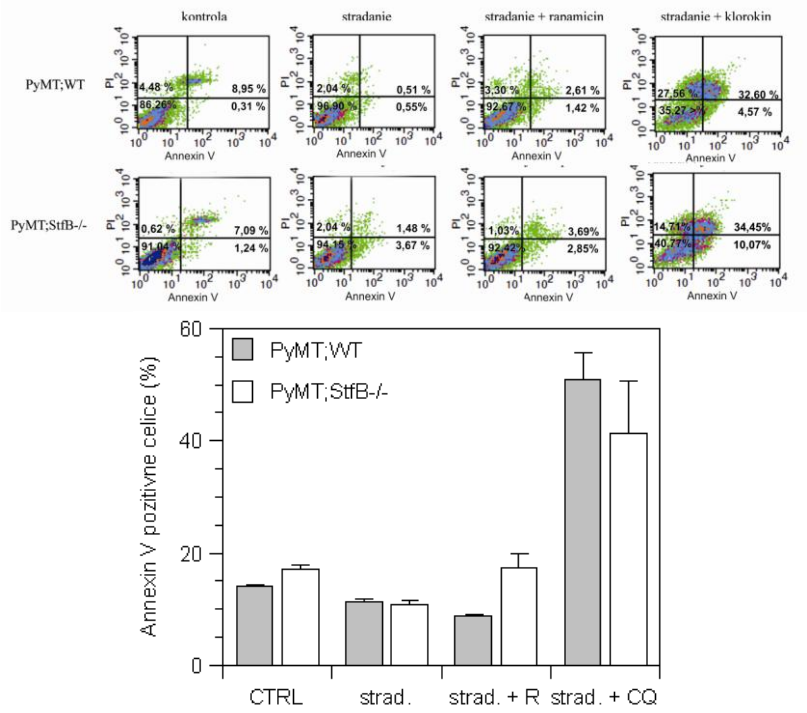
Butinar in sod. so pokazali, da imajo tumorske celice PyMT;StfB-/- zaradi odsotnosti stefina B povišan nivo endogenih reaktivnih kisikovih spojin (ROS) (rezultati niso objavljeni). Prav tako so pokazali, da se ob dodatku eksogenega ROS, $H_2O_2$, v celicah PyMT;StfB-/-, v primerjavi s celicami PyMT;WT, signifikantno poviša nivo celične smrti [123]. Ker so ROS zelo pomembni induktorji avtofagije, nas je zanimalo, ali je ob regulaciji avtofagije v pogojih stradanja mogoče zaznati spremembe v preživetju tumorskih celic PyMT;WT in PyMT;StfB-/-.

Tumorske celice PyMT;WT in PyMT;StfB-/- v pogojih stradanja brez povečanega umiranja lahko preživijo tudi do 48 h. Razlike v preživetju pa se začnejo kazati šele po 72 h, kjer PyMT;StfB-/- umirajo bolj. Statistično značilnih razlik med skupinama nismo zaznali (Slika 40).




Slika 40: *Preživetje tumorskih celic PyMT;WT in PyMT;StfB-/- v pogojih stradanja*. Tumorske celice PyMT;WT in PyMT;StfB-/- smo gojili pri normalnih pogojih v gojišču DMEM z dodanimi 10 % FBS, 1 % glutaMAX$^{TM}$ in 1 % penicilin/streptomicinom in v pogojih stradanja v pufru HBSS pri 37 °C in 5 % $CO_2$ 72 ur.

Zanimalo nas je, ali lahko ob pogojih stradanja in istočasni regulaciji avtofagije zaznamo večje razlike v preživetju med obema skupinama tumorskih celic. Zaradi pospešenega odmiranja obeh skupin tumorskih celic v pogojih stradanja in istočasni regulaciji avtofagije smo tumorske celice tretirali le 24 h. Indukcija avtofagije z 200 nM rapamicinom (R) v pogojih stradanja ne sproži povečane celične smrti. Inhibicija avtofagije s 50 µM klorokinom v pogojih stradanja povzroči povečano celično smrt tako v PyMT;WT kot tudi v PyMT;StfB-/-. Statističnih značilnih razlik med skupinama ni (sSlika 41).




Slika 41: *Sprožitev celične smrti z regulacijo avtofagije v pogojih stradanja.* Tumorske celice PyMT;WT in PyMT;StfB-/- smo gojili pri normalnih pogojih v gojišču DMEM z dodanimi 10 % FBS, 1 % glutaMAX$^{TM}$ in 1 % penicilin/streptomicinom (CTRL), v pogojih stradanja v pufru HBSS (strad.), v pogojih stradanja z dodanim 200 nM induktorjem avtofagije rapamicinom (strad. + R), ter v pogojih stradanja z dodanim 100 µM inhibitorjem avtofagije klorokinom (strad. + CQ), pri 37 °C in 5 % $CO_2$ 24 ur.

# 5 Razprava

Avtofagija je katabolna metabolna pot, pri kateri evkariontski organizmi s pomočjo lizosomov razgrajujejo odvečne in poškodovane komponente. S svojim delovanjem skrbi za ohranjanje homeostaze in prilagajanje organizmov na različne oblike stresa. Enoceličnim organizmom omogoča hitro in učinkovito prilagajanje na stresne pogoje, kot je na primer pomanjkanje hranil v okolju, znotrajceličnim parazitom pa omogoča tudi diferenciacijo in preživetje znotraj gostiteljskega organizma ter v višjih večceličnih sistemih sodeluje tudi pri remodeliranju tkiv, zaščiti organizmov pred razvojem tumorjev in nevrodegenerativnih bolezni, obrambo pred patogenimi organizmi in pripravo antigenskih peptidov za potrebe imunskega sistema.

V celotnem procesu so udeleženi številni z avtofagijo povezani proteini, ki se združujejo v proteinske komplekse in sodelujejo v različnih fazah avtofagnega procesa (povzeto v [145]). Eden takšnih sistemov je tudi ubikvitinu podoben konjugacijski sistem Atg8, pri katerem sodelujejo tudi edine v celotnem procesu avtofagije udeležene proteaze, imenovane avtofagini (Atg4).

Avtofagini so evolucijsko zelo ohranjene cisteinske proteaze, ki so nepogrešljive za potek avtofagije. S procesiranjem naravnega substrata Atg8 omogočijo njegovo konjugacijo na fosfatidiletanolamin (PE) v membrani nastajajočega fagofore. Prav tako z zrelih avtofagosomov v procesu dekonjugacije/delipidacije s površine avtofagosoma odstranjujejo Atg8 ter tako skrbijo za njegovo recikliranje, ki hkrati omogoča tudi nadaljnjo fuzijo avtofagosoma z lizosomom ter razgradnjo zaobjetega tovora [50,146].

Enocelični kinetoplastidni paraziti *Trypanosoma cruzi*, ki povzroča Chagasovo bolezen v Latinski Ameriki, *Trypanosoma brucei*, ki povzroča spalno bolezen v Afriki in *Leismania spp*., ki povzročajo lišmanioze pri ljudeh in živalih, predstavljajo poglavitni zdravstveni problem držav tretjega sveta. Za uspešno kolonizacijo sesalskih gostiteljev ti paraziti nujno potrebujejo avtofagine in avtofagijo, zato je za uspešno spremljanje in zdravljenje omenjenih bolezni nujen razvoj orodij, ki bi omogočala selektivno spremljanje proteolitične aktivnosti parazitskih avtofaginov brez vpliva na človeške Atg4 proteaze.

V genomu *Trypanosome cruzi*, tako kot v genomu sorodnih parazitov *Trypanosome brucei* in *Leishmanie major*, se nahajata zapisa za dva homologa Atg4, Atg4.1 in Atg4.2. Williams in sod. so pokazali, da je Atg4.1, ki se nahaja v parazitu *L. major*, glavni nosilec endopeptidazne aktivnosti, Atg4.2 pa je odgovoren za dekonjugacijo/delipidacijo homologov Atg8 z membrane avtofagosomov [147]. V skladu s temi rezultati tudi oba predstavnika avtofaginov iz parazita *Trypanosoma cruzi* procesirata naravna substrata TcAtg8.1 in TcAtg8.2. TcAtg4.2 je tako glavni nosilec endopeptidazne aktivnosti in oba substrata v pogojih *in vitro* cepi približno 10.000-krat hitreje kakor TcAtg4.1 [18].

Naše funkcijske študije so pokazale številne podobnosti med avtofaginom iz parazita *T. cruzi*, TcAtg4.2 in človeškim ortologom HsAtg4B. Ker ima TcAtg4.2 pri preživetju parazita, tudi znotraj človeškega gostitelja, izjemno pomembno vlogo, predstavlja novo potencialno terapevtsko tarčo pri zdravljenju Chagasove bolezni [18,75].

Zaradi dobre ohranjenosti mehanizma delovanja homologov Atg4 je za razvoj specifičnih komponent, ki bi tarčno ciljale TcAtg4.2 brez vpliva na človeški Atg4B,

potrebna natančna biokemijska karakterizacija obeh homologov Atg4.

Raziskovalne skupine po vsem svetu so za določanje substratne specifičnosti številnih proteaz uporabile kombinatorne substratne knjižnice (angl. *PS-SCL - positional scanning-substrate combinatorial library*). Z uporabo te metode so uspešno določene substratne specifičnosti kaspaz [148], deSUMOilirajočih encimov [134], deubikvitinirajočih encimov [133] in tudi človeškega avtofagina-2 [135]. Tudi mi smo za določanje substratne specifičnosti TcAtg4.2 uporabili PS-SCL ter P2 podknjižnico poleg 19 naravnih L-aminokislinskih preostankov dopolnili z nenaravnimi aminokislinskimi preostanki, kakor so za določanje substratne specifičnosti človeškega Atg4B storili tudi Shu in sod. [135]. Izjemno selektivni sintetični substrati, ki vključujejo tudi nenaravne aminokislinske preostanke, so že uspešno razvili za številne proteaze, med drugim za človeške proteaze katepsin C [149], nevtrofil elastazo [150] in kaspaze [151]. Ti substrati lahko ločijo med proteolitičnimi aktivnostmi proteaz z zelo podobnimi substratnimi specifičnostmi, kar v primeru uporabe naravnih aminokislinskih preostankov do sedaj ni bilo mogoče.

Z uporabo omenjenega pristopa smo razvili optimalen substrat za TcAtg4.2, Ac-KTChaG-AFC ter najselektivnejši substrat, Ac-KKChaG-AFC. Omenjena substrata na poziciji P2 vsebujeta nenaravni analog Phe, cikloheksilalanin (Cha), ki je tudi ključen za selektivno delovanje TcAtg4.2. Cha ima v primerjavi s Phe dodaten $–CH_2–$ linker in cikloheksilni obroč, ki v nasprotju s planarnim fenilalanilnim obročem zaseda konformacijo kadi oziroma stola in v primerjavi s ortologom HsAtg4B nakazuje na drugačno arhitekturo vezave substrata. Na poziciji P2 TcAtg4.2 poleg Cha, ki je daleč najprimernejša aminokislina, dopušča tudi Phe in Tyr.

Nepogrešljivost Gly na poziciji P1 in aromatskega aminokislinskega preostanka na P2 smo dokazali tudi z mutacijami pripadajočih aminokislinskih preostankov v naravnem substratu TcAtg8.2. Kakor človeški homolog HsAtg4B ni mogel procesirali mutant P1 in P2 v človeškem homologu Atg8 LC3 [56], tudi TcAtg4.2 ni bil zmožen procesiranja mutant P1 ter P2 v naravnem substratu TcAtg8.2. V nasprotju s TcAtg4.2 človeški homolog Atg4B na poziciji P2 preferira izključno Phe, ki se nahaja tudi v naravnem substratu LC3, in ne more procesirati substratov, ki na tej poziciji nosijo Cha.

Poleg najpomembnejše razlike v substratnih specifičnostih obeh ortologov na poziciji P2 pa ob primerjavi že objavljenih rezultatov za HsAtg4B [135] ortologa kažeta tudi manjše razlike v aminokislinskih preferencah na pozicijah P3 in P4.

Na naše presenečenje TcAtg4.2 lahko procesira tudi tetrapeptidne substrate, ki na pozicijah P4 in/ali P3 nosijo neoptimalne aminokislinske preostanke. Tako TcAtg4.2 cepi tetrapeptidni substrat Ac-KLChaG-AFC s skoraj enako učinkovitostjo kakor optimalni tetrapeptidni substrati Ac-KTChaG-AFC, Ac-GLChaG-AFC pa procesira s približno trikrat nižjo učinkovitostjo. Dobljene rezultate lahko razložimo s hipotezo kooperativnosti vezavnih mest [152]. Tako ima Cha, v nasprotju s Phe, na poziciji P2 zelo močan vpliv na vezavo sosednjih aminokislinskih preostankov in v kombinaciji z Lys na poziciji P4 izniči negativni efekt neoptimalnega Leu na poziciji P3. Prav tako lahko kooperativnost vezavnih mest dodatno potrdimo tudi z zamenjavo fluorofora ACC z manjšim AFC-jem. Rezultat zamenjave je drastično izboljšanje katalitične učinkovitosti TcAtg4.2 do tetrapeptidnih substratov, kar nakazuje na majhen vezavni žep S1' v TcAtg4.2. Tudi ti rezultati so v skladu z zastopanostjo majhnih aminokislinskih preostankov v naravnih substratih TcAtg8.1 in TcAtg8.2, kjer se na poziciji P1' nahajata Gly oziroma Ser [18].

Dodatni selektivnostni testi, pri katerih smo uporabili človeške avtofaginom funkcijsko podobne citosolne encime, deSUMOilirajoča encima SENP1, SENP2 in deubikvitinirajoč encim (DUB) UCH-L3, so potrdili izključno selektivnost TcAtg4.2 do tetrapeptidnih substratov s Cha na poziciji P2, saj noben izmed testiranih encimov ni kazal afinitete do omenjenih tetrapeptidnih substratov. Rezultati so v skladu z že objavljenimi substratnimi

specifičnostmi SENP-ov in DUB-ov, ki na pozicijah P1 in P2 preferirajo dva Gly [133,134].

Kot kaže, imata poziciji P1 in P2, tako kot pri TcAtg4.2, tudi pri SNEP-ih in DUB-ih poglaviten vpliv na vezavo substratne molekule v režo aktivnega mesta. Velika stranska skupina Cha na poziciji P2 prepreči učinkovito vezavo substrata v režo aktivnega mesta encima, zaradi česar se substrat ne more namestiti v pozicijo, ki bi omogočila učinkovito hidrolizo peptidne vezi substrata. Na osnovi tetrapeptidnega ogrodja najselektivnejšega substrata za TcAtg4.2, Ac-KKChaG-AFC, smo sintetizirali tudi pametno aktivnostno sondo MP001, ki prav tako kaže izjemno dobro selektivnost in inhibira le TcAtg4.2 brez vpliva na katalitično aktivnost človeških citosolnih proteinov HsAtg4B, SENP1, SENP2 in UCH-L3.

Strukturne študije prostega človeškega Atg4B in v kompleksu z LC3 so razkrile, da sta se poleg ohranjenih aminokislinskih preostankov v homologih Atg8 na pozicijah P2 in P1, ki sta nepogrešljiva za nemoteno hidrolizo substratnih molekul Atg8, tudi v Atg4 ohranili vsaj dve domeni, ki sta ključni za aktivnost encima. To sta regulatorna zanka in N-končna domena, ki sta nujni za prepoznavanje in vezavo substrata ter nadaljnje konformacijske spremembe encima, potrebne za uspešno hidrolizo peptidne vezi in delipidacijo Atg8 s fosfatidiletanolamina (PE) v membrani avtofagosoma [51,56].

S prileganjem aminokislinskih zaporedij homologov Atg4 smo ugotovili, da so se domene in tudi aminokislinski preostanki, ki so neposredno udeleženi v hidrolizi substrata, dobro ohranili v številnih homologih Atg4. Tako so se tudi v TcAtg4.2 dobro ohranili aminokislinski preostanki, ki sestavljajo regulatorno zanko (aminokislinski preostanki 258–263 v HsAtg4B), in tisti, ki vzdržujejo njeno konformacijo. To sta Trp 142, ki se nahaja med α-vijačnicama D in E, ter Pro 260 v regulatorni zanki. Trp 142 in Ser 260 tvorita van der Waalsove interakcije in ohranjata regulatorno zanko zaprto.

Ohranila sta se tudi dva zaporedna Gly (Gly 256 in Gly 257 v HsAtg4B), ki se nahajata na N-koncu regulatorne zanke in ob vezavi substrata omogočita njeno tranzicijo iz neaktivne v aktivno konformacijo.

Funkcijske študije različnih mutant TcAtg4.2 in njihova primerjava s študijami na HsAtg4B kažejo na evolucijsko izredno ohranjen mehanizem delovanja homologov Atg4, ki se je ohranil od parazitov vse do človeka. Mutanta z delecijo regulatorne zanke TcAtg4.2 dL (delecija aminokislinskih preostankov 245–248) ne more hidrolizirati niti naravnih niti sintetičnih substratnih molekul v skladu z idejo o kritični vlogi zanke pri ohranjanju katalitične aktivnosti encima. Prav tako je za ohranitev katalitične aktivnosti encima ključna tudi fleksibilnost regulatorne zanke, ki jo vzdržujeta dva ohranjena Gly (Gly 256 in Gly 257 v HsAtg4B) in se nahajata tik pred regulatorno zanko. Z mutacijo enega izmed dveh ohranjenih Gly (Gly 244 v TcAtg4.2/Gly 257 v HsATg4B) v His se zaradi steričnih ovir in/ali uvedenega naboja fleksibilnost regulatorne zanke drastično zmanjša, zaradi česar Tctg4.2 popolnoma izgubi katalitično aktivnost.

V nasprotju s kritično vlogo regulatorne zanke pa ima delecija N-končne domene na katalitično aktivnost TcAtg4.2 le manjši vpliv in je bolj v skladu z idejo, da naj bi bila N-končna domena pomembna pri dekonjugaciji Atg8 s fosfatidiletanolamina v membrani avtofagosoma, kar potrjujejo tudi kristalografske študije kompleksa HsAtg4B in dveh molekul LC3, substratne in nesubstratne molekule. Substratna molekula LC3 se na insercijsko domeno HsAtg4B veže preko vezavnega motiva za Atg4 in omogoči procesiranje novonastalih proAtg8 molekul in izpostavitev C-končnega Gly. Nesubstratna molekula LC3 pa se veže na N-končno domeno HsAtg4B preko vezavnih mest W in L in je najverjetneje udeležena pri stabilizaciji »odprte« konformacije N-konca HsAtg4B, ki omogoča dekonjugacijo Atg8 z membrane avtofagosoma [56].

Za vezavo in procesiranje substrata so poleg aminokislinskih preostankov, ki se nahajajo blizu mesta cepitve polipeptidne verige substrata, pomembni tudi aminokislinski preostanki, ki tvorijo jedro substratne molekule, na katerem se nahaja tudi tako imenovana ubikvitinu podobna domena Atg8. Ta domena se veže na insercijsko domeno, ki je značilna le za avtofagine, in se nahaja daleč stran od reže aktivnega mesta encima. Preko teh interakcij Atg8 povzroči aktivacijo encima in insercijo C-končnega dela substrata v režo aktivnega mesta encima [51]. Zaradi odsotnosti ubikvitinu podobne domene v tetrapeptidnih sintetičnih substratih avtofagini do njih kažejo slabo afiniteto.

Koinkubacija tetrapeptidnih substratov s TcAtg8 divjega tipa je preprečila njihovo procesiranje, kar nakazuje na direktno kompeticijo obeh substratov za vezavo v reži aktivnega mesta encima. Koinkubacija C-končno skrajšanih mutant TcAtg8, ki ohranijo substratna vezavna mesta S5 – S1 v encimu prosta in tetrapeptidnih substratov, pa ni izboljšala hitrosti cepitve tetrapeptidnih substratov, zaradi česar sklepamo, da prisotnost ubikvitinu podobne domene brez C-končnega dela substrata sama po sebi ni dovolj za aktivacijo encima. Tudi ta rezultat sovpada s študijami HsAtg4B in LC3 ter tudi našimi študijami na TcAtg8.2 mutantah P1 in P2, kjer je Phe 119, ki se nahaja na C-koncu LC3, nujno potreben za premik Trp 142 v HsAtg4B in insercijo polipeptidne verige substrata v režo aktivnega mesta encima [51]. Prav nasprotno pa se avtofaginom funkcijsko podobni deubikvitinirajoči encimi, med katere spada tudi IsoT, ob koinkubaciji ubikvitina in sintetičnega substrata aktivirajo [134], kar nakazuje na različen mehanizem hidrolize substratnih molekul med funkcijsko podobnimi encimi.

Tetrapeptidna fluorogena substrata Ac-KTChaG-AFC in Ac-KKChaG-AFC, ki sta se izkazala kot najboljša substrata za TcAtg4.2, funkcijsko podobni človeški citosolni proteini HsAtg4B, SENP1, SENP2 in UCH-L3 niso sposobni cepiti. Prav tako tudi pametna aktivnostna sonda MP001, razvita na osnovi ogrodja KKChaG, ni inhibirala nobenega izmed funkcijsko podobnih človeških encimov. V nasprotju z njimi pa človeški katepsini, predvsem katepsin L zelo dobro cepi oba substrata. Posledično je tudi pametna aktivnostna sonda MP001 zelo dober inhibitor človeških katepsinov. Zato je razvoj selektivnih Atg4 substratov in inhibitorjev, ki bi delovali na celičnem nivoju, kjer so katepsini udeleženi tudi pri razgradnji Atg8/LC3, v nekonjugirani obliki vprašljiv. Prav tako je vprašljivo tudi spremljanje Atg4 katalitične aktivnosti s tetrapeptidnimi fluorogenimi substrati v živih parazitih, v katerih se nahaja kruzipain, katepsinu L podobna cisteinska proteaza [153,154], za katerega, kakor za TcAtg4.2, Cha na poziciji P2 predstavlja optimalen aminokislinski preostanek [155]. Kljub zapletom pri študijah na celičnem nivoju pa so dobljeni substrati in pametna aktivnostna sonda MP001 v sedanji obliki zelo primerni za študije *in vitro* in različne presejalne teste.

Podrobna karakterizacija TcAtg4.2, poglavitnega avtofagina v parazitu *T. cruzi*, je pokazala številne podobnosti s človeškim HsAtg4B, ki so v skladu z idejo o evolucijski ohranjenosti celotnega procesa avtofagije in njeni pomembni vlogi pri preživetju in ohranjanju homeostaze v evkariontskih organizmih. Enako velja tudi za podobnost v substratnih specifičnostih obeh homologov. Z uporabo PS-SCL in nenaravnih aminokislinskih preostankov smo kljub temu lahko določili razlike, na podlagi katerih smo uspešno razvili selektivne tetrapeptide substrate. Najpomembnejša razlika v substratnih specifičnostih obeh ortologov je pozicija P2, kjer TcAtg4.2 preferenčno prepoznava le nenaravni aminokislinski preostanek Cha, človeški HsAtg4B pa ga sploh ne tolerira. Prav tako TcAtg4.2 na poziciji P1' prepoznava manjše aminokislinske preostanke, ki bi pri razvoju specifičnih substratov in inhibitorjev za TcAtg4.2 lahko povečali njihovo selektivnost. Naši rezultati tako predstavljajo osnovo za razvoj selektivnih substratov in inhibitorjev za TcAtg4.2, ki bi pripeti na skupine, ki se tarčno

usmerjajo v citosol in se tako izognejo prebavnim vakuolam in neselektivni razgradnji, lahko omogočali tudi sledenje in regulacijo avtofagije v živih parazitih.

Fiziološka vloga avtofagije je ohranjanje celične homeostaze v normalnih in stresnih pogojih. Izkoriščanje avtofagije kot preživitvenega mehanizma tumorskim celicam omogoča prilagoditev na neugodne in stresne pogoje v tumorskem mikrookolju, kot so hipoksija, kislo okolje ter pomanjkanje hranil. Hkrati ima avtofagija pri nastanku in razvoju tumorjev kontradiktorno vlogo. Številne vrste tumorskih celic imajo v primerjavi z normalnimi tkivi zmanjšan nivo avtofagije, ki se kaže v zmanjšani količini LC3 in nekaterih drugih Atg proteinov. Posledica znižanja avtofagije je pospešeno kopičenje poškodovanih proteinov, organelov in poškodovane in/ali mutirane DNA ter zvišan oksidativni stres, ki so gonilo karcinogeneze v začetnih fazah razvoja tumorjev. Rezultat monoalelne delecije gena za *beklin 1*, ki jo najdemo v številnih humanih tumorjih, kot so rak dojke, jajčnikov in prostate, je znižana avtofagija. Znižanje nivoja avtofagije pri teh vrstah tumorjev omogoča hitrejšo celično proliferacijo in pospešeno tumorigenezo [25], medtem ko jo prekomerno izražanje proteina beklin-1 inhibira [93], kar je v skladu s tumor-supresorsko vlogo avtofagije pri preprečevanju razvoja malignih transformacij [156,157].

Tumor-supresorsko vlogo avtofagije so potrdili tudi poskusi na miših z izbitim genom za *atg4c*, ki so pokazali, da se miši sicer razvijajo normalno, vendar imajo v pogojih stradanja v primerjavi z mišmi divjega tipa znižano avtofagijo ter so bolj dovzetne za razvoj kemijsko induciranih fibrosarkomov [94]. V nasprotju z znižano avtofagijo, ki je gonilo tumorigeneze v zgodnjih fazah razvoja številnih humanih tumorjev, se v kasnejših fazah razvoja kot odgovor na hipoksijo, acidozo in pomanjkanje nutrientov avtofagija poveča. Tako zvišano avtofagijo najdemo v poznih stadijih humanega raka črevesja [98] in dojke [99], melanoma [100], hepatoma [101] in malignega glioma [102]. V zadnjem času se protumorigena funkcija avtofagije nanaša tudi na njeno protektivno vlogo, ki omogoča preživetje tumorskih celic pri zdravljenju pacientov s konvencionalnimi antitumorski terapijami, kot so radiacija [103,158] in kemoterapije z doksorubicinom [159], temozolomidom [160] in etopozidom [161] ter tamoksifenom [162]. Aktivira se ob terapevtsko induciranem celičnem stresu in ima ključno vlogo pri preživetju in razvoju rezistence tumorskih celic na konvencionalne antitumorske terapije. S farmakološko ali genetsko inhibicijo protektivne avtofagije se preživetje tumorskih celic in njihova rezistenca na antitumorska zdravljenja onemogoči, s čimer se poveča eliminacija rezistentnih tumorskih celic in izboljša učinkovitost antitumorskih terapij (povzeto v [163]).

Wei in sod. so na mišjem modelu raka dojke MMTV-PyMT s pogojnim izbitjem gena za *FIP200*, ki sodeluje pri iniciaciji avtofagije, v tumorskih celicah potrdili protumorigeno funkcijo avtofagije. Zaradi okvarjene avtofagije so se v tumorskih celicah akumulirali p62/SQSTM1 pozitivni agregati, znižal se je nivo pretvorbe LC3. Prav tako se je povečalo število okvarjenih mitohondrijev. Posledično se je zvišal nivo reaktivnih kisikovih spojin (ROS) in število okvar DNA. Povečala se je tudi celična smrt tumorskih celic *in vivo*, medtem ko razlike v celični smrti v tumorskih celicah, gojenih v pogojih *in vitro*, niso bile opažene, kar nakazuje na vpletenost mikrookoljskih stresorjev na preživetje tumorskih celic, katerih v pogojih *ex vivo* ni bilo [164].

Butinar in sod. so pokazali, da imajo tumorske celice MMTV-PyMT;StfB-/- zaradi odsotnosti stefina B povišan nivo endogenih ROS (rezultati niso objavljeni) ter da so v primerjavi s tumorskimi celicami divjega tipa ob dodatku aminokislinskega metilnega estra Leu-Leu-OMe ali nizkih koncentracij eksogenega $H_2O_2$, ki destabilizirata membrane lizosomov in mitohondrijev, podvržene pospešeni in obsežnejši apoptozi [123].

Zaradi povišanega nivoja ROS-ov, ki so dobro poznani induktorji avtofagije [9,59],

smo v PyMT;StfB-/- pričakovali povišan nivo avtofagije. V skladu s pričakovanji smo z imunološko detekcijo LC3 pokazali, da imajo tumorske celice PyMT;StfB-/- v primerjavi s tumorskimi celicami PyMT;WT povišan nivo obeh oblik LC3, citosolne (LC3 I) in membransko vezane oblike (LC3 II). Z detekcijo annexin V pozitivnih celic smo ugotovili, da sta obe skupini tumorskih celic v mediju brez hranil brez težav preživeli tudi do 48 h. Razlike so se pojavile šele po 72 h stradanja, kjer so tumorske celice PyMT;StfB-/- v primerjavi s tumorskimi celicami PyMT;WT umirale hitreje, vendar brez statistično značilnih razlik. Prav tako stradanje (24 h) s sočasno indukcijo avtofagije z rapamicinom pri nobeni skupini tumorskih celic ni vplivalo na preživetje. Pri stradanju (24 h) in sočasni inhibiciji avtofagije s klorokinom pa sta obe skupini tumorskih celic bili podvrženi pospešeni apoptozi, prav tako brez statistično značilnih razlik. Rezultati so v nasprotju s pričakovanji, saj bi zaradi povišanega nivoja ROS in posledično tudi zvišanega nivoja LC3 v PyMT;StfB-/- pričakovali, da je preživetje teh tumorskih celic bolj odvisno od avtofagije, kakor preživetje PyMT;WT. Wei in sod. [164] so dokazali vpletenost tumorskega mikrookolja na regulacijo avtofagije v tumorskih celicah PyMT v pogojih *in vivo* ter na spremenjen nivo preživetja pri njihovem gojenju v pogojih *ex vivo*. Ker smo tudi mi uporabili tumorske celice PyMT, lahko predpostavimo, da je bila odsotnost statistično značilnih razlik med skupinama kljub povišanemu nivoju ROS-ov v tumorskih celicah PyMT;StfB-/ povezana z gojenjem tumorskih celic v pogojih *ex vivo*.

Za boljše razumevanje avtofagije ter določanje potencialne vloge stefina B pri njeni regulaciji bi tudi mi potrebovali dodatne študije *in vivo*. Kljub temu lahko na podlagi rezultatov zaključimo, da je za preživetje tumorskih celic PyMT v pogojih dolgotrajnega stradanja ključna ohranjena avtofagija. Iz dobljenih rezultatov lahko zaključimo tudi, da stefin B pri gojenju tumorskih celic *ex vivo* ni imel bistvenega vpliva na potek avtofagije, saj so se tumorske celice PyMTStfB-/- kljub zvišanemu nivoju ROS ob indukciji oz. inhibiciji avtofagije obnašale primerljivo kakor tumorske celice divjega tipa. V nadaljnjih fazah raziskav bi bilo poleg študij *in vivo* zanimivo raziskati natančen izvor ROS v PyMT;StfB-/-, mehanizem njihovega nastanka, morfološko analizo mitohondrijev in potencialne neinhibitorne vloge stefina B v povezavi s homeostazo mitohondrijev in apoptozo. Prav tako bi bilo zanimivo preveriti tudi, ali bi z inhibicijo avtofagije lahko dosegli senzitizacijo tumorskih celic na konvencionalna antitumorska zdravljenja in ali bi s takšno strategijo lahko raziskali potencialne povezave med stefinom B in avtofagijo.

# 6 Zaključki

Uspešno smo okarakterizirali cisteinsko proteinazo avtofagin-2 iz parazita *T. cruzi*, TcAtg4.2. S pomočjo kombinatorne tetrapeptidne fluorogene knjižnice smo določili tudi njegovo substratno specifičnost. S podrobno analizo in primerjavo že obstoječih rezultatov substratne specifičnosti človeškega ortologa HsAtg4B ter naših rezultatov smo uspešno sintetizirali specifična tetrapeptidna substrata za TcAtg4.2, Ac-KTChaG-AFC in Ac-KKChaG-AFC, ki sta v trenutni obliki primerna za uporabo v študijah *in vitro*. Z mutagenezo aminokislinskih preostankov, ki so ključni za regulacijo katalitične aktivnosti TcAtg4.2, smo dokazali evolucijsko ohranjenost mehanizma regulacije aktivnosti in katalize dveh evolucijsko ohranjenih ortologov, TcAtg4.2 in HsAtg4B.

Pokazali smo, da imajo tumorske celice z izbitim genom za *stefin B* v primerjavi s tumorskimi celicami divjega tipa povišan bazalni nivo avtofagije ter da ima avtofagija pri obeh skupinah tumorskih celic ključno vlogo pri ohranjanju celične homeostaze. Zaradi odsotnosti statistično značilnih razlik med obema skupinama pri različnih tretiranjih lahko sklepamo, da stefin B najverjetneje ni udeležen pri regulaciji avtofagije. Za potrditev te hipoteze bodo potrebne nadaljnje študije *in vivo*, ki bodo potrdile ali ovrgle potencialno vlogo stefina B pri regulaciji avtofagije v tumorskih celicah.

# Zahvale

Doktorsko delo sem opravila na Odseku za biokemijo, molekularno in strukturno biologijo B1, na Institutu »Jožef Stefan« v okviru programske skupine »Proteoliza in njena regulacija« in Centra odličnosti za integrirane pristope v kemiji in biologiji proteinov »CIPKeBiP« pod mentorstvom prof. ddr. Borisa Turka. Za mentorstvo na podiplomskem študiju se mu iskreno zahvaljujem.

Dr. Dejanu Cagliču se zahvaljujem za ves trud, čas in energijo, ki jo je vložil v vodenje mojega raziskovalnega dela ter prijetno vzdušje v laboratoriju.

Prof. dr. Veroniki Stoka se zahvaljujem za kritičen pregled doktorske disertacije kot tudi za vse nasvete in pomoč tekom raziskovalnega dela. Prav tako se za kritičen pregled doktorske disertacije zahvaljujem tudi doc. dr. Marku Fonoviću in prof. dr. Ani Plemenitaš.

Prof. dr. Marcinu Dragu, dr. Marcinu Porebi, Aleksandri Wilk in Agati Borowik (Tehniška univerza v Wroclawu, Fakulteta za kemijo, oddelek za bioorgansko kemijo, Wroclaw, Poljska) se zahvaljujem za sintezo fluorogenih substratov in pametne aktivnostne sonde.

Prof. dr. Guyju Salvesenu (Medicinski raziskovalni inštitut Sanford-Burnham, San Diego (La Jolla), Californija) se zahvaljujem za DNA konstrukte, ki nosijo genske zapise za izražanje rekombinantnih proteinov SENP1, SENP2 in UCH-L3.

Dr. Mihi Butinarju se zahvaljujem za pripravo mišjih primarnih tumorskih celic MMTV-PyMT ter za pomoč pri eksperimentalnem delu in analizi rezultatov pretočne citometrije. Zahvaljujem se mu tudi za ves »neznanstveni« čas in trud.

Zahvaljujem se tudi prof. dr. Evi Žerovnik, dr. Iztoku Dolencu, dr. Mihi Renku in dr. Marku Miheliču za pomoč pri uvajanju novih tehnik in interpretaciji rezultatov.

Ivici Štefe se zahvaljujem za pripravo rekombinantnih človeških cisteinskih katepsinov, Mojci Trstenjak Prebanda pa za pomoč pri kloniranju.

Zahvaljujem se tudi dr. Georgyju Mikhaylovu, Tamari Marič, dr. Katarini Maher, dr. Miri Polajnar, Lovru Kramerju, Nežki Kavčič, dr. Katarini Pegan in vsem sodelavcem odseka B1 za pomoč in prijetno počutje na odseku.

Nazadnje se želim zahvaliti Mihi ter sestri, mami in očetu za vso podporo v dobrih in slabih trenutkih.

# Literatura in viri


1. Hershko A, Ciechanover A. The ubiquitin system. *Annual review of biochemistry.* 1998;67:425-479.

2. Takeshige K, Baba M, Tsuboi S, Noda T, Ohsumi Y. Autophagy in yeast demonstrated with proteinase-deficient mutants and conditions for its induction. *The Journal of cell biology.* Oct 1992;119(2):301-311.

3. Bjorkoy G, Lamark T, Brech A, et al. p62/SQSTM1 forms protein aggregates degraded by autophagy and has a protective effect on huntingtin-induced cell death. *The Journal of cell biology.* Nov 21 2005;171(4):603-614.

4. Bernales S, McDonald KL, Walter P. Autophagy counterbalances endoplasmic reticulum expansion during the unfolded protein response. *PLoS biology.* Nov 2006;4(12):e423.

5. Shirihai OS, Song M, Dorn GW, 2nd. How Mitochondrial Dynamism Orchestrates Mitophagy. *Circulation research.* May 22 2015;116(11):1835-1849.

6. Chen Y, McMillan-Ward E, Kong J, Israels SJ, Gibson SB. Mitochondrial electron-transport-chain inhibitors of complexes I and II induce autophagic cell death mediated by reactive oxygen species. *Journal of cell science.* Dec 1 2007;120(Pt 23):4155-4166.

7. Sanjuan MA, Dillon CP, Tait SW, et al. Toll-like receptor signalling in macrophages links the autophagy pathway to phagocytosis. *Nature.* Dec 20 2007;450(7173):1253-1257.

8. Wang Y, Weiss LM, Orlofsky A. Host cell autophagy is induced by Toxoplasma gondii and contributes to parasite growth. *J Biol Chem.* Jan 16 2009;284(3):1694-1701.

9. Long X, Ortiz-Vega S, Lin Y, Avruch J. Rheb binding to mammalian target of rapamycin (mTOR) is regulated by amino acid sufficiency. *J Biol Chem.* Jun 24 2005;280(25):23433-23436.

10. Kim E, Goraksha-Hicks P, Li L, Neufeld TP, Guan KL. Regulation of TORC1 by Rag GTPases in nutrient response. *Nature cell biology.* Aug 2008;10(8):935-945.

11. Byfield MP, Murray JT, Backer JM. hVps34 is a nutrient-regulated lipid kinase required for activation of p70 S6 kinase. *J Biol Chem.* Sep 23 2005;280(38):33076-33082.

12. Chen JL, Lin HH, Kim KJ, Lin A, Forman HJ, Ann DK. Novel roles for protein kinase Cdelta-dependent signaling pathways in acute hypoxic stress-induced autophagy. *J Biol Chem.* Dec 5 2008;283(49):34432-34444.

13. Papandreou I, Lim AL, Laderoute K, Denko NC. Hypoxia signals autophagy in tumor cells via AMPK activity, independent of HIF-1, BNIP3, and BNIP3L. *Cell death and differentiation.* Oct 2008;15(10):1572-1581.

14. Vasseur S, Afzal S, Tardivel-Lacombe J, Park DS, Iovanna JL, Mak TW. DJ-1/PARK7 is an important mediator of hypoxia-induced cellular responses. *Proceedings of the National Academy of Sciences of the United States of America.* Jan 27 2009;106(4):1111-1116.

15. Wada Y, Sun-Wada GH, Kawamura N, Aoyama M. Role of autophagy in embryogenesis. *Current opinion in genetics & development.* Aug 2014;27:60-66.

16. Wang S, Li B, Qiao H, et al. Autophagy-related gene Atg5 is essential for astrocyte differentiation in the developing mouse cortex. *EMBO reports.* Oct 2014;15(10):1053-1061.

17. Lv X, Jiang H, Li B, et al. The crucial role of Atg5 in cortical neurogenesis during early brain development. *Scientific reports.* 2014;4:6010.

18. Alvarez VE, Kosec G, Sant'Anna C, Turk V, Cazzulo JJ, Turk B. Autophagy is involved in nutritional stress response and differentiation in Trypanosoma cruzi. *J Biol Chem.* Feb 8 2008;283(6):3454-3464.

19. Barquilla A, Crespo JL, Navarro M. Rapamycin inhibits trypanosome cell growth by preventing TOR complex 2 formation. *Proceedings of the National Academy of Sciences of the United States of America.* Sep 23 2008;105(38):14579-14584.

20. Shapiro IM, Layfield R, Lotz M, Settembre C, Whitehouse C. Boning up on autophagy: the role of autophagy in skeletal biology. *Autophagy.* Jan 2014;10(1):7-19.

21. Mizushima N, Levine B. Autophagy in mammalian development and differentiation. *Nature cell biology.* Sep 2010;12(9):823-830.

22. Gozuacik D, Kimchi A. Autophagy as a cell death and tumor suppressor mechanism. *Oncogene.* Apr 12 2004;23(16):2891-2906.

23. Lorin S, Hamai A, Mehrpour M, Codogno P. Autophagy regulation and its role in cancer. *Seminars in cancer biology.* Oct 2013;23(5):361-379.

24. Levine B, Deretic V. Unveiling the roles of autophagy in innate and adaptive immunity. *Nature reviews. Immunology.* Oct 2007;7(10):767-777.

25. Qu X, Yu J, Bhagat G, et al. Promotion of tumorigenesis by heterozygous disruption of the beclin 1 autophagy gene. *The Journal of clinical investigation.* Dec 2003;112(12):1809-1820.

26. Menzies FM, Fleming A, Rubinsztein DC. Compromised autophagy and neurodegenerative diseases. *Nature reviews. Neuroscience.* May 20 2015;16(6):345-357.

27. Tanaka Y, Guhde G, Suter A, et al. Accumulation of autophagic vacuoles and cardiomyopathy in LAMP-2-deficient mice. *Nature.* Aug 24 2000;406(6798):902-906.

28. Orvedahl A, Alexander D, Talloczy Z, et al. HSV-1 ICP34.5 confers neurovirulence by targeting the Beclin 1 autophagy protein. *Cell host & microbe.* Mar 15 2007;1(1):23-35.

29. Yoshimori T, Noda T. Toward unraveling membrane biogenesis in mammalian autophagy. *Current opinion in cell biology.* Aug 2008;20(4):401-407.

30. Xie Z, Klionsky DJ. Autophagosome formation: core machinery and adaptations. *Nature cell biology.* Oct 2007;9(10):1102-1109.

31. Lecaille F, Cotton J, McKerrow JH, et al. Reversible inhibition of cathepsin L-like proteases by 4-mer pseudopeptides. *FEBS Lett.* Nov 2 2001;507(3):362-366.

32. Mizushima N, Levine B, Cuervo AM, Klionsky DJ. Autophagy fights disease through cellular self-digestion. *Nature.* Feb 28 2008;451(7182):1069-1075.

33. Ding WX, Manley S, Ni HM. The emerging role of autophagy in alcoholic liver disease. *Experimental biology and medicine.* May 1 2011;236(5):546-556.

34. Lynch-Day MA, Klionsky DJ. The Cvt pathway as a model for selective autophagy. *FEBS Lett.* Apr 2 2010;584(7):1359-1366.

35. Jung CH, Ro SH, Cao J, Otto NM, Kim DH. mTOR regulation of autophagy. *FEBS Lett.* Apr 2 2010;584(7):1287-1295.

36. Itakura E, Kishi C, Inoue K, Mizushima N. Beclin 1 forms two distinct phosphatidylinositol 3-kinase complexes with mammalian Atg14 and UVRAG. *Molecular biology of the cell.* Dec 2008;19(12):5360-5372.

37. Kihara A, Noda T, Ishihara N, Ohsumi Y. Two distinct Vps34 phosphatidylinositol 3-kinase complexes function in autophagy and carboxypeptidase Y sorting in Saccharomyces cerevisiae. *The Journal of cell biology.* Feb 5 2001;152(3):519-530.

38. Sun Q, Fan W, Chen K, Ding X, Chen S, Zhong Q. Identification of Barkor as a mammalian autophagy-specific factor for Beclin 1 and class III phosphatidylinositol 3-kinase. *Proceedings of the National Academy of Sciences of the United States of America.* Dec 9 2008;105(49):19211-19216.

39. Nice DC, Sato TK, Stromhaug PE, Emr SD, Klionsky DJ. Cooperative binding of the cytoplasm to vacuole targeting pathway proteins, Cvt13 and Cvt20, to phosphatidylinositol 3-phosphate at the pre-autophagosomal structure is required for selective autophagy. *J Biol Chem.* Aug 16 2002;277(33):30198-30207.

40. Obara K, Sekito T, Niimi K, Ohsumi Y. The Atg18-Atg2 complex is recruited to autophagic membranes via phosphatidylinositol 3-phosphate and exerts an essential function. *J Biol Chem.* Aug 29 2008;283(35):23972-23980.

41. Hayashi-Nishino M, Fujita N, Noda T, Yamaguchi A, Yoshimori T, Yamamoto A. Electron tomography reveals the endoplasmic reticulum as a membrane source for autophagosome formation. *Autophagy.* Feb 2010;6(2):301-303.

42. Young AR, Chan EY, Hu XW, et al. Starvation and ULK1-dependent cycling of mammalian Atg9 between the TGN and endosomes. *Journal of cell science.* Sep 15 2006;119(Pt 18):3888-3900.

43. Reggiori F, Shintani T, Nair U, Klionsky DJ. Atg9 cycles between mitochondria and the pre-autophagosomal structure in yeasts. *Autophagy.* Jul 2005;1(2):101-109.

44. Juhasz G, Neufeld TP. Autophagy: a forty-year search for a missing membrane source. *PLoS biology.* Feb 2006;4(2):e36.

45. Suzuki K, Kubota Y, Sekito T, Ohsumi Y. Hierarchy of Atg proteins in pre-autophagosomal structure organization. *Genes to cells : devoted to molecular & cellular mechanisms.* Feb 2007;12(2):209-218.

46. Geng J, Klionsky DJ. The Atg8 and Atg12 ubiquitin-like conjugation systems in macroautophagy. 'Protein modifications: beyond the usual suspects' review series. *EMBO reports.* Sep 2008;9(9):859-864.

47. Kuma A, Mizushima N, Ishihara N, Ohsumi Y. Formation of the approximately 350-kDa Apg12-Apg5.Apg16 multimeric complex, mediated by Apg16 oligomerization, is essential for autophagy in yeast. *J Biol Chem.* May 24 2002;277(21):18619-18625.

48. Xie Z, Nair U, Klionsky DJ. Atg8 controls phagophore expansion during autophagosome formation. *Molecular biology of the cell.* Aug 2008;19(8):3290-3298.

49. Jager S, Bucci C, Tanida I, et al. Role for Rab7 in maturation of late autophagic vacuoles. *Journal of cell science.* Sep 15 2004;117(Pt 20):4837-4848.

50. Kirisako T, Ichimura Y, Okada H, et al. The reversible modification regulates the membrane-binding state of Apg8/Aut7 essential for autophagy and the cytoplasm to vacuole targeting pathway. *The Journal of cell biology.* Oct 16 2000;151(2):263-276.

51. Sugawara K, Suzuki NN, Fujioka Y, Mizushima N, Ohsumi Y, Inagaki F. Structural basis for the specificity and catalysis of human Atg4B responsible for mammalian autophagy. *J Biol Chem.* Dec 2 2005;280(48):40058-40065.

52. Tanida I, Ueno T, Kominami E. Human light chain 3/MAP1LC3B is cleaved at its carboxyl-terminal Met121 to expose Gly120 for lipidation and targeting to autophagosomal membranes. *J Biol Chem.* Nov 12 2004;279(46):47704-47710.

53. Marino G, Uria JA, Puente XS, Quesada V, Bordallo J, Lopez-Otin C. Human autophagins, a family of cysteine proteinases potentially implicated in cell degradation by autophagy. *J Biol Chem.* Feb 7 2003;278(6):3671-3678.

54. Li M, Hou Y, Wang J, Chen X, Shao ZM, Yin XM. Kinetics comparisons of mammalian Atg4 homologues indicate selective preferences toward diverse Atg8 substrates. *J Biol Chem.* Mar 4 2011;286(9):7327-7338.

55. Noda NN, Ohsumi Y, Inagaki F. ATG systems from the protein structural point of view. *Chemical reviews.* Apr 2009;109(4):1587-1598.

56. Satoo K, Noda NN, Kumeta H, et al. The structure of Atg4B-LC3 complex reveals the mechanism of LC3 processing and delipidation during autophagy. *Embo J.* May 6 2009;28(9):1341-1350.

57. Li FJ, Shen Q, Wang C, Sun Y, Yuan AY, He CY. A role of autophagy in Trypanosoma brucei cell death. *Cellular microbiology.* Aug 2012;14(8):1242-1256.

58. Weidberg H, Shvets E, Shpilka T, Shimron F, Shinder V, Elazar Z. LC3 and GATE-16/GABARAP subfamilies are both essential yet act differently in autophagosome biogenesis. *Embo J.* Jun 2 2010;29(11):1792-1802.

59. Scherz-Shouval R, Shvets E, Fass E, Shorer H, Gil L, Elazar Z. Reactive oxygen species are essential for autophagy and specifically regulate the activity of Atg4. *Embo J.* Apr 4 2007;26(7):1749-1760.

60. Longatti A, Tooze SA. Vesicular trafficking and autophagosome formation. *Cell death and differentiation.* Jul 2009;16(7):956-965.

61. Klebig C, Seitz S, Arnold W, et al. Characterization of {gamma}-aminobutyric acid type A receptor-associated protein, a novel tumor suppressor, showing reduced expression in breast cancer. *Cancer research.* Jan 15 2005;65(2):394-400.

62. Comes F, Matrone A, Lastella P, et al. A novel cell type-specific role of p38alpha in the control of autophagy and cell death in colorectal cancer cells. *Cell death and differentiation.* Apr 2007;14(4):693-702.

63. Schwarten M, Mohrluder J, Ma P, et al. Nix directly binds to GABARAP: a possible crosstalk between apoptosis and autophagy. *Autophagy.* Jul 2009;5(5):690-698.

64. Tanida I, Wakabayashi M, Kanematsu T, et al. Lysosomal turnover of GABARAP-phospholipid conjugate is activated during differentiation of C2C12 cells to myotubes without inactivation of the mTor kinase-signaling pathway. *Autophagy.* Oct-Dec 2006;2(4):264-271.

65. Sugawara K, Suzuki NN, Fujioka Y, Mizushima N, Ohsumi Y, Inagaki F. The crystal structure of microtubule-associated protein light chain 3, a mammalian homologue of Saccharomyces cerevisiae Atg8. *Genes to cells : devoted to molecular & cellular mechanisms.* Jul 2004;9(7):611-618.

66. Kouno T, Mizuguchi M, Tanida I, et al. Solution structure of microtubule-associated protein light chain 3 and identification of its functional subdomains. *J Biol Chem.* Jul 1 2005;280(26):24610-24617.

67. Kabeya Y, Mizushima N, Ueno T, et al. LC3, a mammalian homologue of yeast Apg8p, is localized in autophagosome membranes after processing. *Embo J.* Nov 1 2000;19(21):5720-5728.

68. Kabeya Y, Mizushima N, Yamamoto A, Oshitani-Okamoto S, Ohsumi Y, Yoshimori T. LC3, GABARAP and GATE16 localize to autophagosomal membrane depending on form-II formation. *Journal of cell science.* Jun 1 2004;117(Pt 13):2805-2812.

69. Tanida I, Ueno T, Kominami E. LC3 conjugation system in mammalian autophagy. *The international journal of biochemistry & cell biology.* Dec 2004;36(12):2503-2518.

70. Koopmann R, Muhammad K, Perbandt M, Betzel C, Duszenko M. Trypanosoma brucei ATG8: structural insights into autophagic-like mechanisms in protozoa. *Autophagy.* Nov 2009;5(8):1085-1091.

71. Levine B, Kroemer G. Autophagy in the pathogenesis of disease. *Cell.* Jan 11 2008;132(1):27-42.

72. Kourtis N, Tavernarakis N. Autophagy and cell death in model organisms. *Cell death and differentiation.* Jan 2009;16(1):21-30.

73. Kuma A, Hatano M, Matsui M, et al. The role of autophagy during the early neonatal starvation period. *Nature.* Dec 23 2004;432(7020):1032-1036.

74. Singh R, Kaushik S, Wang Y, et al. Autophagy regulates lipid metabolism. *Nature.* Apr 30 2009;458(7242):1131-1135.

75. Duszenko M, Ginger ML, Brennand A, et al. Autophagy in protists. *Autophagy.* Feb 2011;7(2):127-158.

76. De Souza W. Basic cell biology of Trypanosoma cruzi. *Current pharmaceutical design.* 2002;8(4):269-285.

77. Contreras VT, Morel CM, Goldenberg S. Stage specific gene expression precedes morphological changes during Trypanosoma cruzi metacyclogenesis. *Molecular and biochemical parasitology.* Jan 1985;14(1):83-96.

78. Alvarez VE, Kosec G, Sant Anna C, Turk V, Cazzulo JJ, Turk B. Blocking autophagy to prevent parasite differentiation: a possible new strategy for fighting parasitic infections? *Autophagy.* Apr 2008;4(3):361-363.

79. Sanderson CJ, de Souza W. A morphological study of the interaction between Trypanosoma cruzi and rat eosinophils, neutrophils and macrophages in vitro. *Journal of cell science.* Jun 1979;37:275-286.

80. Barrias ES, de Carvalho TM, De Souza W. Trypanosoma cruzi: Entry into Mammalian Host Cells and Parasitophorous Vacuole Formation. *Frontiers in immunology.* 2013;4:186.

81. World-Health-Organization. *Chagas disease: control and elimination* 22th April 2010 2010.

82. Coura JR. Chagas disease: what is known and what is needed--a background article. *Memorias do Instituto Oswaldo Cruz.* Oct 30 2007;102 Suppl 1:113-122.

83. Ribeiro AL, Nunes MP, Teixeira MM, Rocha MO. Diagnosis and management of Chagas disease and cardiomyopathy. *Nat Rev Cardiol.* Oct 2012;9(10):576-589.

84. Prata A. Clinical and epidemiological aspects of Chagas disease. *The Lancet infectious diseases.* Sep 2001;1(2):92-100.

85. Marr JJ, Docampo R. Chemotherapy for Chagas' disease: a perspective of current therapy and considerations for future research. *Reviews of infectious diseases.* Nov-Dec 1986;8(6):884-903.

86. Franke de Cazzulo BM, Martinez J, North MJ, Coombs GH, Cazzulo JJ. Effects of proteinase inhibitors on the growth and differentiation of Trypanosoma cruzi. *FEMS microbiology letters.* Nov 15 1994;124(1):81-86.

87. Harth G, Andrews N, Mills AA, Engel JC, Smith R, McKerrow JH. Peptide-fluoromethyl ketones arrest intracellular replication and intercellular transmission of Trypanosoma cruzi. *Molecular and biochemical parasitology.* Mar 1993;58(1):17-24.

88. Meirelles MN, Juliano L, Carmona E, et al. Inhibitors of the major cysteinyl proteinase (GP57/51) impair host cell invasion and arrest the intracellular development of Trypanosoma cruzi in vitro. *Molecular and biochemical parasitology.* Jun 1992;52(2):175-184.

89. Barr SC, Warner KL, Kornreic BG, et al. A cysteine protease inhibitor protects dogs from cardiac damage during infection by Trypanosoma cruzi. *Antimicrobial agents and chemotherapy.* Dec 2005;49(12):5160-5161.

90. Futreal PA, Soderkvist P, Marks JR, et al. Detection of frequent allelic loss on proximal chromosome 17q in sporadic breast carcinoma using microsatellite length polymorphisms. *Cancer research.* May 1 1992;52(9):2624-2627.

91. Gao X, Zacharek A, Salkowski A, et al. Loss of heterozygosity of the BRCA1 and other loci on chromosome 17q in human prostate cancer. *Cancer research.* Mar 1 1995;55(5):1002-1005.

92. Russell SE, Hickey GI, Lowry WS, White P, Atkinson RJ. Allele loss from chromosome 17 in ovarian cancer. *Oncogene.* Oct 1990;5(10):1581-1583.

93. Liang XH, Jackson S, Seaman M, et al. Induction of autophagy and inhibition of tumorigenesis by beclin 1. *Nature.* Dec 9 1999;402(6762):672-676.

94. Marino G, Salvador-Montoliu N, Fueyo A, Knecht E, Mizushima N, Lopez-Otin C. Tissue-specific autophagy alterations and increased tumorigenesis in mice deficient in Atg4C/autophagin-3. *J Biol Chem.* Jun 22 2007;282(25):18573-18583.

95. Mathew R, Karantza-Wadsworth V, White E. Role of autophagy in cancer. *Nature reviews. Cancer.* Dec 2007;7(12):961-967.

96. Mathew R, Karp CM, Beaudoin B, et al. Autophagy suppresses tumorigenesis through elimination of p62. *Cell.* Jun 12 2009;137(6):1062-1075.

97. Turcotte S, Chan DA, Sutphin PD, Hay MP, Denny WA, Giaccia AJ. A molecule targeting VHL-deficient renal cell carcinoma that induces autophagy. *Cancer cell.* Jul 8 2008;14(1):90-102.

98. Ogier-Denis E, Houri JJ, Bauvy C, Codogno P. Guanine nucleotide exchange on heterotrimeric Gi3 protein controls autophagic sequestration in HT-29 cells. *J Biol Chem.* Nov 8 1996;271(45):28593-28600.

99. Liang XH, Yu J, Brown K, Levine B. Beclin 1 contains a leucine-rich nuclear export signal that is required for its autophagy and tumor suppressor function. *Cancer research.* Apr 15 2001;61(8):3443-3449.

100. Proikas-Cezanne T, Waddell S, Gaugel A, Frickey T, Lupas A, Nordheim A. WIPI-1alpha (WIPI49), a member of the novel 7-bladed WIPI protein family, is aberrantly expressed in human cancer and is linked to starvation-induced autophagy. *Oncogene.* Dec 16 2004;23(58):9314-9325.

101. Susan PP, Dunn WA, Jr. Starvation-induced lysosomal degradation of aldolase B requires glutamine 111 in a signal sequence for chaperone-mediated transport. *Journal of cellular physiology.* Apr 2001;187(1):48-58.

102. Ito H, Daido S, Kanzawa T, Kondo S, Kondo Y. Radiation-induced autophagy is associated with LC3 and its inhibition sensitizes malignant glioma cells. *International journal of oncology.* May 2005;26(5):1401-1410.

103. Paglin S, Hollister T, Delohery T, et al. A novel response of cancer cells to radiation involves autophagy and formation of acidic vesicles. *Cancer research.* Jan 15 2001;61(2):439-444.

104. Livesey KM, Tang D, Zeh HJ, Lotze MT. Autophagy inhibition in combination cancer treatment. *Current opinion in investigational drugs.* Dec 2009;10(12):1269-1279.

105. Rossi A, Deveraux Q, Turk B, Sali A. Comprehensive search for cysteine cathepsins in the human genome. *Biological chemistry.* May 2004;385(5):363-372.

106. Turk V, Stoka V, Vasiljeva O, et al. Cysteine cathepsins: from structure, function and regulation to new frontiers. *Biochim Biophys Acta.* Jan 2012;1824(1):68-88.

107. Turk B, Turk D, Turk V. Protease signalling: the cutting edge. *Embo J.* Apr 4 2012;31(7):1630-1643.

108. Turk B, Turk D, Salvesen GS. Regulating cysteine protease activity: essential role of protease inhibitors as guardians and regulators. *Current pharmaceutical design.* 2002;8(18):1623-1637.

109. Rawlings ND, Barrett AJ. Evolution of proteins of the cystatin superfamily. *Journal of molecular evolution.* Jan 1990;30(1):60-71.

110. Abrahamson M, Barrett AJ, Salvesen G, Grubb A. Isolation of six cysteine proteinase inhibitors from human urine. Their physicochemical and enzyme kinetic properties and concentrations in biological fluids. *J Biol Chem.* Aug 25 1986;261(24):11282-11289.

111. Sloane BF, Dunn JR, Honn KV. Lysosomal cathepsin B: correlation with metastatic potential. *Science.* Jun 5 1981;212(4499):1151-1153.

112. Gocheva V, Joyce JA. Cysteine cathepsins and the cutting edge of cancer invasion. *Cell cycle.* Jan 1 2007;6(1):60-64.

113. Gabrijelcic D, Svetic B, Spaic D, et al. Cathepsins B, H and L in human breast carcinoma. *European journal of clinical chemistry and clinical biochemistry : journal of the Forum of European Clinical Chemistry Societies.* Feb 1992;30(2):69-74.

114. Talieri M, Papadopoulou S, Scorilas A, et al. Cathepsin B and cathepsin D expression in the progression of colorectal adenoma to carcinoma. *Cancer letters.* Mar 8 2004;205(1):97-106.

115. Campo E, Munoz J, Miquel R, et al. Cathepsin B expression in colorectal carcinomas correlates with tumor progression and shortened patient survival. *The American journal of pathology.* Aug 1994;145(2):301-309.

116. Kos J, Lah TT. Cysteine proteinases and their endogenous inhibitors: target proteins for prognosis, diagnosis and therapy in cancer (review). *Oncology reports.* Nov-Dec 1998;5(6):1349-1361.

117. Jedeszko C, Sloane BF. Cysteine cathepsins in human cancer. *Biological chemistry.* Nov 2004;385(11):1017-1027.

118. Sokol JP, Schiemann WP. Cystatin C antagonizes transforming growth factor beta signaling in normal and cancer cells. *Molecular cancer research : MCR.* Mar 2004;2(3):183-195.

119. Gocheva V, Zeng W, Ke D, et al. Distinct roles for cysteine cathepsin genes in multistage tumorigenesis. *Genes & development.* Mar 1 2006;20(5):543-556.

120. Vasiljeva O, Papazoglou A, Kruger A, et al. Tumor cell-derived and macrophage-derived cathepsin B promotes progression and lung metastasis of mammary cancer. *Cancer research.* May 15 2006;66(10):5242-5250.

121. Strojan P, Budihna M, Smid L, et al. Prognostic significance of cysteine proteinases cathepsins B and L and their endogenous inhibitors stefins A and B in patients with squamous cell carcinoma of the head and neck. *Clinical cancer research : an official journal of the American Association for Cancer Research.* Mar 2000;6(3):1052-1062.

122. Kos J, Krasovec M, Cimerman N, Nielsen HJ, Christensen IJ, Brunner N. Cysteine proteinase inhibitors stefin A, stefin B, and cystatin C in sera from patients with colorectal cancer: relation to prognosis. *Clinical cancer research : an official journal of the American Association for Cancer Research.* Feb 2000;6(2):505-511.

123. Butinar M, Prebanda MT, Rajkovic J, et al. Stefin B deficiency reduces tumor growth via sensitization of tumor cells to oxidative stress in a breast cancer model. *Oncogene.* Jun 26 2014;33(26):3392-3400.

124. Guy CT, Cardiff RD, Muller WJ. Induction of mammary tumors by expression of polyomavirus middle T oncogene: a transgenic mouse model for metastatic disease. *Molecular and cellular biology.* Mar 1992;12(3):954-961.

125. Turk B. Targeting proteases: successes, failures and future prospects. *Nature reviews. Drug discovery.* Sep 2006;5(9):785-799.

126. Schechter I, Berger A. On the size of the active site in proteases. I. Papain. *Biochemical and biophysical research communications.* Apr 20 1967;27(2):157-162.

127. Rano TA, Timkey T, Peterson EP, et al. A combinatorial approach for determining protease specificities: application to interleukin-1beta converting enzyme (ICE). *Chemistry & biology.* Feb 1997;4(2):149-155.

128. Hu HY, Vats D, Vizovisek M, et al. In vivo imaging of mouse tumors by a lipidated cathepsin S substrate. *Angewandte Chemie.* Jul 14 2014;53(29):7669-7673.

129. Sanman LE, Bogyo M. Activity-based profiling of proteases. *Annual review of biochemistry.* 2014;83:249-273.

130. Kuhelj R, Dolinar M, Pungercar J, Turk V. The preparation of catalytically active human cathepsin B from its precursor expressed in Escherichia coli in the form of inclusion bodies. *Eur J Biochem.* Apr 15 1995;229(2):533-539.

131. Bromme D, Nallaseth FS, Turk B. Production and activation of recombinant papain-like cysteine proteases. *Methods.* Feb 2004;32(2):199-206.

132. Mihelic M, Dobersek A, Guncar G, Turk D. Inhibitory fragment from the p41 form of invariant chain can regulate activity of cysteine cathepsins in antigen presentation. *J Biol Chem.* May 23 2008;283(21):14453-14460.

133. Drag M, Mikolajczyk J, Bekes M, et al. Positional-scanning fluorigenic substrate libraries reveal unexpected specificity determinants of DUBs (deubiquitinating enzymes). *The Biochemical journal.* Nov 1 2008;415(3):367-375.

134. Drag M, Mikolajczyk J, Krishnakumar IM, Huang Z, Salvesen GS. Activity profiling of human deSUMOylating enzymes (SENPs) with synthetic substrates suggests an unexpected specificity of two newly characterized members of the family. *The Biochemical journal.* Jan 15 2008;409(2):461-469.

135. Shu CW, Drag M, Bekes M, Zhai D, Salvesen GS, Reed JC. Synthetic substrates for measuring activity of autophagy proteases: autophagins (Atg4). *Autophagy.* Oct 2010;6(7):936-947.

136. Zhang Y, Cremer PS. Interactions between macromolecules and ions: The Hofmeister series. *Current opinion in chemical biology.* Dec 2006;10(6):658-663.

137. Yang Z. Hofmeister effects: an explanation for the impact of ionic liquids on biocatalysis. *Journal of biotechnology.* Oct 12 2009;144(1):12-22.

138. Whitmore L, Wallace BA. Protein secondary structure analyses from circular dichroism spectroscopy: methods and reference databases. *Biopolymers.* May 2008;89(5):392-400.

139. Andrade MA, Chacon P, Merelo JJ, Moran F. Evaluation of secondary structure of proteins from UV circular dichroism spectra using an unsupervised learning neural network. *Protein Eng.* Jun 1993;6(4):383-390.

140. Biasini M, Bienert S, Waterhouse A, et al. SWISS-MODEL: modelling protein tertiary and quaternary structure using evolutionary information. *Nucleic Acids Res.* Jul 2014;42(Web Server issue):W252-258.

141. Ma J, Wang S, Zhao F, Xu J. Protein threading using context-specific alignment potential. *Bioinformatics.* Jul 1 2013;29(13):i257-265.

142. Repnik U, Stoka V, Turk V, Turk B. Lysosomes and lysosomal cathepsins in cell death. *Biochimica et biophysica acta.* Jan 2012;1824(1):22-33.

143. Turk B, Turk V. Lysosomes as "suicide bags" in cell death: myth or reality? *J Biol Chem.* Aug 14 2009;284(33):21783-21787.

144. Klionsky DJ, Abdalla FC, Abeliovich H, et al. Guidelines for the use and interpretation of assays for monitoring autophagy. *Autophagy.* Apr 2012;8(4):445-544.

145. He C, Klionsky DJ. Regulation mechanisms and signaling pathways of autophagy. *Annu Rev Genet.* 2009;43:67-93.

146. Ichimura Y, Kirisako T, Takao T, et al. A ubiquitin-like system mediates protein lipidation. *Nature.* Nov 23 2000;408(6811):488-492.

147. Williams RA, Woods KL, Juliano L, Mottram JC, Coombs GH. Characterization of unusual families of ATG8-like proteins and ATG12 in the protozoan parasite Leishmania major. *Autophagy.* Feb 2009;5(2):159-172.

148. Thornberry NA, Rano TA, Peterson EP, et al. A combinatorial approach defines specificities of members of the caspase family and granzyme B. Functional relationships established for key mediators of apoptosis. *J Biol Chem.* Jul 18 1997;272(29):17907-17911.

149. Poreba M, Mihelic M, Krai P, et al. Unnatural amino acids increase activity and specificity of synthetic substrates for human and malarial cathepsin C. *Amino acids.* Apr 2014;46(4):931-943.

150. Kasperkiewicz P, Poreba M, Snipas SJ, et al. Design of ultrasensitive probes for human neutrophil elastase through hybrid combinatorial substrate library profiling. *Proceedings of the National Academy of Sciences of the United States of America.* Feb 18 2014;111(7):2518-2523.

151. Poreba M, Kasperkiewicz P, Snipas SJ, Fasci D, Salvesen GS, Drag M. Unnatural amino acids increase sensitivity and provide for the design of highly selective caspase substrates. *Cell death and differentiation.* Sep 2014;21(9):1482-1492.

152. Boyd SE, Kerr FK, Albrecht DW, de la Banda MG, Ng N, Pike RN. Cooperative effects in the substrate specificity of the complement protease C1s. *Biol Chem.* May-Jun 2009;390(5-6):503-507.

153. Kosec G, Alvarez V, Cazzulo JJ. Cysteine proteinases of Trypanosoma cruzi: from digestive enzymes to programmed cell death mediators. *Biocell : official journal of the Sociedades Latinoamericanas de Microscopia Electronica ... et. al.* Dec 2006;30(3):479-490.

154. Jose Cazzulo J, Stoka V, Turk V. The major cysteine proteinase of Trypanosoma cruzi: a valid target for chemotherapy of Chagas disease. *Current pharmaceutical design.* Aug 2001;7(12):1143-1156.

155. Lecaille F, Authie E, Moreau T, Serveau C, Gauthier F, Lalmanach G. Subsite specificity of trypanosomal cathepsin L-like cysteine proteases. Probing the S2 pocket with phenylalanine-derived amino acids. *Eur J Biochem.* May 2001;268(9):2733-2741.

156. Yue Z, Jin S, Yang C, Levine AJ, Heintz N. Beclin 1, an autophagy gene essential for early embryonic development, is a haploinsufficient tumor suppressor. *Proceedings of the National Academy of Sciences of the United States of America.* Dec 9 2003;100(25):15077-15082.

157. Edinger AL, Thompson CB. Defective autophagy leads to cancer. *Cancer cell.* Dec 2003;4(6):422-424.

158. Apel A, Herr I, Schwarz H, Rodemann HP, Mayer A. Blocked autophagy sensitizes resistant carcinoma cells to radiation therapy. *Cancer research.* Mar 1 2008;68(5):1485-1494.

159. Zhao D, Yuan H, Yi F, Meng C, Zhu Q. Autophagy prevents doxorubicininduced apoptosis in osteosarcoma. *Molecular medicine reports.* May 2014;9(5):1975-1981.

160. Kanzawa T, Germano IM, Komata T, Ito H, Kondo Y, Kondo S. Role of autophagy in temozolomide-induced cytotoxicity for malignant glioma cells. *Cell death and differentiation.* Apr 2004;11(4):448-457.

161. Xie BS, Zhao HC, Yao SK, et al. Autophagy inhibition enhances etoposide-induced cell death in human hepatoma G2 cells. *International journal of molecular medicine.* Apr 2011;27(4):599-606.

162. Qadir MA, Kwok B, Dragowska WH, et al. Macroautophagy inhibition sensitizes tamoxifen-resistant breast cancer cells and enhances mitochondrial depolarization. *Breast cancer research and treatment.* Dec 2008;112(3):389-403.

163. Kondo Y, Kanzawa T, Sawaya R, Kondo S. The role of autophagy in cancer development and response to therapy. *Nature reviews. Cancer.* Sep 2005;5(9):726-734.

164. Avruch J, Lin Y, Long X, Murthy S, Ortiz-Vega S. Recent advances in the regulation of the TOR pathway by insulin and nutrients. *Current opinion in clinical nutrition and metabolic care.* Jan 2005;8(1):67-72.

# Kazalo slik

Slika 1: *Potek nastajanja avtofagosoma* (povzeto po [29]). PAS (angl. *phagophore assembly site*) predstavlja mesto nastanka fagofore. Slednja s pomočjo proteinov Atg raste in zaobjame celične komponente. Nastane vezikel, imenovan avtofagosom. Le-ta se združi z lizosomom v avtolizosom, kjer poteče razgradnja zajete vsebine. ..... 2

Slika 2: *Oblike avtofagije* (povzeto po [32]). Pojem avtofagije zajema tri različne procese razgradnje celičnih komponent: makroavtofagijo, mikroavtofagijo in od šaperonov odvisno avtofagijo (CMA). ..... 2

Slika 3: *Kompleksi Atg, ki omogočajo nastanek avtofagosoma* (povzeto po [33]). Za avtofagijo je značilen nastanek avtofagosoma. Pri njegovem nastajanju sodelujejo vsaj štirje med seboj natančno usklajeni kompleksi Atg: (1) Kompleks ULK1-Atg13-FIP200 je odgovoren za iniciacijo avtofagije. (2) Kompleks Vps34-Beklin 1 (PI3-kinaza razreda III) sodeluje pri nukleaciji. (3) Kompleks Atg9-Atg2-Atg18 na PAS prinaša lipide in omogoča rast in širitev fagofore. (4) Konjugacijska sistema, Atg5-Atg12-Atg16 ter sesalski homolog Atg8, LC3, uravnavata podaljšanje membrane avtofagosoma. ..... 3

Slika 4: *Tridimenzionalna struktura človeškega Atg4B* (povzeto po [55]). Človeški Atg4B (koda PDB: 2CY7) ima papainu podobno zvitje, sestavljeno iz devetih α-vijačnic (roza) in 13 β-trakov (modra). Aminokislinski preostanki katalitične triade so prikazani z rdečo, z zeleno je prikazan aminokislinski preostanek, ki gradi oksaanionsko luknjo. V kvadratu, ki ga omejuje prekinjena črta, je prikazana insercijska regija, ki predstavlja strukturno posebnost avtofaginov. ..... 6

Slika 5: *Konformacijske spremembe HsAtg4B ob vezavi substrata* (povzeto po [56]). Ob nastanku kompleksa HsAtg4B-LC3 regulatorna zanka in N-končni del encima spremenita konformacijo in omogočita procesiranje substratne molekule. S črno je označena »zaprta«, neaktivna konformacija avtofagina, z rdečo pa »odprta«, aktivna konformacija encima. S kvadratom, obdanim s prekinjeno črto, je označena insercijska regija, na katero se veže substratna molekula. ..... 6

Slika 6: *Struktura ubikvitina in človeških homologov Atg8* (povzeto po [55]). Vse molekule so predstavljene v enaki orientaciji. α-vijačnice so predstavljene z roza barvo, β-ploskve z modro. Posebna značilnost homologov Atg8 sta α-vijačnici α1 in α2, ki tvorita N-končno helično domeno. LC3 se v pogojih *in vitro* preko te domene veže na tubulin in mikrotubule. Kode PDB: ubikvitin – 1UB1, GATE-16 – 1EO6, GABARAP – 1GNU, LC3 – 1UGM. ..... 8

Slika 7: *Tridimenzionalna struktura TbAtg8.2 in superpozicija homologov Atg8* [70]. (A) Kristalna struktura *Trypanosoma brucei* Atg8.2. (B) Superpozicija homologov Atg8: rdeča – TbAtg8B, modra – GATE-16 (*Bos taurus*, koda PDB: Ieo6), zelena – LC3 (*Rattus norvegicus*, koda PDB: Iugm), rjava – GABARAP (*Rattus norvegicus*, koda PDB: Ikjt). ..... 8

Slika 8: *Življenjski cikel parazita Trypanosoma cruzi* [78]. Življenjski cikel *T. cruzi* vključuje štiri razvojne stopnje. Replikativni obliki sta epimastigot v insektnem vektorju in amastigot v sesalskih gostiteljih ter infektivni obliki metaciklični in krvni tripomastigot pri insektih in sesalcih. .....10

Slika 9: *Geografska porazdelitev ljudi, okuženih s T. cruzi v letu 2012* [83]. Največ ljudi, okuženih s *T. cruzi*, živi na področju Latinske Amerike, z migracijami latinskoameriških prebivalcev se je bolezen razširila tudi na ostale predele sveta. .....11

Slika 10: *Schechterjeva in Bergerjeva nomenklatura* (povzeto po [126]). Poimenovanje aminokislinskih preostankov okoli cepitvenega mesta v substratu in v vezavnem žepu encima.....15

Slika 11: *Zgradba fluorogene kombinatorne tetrapeptidne knjižnice*. Fluorogena kombinatorna tetrapeptidna knjižnica je sestavljena iz treh podknjižnic: P2, P3 in P4. Legenda: Mix – izokinetična mešanica vseh naravnih aminokislinskih preostankov, AA – preučevani aminokislinski preostanki na želeni poziciji (P2, P3 oz. P4), tričrkovna oznaka aminokislin – fiksirani aminokislinski preostanki. .....27

Slika 12: *Zgradba optimizirane substratne knjižnice*. Optimizirana substratna knjižnica je sestavljena iz enajstih substratov. 28

Slika 13: *Poliakrilamidna gelska elektroforeza v prisotnosti NaDS (12,5 % gel) očiščenih rekombinantnih proteinov*. Relativne molekulske mase očiščenih rekombinantnih proteinov ustrezajo izračunanim relativnim molekulskim masam rekombinantnih proteinov, izraženih v fuziji s histidinskim priveskom. .....31

Slika 14: *Poliakrilamidna gelska elektroforeza v prisotnosti NaDS (12,5 %) cepitev TcAtg8.1 in TcAtg8.2 s TcAtg4.2 divjega tipa (WT) in katalitično mutanto TcAtg4.2 C91S.* 50 ng TcAtg4.2 WT oz. TcAtg4.2 C9S in 2 µg TcAtg8.1 oz. TcAtg8.2 smo inkubirali v reakcijskem pufru (20 mM Tris-HCl pH 7,5, 150 mM NaCl, 5 mM DTT) pri 37 °C in stresanju 300 obr./min. Vzorčenje je potekalo v časovnih presledkih 0 min, 30 min, 60 min, 90 min in 120 min. Reakcijo smo prekinili z dodatkom 6 × pufra SDS in inkubacijo alikvotov pri 100 °C 5 min. .....32

Slika 15:*Poliakrilamidna gelska elektroforeza v prisotnosti NaDS (12,5 %) kinetike cepitev TcAtg8.1 in TcAtg8.2 s TcAtg4.2.* 0-150 ng TcAtg4.2 in 2 µg TcAtg8.1 oz. TcAtg8.2 smo inkubirali v reakcijskem pufru (20 mM Tris-HCl pH 7,5, 150 mM NaCl, 5 mM DTT) pri 37 °C in stresanju 300 obr./min. Reakcijo smo po 60 min prekinili z dodatkom 6 × pufra SDS in inkubacijo vzorcev pri 100 °C 5 min. .....32

Slika 16: *Vpliv aminokislinskega zaporedja na hitrost cepitve tetrapeptidnih fluorogenih substratov.* 4 µg TcAtg4.2 in 100 µM tetrapeptidnih fluorogenih substratov (Ac-ETFG-AFC, Ac-GTFG-AFC, AC-NTFG-AFC in Ac-STFG-AFC) smo inkubirali v 100 µl reakcijskega pufra (20 mM Tris-HCl pH 7,5, 150 mM NaCl, 5 mM DTT). Cepitve fluorogenih substratov smo spremljali na fluorimetru za mikrotitrske plošče (Safire, Tecan) pri vzbujanju $\lambda$ = 400 nm in emisiji $\lambda$ = 505 nm pri 37 °C 30 min. .....33

Slika 17: *Vpliv prisotnosti kozmotropnih soli na katalitično aktivnost TcAtg4.2.* Levo: 4 µg TcAtg4.2 in 100 µM Ac-ETFG-AFC smo inkubirali v 100 µl reakcijskega pufra (50 mM Tris-HCl pH 8,0, 1 M kozmotropna sol, 5 mM DTT). Desno: 4 µg TcAtg4.2 in 100 µM Ac-ETFG-AFC smo inkubirali v 100 µl reakcijskega pufra (50 mM Tris-HCl pH 8,0, 0–1,5 M $K_2HPO_4$, 5 mM DTT). Cepitev fluorogenega substrata smo spremljali na fluorimetru za mikrotitrske plošče (Safire, Tecan) pri vzbujanju λ = 400 nm in emisiji λ = 505 nm pri 37 °C 30 min. ..... 34

Slika 18: *Vpliv koncentracije $K_2HPO_4$ na urejenost sekundarne strukture TcAtg4.2.* Za merjenje daljnega-UV CD spektra (250–195 nm) smo uporabili proteinsko koncentracijo $A_{280}$ = 0,1. Podatke smo odčitavali v korakih po 1 nm. Izmerjene eliptične vrednosti smo preračunali s pomočjo enačbe, opisane v poglavju 3.3.2. ..... 34

Slika 19: *Vpliv dolžine polipeptidne verige na katalitično aktivnost TcAtg4.2*. 4 µg TcAtg4.2 in 100 µM fluorogene tetra-, heksa- in oktapeptide smo inkubirali v 100 µl reakcijskega pufra (50 mM Tris-HCl pH 8, 0,5 M $K_2HPO_4$, 5 mM DTT). Cepitve fluorogenih substratov smo spremljali na fluorimetru za mikrotitrske plošče (Safire, Tecan) pri vzbujanju λ = 355 nm in emisiji λ = 460 nm pri 37 °C 30 min. ..... 35

Slika 20: *pH profil encimske aktivnosti TcAtg4.2*. 4 µg TcAtg4.2 in 100 µM Ac-ETFG-AFC smo inkubirali v reakcijskih pufrih z različnimi pH (pH 6,5–9,0, 0,5 M $K_2HPO_4$, 5 mM DTT). Cepitev fluorogenega substrata smo spremljali na fluorimetru za mikrotitrske plošče (Safire, Tecan) pri vzbujanju λ = 400 nm in emisiji λ = 505 nm pri 37 °C 30 min. ..... 35

Slika 21: *Dendogram homologov Atg4.* Za izračun evolucijske oddaljenosti med homologi Atg4 smo uporabili metodo združevanja sosedov. Uporabili smo privzete nastavitve programa MEGA6, ki so se v več študijah izkazale za najoptimalnejše. ..... 36

Slika 22: *Poravnava aminokislinskih zaporedij katalitične domene homologov Atg4.* Prileganje aminokislinskih zaporedij katalitične domene človeških HsAtg4A (Genebank koda: NP_443168.2) in HsAtg4B (NM_013325), *T. cruzi* TcAtg4.1 (DQ768297.1) in TcAtg4.2 (DQ768298), *L major* LmAtg4.1(XM_001685663) in LmAtg4.2 (XM_001684564), *T. brucei* TbAtg4.1 (DQ768297.1) in TbAtg4.2 (XM_824593.1) ter kvasnega Atg4 (NP_014176.2). * – katalitični cisteinski preostanki, temno-siv okvirček – 4 aminokislinski preostanki, ki tvorijo regulatorno zanko, z belo označen S246 znotraj regulatorne zanke tvori van der Waalsove interakcije s Trp158 (z belo označen W v sivem okvirčku), rdeč Gly – omogoča fleksibilnost regulatorne zanke. ..... 37

Slika 23: *Superpozicija struktur človeških avtofaginov HsAtg4A in HsAtg4B ter modelov struktur TcAtg4.2.* Modela strukture TcAtg4.2 sta narejena na osnovi človeških HsAtg4A (koda PDB: 2p82) in HsAtg4B (koda PDB: 2d1i). Levo: Superpozicija struktur človeškega HsAtg4A (zelena) in HsAtg4B (rumena). Desno: Superpozicija modelov strukture TcAtg4.2 narejenih s programoma za napovedovanje struktur Swiss-Model (modra) in RaptoX (roza). Slike so narejene v programu PyMOL, verzija 1.3r1 edu (Schrödinger, LLC, USA). ..... 38

Slika 24: *Vpliv modifikacij TcAtg4.2 na hitrost cepitve naravnega substrata TcAtg8.1*. 0-150 ng TcAtg4.2 WT in mutant TcAtg4.2 dL, W158A, G244H, S246D, S246P, dN18 in dN24 in 2 µg TcAtg8.1 smo inkubirali v reakcijskem pufru (20 mM Tris-HCl pH 7,5, 150 mM NaCl, 5 mM DTT) pri 37 °C in stresanju 300 obr./min. Reakcijo smo po 60 min prekinili z dodatkom 6 × pufra SDS in inkubacijo vzorcev pri 100 °C 5 min. .....39

Slika 25: *Primerjava hitrosti cepitev Ac-ETFG-AFC s TcAtg4.2 WT, dN18, dN24 in dL*. 4 µg TcAtg4.2 WT in njegovih mutant TcAtg4.2 dN18, dN24 in dL ter 100 µM tetrapeptidnega fluorogenega substrata Ac-ETFG-AFC smo inkubirali v 100 µl reakcijskega pufra (20 mM Tris-HCl pH 8,0, 0,5 M $K_2HPO_4$, 5 mM DTT). Cepitev fluorogenega substrata smo spremljali na fluorimetru za mikrotitrske plošče (Safire, Tecan) pri vzbujanju $\lambda = 400$ nm in emisiji $\lambda = 505$ nm pri 37 °C 30 min. .....40

Slika 26: *Primerjava daljnega- in bližnjega-UV CD spektra TcAtg4.2 WT in TcAtg4.2 dL*. Levo: daljni-UV CD spekter. Za merjenje daljnega-UV CD spektra (250–195 nm) smo uporabili proteinsko koncentracijo $A_{280} = 0,1$. Podatke smo odčitavali v korakih po 1 nm. Desno: bližnji-UV CD spekter. Za merjenje bližnjega-UV CD spektra (320–250 nm) smo uporabili proteinsko koncentracijo med $A_{280} = 1,1$ in $A_{280} = 1,6$. Podatke smo odčitavali v korakih po 0,5 nm. Izmerjene eliptične vrednosti smo preračunali s pomočjo enačbe, opisane v poglavju 3.3.2. .....40

Slika 27: *Shematski prikaz C-končno skrajšanih konstruktov TcAtg8.1 ΔC8 in TcAtg8.2 ΔC14*. Siva – izbrisani aminokislinski preostanki v skrajšanih Atg8 konstruktih. Puščica – mesto cepitve peptidne verige v substratih divjega tipa (wt). .....41

Slika 28: *Vpliv koinkubacije naravnih substratov TcAtg8 in sintetičnega substrata Ac-ETFG-AFC na afiniteto TcAtg4.2 do sintetičnega substrata.* V reakcijskem pufru (20 mM Tris-HCl pH 7,5, 150 mM NaCl, 5 mM DTT) smo TcAtg4.2 in naravna substrata divjega tipa (TcAtg8.1 in TcAtg8.2) ter njuni C-končno skrajšani različici (TcAtg8.1 ΔC8 in TcAtg82 ΔC14) v razmerjih med 0 in 25 koinkubirali z 250 µM tetrapeptidnim fluorogenim substratom Ac-ETFG-AFC. Cepitev fluorogenega substrata smo spremljali na fluorimetru za mikrotitrske plošče (Safire, Tecan) pri vzbujanju $\lambda = 400$ nm in emisiji $\lambda = 505$ nm pri 37 °C 30 min. .....41

Slika 29: *Določanje substratne specifičnosti TcAtg4.2.* (A) Zgradba kombinatorne substratne knjižnice. (B) Pregled substratne specifičnosti TcAtg4.2 na pozicijah P2, P3 in P4. .....42

Slika 30: *Vpliv zamenjave aminokislinskih preostankov na pozicijah P1, P2, P3 in P4 na hitrost cepitve TcAtg8.2 s TcAtg4.2*. 0–150 ng TcAtg4.2 in 2 µg TcAtg8.2 WT in njegovih mutant P1 (G131A), P2 (F130S), P3 (T129H) in P4 (S128G) smo inkubirali v reakcijskem pufru (20 mM Tris-HCl pH 7,5, 150 mM NaCl, 5 mM DTT) pri 37 °C in stresanju 300 obr./min. Reakcijo smo po 60 min prekinili z dodatkom 6 × pufra SDS in inkubacijo vzorcev pri 100 °C 5 min. .....43

Slika 31*: Spremljanje hitrosti razgradnje substratov v optimizirani substratni tetrapeptidni knjižnici s TcAtg4.2 in HsAtg4B.* 4 µg TcAtg4.2 oz. HsAtg4B smo inkubirali z 250 µM tetrapeptidnimi fluorogenimi substrati v reakcijskem pufru za TcAtg4.2 (25 mM Tris-HCl pH 8,0, 0,5 M $K_2HPO_4$, 5 mMDTT) oz. v reakcijskem pufru za HsAtg4B (25 mM Tris-HCl pH 7,5, 0,5 M $Na_3C_3H_5O(COO)_3$, 5 mMDTT). Hitrost cepitev fluorogenih substratov smo spremljali na fluorimetru za mikrotitrske plošče (Safire, Tecan) pri vzbujanju λ = 355 nm in emisiji λ = 460 nm pri 37 °C 30 min. ..... 44

Slika 32: *Cepitve izbranih tetrapeptidnih substratov s TcAtg4.2 in človeškimi citosolnimi proteini HsAtg4B, SENP1, SENP2 in UCH-L3.* 4 µg TcAtg4.2, HsAtg4B, SENP1, SENP2 oz. UCH-L3 smo inkubirali z 250 µM tetrapeptidnimi fluorogenimi substrati v reakcijskem pufru za TcAtg4.2 (25 mM Tris-HCl pH 8,0, 0,5 M $K_2HPO_4$, 5 mM DTT) oz. v reakcijskem pufru za preostale encime (25 mM Tris-HCl pH 7,5, 0,5 M $Na_3C_3H_5O(COO)_3$, 5 mM DTT). Hitrost cepitev fluorogenih substratov smo spremljali na fluorimetru za mikrotitrske plošče (Safire, Tecan) pri vzbujanju λ = 400 nm in emisiji λ = 505 nm pri 37 °C 30 min. ..... 45

Slika 33: Cepitve *T. cruzi* homologov, Atg8 TcAtg8.1 in TcAtg8.2 s človeškimi katepsini B, K, L in S. 40 ng rekombinantnih katepsinov B, K, L in S smo v reakcijskem pufru BANA (15 mM $Na_2HPO_4$, 88 mM $KH_2PO_4$ pH 6,0, 1 mM EDTA, 0,1 % PEG-6000, 5 mM DTT) inkubirali z 2 µg TcAtg8.1 oz TcAtg8.2 pri 37 °C. Reakcijo smo po 60 min prekinili z dodatkom 6 × pufra SDS in inkubacijo vzorcev pri 100 °C 5 min. ..... 45

Slika 34: *Cepitve izbranih tetrapeptidnih substratov s človeškimi cisteinskimi katepsini B, K, L in S.* 5–20 nM rekombinantne katepsine B, K, L in S smo v reakcijskem pufru BANA (15 mM $Na_2HPO_4$, 88 mM $KH_2PO_4$ pH 6,0, 1 mM EDTA, 0,1 % PEG-6000, 5 mM DTT) inkubirali s 100 µM tetrapeptidnimi substrati. Hitrosti cepitev fluorogenih substratov smo spremljali na fluorimetru za mikrotitrske plošče (Safire, Tecan) pri vzbujanju λ = 400 nm in emisiji λ = 505 nm pri 37 °C 30 min. ..... 46

Slika 35: *Shematski prikaz pametne aktivnostne sonde MP001*. Pametno aktivnostno sondo MP001 smo sintetizirali na osnovi tetrapeptidnega substrata KKChaG. Na N-koncu sonde je preko linkerja pripet biotin, na C-koncu peptida pa je pripet metilni ester, ki se ob hidrolizi peptidne vezi kovalentno poveže s katalitičnim cisteinskim preostankom v reži aktivnega mesta encima. ..... 46

Slika 36: *Inhibicija TcAtg4.2 s pametno aktivnostno sondo MP001*. Levo: Prikaz aktivnosti TcAtg4.2 (v %) v odvisnosti od naraščajoče koncentracije MP001 (v mM). Desno: Prikaz aktivnosti TcAtg4.2 (v %) v odvisnosti od naravnega logaritma koncentracije MP001 (v M). TcAtg4.2 in MP001 smo v različnih molarnih razmerjih predinkubirali v 50 µl reakcijskega pufra (25 mM Tris-HCl pH 8,0, 0,5 M $K_2HPO_4$, 5 mM DTT) pri 37 °C 10 min. Nato smo k TcAtg4.2 in MP001 dodali še 50 µl reakcijskega pufra, ki je vseboval 100 µM Ac-KKChaG-AFC. Hitrost cepitve smo spremljali na fluorimetru za mikrotitrske plošče (Safire, Tecan) pri vzbujanju λ = 400 nm in emisiji λ = 505 nm pri 37 °C 30 min. ..... 47

Slika 37: *Inhibicija človeških citosolnih cisteinskih proteaz s pametno aktivnostno sondo MP001*. HsAtg4B, SENP1, SENP2 in UCH-3 ter MP001 smo v različnih molarnih razmerjih predinkubirali v 50 µl reakcijskega pufra (25 mM Tris-HCl pH 7,5, 0,5 M $Na_3C_3H_5O(COO)_3$, 5 mM DTT) pri 37 °C 10 min. Nato smo k encimom in MP001 dodali še 50 µl reakcijskega pufra, ki je vseboval 100 µM Ac-KKChaG-AFC. Hitrost cepitve smo spremljali na fluorimetru za mikrotitrske plošče (Safire, Tecan) pri vzbujanju λ = 400 nm in emisiji λ = 505 nm pri 37 °C 30 min. .....47

Slika 38: *Inhibicija človeških katepsinov B, K, L in S s pametno aktivnostno sondo MP001*. 5 - 20 nM rekombinantnih katepsinov ter MP001 smo v različnih molarnih razmerjih predinkubirali v 50 µl reakcijskega pufra BANA (15 mM $Na_2HPO_4$, 88 mM $KH_2PO_4$ pH 6,0, 1 mM EDTA, 0,1 % PEG-6000, 5 mM DTT). Nato smo k mešanici katepsinov in MP001 dodali še 50 µl reakcijskega pufra, ki je vseboval 100 µM Ac-KKChaG-AFC. Hitrost cepitve smo spremljali na fluorimetru za mikrotitrske plošče (Safire, Tecan) pri vzbujanju λ = 400 nm in emisiji λ = 505 nm pri 37 °C 30 min. .....48

Slika 39: *Imunološka detekcija LC3 v tumorskih celicah PyMT;WT in PyMT;StfB-/-*. Tumorske celice PyMT;WT in PyMT;StfB-/- smo gojili pri normalnih pogojih v gojišču DMEM z dodanimi 10 % FBS, 1 % glutaMAX™ in 1 % penicilin/streptomicinom, v pogojih stradanja v pufru HBSS ter v pogojih stradanja z dodanim 100 µM inhibitorjem avtofagije klorokinom pri 37 °C in 5 % $CO_2$ 2,5 uri. .....49

Slika 40: *Preživetje tumorskih celic PyMT;WT in PyMT;StfB-/- v pogojih stradanja*. Tumorske celice PyMT;WT in PyMT;StfB-/- smo gojili pri normalnih pogojih v gojišču DMEM z dodanimi 10 % FBS, 1 % glutaMAX™ in 1 % penicilin/streptomicinom in v pogojih stradanja v pufru HBSS pri 37 °C in 5 % $CO_2$ 72 ur. .....49

Slika 41: *Sprožitev celične smrti z regulacijo avtofagije v pogojih stradanja.* Tumorske celice PyMT;WT in PyMT;StfB-/- smo gojili pri normalnih pogojih v gojišču DMEM z dodanimi 10 % FBS, 1 % glutaMAX™ in 1 % penicilin/streptomicinom (CTRL), v pogojih stradanja v pufru HBSS (strad.), v pogojih stradanja z dodanim 200 nM induktorjem avtofagije rapamicinom (strad. + R), ter v pogojih stradanja z dodanim 100 µM inhibitorjem avtofagije klorokinom (strad. + CQ), pri 37 °C in 5 % $CO_2$ 24 ur. .....50

# Priloge

V času trajanja doktorskega študija sta bila objavljena dva raziskovalna članka, s prvim avtorstvom in s koavtorstvom:

Rajkovic J, Poreba M, Caglic D, et al. Biochemical Characterization and Substrate Specificity of Autophagin-2 from the Parasite Trypanosoma cruzi. *J Biol Chem.* 2015 Oct 7. Doi: 10.1074/jbc.M115.687764

Butinar M, Trstenjak-Prebanda M, Rajković J, et al. Stefin B deficiency reduces tumor growth via sensitisation of tumor cell to oxidative stress in a breast cancer model. *Oncogene*, 2013 Avt 19. Doi: 10.1038/onc.2013.314

**JBC Papers in Press. Published on October 7, 2015 as Manuscript M115.687764**
**The latest version is at http://www.jbc.org/cgi/doi/10.1074/jbc.M115.687764**


# Biochemical Characterization and Substrate Specificity of Autophagin-2 from the Parasite *Trypanosoma cruzi*

**Jelena Rajković[*†‡], Marcin Poreba[II], Dejan Caglič[*§], Robert Vidmar[*†], Aleksandra Wilk[II], Agata Borowik[II], Guy Salvesen[¶], Vito Turk[*], Marcin Drag[II] and Boris Turk[*‡¥]**

[*] Department of Biochemistry and Molecular and Structural Biology, Jožef Stefan Institute, Jamova Cesta 39, SI-1000 Ljubljana, Slovenia
[†] Jožef Stefan International Postgraduate School, Jamova Cesta 39, SI-1000 Ljubljana, Slovenia
[‡] Centre of Excellence for Integrated Approaches in Chemistry and Biology of Proteins, Jamova Cesta 39, SI-1000 Ljubljana, Slovenia
[§] Department of Chemistry, The Scripps Research Institute , 10550 North Torrey Pines Road, La Jolla, CA 92037, USA
[II] Department of Bioorganic Chemistry, Faculty of Chemistry, Wroclaw University of Technology, Wyb. Wyspianskiego 27, 50-370 Wroclaw, Poland
[¶] Sanford-Burnham Medical Research Institute, Program in Cell Death and Survival Networks, 10901 North Torrey Pines Road, La Jolla, CA 92037, USA
[¥] Faculty of Chemistry and Chemical Technology, University of Ljubljana, Jamova Cesta 39, SI-1000 Ljubljana, Slovenia

**Running title:** Biochemical characterization of TcAtg4.2

To whom correspondence should be addressed: Prof. Boris Turk, Department of Biochemistry and Molecular and Structural Biology, Jožef Stefan Institute, Jamova Cesta 39, SI-1000 Ljubljana, Slovenia, Telephone: (386) 1 477 37 72, FAX: (+386) 1 477 39 84, E-mail: boris.turk@ijs.si

**Keywords:** Autophagy; *Trypanosoma cruzi*; Atg4; Atg8; fluorogenic substrates; positional-scanning substrate combinatorial library (PS-SCL)

Downloaded from http://www.jbc.org/ at Jozef Stefan Institut on October 11, 2015



**Copyright 2015 by The American Society for Biochemistry and Molecular Biology, Inc.**

**Background:** Successful colonization of humans by the parasite *Trypanosoma cruzi* critically depends on intact parasite autophagy and autophagin-2.
**Results:** *T. cruzi* autophagin-2, in contrast to human autophagin-1, exhibits substantial preference towards the unnatural amino acid cyclohexylalanine in the P2 position.
**Conclusion:** Selective fluorogenic substrates, which are only recognized by *T. cruzi* autophagin-2, were synthesized.
**Significance:** These selective substrates have a potential for screening of *T. cruzi* autophagin-2 specific inhibitors.

**ABSTRACT**

The genome of the parasite *Trypanosoma cruzi* encodes two copies of autophagy-related cysteine proteases, Atg4.1 and Atg4.2. *T. cruzi* autophagin-2 (TcAtg4.2) carries the majority of proteolytic activity and is responsible for processing of Atg8 proteins near the carboxy-terminus, exposing a conserved glycine. This enables progression of autophagy and differentiation of the parasite, which is required for successful colonization of humans. The mechanism of substrate hydrolysis by Atg4 was found to be highly conserved among the species as critical mutations in the TcAtg4.2, including mutation of the conserved Gly244 residue in the hinge region enabling flexibility of the regulatory loop, and deletion of the regulatory loop, completely abolished processing capacity of the mutants. Using Positional Scanning-Substrate Combinatorial Library (PS-SCL) we determined that TcAtg4.2 tolerates a broad spectrum of amino acids in the P4 and P3 positions, similar to the human orthologue autophagin-1 (HsAtg4B). In contrast, both human and trypanosome Atg4 orthologues exhibited exclusive preference for aromatic amino acid residues in the P2 position, and for Gly in the P1 position, which is absolutely conserved in the natural Atg8 substrates. Using an extended P2 substrate library, which also included the unnatural amino acid cyclohexylalanine (Cha) derivative of Phe, we generated highly selective tetrapeptide substrates acetyl-Lys-Lys-Cha-Gly-AFC (Ac-KKChaG-AFC) and acetyl-Lys-Thr-Cha-Gly-AFC (Ac-KTChaG-AFC). Although these substrates were cleaved by cathepsins, making them unsuitable for analysis of complex cellular systems, they were recognized exclusively by TcAtg4.2, but not by HsAtg4B nor by the structurally related human proteases SENP1, SENP2 and UCH-L3.

## INTRODUCTION

Autophagy is a lysosome- and/or vacuole-dependent mechanism of degradation of intracellular constituents, highly conserved through evolution (1). It enables cells to adopt the extracellular and intracellular stress such as nutrient and growth factor deprivation (2-4), hypoxia (5-7), removal of excessive and damaged cytosolic proteins (8) and organelles (9-12) and invading pathogens (13,14). It also plays a crucial role during the development (15,16), differentiation (17,18), embryogenesis (19) and tissue remodeling in various organisms (20-22). Formation of autophagosomes and execution of autophagy critically depend on proteolytic processing of the Atg8 and its subsequent conjugation to the phosphatydilethanolamine (PE) in the expanding phagophore membrane. The protease responsible for the processing of proAtg8 homologues, the Atg4 cysteine protease, cleaves the peptide bond after the conserved glycine residue at the C-terminus of the protein (23-25). The processed Atg8 is further transferred to Atg7 (E1 activating enzyme) and Atg3 (E2 conjugating enzyme) and finally conjugated to the PE moiety in the phagophore membrane. After autophagosome formation, the Atg8-PE complex is deconjugated by the same Atg4 protease, leading to the release of Atg8 from the outer phagosome membrane. The whole conjugating reaction is reminiscent of the ubiquitin-proteasome system, where deubiquitinating enzymes participate in the control of ubiquitin and ubiquitin-like modifiers.

The core machinery of macroautophagy, which clears non-selectively engulfed cargo, is evolutionary highly conserved among all eukaryotes, from unicellular organisms, such as yeast, protozoan pathogens and free living protists, to fungi, plants and mammals including humans (26-28).

The flagellated protozoan *Trypanosoma cruzi* is the causative agent of Chagas disease, a prevalent health problem in Central and Latin America, with estimated 7-8 million people infected (29). The *T. cruzi* life cycle alternates between the insect vector and the mammalian host and involves four developmental stages, two replicative forms, and two infective forms. All four



Downloaded from http://www.jbc.org/ at Jozef Stefan Institut on October 11, 2015

forms are needed for successful colonization of both hosts and for the survival of the parasite (30). The differentiation process is characterized by massive metabolic and morphological changes, which critically depend on an activated autophagic pathway. Using bioinformatic analysis, a functional Atg8 ubiquitin-like conjugating system has been identified in the parasite (Atg3, Atg4, Atg7 and Atg8), whereas the major components of the Atg12 conjugation system have not been identified as yet (26). *T. cruzi* genome encodes two Atg4 and two Atg8 homologues, TcAtg4.1 (Uniprot code: A6XG54), the proteolytically less active variant, and TcAtg4.2 (Uniprot code: A6XG55), which carries the majority of proteolytic activity and is responsible for the processing of TcAtg8.1 and TcAtg8.2 (2008-02-08 nomenclature). Moreover, TcAtg4.2 and TcAtg8.1 were already characterized as yeast Atg4 and Atg8 counterparts able to complement autophagy in *S. cerevisiae atg4Δ* and *atg8Δ* strains, consistent with a very high degree of conservation of the autophagy pathway, whereas the physiological function of TcAtg4.1 is not clear, although it was able to compensate for the loss of Atg4 in yeast (31).

Since successful monitoring and treatment of Chagas' disease would largely benefit from development of tools for specific monitoring of the activity of TcAtg4.2 from the parasite, the major goal of our study was to characterize the *T. cruzi* autophagin-2 (TcAtg4.2). We took advantage of a combinatorial tetrapeptide substrate library and determined the substrate specificity of TcAtg4.2. Moreover, by comparison of specificities of human Atg4B and TcAtg4.2 selective tetrapeptide substrates Ac-KTChaG-AFC and Ac-KKChaG-AFC were synthesized. Both substrates showed good selectivity for TcAtg4.2 and were very poorly recognized by HsAtg4B as well as by human cytosolic proteins SENP1, SENP2 and UCH-L3.

## EXPERIMENTAL PROCEDURES

*Construction of Plasmids*–Preparation of the plasmids carrying the sequences encoding wild-type TcAtg4.2, TcAtg8.1 and TcAtg8.2 was described previously (31). Catalytically inactive mutant TcAtg4.2 C91S (Ser was selected as structurally most similar to Cys), mutant lacking the regulatory loop (amino acids 245-258) TcAtg4.2 dL, TcAtg4.2 W158A, G244H, S246D and S246P were generated using QuikChange™ (Stratagene) with oligonucleotides 5'-ATCTCTTCTGG-GGATCCATGATCCGGACAGG-3' and 5'-CCT-GTCCGGATCATGGATCCCCAGAAGAGAT-3' for TcAtg4.2 C91S, 5'-CTCGATAGGCATT-CTTGGAGGTGCGTTATTCCTCTTT-3', 5'-AA-AGAGGAATAACGCACCTCCAAGAATGCCT-ATCGAG-3' for TcAtg4.2 dL, 5'-GTTAACTGC-GGTGAGGCGTTTGGGCCAACGCC-3' and 5'-GGCGTTGGCCCAAACGCCTCACCGCAGT-TAAC-3' for TcAtg4.2 W158A, 5'-AGCT-CGATAGGCATTCTTGGACACAAATCTCGC-TCCGCGTTATTC-3' and 5'-GAATAACGC-GGAGCGAGATTTGTGTCCAAGAATGCCTAT CGAGCT-3' for TcAtg4.2 G244H, 5'-CTCGATA-GGCATTCTTGGAGGTAAAGATCGCTCCGC-GTTA-3' and 5'-TAACGCGGAGCGATCTTTAC-CTCCAAGAATGCCTATCGAG-3' for TcAtg4.2 S246D, 5'-CGATAGGCATTCTTGGAGGTAAA-CCGCGCTCCGCGTTA-3' and 5'-TAACGCG-GAGCGCGGTTTACCTCCAAGAATGCCTATC -G-3' for TcAtg4.2 S246P. TcAtg4.2 mutants lacking first 18 in TcAtg4.2 dN18 and 24 amino acid residues in TcAtg4.2 dN24 we generated by PCR using the forward primers 5'-AACAT-ATGTTAGCGATTAAGGCTGTGT-3' for TcATg4.2 dN18 and 5'-TAACATATGAATTG-TATGTTTCGCCTCCGG-3' for TcAtg4.2 dN24 both carrying *Nde*I restriction site and the reverse primer 5'-AAGGATCCTACTCCGCCACGTCC-3' with included *Bam*HI restriction site. The amplified PCR fragments were digested by *Nde*I and *Bam*HI (New England Biolabs) and cloned into the pET-28a(+) bacterial expression vector (Novagen). TcAtg8.2 S128G, A129H, F130S and G131A mutants were generated using QuikChange™ (Stratagene) with oligonucleotides for TcAtg8.2 S128G: 5'-GACATAC-AGCATTGAGGGCGCCTTTGGCGGT-3' and 5'-ACCGCCAAAGGCGCCCTCAATGCTGTATG-TC-3', TcAtg8.2 A129H: 5'-TACAGCATTGAGA-GCCACTTTGGCGGTGCGGC-3' and 5'-GCCG-CACCGCCAAAGTGGCTCTCAATGCTGTA-3', TcAtg8.2 F130S: 5'-CAGCATTGAGAGCGCCT-CTGGCGGTGC-3' and 5'-GCACCGCCAGAGG-CGCTCTCAATGCTG-3' and TcAtg8.2 G131A: 5'-GAGCGCCTTTGCCGGTGCGGCTG-3' and 5'-CAGCCGCACCGGCAAAGGCGCTC-3'. We also prepared C-terminally truncated TcAtg8.1 and TcAtg8.2 ΔC mutants, which are lacking five



Downloaded from http://www.jbc.org/ at Jozef Stefan Institut on October 11, 2015

amino acids upstream of the conserved Glycine in the scissile bond. The TcAtg8.1 ΔC8 mutant was generated by PCR using the forward primer 5'-ACGTCATATGGCGCCAAAGAAATTGG-3' and the reverse primer 5'-ACGTGGATCCTC-AACCCGAGTACTTTATGTA-3'. The TcAtg8.2 ΔC13 mutant was generated by PCR using the forward primer 5'-ACGTCATATGGCACGCA-AATATCGCTAC-3' and the reverse primer 5'-ACGTGGATCCTCAAATGCTGTATGTCATGT A-3'. Forward primers included *Nde*I restriction site and reverse primers included *Bam*HI restriction site. The PCR fragments were digested with *Nde*I and *Bam*HI restriction enzymes (New England Biolabs) and inserted into pET28a(+). Human autophagin-1 (HsAtg4B) (GeneService, Nottingham, UK) was amplified by PCR using the primers designed for In-Fusion™ cloning (32). Preparation of the plasmids carrying the sequences encoding DeSUMOylating and deubiquitinating enzymes and cysteine cathepsins B, K, L and S was described previously (33-37).

*Expression and purification of recombinant proteins*–All plasmids were introduced into *Escherichia coli BL21* (DE3) strain. Transformants were stimulated to produce recombinant proteins by incubation with 0.5 mM IPTG at 28°C for 4 h expressing TcAtg8 proteins and 25°C for 6 h expressing TcAtg4.2 and HsAtg4B. All proteins were expressed as fusion protein with a $His_6$-tag and were allowed to bind to HisTrap FF crude columns (GE Healthcare) and eluted with buffer containing 250 mM imidazole. DeSUMOylating and deubiquitinating enyzmes were produced and purified as previously described (33,34). Human cathepsins were produced and purified as previously described (35-37). Purity and the relative molecular masses of the purified proteins were verified by SDS-PAGE (12.5% gel) followed by Coomassie Brilliant Blue (CBB) staining.

*Circular dichroism (CD) spectroscopy*–Far-UV CD spectra of TcAtg4.2 were recorded in an Aviv 62 ADS CD spectropolarimeter (Aviv Biomedical, Lakewood Township, NJ, USA) equipped with a thermoelectric sample holder for temperature control as described (38). Briefly, samples (0.1 mg/ml) were measured in 0.1 cm cell and at the bandwidth of 1 nm, whereas the temperature was maintained at 25 °C throughout. Data were collected every nm and the mean residue ellipticity in deg $cm^2$/mol was calculated using a mean weight of 109/residue (MRW).

*In Vitro Cleavage of TcAtg8 proteins*–For cleavage assay of recombinant TcAtg8 constructs by recombinant TcAtg4.2, 1-4 µg of TcAtg8 proteins were incubated with 0-150 ng of TcAtg4.2 in 20 µl reaction buffer, containing 20 mM Tris-HCl pH 7.5, 150 mM NaCl and 5 mM DTT. To determine the ability of TcAtg4.2 to cleave wild-type and mutated TcAtg8 molecules with substituted amino acid residues in positions P4, P3, P2 and P1 the samples were incubated at 37°C for the designated times. To determine the catalytic efficiency of the enzyme we used the equation: $k_{cat}/K_m = \ln 2/(t \times EC_{50})$ where $EC_{50}$ is the enzyme concentration at which 50% conversion of the substrate is obtained (39,40). Reactions were stopped by addition of 6× SDS loading dye and incubation at 100°C for 5 min.

*Synthesis and characterization of single tetrapeptide-AFC (7-amino-4-trifluoromethyl-coumarin) substrates*–To synthesize Boc-Gly-AFC, one eq. of Boc-Gly-COOH and one eq. of AFC were dissolved in anhydrous pyridine and cooled in ice/NaCl bath to -15°C. To this mixture 1.4 eq. of $POCl_3$ was added dropwise in the period of 10 minutes. The reaction was carried out at -15°C and the progress was monitored using TLC analysis. After the reaction was completed (60 minutes) the mixture was dissolved in ethyl acetate and extracted with 5% citric acid (2x), 5% $NaHCO_3$ (2x) and brine (2x). The organic fraction was dried over $MgSO_4$ and ethyl acetate was then removed under reduced pressure to obtain Boc-Gly-AFC, which was used for further synthesis without additional purification. In a separate synthesis N-acetylated tripeptides with free carboxylic group at the C-terminus were synthesized similar as described previously and used without further purification (41). To synthesize Ac-peptide-Gly-AFC substrates one eq. of Boc-Gly-AFC was dissolved in 50% TFA in DCM (with 2.5% of triisoprooylsilane as a scavenger) the Boc deprotection reaction was carried out for 30 minutes. After the reaction was completed, TFA and DCM were removed under reduced pressure to obtain $NH_2$-Gly-AFC. Next, $NH_2$-Gly-AFC was dissolved in a minimal amount of DMF, followed by the addition of one eq. of Ac-peptide-COOH and one eq. of HBTU. Finally, three eq. of DIPEA were added and the coupling



Downloaded from http://www.jbc.org/ at Jozef Stefan Institut on October 11, 2015

reaction was carried out for 3 hours. After the reaction was completed, as judged by HPLC analysis, the mixture was diluted in ethyl acetate and extracted with 5% citric acid (2x), 5% $NaHCO_3$ (2x) and brine (2x). The organic fraction was dried over $MgSO_4$ and the ethyl acetate was then removed under reduced pressure to obtain crude Ac-peptide-Gly-AFC. Next, all protecting groups were removed in 50% TFA in DCM (with 2.5% of triisoprooylsilane as a scavenger) for 1 hour. Finally, the crude product was purified by HPLC on a Waters M600 solvent delivery module with a Waters M2489 detector system using a semi-preparative Waters Spherisorb S10ODS2 column. The solvent composition was as follows: phase A (water/0.1% TFA) and phase B (acetonitrile/0.1% TFA). The purity of each compound was verified by analytical HPLC system using a Waters Spherisorb S5ODS2 column. The molecular weight of each Ac-peptide-Gly-AFC substrate was determined by high-resolution mass spectrometry using a High Resolution Mass Spectrometer WATERS LCT premier XE with Electrospray Ionization (ESI) and Time of Flight (TOF) module.

*Synthesis of the fluorogenic tetrapeptide-ACC (7-amino-4-carbamoylmethylcoumarin) positional scanning-synthetic combinatorial peptide library (PS-SCL)*–The PS-SCL was synthesized using semiautomatic FlexChem Peptide Synthesis System (model 202) as described earlier (33,34,40). All substrates from each sublibrary (P4, P3 and P2) were dissolved in DMSO at a concentration of 50 mM or 20 mM and stored at -20°C until use.

*Effect of pH and salts on TcAtg4.2 activity*– The effect of different salts on TcAtg4.2 activity was determined by incubating 4 µM enzyme with 100 µM Ac-ETFG-AFC in the presence of 1 M salt in 25 mM Tris-HCl, pH 8.0 and 5 mM DTT. The optimal pH of TcAtg4.2 was determined by incubation of 4 µM enzyme and 100 µM Ac-ETFG-AFC in 50 mM reaction buffer, containing MES buffer (pH 6.0 and 6.5), HEPES buffer (pH 7.0 and pH 7.5), Tris-HCl (pH 8.0 and pH 8.5) and Bistris propane buffer (pH 9.0) in presence of 500 mM $K_2HPO_4$ and 5 mM DTT. The enzyme was activated with DTT for 10 min at 37°C before adding to the wells containing substrate. The reaction volume was 100 µl. Release of AFC fluorophore was monitored continuously with excitation at 400 nm and emission at 505 nm. The total assay time was 30 min, and only the liner portions of the progress curves was used to calculate velocity.

*Assay of the PS-SCL*–All reactions were assayed at 37°C in 25 mM Tris-HCl pH 8.0 containing 500 mM $K_2HPO_4$ and 5 mM DTT. The enzyme was activated with DTT for 10 min at 37°C before being added to the wells containing substrates. Standard reaction conditions were reaction volume 100 µL, final enzyme concentration 4 µM and final substrate concentration 250 µM, which is similar to conditions used for DeSUMOylating and deubiquitinating enzymes, and HsATG4B (250-500 µM) (33,34,40). Release of the ACC fluorophore was measured at an excitation wavelength of 355 nm and emission wavelength of 460 nm for 30 min. Only the linear portions of the progress curves were used for further analysis. In each sublibrary the substrate with the highest RFU (relative fluorescence units) value was set to 100%. The other results were adjusted accordingly to the 100% of the best substrate. The difference between individual values was in every case smaller than 10%. The $k_{cat}/K_m$ of TcAtg4.2 was determined using nonlinear regression analysis of a series of progress curves using the equation: $k_{cat}/K_m$ = slope/E.

*Assay of SENPs, DUBs and cysteine cathepsins B, K, L and S*–The enzymatic activities of recombinant SENP1, SENP2 and UCH-L3 were previously confirmed with the cleavage of the optimal fluorogenic synthetic tetrapeptidic substrates Ac-QTGG-ACC for SENPs and Ac-LRGG-AC for UCH-L3 (33,34). All reactions were assayed at 37°C in 25 mM Tris-HCl pH 7.5 containing 500 mM $Na_3C_3H_5(COO)_3$ and 5 mM DTT. The enzymes were activated for 10 min at 37°C in the same DTT-containing buffer before they were added to the wells containing substrates. Standard reaction conditions were 100 µL reaction volume, 4-6 µM final enzyme concentration and 100 µM final substrate concentration. The enzymatic activities of recombinant cathepsins were confirmed with cleavage of Cbz-FR-AMC, Cbz-RR-AMC and Cbz-FVR-AMC. Standard reaction conditions for the cleavage of synthetic substrates were 100 µL reaction volume (100 mM BANA, pH 6.5, containing 0.1% PEG-6000 and 5 mM DTT), 10-50 nM final enzyme concentration



Downloaded from http://www.jbc.org/ at Jozef Stefan Institut on October 11, 2015

and 100 µM final substrate concentration. In order to evaluate cleavage of recombinant Atg8 homologues TcAtg8.1, TcAtg8.2 and human GABARAPL2/GATE-16 with recombinant human cathepsins B, K, L and S, substrates and enzymes were incubated at a 50 : 1 molar ratio in 20 µl BANA buffer pH 6.5, containing 0.1 % PEG-6000 and 5 mM DTT for 1 h at 37°C. Reactions were stopped by addition of 6× SDS loading dye and incubation at 100°C for 5 min. The samples were then loaded on 16% Tricine-SDS-gels and separated (42).

**RESULTS**

*Kinetics of TcAtg8.1 and TcAtg8.2 cleavage with TcAtg4.2*–Recombinant TcAtg4.2 and human Atg4B autophagins, and Atg8 homologs TcAtg8.1 and TcAtg8.2 were expressed in *E. coli* BL21 (DE3) host strain and purified using a $Ni^{2+}$-NTA column. Relative molecular masses and purity of proteins was verified by SDS-PAGE (12.5% gel) followed by Coomassie Brilliant Blue (CBB) staining (Fig. 1A). In order to confirm that the recombinant TcAtg4.2 is catalytically active the enzyme was incubated with its natural substrates TcAtg8.1 and TcAtg8.2 (31). Processing of the substrates was monitored by SDS-PAGE and $k_{cat}/K_m$ values of $3.7 \times 10^3$ $M^{-1}$ $s^{-1}$ and $3.4 \times 10^3$ $M^{-1}$ $s^{-1}$ were determined for processing TcAtg8.1 and TcAtg8.2, respectively, using the same method as described previously for caspases (39). In the control experiment, TcAtg8.1 and TcAt8.2 proteins were incubated in the reaction buffer in the absence of TcAtg4.2 and no processing could be detected (Fig. 1B).

Alignment of amino acid sequences of multiple autophagin orthologues revealed a highly conserved amino acid sequence around Cys74, which is the catalytic Cys in human autophagin-1 (Fig. 3D). In order to evaluate the importance of its equivalent in TcAtg4.2, Cys91, the latter was mutated into a Ser. When TcAtg8.1 and TcAtg8.2 proteins were incubated with the TcAtg4.2 C91S mutant processing of proTcAtg8.1 or proTcAtg8.2 was abolished, suggesting that Cys91 is indeed the active site Cys residue in TcAtg4.2. Prolonged incubation of TcAtg4.2 C91S with Atg8.1 (24 h) resulted in a very minor proteolysis, which was ~ 10,000 times lower than the enzymatic activity of the wild-type TcAtg4.2, similar to what was observed earlier for TcAtg4.1 (31) (Fig. 1B). This is in agreement with previous results on human Atg4B, where a very minor activity of Cys74Ser on Atg8 substrates was observed (43). In addition, in adenoviral protease replacement of the active site Cys to Ser also resulted in a protease with substantially diminished activity (44,45).

*Biochemical characterization of TcAtg4.2*–In addition to processing natural substrates, human autophagin-1 (HsAtg4B) was found to be able to process small synthetic fluorogenic tetrapeptide substrates (40). The cleavage of tetrapeptide fluorogenic substrates was not very efficient, but could be enhanced in the presence of an optimal kosmotropic salt. Based on the high homology between the human Atg4B and TcAtg4.2, four tetrapeptide substrates carrying AFC (7-amino-4-trifluoromethylcoumarin) fluorophore, which were found to be cleaved by HsAtg4B, were therefore used for the initial biochemical analyses. Ac-GTFG-AFC and Ac-STFG-AFC substrates were derived from the HsAtg4B PS-SCL, whereas Ac-NTFG-AFC and Ac-ETFG-AFC were derived from the human Atg4 substrates GATE-16 and LC3, respectively. The hydrolysis of Ac-ETFG-AFC by TcAtg4.2 was substantially more efficient than of the other three substrates. However, all reactions exhibited very slow kinetics (Fig. 2A). The latter was therefore used for further biochemical characterization of the TcAtg4.2. The enzyme was found to be active between pH 6.5 and 8.5 with the maximum activity at pH 8.0, whereas its activity dropped sharply at pH 9.0 (Fig. 2B). Since it is known that kosmotropic salts can significantly enhance proteolytic activities of various proteases (33,34,40) we applied this approach also to TcAtg4.2. The activity dramatically increased at high concentration of various citrate, phosphate and sulfate salts, with the highest activity observed in the presence of $K_2HPO_4$ (Fig. 2C). A titration experiment showed that the proteolytic activity of TcAtg4.2 increased with the increasing salt concentration even above 1 M (Fig. 2D). However, at high salt concentrations ($\geq$ 1 M) the enzyme started to precipitate. Circular dichroism measurements in the far-UV and deconvolution analyses made with the Dichroweb software (46,47) showed unfavorable changes in the enzyme conformation when $K_2HPO_4$ concentration was increased from 0.5 M to 1.0 M. A significant decrease in α-helix (from ~60% to 40%, respectively) and β-sheet (from 10% to 3%,



Downloaded from http://www.jbc.org/ at Jozef Stefan Institut on October 11, 2015

respectively) content was thus observed at 1.0 M salt. Moreover, protein precipitation seen at 1.0 M $K_2HPO_4$ also resulted in decreased ellipticity (Fig. 2E) and therefore 0.5 M $K_2HPO_4$ was used in all further experiments. In addition, the cleavage efficacy of the enzyme was improved by elongation of the synthetic substrates, as demonstrated using tetra- (ETFG), hexa- (SQETFG) and octapeptides (YASQETFG) based on the sequence of the natural substrate LC3B, which were designed for HsAtg4B (40) (Fig. 2F). In a control experiment, active site Cys91 was mutated into Ser, which has almost completely abolished substrate processing (Fig. 2G).

*Structure-function basis for TcAtg4.2 substrate hydrolysis*–During the evolution of eukaryotes *ATG4* genes multiplied. There is only one Atg4 member in yeast possessing both, endopeptidase and isopeptidase activity (25). Two members were found in kinetoplastid parasites T. cruzi, T. brucei and L. major (Atg4.1 and Atg4.2), where LmAtg4.1 possesses endopeptidase activity and LmAtg4.2 possesses isopeptidase activity (31,48,49), whereas four members have been found in mammals, (autophagin-1/Atg4B, autophagin-2/Atg4A, autophagin-3/Atg4C and autophagin-4/Atg4D). However, mammalian autophagins have different tissue distribution as well as catalytic properties. Among them, only Atg4A and Atg4B are catalytically active with Atg4B carrying the highest catalytic activity. In addition, Atg4B is the most important autophagin involved in basal macroautophagy in mammals (43,50,51).

To interpret substrate hydrolysis of TcAtg4.2 at the molecular level, we first analysed the phylogenetic relationship between TcAtg4.2 and other Atg4 othologues, using a phylogenetic tree construction program MEGA6 based on distances of amino acid sequences from five species (human, yeast, *Trypanosoma cruzi*, *Trypanosoma brucei* and *Leishmania major*).

The dendrogram placed TcAtg4.2 near TbAtg4.2 and LmAtg4.1, the latter two carrying the majority of endopeptidase activity in these species, with sequence identity of 45% and 34.5%, respectively (Fig. 3A). Moreover, the TcAtg4.2 amino acid sequence exhibits 21.3% and 22.2% identity with the sequences of HsAtg4A and HsAtg4B, respectively, with several conserved regions that share higher local identity to both human autophagins. To explore whether the mechanism of action of TcAtg4.2 is indeed highly conserved as compared to HsAtg4B, the SWISS-MODEL structure homology-modeling server (52-55) and RaptorX web server (56) were used to model the 3D structure of TcAtg4.2 as no crystal structure of autophagins from the trypanosomatids family of parasites is available. To construct the TcAtg4.2 3D model, the structures of the human homologues HsAtg4A (PDB code 2p82) and HsAtg4B (PDB code 2d1i) were used as templates (Fig. 3B). The SWISS-MODELs' global and per-residue model quality was assessed using the QMEAN scoring function with integrated Z-score (57). The QMEAN value of 0.63 indicates a good quality of the predicted model. In addition, the RaptorXs' quality evaluation parameters P-value ($3.4 \times 10^{-12}$), score (286) and uGDT/GDT (236/76) also indicate good quality of the predicted 3D model (Fig. 3C), suggesting that both constructed models are appropriate for further studies. Using this TcAtg4.2 model and the sequence alignment (Fig. 3D) several TcAt4.2 mutants were then prepared to study functional conservation of the structural elements involved in substrate hydrolysis (58,59). The first is the regulatory loop region comprising residues 258-263 (HsAtg4B numbering), which shares very high sequence homology throughout different species. In human Atg4B the loop covers the active site Cys74 residue and occupies the active site cleft in the free enzyme, thereby preventing substrate hydrolysis. The closed conformation of the loop in the enzyme free form is maintained by limited interactions of the loop with the neighboring side chains, where the majority of van der Waals interactions are formed between the side chain of Trp142, which is located in the loop between helices D and E, and Pro260 in the regulatory loop. However, upon substrate binding Phe119 and Gly120 from the C-terminal tail of LC3B interact with Trp142 of HsAtg4B and open the regulatory loop. In addition, neighboring interactions between Pro260 (equivalent to Ser246 in TcAtg4.2) in this loop and Trp142 (equivalent to Trp158 in TcAtg4.2) in vicinity embrace the C-terminal tail of LC3B and position the scissile bond in the proximity of the catalytic Cys residue, as seen in the crystal structure of Atg4B-LC3B complex (59), thereby enabling processing of the substrate. To address the role of the loop in TcAtg4.2, the corresponding

Downloaded from http://www.jbc.org/ at Jozef Stefan Institut on October 11, 2015

residues (245-248) were deleted to generate the TcAtg4.2 dL mutant. The deletion of regulatory loop resulted in a complete loss of processing capacity, indicating its critical role in substrate hydrolysis in particular in positioning the C-terminus of Atg8 (Fig. 4A).

Next, the role of the highly conserved Pro260 (Ser246 in TcAtg4.2) in this loop was addressed. First, Ser246 was mutated into Pro, which slightly enhanced proteolytic activity of TcAtg4.2, in agreement with earlier data demonstrating that Pro260 is not critical for the activity of HsAtg4B on its natural substrate LC3 (58). However, mutating Ser246 into Asp resulted in a significant enhancement of the proteolytic activity of TcAtg4.2 (Fig. 4A). Since the flexibility of the regulatory loop in Atg4 is maintained by two conserved Gly residues (Gly256 and Gly257 in human Atg4B) at the N-terminus of the regulatory loop, one of them (Gly244 in TcAtg4.2/ Gly257 in HsAtg4B) was mutated into His, resulting in a complete loss of processing capacity (Fig. 4A). Having shown the importance of the regulatory loop and its flexibility, we next addressed the role of Trp158, the TcAtg4.2 equivalent of HsAtg4B Trp142. Upon mutation into Ala, only weak processing of TcAtg8.1 was observed, in agreement with previous results on HsAtg4B Trp142Ala mutant (58). Since in the crystal structure of HsAtg4 complex with LC3 (59), Trp142 residue was moved from its normal position, we next wanted to explore, whether it would be possible to monitor this movement by changes of tryptophan fluorescence. Therefore, fluorescence spectra of the wild-type TcAtg4.2 and the Trp158Ala mutant were compared. Unfortunately, no difference was observed, suggesting that the fluorescence intensity of Trp158 is not sufficient to allow its monitoring (data not shown).

The second important region in HsAtg4B is the N-terminal tail, which masks the exit of the catalytic site of the free enzyme (40,59). We therefore prepared two TcAtg4.2 mutants, TcAtg4.2 dN18 and TcAtg4.2 dN24, lacking the first 18 or 24 amino acid residues, respectively. When compared with WT TcAtg4.2, the activity of the two mutants towards TcAtg8.1 was almost the same ($k_{cat}/K_m$ = 3.7 × $10^3$ $M^{-1}$ $s^{-1}$, 3.1 × $10^3$ $M^{-1}$ $s^{-1}$ and 2.8 × $10^3$ $M^{-1}$ $s^{-1}$ for WT TcAtg4.2, TcAtg4.2 dN18 and TcAtg4.2 dN24, respectively; Fig. 4A). Similarly as for the natural substrate, the activity of the mutants on the small synthetic substrate Ac-ETFG-AFC was only slightly affected. TcAtg4.2 dN18 exhibited somewhat diminished activity, whereas the activity of TcAtg4.2 dN24 was moderately increased (Fig. 4B).

As full-length Atg8 is required for efficient hydrolysis, we co-incubated TcAtg4.2 with full length TcAtg8.1 and TcAtg8.2 and their C-terminally truncated forms, lacking five amino acid residues upstream of the P1 glycine, TcAtg8.1 ΔC8 (residues 1 – 116) and TcAtg8.2 ΔC13 (residues 1 – 126) (Fig. 4C). Using a similar strategy, i.e. by co-incubating the deubiquitinating enzyme IsoT with its natural substrate ubiquitin, Drag et al. (33) observed a 20-fold enhancement of the cleavage of the synthetic tetrapeptide Ac-LRGG-AFC. However, the two truncated versions failed to significantly enhance hydrolysis of the Ac-ETFG-AFC substrate by TcAtg4.2, whereas both full length natural substrates completely prevented cleavage of the synthetic substrate, suggesting a direct competition between both substrates for the binding into the active site cleft of the enzyme (Fig. 4D and E).

*A positional scanning of the tetrapeptide fluorogenic substrate library (PS-SCL) revealed high preference for cyclohexylalanine in the P2 position*–In order to identify the optimal amino acid sequence of a tetrapeptide substrate for TcAtg4.2 we designed a PS-SCL. In all sublibraries a glycine residue was fixed in the P1 position, due to the absolute requirement of ATG4 proteases for a glycine in this position (Fig. 5A) (31,60). The P2 sublibrary was designed by fixing P1, P3 and P4 residues with Gly, Glu and Ser, respectively. The P2 position sublibrary included 19 natural and three non-natural amino acids, nor-leucine (O), cyclohexylalanine (Cha) and homoPhenylalanine (hPhe). Since HsAtg4B shows high preference towards Phe in the P2 position unnatural amino acids were used to possibly improve substrate specificity. P3 and P4 sublibraries included only natural L-amino acids. The PS-SCL contained two sublibraries for determination of the optimal amino acid residues in the P4 position. The Ac-XTFG-ACC sublibrary with last three amino acids proximal to the cleavage site identical to the natural substrate TcAtg8.1 and Ac-XAFG-ACC with amino acid sequence corresponding to the sequence of the



Downloaded from http://www.jbc.org/ at Jozef Stefan Institut on October 11, 2015

TcAtg8.2 homologue. All substrates in the PS-SCL were conjugated to the 7-amino-4-carbamoylmethylcoumarin (ACC) fluorophore. Screening of the P2 sublibrary revealed an almost exclusive selectivity of TcAtg4.2 towards the unnatural amino acid residue cyclohexylalanine (Cha). In contrast, screening of the P3 and P4 sublibraries revealed a much broader specificity in these two positions. In the P3 position the most preferred residue was arginine, followed by threonine, alanine and lysine, whereas the enzyme exhibited preference for tryptophan, followed by lysine, in the P4 position (Fig. 5B). To further evaluate these findings several mutants of the natural TcAtg4.2 substrate, TcAtg8.2, were prepared including P2 F130S, P3 T129H and P4 S128G mutants. All three included mutations to non-preferred residues based on PS-SCL results. In addition, the P1 G131A mutant, which is known to prevent the cleavage (31) was used as a positive control. In addition to Gly in the P1 position also Phe in the P2 position, as in HsAtg4B (59,61), was found to be critical for cleavage of natural substrates, whereas substitutions in P4 and P3 positions had only a minor effect (Fig. 5C).

*Searching for optimal synthetic substrate for the TcAtg4.2*–Based on the TcAtg4.2 specificity obtained in PS-SCL and previous data for HsAtg4B (40) a new tetrapeptide library was synthesized consisting of eleven substrates. Seven of them carried cyclohexylalanine (Cha) in the P2 position and were expected to be cleaved preferably by TcAtg4.2 rather than by the human orthologue HsAtg4B. The other four substrates carried Phe in the P2 position, which is preferred by HsAtg4B and were selected for comparison. Based on the screening results, Lys or Trp were fixed in the P4 position as the two preferred residues for TcATg4.2 in eight substrates, six in combination with Cha in the P2 position and two with Phe in the P2. Among them, KLChaG and KLFG contained a Leu in the P3 position, which was found unfavorable for TcATg4.2, but highly favorable in this position for HsAtg4B. The last Cha-containing substrate was GLChaG with the non-preferred amino acids Gly in the P4 position and Leu in the P3 position, which was expected to be only poorly cleaved by TcAtg4.2. Finally, the GLFG and GTFG substrates were included in the group as the preferred substrates of HsAtg4B (40).

As expected, TcAtg4.2 cleaved substrates containing Cha in the P2 position much more efficiently than those with a Phe. The best substrate for TcAtg4.2 was found to be Ac-KTChaG-ACC, followed by Ac-KKChaG-ACC with $k_{cat}/K_m$ values of 2.1 ± 0.23 $M^{-1}$ $s^{-1}$ and 3.0 ± 0.15 $M^{-1}$ $s^{-1}$, respectively (Fig. 6A). These results confirmed TcAtg4.2 specificity determined with the PS-SCL. In contrast, HsAtg4B cleaved best Ac-GTFG-ACC and Ac-GLFG-ACC, in agreement with previous results (40). In order to improve catalysis and quantum yield, the ACC fluorophore was substituted with AFC in the best two TcAtg4.2 substrates, KTChaG and KKChaG, yielding $k_{cat}/K_m$ values of 112 ± 7.6 $M^{-1}$ $s^{-1}$ and 137 ± 8.2 $M^{-1}$ $s^{-1}$, respectively.

*Selectivity of tetrapeptide substrates against other proteases*–Autophagins participate in an ubiquitin-like conjugating cascade, where they possess activity reminiscent of deubiquitinating (DUBs) and deSUMOylating (SENPs) enzymes, which mediate processing and deconjugation of ubiquitin and SUMO proteins. Therefore we decided to test eight tetrapeptide substrates for their selectivity against human proteases deSUMOylating (SENP) proteins SENP1 and SENP2, and Deubiquitinating (DUB) protein UCH-L3. These substrates included Ac-GTFG-AFC and Ac-STFG-AFC derived from the HsAtg4B PS-SCL, Ac-NTFG-AFC and Ac-ETFG-AFC bearing amino acid sequences of the human Atg4 substrates GATE-16 and LC3, Ac-KKChaG-AFC and Ac-KTChaG-AFC as two best substrates for TcAtg4.2, and, finally Ac-SAChaG-AFC and Ac-ATChaG-AFC, bearing amino acid sequences from TcAtg8.1 and TcAtg8.2 with Cha in the P2 position (Fig. 6B).However, none of the proteases tested exhibited any significant activity against any of the substrates in comparison with TcAtg4.2, which was used as a positive control.

As human lysosomal cysteine cathepsins are known to participate in the final stages of autophagy by degrading the sequestered material including the Atg8 homologues (62,63), we next incubated human recombinant cathepsins B, K, L and S with TcAtg8.1 and TcAtg8.2. All tested cathepsins degraded TcAtg8.1 as well as TcAtg8.2 very effectively (Fig. 6C). Therefore, we additionally tested four synthetic tetrapeptide substrates against the cathepsins. In addition to Ac-KKChaG-AFC and Ac-KTChaG-AFC, the two



Downloaded from http://www.jbc.org/ at Jozef Stefan Institut on October 11, 2015

best substrates for TcAtg4.2, Ac-SAChaG-AFC and Ac-ATChaG-AFC, bearing amino acid sequences from the TcAtg8.1 and TcAtg8.2 with Cha instead of a Phe in the P2 position were used. However, cysteine cathepsins, in particular cathepsin L, were far more efficient in cleaving all tetrapeptide substrates than the other enzymes tested (Fig. 6D). Using MALDI-TOF mass spectrometry analysis we confirmed that cathepsins cleaved the synthetic AFC substrates at the same position as TcAtg4.2 (Data not shown).

## DISCUSSION

ATG4 proteases (autophagins) are responsible for processing Atg8 proteins for their successful conjugation to the phosphatydilethanolamine, which is critical for autophagosome formation, as well as for their subsequent deconjugation, which enables the release of ATG8 proteins from the phagosome membrane. *Trypanosoma cruzi*, like other related parasites *Trypanosoma brucei* and *Leishmania major* genomes, encodes two copies of Atg4 proteins, Atg4.1 and Atg4.2. Williams et al. (48) demonstrated that in *L. major* Atg4.1 carries the majority of endopeptidase activity, while Atg4.2 is predominantly responsible for the delipidation of Atg8 homologues from the autophagosomal membrane. In agreement with these findings, both Trypanosoma autophagins are able to process natural substrates TcAtg8.1 and TcAtg8.2, with TcAtg4.2 exhibiting the majority of the proteolytic activity *in vitro*, whereas Atg4.1 exhibited approximately 10,000-fold lower proteolytic efficiency (31).

All our functional studies pointed out substantial similarity between TcAtg4.2 and HsAtg4B. Due to this high conservation of the ATG4 proteases through evolution and the potential of TcATG4.2 as a therapeutic target for Chagas disease (17,26), there is a need to develop selective assays that would discriminate between Trypanosoma and human autophagins to avoid potential off target effects of TcATG4.2-targeting compounds. We took advantage of the PS-SCL, which had been successfully applied to define preferred specificity of a number of proteases, including caspases (64), deSUMOylating enzymes (SENPs) (34), deubiquitinating enzymes (DUBs) (33), and human autophagins (40). The expanded P2 sublibrary, which additionally contained several unnatural amino acids, enabled generation of selective substrates, with which we were able to distinguish between the activities of closely related homologues human Atg4B and *T. cruzi* Atg4.2. The use of unnatural amino acids has been successfully applied to identify substantially improved substrates of several other proteases including human cathepsin C (65), neutrophil elastase (41) and caspases (66). Using this approach, we were able to identify Ac-KKChaG-AFC as an optimal substrate distinguishing TcAtg4.2 from HsAtg4B. The substrate contains in the P2 position the unnatural Phe homologue cyclohexylalanine (Cha), which was found to be the major selectivity determinant, thereby confirming the validity of the approach to include unnatural amino acids. Since Cha contains a methyl group linked to the cyclohexyl ring, which in contrast to the planar phenyl ring occupies a chair or bath conformation, we suggest that the S2 binding site in TcAtg4.2 has a different architecture than the human orthologue. In addition to Cha, which was found to be by far preferred P2 residue for TcATG4.2, aromatic residues such as Phe and Tyr were also tolerated in this position. As found in human Atg4B and its natural substrate LC3 (40,58) and also in TcAtg8.2, both P1 Gly and a P2 aromatic residue in the substrate polypeptide chain are critical for substrate recognition by TcAtg4.2. In addition, the two enzymes exhibited some minor differences in P3 and P4 specificities as revealed on the basis of comparison of our results for TcAtg4.2 with the previous results for HsAtg4B (40). Surprisingly, TcAtg4.2 was found to cleave Ac-KLChaG-ACC with almost the same efficiency as Ac-KKChaG-ACC, and even Ac-GLChaG-ACC with about 3-fold lower efficiency. These results could be due to subsite cooperativity (27). Cha in the P2 position thereby seems to have an enormous effect on the adjacent positions, much stronger than Phe, which was fixed in this position in the original libraries (Fig. 6). Moreover, when this was combined with a Lys in the P4 position, the negative effect of a Leu in the P3 position was completely overcome. In addition, the finding that the replacement of the larger ACC fluorophore with the smaller AFC dramatically (~50-fold) increased $k_{cat}/K_m$ values for two best substrates, Ac-KTChaG and Ac-KKChaG, suggests that the S1' subsite of TcAtg4.2 is relatively small and

Downloaded from http://www.jbc.org/ at Jozef Stefan Institut on October 11, 2015

tolerates smaller residues such as those found in the natural substrates TcAtg8.1 and TcAtg8.2, where Gly and Ser, respectively, are found in the P1' position (31).

Interestingly, Ac-KTChaG-AFC and Ac-KKChaG-AFC, which were the best substrates for TcAtg4.2, were only very poor substrates for the functionally-related human cytosolic proteins HsAtg4B, SENP1 and 2 and UCH-L3, but very good substrates for human cysteine cathepsins B and L. This might pose a serious problem in further design of selective Atg4 substrates that would work in cellular assays, as cathepsins, which are normally involved in the turnover of Atg8/LC3, may cleave them resulting in false positive results, but should not pose a problem for *in vitro* screening. Similarly, a cathepsin L-related enzyme cruzipain is present in *T. cruzi* (67,68), which might additionally complicate *in vivo* screening in the parasite, since the enzyme, as TcAtg4.2, prefers Cha in the P2 position (69). Replacement of Cha with other nonnatural Phe derivatives might therefore be an alternative to improve specificity of the substrates.

In addition to the residues intimately involved in substrate hydrolysis there are two additional domains critically important for substrate recognition and binding that require major conformational changes for efficient substrate hydrolysis as revealed by structural analysis of human Atg4B (58,59). These are the regulatory loop, under which the catalytic Cys residue is buried and functions as an autoinhibitory peptide, and the N-terminal tail of the enzyme. Deletion of the regulatory loop or reduction of the loop flexibility as a consequence of mutation of one of the two conserved glycines preceding it resulted in a complete loss of processing capacity of the protein. In contrast, deletion of the N-terminal region had only a minor effect on substrate hydrolysis, suggesting that the N-terminal domain plays only a minor role in hydrolysis of both natural and small substrates. This supports the idea that the N-terminal region is more important for deconjugation activity of the enzyme, as suggested earlier (59). Atg4 contains a unique inserted regional exosite distant from the catalytic site that binds the ubiquitin-like domain of Atg8/LC3, termed the ubiquitin-binding domain. Binding to this site is hypothesized to induce a conformational change that activates the enzyme and enables entrance of the C-terminus of the substrate into the active site cleft (58). The lack of this domain interaction explains the very inefficient hydrolysis of tetrapeptide substrates. However, the addition of ubiquitin-like domain in *trans* did not improve tetrapeptide substrate hydrolysis as shown by co-incubating the enzyme and tetrapeptide substrate with C-terminal truncation mutants of TcAtg8 lacking the C-terminal residues. This stands in contrast to the activation of the deubiquitinating enzyme IsoT by a similar approach (33), suggesting that substrate hydrolysis differs between these functionally related enzymes.

In summary, we have thoroughly characterized TcAtg4.2, the major autophagin of the *T. cruzi* parasite. The enzyme resembles its human orthologue Atg4B in many properties, in agreement with the very high conservation of the autophagy through evolution. Although the two enzymes share very similar substrate specificity, using PS-SCL we were able to demonstrate that the Trypanosoma autophagin exhibited substantial preference towards the unnatural amino acid cyclohexylalanine (Cha) in the P2 position, which was not accepted by the human orthologue, as well as for a smaller group in the P1' position. This represents a solid basis for the development of *T. cruzi* Atg4.2 specific substrates, which should, however, be conjugated to moieties that could deliver the substrate specifically into the cytosol in order to avoid their non-specific cleavage in the degradative organelles of living cells. If successful, the strategy might also allow tracking of autophagy in the living parasites.

Downloaded from http://www.jbc.org/ at Jozef Stefan Institut on October 11, 2015

**Acknowledgements**
We thank Ivica Štefe and Matej Vizovišek for preparing cysteine cathepsins.

**Conflict of interest**
The authors declare that they have no conflicts of interest with the contents of this article.

**Author contribution**
Marcin Poreba, Marcin Drag, Aleksandra Wilk and Agata Borowik synthesized synthetic fluorogenic substrates and libraries. Robert Vidmar performed MALDI-TOF analysis. Dejan Caglič designed pOPINF-Atg4B construct. Dejan Caglič, Jelena Rajković, Guy Salvesen, Vito Turk and Boris Turk designed the experiments. Jelena Rajković and Marcin Poreba performed the experiments. Jelena Rajković and Boris Turk wrote the paper with editorial input from Marcin Drag and Guy Salvesen.

## REFERENCES

1. Yorimitsu, T., and Klionsky, D. J. (2005) Autophagy: molecular machinery for self-eating. *Cell death and differentiation* **12 Suppl 2**, 1542-1552
2. Long, X., Ortiz-Vega, S., Lin, Y., and Avruch, J. (2005) Rheb binding to mammalian target of rapamycin (mTOR) is regulated by amino acid sufficiency. *J Biol Chem* **280**, 23433-23436
3. Kim, E., Goraksha-Hicks, P., Li, L., Neufeld, T. P., and Guan, K. L. (2008) Regulation of TORC1 by Rag GTPases in nutrient response. *Nature cell biology* **10**, 935-945
4. Byfield, M. P., Murray, J. T., and Backer, J. M. (2005) hVps34 is a nutrient-regulated lipid kinase required for activation of p70 S6 kinase. *J Biol Chem* **280**, 33076-33082
5. Chen, J. L., Lin, H. H., Kim, K. J., Lin, A., Forman, H. J., and Ann, D. K. (2008) Novel roles for protein kinase Cdelta-dependent signaling pathways in acute hypoxic stress-induced autophagy. *J Biol Chem* **283**, 34432-34444
6. Papandreou, I., Lim, A. L., Laderoute, K., and Denko, N. C. (2008) Hypoxia signals autophagy in tumor cells via AMPK activity, independent of HIF-1, BNIP3, and BNIP3L. *Cell death and differentiation* **15**, 1572-1581
7. Vasseur, S., Afzal, S., Tardivel-Lacombe, J., Park, D. S., Iovanna, J. L., and Mak, T. W. (2009) DJ-1/PARK7 is an important mediator of hypoxia-induced cellular responses. *Proc Natl Acad Sci U S A* **106**, 1111-1116
8. Bjorkoy, G., Lamark, T., Brech, A., Outzen, H., Perander, M., Overvatn, A., Stenmark, H., and Johansen, T. (2005) p62/SQSTM1 forms protein aggregates degraded by autophagy and has a protective effect on huntingtin-induced cell death. *J Cell Biol* **171**, 603-614
9. Bernales, S., McDonald, K. L., and Walter, P. (2006) Autophagy counterbalances endoplasmic reticulum expansion during the unfolded protein response. *PLoS biology* **4**, e423
10. Yorimitsu, T., Nair, U., Yang, Z., and Klionsky, D. J. (2006) Endoplasmic reticulum stress triggers autophagy. *J Biol Chem* **281**, 30299-30304
11. Zhang, H., Bosch-Marce, M., Shimoda, L. A., Tan, Y. S., Baek, J. H., Wesley, J. B., Gonzalez, F. J., and Semenza, G. L. (2008) Mitochondrial autophagy is an HIF-1-dependent adaptive metabolic response to hypoxia. *J Biol Chem* **283**, 10892-10903
12. Sandoval, H., Thiagarajan, P., Dasgupta, S. K., Schumacher, A., Prchal, J. T., Chen, M., and Wang, J. (2008) Essential role for Nix in autophagic maturation of erythroid cells. *Nature* **454**, 232-235
13. Sanjuan, M. A., Dillon, C. P., Tait, S. W., Moshiach, S., Dorsey, F., Connell, S., Komatsu, M., Tanaka, K., Cleveland, J. L., Withoff, S., and Green, D. R. (2007) Toll-like receptor signalling in macrophages links the autophagy pathway to phagocytosis. *Nature* **450**, 1253-1257



Downloaded from http://www.jbc.org/ at Jozef Stefan Institut on October 11, 2015

14. Wang, Y., Weiss, L. M., and Orlofsky, A. (2009) Host cell autophagy is induced by Toxoplasma gondii and contributes to parasite growth. *J Biol Chem* **284**, 1694-1701
15. Wang, S., Li, B., Qiao, H., Lv, X., Liang, Q., Shi, Z., Xia, W., Ji, F., and Jiao, J. (2014) Autophagy-related gene Atg5 is essential for astrocyte differentiation in the developing mouse cortex. *EMBO reports* **15**, 1053-1061
16. Lv, X., Jiang, H., Li, B., Liang, Q., Wang, S., Zhao, Q., and Jiao, J. (2014) The crucial role of Atg5 in cortical neurogenesis during early brain development. *Scientific reports* **4**, 6010
17. Alvarez, V. E., Kosec, G., Sant Anna, C., Turk, V., Cazzulo, J. J., and Turk, B. (2008) Blocking autophagy to prevent parasite differentiation: a possible new strategy for fighting parasitic infections? *Autophagy* **4**, 361-363
18. Barquilla, A., Crespo, J. L., and Navarro, M. (2008) Rapamycin inhibits trypanosome cell growth by preventing TOR complex 2 formation. *Proc Natl Acad Sci U S A* **105**, 14579-14584
19. Wada, Y., Sun-Wada, G. H., Kawamura, N., and Aoyama, M. (2014) Role of autophagy in embryogenesis. *Current opinion in genetics & development* **27**, 60-66
20. Shapiro, I. M., Layfield, R., Lotz, M., Settembre, C., and Whitehouse, C. (2014) Boning up on autophagy: the role of autophagy in skeletal biology. *Autophagy* **10**, 7-19
21. Levine, B., and Klionsky, D. J. (2004) Development by self-digestion: molecular mechanisms and biological functions of autophagy. *Developmental cell* **6**, 463-477
22. Mizushima, N., and Levine, B. (2010) Autophagy in mammalian development and differentiation. *Nature cell biology* **12**, 823-830
23. Hemelaar, J., Lelyveld, V. S., Kessler, B. M., and Ploegh, H. L. (2003) A single protease, Apg4B, is specific for the autophagy-related ubiquitin-like proteins GATE-16, MAP1-LC3, GABARAP, and Apg8L. *J Biol Chem* **278**, 51841-51850
24. Tanida, I., Sou, Y. S., Ezaki, J., Minematsu-Ikeguchi, N., Ueno, T., and Kominami, E. (2004) HsAtg4B/HsApg4B/autophagin-1 cleaves the carboxyl termini of three human Atg8 homologues and delipidates microtubule-associated protein light chain 3- and GABAA receptor-associated protein-phospholipid conjugates. *J Biol Chem* **279**, 36268-36276
25. Kirisako, T., Ichimura, Y., Okada, H., Kabeya, Y., Mizushima, N., Yoshimori, T., Ohsumi, M., Takao, T., Noda, T., and Ohsumi, Y. (2000) The reversible modification regulates the membrane-binding state of Apg8/Aut7 essential for autophagy and the cytoplasm to vacuole targeting pathway. *J Cell Biol* **151**, 263-276
26. Duszenko, M., Ginger, M. L., Brennand, A., Gualdron-Lopez, M., Colombo, M. I., Coombs, G. H., Coppens, I., Jayabalasingham, B., Langsley, G., de Castro, S. L., Menna-Barreto, R., Mottram, J. C., Navarro, M., Rigden, D. J., Romano, P. S., Stoka, V., Turk, B., and Michels, P. A. (2011) Autophagy in protists. *Autophagy* **7**, 127-158
27. Yang, Z., and Klionsky, D. J. (2009) An overview of the molecular mechanism of autophagy. *Curr Top Microbiol Immunol* **335**, 1-32
28. Meijer, W. H., van der Klei, I. J., Veenhuis, M., and Kiel, J. A. (2007) ATG genes involved in non-selective autophagy are conserved from yeast to man, but the selective Cvt and pexophagy pathways also require organism-specific genes. *Autophagy* **3**, 106-116
29. WHO. (2010) Sixty-third World Health Assembly Report;Chagas disease: control and elimination A63/17. *Geneva, Switzerland. World Health Organization*
30. De Souza, W. (2002) Basic cell biology of Trypanosoma cruzi. *Current pharmaceutical design* **8**, 269-285
31. Alvarez, V. E., Kosec, G., Sant'Anna, C., Turk, V., Cazzulo, J. J., and Turk, B. (2008) Autophagy is involved in nutritional stress response and differentiation in Trypanosoma cruzi. *J Biol Chem* **283**, 3454-3464


Downloaded from http://www.jbc.org/ at Jozef Stefan Institut on October 11, 2015

32. Berrow, N. S., Alderton, D., Sainsbury, S., Nettleship, J., Assenberg, R., Rahman, N., Stuart, D. I., and Owens, R. J. (2007) A versatile ligation-independent cloning method suitable for high-throughput expression screening applications. *Nucleic acids research* **35**, e45
33. Drag, M., Mikolajczyk, J., Bekes, M., Reyes-Turcu, F. E., Ellman, J. A., Wilkinson, K. D., and Salvesen, G. S. (2008) Positional-scanning fluorigenic substrate libraries reveal unexpected specificity determinants of DUBs (deubiquitinating enzymes). *The Biochemical journal* **415**, 367-375
34. Drag, M., Mikolajczyk, J., Krishnakumar, I. M., Huang, Z., and Salvesen, G. S. (2008) Activity profiling of human deSUMOylating enzymes (SENPs) with synthetic substrates suggests an unexpected specificity of two newly characterized members of the family. *The Biochemical journal* **409**, 461-469
35. Bromme, D., Nallaseth, F. S., and Turk, B. (2004) Production and activation of recombinant papain-like cysteine proteases. *Methods* **32**, 199-206
36. Kuhelj, R., Dolinar, M., Pungercar, J., and Turk, V. (1995) The preparation of catalytically active human cathepsin B from its precursor expressed in Escherichia coli in the form of inclusion bodies. *Eur J Biochem* **229**, 533-539
37. Mihelic, M., Dobersek, A., Guncar, G., and Turk, D. (2008) Inhibitory fragment from the p41 form of invariant chain can regulate activity of cysteine cathepsins in antigen presentation. *J Biol Chem* **283**, 14453-14460
38. Polajnar, M., Vidmar, R., Vizovisek, M., Fonovic, M., Kopitar-Jerala, N., and Zerovnik, E. (2013) Influence of partial unfolding and aggregation of human stefin B (cystatin B) EPM1 mutants G50E and Q71P on selective cleavages by cathepsins B and S. *Biological chemistry* **394**, 783-790
39. Stennicke, H. R., and Salvesen, G. S. (2000) Caspase assays. *Methods in enzymology* **322**, 91-100
40. Shu, C. W., Drag, M., Bekes, M., Zhai, D., Salvesen, G. S., and Reed, J. C. (2010) Synthetic substrates for measuring activity of autophagy proteases: autophagins (Atg4). *Autophagy* **6**, 936-947
41. Kasperkiewicz, P., Poreba, M., Snipas, S. J., Parker, H., Winterbourn, C. C., Salvesen, G. S., and Drag, M. (2014) Design of ultrasensitive probes for human neutrophil elastase through hybrid combinatorial substrate library profiling. *Proceedings of the National Academy of Sciences of the United States of America* **111**, 2518-2523
42. Schagger, H. (2006) Tricine-SDS-PAGE. *Nature protocols* **1**, 16-22
43. Li, M., Hou, Y., Wang, J., Chen, X., Shao, Z. M., and Yin, X. M. (2011) Kinetics comparisons of mammalian Atg4 homologues indicate selective preferences toward diverse Atg8 substrates. *J Biol Chem* **286**, 7327-7338
44. Grierson, A. W., Nicholson, R., Talbot, P., Webster, A., and Kemp, G. (1994) The protease of adenovirus serotype 2 requires cysteine residues for both activation and catalysis. *J Gen Virol* **75 ( Pt 10)**, 2761-2764
45. Rancourt, C., Tihanyi, K., Bourbonniere, M., and Weber, J. M. (1994) Identification of active-site residues of the adenovirus endopeptidase. *Proc Natl Acad Sci U S A* **91**, 844-847
46. Whitmore, L., and Wallace, B. A. (2008) Protein secondary structure analyses from circular dichroism spectroscopy: methods and reference databases. *Biopolymers* **89**, 392-400
47. Andrade, M. A., Chacon, P., Merelo, J. J., and Moran, F. (1993) Evaluation of secondary structure of proteins from UV circular dichroism spectra using an unsupervised learning neural network. *Protein engineering* **6**, 383-390
48. Williams, R. A., Woods, K. L., Juliano, L., Mottram, J. C., and Coombs, G. H. (2009) Characterization of unusual families of ATG8-like proteins and ATG12 in the protozoan parasite Leishmania major. *Autophagy* **5**, 159-172


Downloaded from http://www.jbc.org/ at Jozef Stefan Institut on October 11, 2015

49. Herman, M., Gillies, S., Michels, P. A., and Rigden, D. J. (2006) Autophagy and related processes in trypanosomatids: insights from genomic and bioinformatic analyses. *Autophagy* **2**, 107-118
50. Marino, G., Uria, J. A., Puente, X. S., Quesada, V., Bordallo, J., and Lopez-Otin, C. (2003) Human autophagins, a family of cysteine proteinases potentially implicated in cell degradation by autophagy. *J Biol Chem* **278**, 3671-3678
51. Fernandez, A. F., and Lopez-Otin, C. (2015) The functional and pathologic relevance of autophagy proteases. *J Clin Invest* **125**, 33-41
52. Biasini, M., Bienert, S., Waterhouse, A., Arnold, K., Studer, G., Schmidt, T., Kiefer, F., Cassarino, T. G., Bertoni, M., Bordoli, L., and Schwede, T. (2014) SWISS-MODEL: modelling protein tertiary and quaternary structure using evolutionary information. *Nucleic acids research* **42**, W252-258
53. Arnold, K., Bordoli, L., Kopp, J., and Schwede, T. (2006) The SWISS-MODEL workspace: a web-based environment for protein structure homology modelling. *Bioinformatics* **22**, 195-201
54. Kiefer, F., Arnold, K., Kunzli, M., Bordoli, L., and Schwede, T. (2009) The SWISS-MODEL Repository and associated resources. *Nucleic acids research* **37**, D387-392
55. Guex, N., Peitsch, M. C., and Schwede, T. (2009) Automated comparative protein structure modeling with SWISS-MODEL and Swiss-PdbViewer: a historical perspective. *Electrophoresis* **30 Suppl 1**, S162-173
56. Ma, J., Wang, S., Zhao, F., and Xu, J. (2013) Protein threading using context-specific alignment potential. *Bioinformatics* **29**, i257-265
57. Benkert, P., Biasini, M., and Schwede, T. (2011) Toward the estimation of the absolute quality of individual protein structure models. *Bioinformatics* **27**, 343-350
58. Sugawara, K., Suzuki, N. N., Fujioka, Y., Mizushima, N., Ohsumi, Y., and Inagaki, F. (2005) Structural basis for the specificity and catalysis of human Atg4B responsible for mammalian autophagy. *J Biol Chem* **280**, 40058-40065
59. Satoo, K., Noda, N. N., Kumeta, H., Fujioka, Y., Mizushima, N., Ohsumi, Y., and Inagaki, F. (2009) The structure of Atg4B-LC3 complex reveals the mechanism of LC3 processing and delipidation during autophagy. *The EMBO journal* **28**, 1341-1350
60. Tanida, I., Ueno, T., and Kominami, E. (2004) Human light chain 3/MAP1LC3B is cleaved at its carboxyl-terminal Met121 to expose Gly120 for lipidation and targeting to autophagosomal membranes. *J Biol Chem* **279**, 47704-47710
61. Noda, N. N., Ohsumi, Y., and Inagaki, F. (2009) ATG systems from the protein structural point of view. *Chemical reviews* **109**, 1587-1598
62. Turk, B., and Turk, V. (2009) Lysosomes as "suicide bags" in cell death: myth or reality? *J Biol Chem* **284**, 21783-21787
63. Repnik, U., Stoka, V., Turk, V., and Turk, B. (2012) Lysosomes and lysosomal cathepsins in cell death. *Biochimica et biophysica acta* **1824**, 22-33
64. Thornberry, N. A., Rano, T. A., Peterson, E. P., Rasper, D. M., Timkey, T., Garcia-Calvo, M., Houtzager, V. M., Nordstrom, P. A., Roy, S., Vaillancourt, J. P., Chapman, K. T., and Nicholson, D. W. (1997) A combinatorial approach defines specificities of members of the caspase family and granzyme B. Functional relationships established for key mediators of apoptosis. *J Biol Chem* **272**, 17907-17911
65. Poreba, M., Mihelic, M., Krai, P., Rajkovic, J., Krezel, A., Pawelczak, M., Klemba, M., Turk, D., Turk, B., Latajka, R., and Drag, M. (2014) Unnatural amino acids increase activity and specificity of synthetic substrates for human and malarial cathepsin C. *Amino acids* **46**, 931-943
66. Poreba, M., Kasperkiewicz, P., Snipas, S. J., Fasci, D., Salvesen, G. S., and Drag, M. (2014) Unnatural amino acids increase sensitivity and provide for the design of highly selective caspase substrates. *Cell death and differentiation* **21**, 1482-1492


Downloaded from http://www.jbc.org/ at Jozef Stefan Institut on October 11, 2015

67. Kosec, G., Alvarez, V., and Cazzulo, J. J. (2006) Cysteine proteinases of Trypanosoma cruzi: from digestive enzymes to programmed cell death mediators. *Biocell* **30**, 479-490
68. Cazzulo, J. J., Stoka, V., and Turk, V. (2001) The major cysteine proteinase of Trypanosoma cruzi: a valid target for chemotherapy of Chagas disease. *Curr Pharm Des* **7**, 1143-1156
69. Lecaille, F., Authie, E., Moreau, T., Serveau, C., Gauthier, F., and Lalmanach, G. (2001) Subsite specificity of trypanosomal cathepsin L-like cysteine proteases. Probing the S2 pocket with phenylalanine-derived amino acids. *Eur J Biochem* **268**, 2733-2741

## FOOTNOTES

The work has been supported by Slovene Research Agency (grant P1-0140 to B.T.), by a statutory activity subsidy from the Polish Ministry of Science and Higher Education for the Faculty of Chemistry at Wroclaw University of Technology, and by NIH grant R01GM09040.

Abbreviations used are: Ac, acetyl; ACC, 7-amino-4-carbamoylmethylcoumarin; AFC, 7-amino-4-trifluoromethylcoumarin; Boc, tert -butoxycarbonyl; DTT, dithiothreitol; DUB, deubiquitinating enzyme; IPTG, isopropyl-β-D-galactopyranoside; PS-SCL, positional scanning substrate combinatorial library; SUMO, small ubiquitin-related modifier; SENP, Sentrin/SUMO-specific protease.

## FIGURE LEGENDS

**FIGURE 1.** (A) Expression and purification of recombinant proteins. Proteins were expressed in *Escherichia coli BL21* (DE3) strain. All proteins were expressed in fusion with $His_6$-tag. Expressed recombinant proteins were purified using HisTrap FF crude columns (GE Healthcare). Purity and relative molecular masses of recombinant proteins were determined with SDS-PAGE with Coomassie Brilliant Blue (CBB). Molecular markers are indicated in kilodaltons (kDa). (B) Time-course of TcAtg4.2 cleavage of TcAtg8.1 and TcAtg8.2. Recombinant wild-type TcATg4.2 (WT) and catalytic mutant TcAtg4.2 C91S were incubated with TcAtg8.1 for designated times. Cleavage was analyzed with SDS-PAGE and Coomassie Brilliant Blue (CBB) staining. In the control experiment TcAtg8.1 and TcAtg8.2 were incubated in the absence of recombinant TcAtg4.2. Other experimental details are in Materials and Methods.

**FIGURE 2.** Biochemical characterization of TcAtg4.2. All experimental details are described in the Materials and Methods. (A) TcAtg4.2 cleavage of Ac-ETFG-AFC, Ac-STFG-AFC, Ac-NTFG-AFC and Ac-GTFG-AFC. TcAtg4.2 cleaves Ac-ETFG-AFC 7.4, 6.3 and 2.2 more efficient than Ac-STFG-AFC, Ac-NTFG-AFC and Ac-GTFG-AFC, respectively. The y-axis represents RFU per sec. Only the linear portions of the progress curves were used to calculate velocity. (B) pH dependence of TcAtg4.2 activity was assayed in 50 mM buffers of various pH values in the presence of 0.5 M $K_2HPO_4$ and 5 mM DTT. The concentrations of enzyme and Ac-ETFG-AFC were 4 μM and 100 μM, respectively. (C) To evaluate the effect of buffer composition on TcAtg4.2 activity the enzyme was incubated with non-Hoffmeister and Hoffmeister salts. The latter increase proteolytic activity of the enzyme. The non-Hofmeister salts NaCl, KCl and $(NH)_4Cl$ were used as a control to rule out the effects from alteration of ionic strength. (D) Effect of $K_2HPO_4$ concentration on proteolytic activity of TcAtg4.2. (E) Effect of $K_2HPO_4$ concentration on conformation of TcAtg4.2. Far-UV CD spectra of TcAtg4.2 in the absence or presence of different $K_2HPO_4$ concentrations shows unfavorable changes in the enzyme conformation when salt concentrations exceeds 0.5 M. (F) The effect of substrate length on TcAtg4.2 activity. TcAtg4.2 activity was measured in the presence of synthetic tetra-, hexa-, and octapeptide substrates, and was found to increase with the increasing length of the substrate. (G) Cys 91 to Ser mutation abolishes the activity of TcAtg4.2. The S.D. values in all experiments were calculated from at least three independent measurements.



Downloaded from http://www.jbc.org/ at Jozef Stefan Institut on October 11, 2015

**FIGURE 3.** Homology modeling of TcAtg4.2 on basis of human Atg4A and Atg4B. (A) Multiple alignment of amino acid sequences was performed using CLUSTAL W for neighbour-joining tree construction (MEGA version 6). The scale indicates distance. (B) Superposition of templates: HsAtg4A in green (PDB code 2P82) and HsAtg4B in orange (PDB code 2D1I). (C) Superposition of TcAtg4.2 3D models derived by Swiss-model (in blue) and RaptorX web server (in pink). (D) Amino acid alignment of the predicted catalytic domain of *T. cruzi* Atg4 aligned with those of *L. major*, *T. brucei*, *H. sapiens* and *C. cerevisiae*. Genebank accession numbers are: T. cruzi Atg4.1 (DQ768297.1) and Atg4.2 (DQ768298), L. major Atg4.1 (XM_001685663) and Atg4.2 (XM_001684564), T. brucei Atg4.1 (DQ768297.1) and Atg4.2 (XM_824593.1), human Atg4B (NM_013325) and Atg4A (NP_443168.2) and yeast Atg4 (NP_014176.2). * - catalytic Cys, white – in HsAtg4B side chains of Trp142 and P260 form van der Waals interactions and keep regulatory loop in closed conformation in the enzyme free form, red – in HsAtg4B Gly257 enables flexibility of the regulatory loop, gray box - four amino acids corresponding to the predicted regulatory loop which covers the active site cleft of Atg4 proteins.

**FIGURE 4.** Structure-function studies of TcAtg4.2 and TcAtg8.1 and TcAtg8.2. Wild-type TcAtg4.2 (WT), regulatory loop deletion mutant TcAtg4.2 (dL), TcAtg4.2 S246P, S246D, G244H, W158A and two N-terminal deletion mutants (dN18 and dN24) were prepared. (A) TcAtg4.2 S246P, S246D, dN18 and dN24 mutants show only a minor effect on the catalytic activity of TcAtg4.2 towards TcAtg8.1. In contrast, TcAtg4.2 dL, G244H and W158A mutants lost the ability to process TcAtg8.1. (B) In accordance with previous results, deletion of N-terminal tail domain has only a minor effect on the proteolytic activity of the enzyme towards tetrapeptide substrate and TcAtg4.2 dL mutant failed to process the tetrapeptide substrate. (C) Schematic presentation of truncated natural substrates TcAtg8.1 ΔC8 (amino acids 1 to 116) and TcAtg8.2 ΔC14 (amino acids 1 to 126), lacking five amino acid residues upstream of the P1 Gly (Gly121 in TcAtg8.1 and Gly131 in TcAtg8.2). (D) Effect of increasing concentration of full length TcAtg8.1 (black dots) and TcAtg8.1 ΔC8 (white dots) on the TcAtg4.2 activity towards Ac-ETFG-AFC. (E) Effect of increasing concentration of full length TcAtg8.2 (black dots) and TcAtg8.2 ΔC13 (white dots) on the TcAtg4.2 activity towards Ac-ETFG-AFC. The S.D. values in all experiments were calculated from at least three independent measurements.

**FIGURE 5.** Substrate specificity of TcAtg4.2. (A) Schematic representation of sublibraries used in the positional scanning. (B) Positional scanning of the tetrapeptide fluorogenic substrate library revealed high preference of TcAtg4.2 for cyclohexylalanine in the P2 position. In P3 and P4 positions broad spectrum of amino acids is tolerated. ACC fluorescence was monitored at excitation wavelength of 455 nm and emission wavelength of 460 nm. The x-axis shows 'natural' amino acids written in the standard one-letter code. 'Unnatural' amino acids are indicated as follows: O, norleucine; Cha, cyclohexylalanine; hPhe, homoPhenylalanine. The y-axis represents the average relative activity expressed as a percentage of that observed with the "best" amino acid. Standard deviation shown is <10%. Data represent the mean ± S.D. of at least three independent experiments. (C) Wild type TcAtg8.2 and its mutants P1 G131A, P2 F130S, P3 T129H and P4 S128G were incubated in the presence of different concentrations of TcAtg4.2. Replacement of P1 Gly and P2 Phe abolished the ability of TcAtg4.2 to process TcAtg8.2, whereas replacements of amino acids in P3 and P4 positions have only a minor effect on cleavage of the natural substrate TcAtg8.2. Cleavage was analyzed by SDS-PAGE and Coomassie Brilliant Blue (CBB) staining.

**FIGURE 6.** Selectivity of tetrapeptide and protein substrates against autophagins and related enzymes, and cysteine cathepins. (A) *T. cruzi* Atg4.2 (TcAtg4.2) and human Atg4B (HsAtg4B) were incubated with seven tetrapeptide substrates carrying cyclohexlalanine (Cha) and four carrying Phe at P2. The best substrates for TcAtg4.2 were found to be Ac-KTChaG-ACC and Ac-KKChaG-ACC and were not processed by HsAtg4B. ACC release was monitored at excitation wavelength of 455 nm and emission wavelength of 460 nm. (B) For improvement of catalysis the ACC fluorophore in tetrapeptide substrates was substituted with AFC. Tetrapeptide substrates indicated on the x-axis were tested against TcAtg4.2 and HsAtg4B, deSUMOylating enzymes SENP1, SENP2 and deubiquitinating enzyme UCH-L3. The $k_{cat}/K_m$ was determined using nonlinear regression fitting of a series of progress curves using the equation:



Downloaded from http://www.jbc.org/ at Jozef Stefan Institut on October 11, 2015

$k_{cat}/K_m$ = slope/E. The y-axis represents the average relative activity expressed as a percentage of that observed with the "best" amino acid. Standard deviation shown is <10%. (C) Atg8 homologues, human GABARAPL2/GATE-16 and *T. cruzi* TcAtg8.1 and TcAtg8.2 were incubated with recombinant human cathepsins B, K, L and S. All were found to process GABARAPL2/GATE-16 and all except cathepsin B were able to degrade TcAtg8.1 and TcAtg8.2. (D) Two best substrates for TcAtg4.2 Ac-KKChaG-AFC and Ac-KTChaG-AFC as well as Ac-SAChaG-AFC and Ac-ATChaG-AFC, bearing amino acid sequences from the TcAtg8.1 and TcAtg8.2 with Cha in the P2 were tested on human cysteine cathepsinsB, K, L and S. Particularly cathepsin L was able to cleave all substrates very efficiently. The S.D. values in all experiments were calculated from at least three independent measurements.

Downloaded from http://www.jbc.org/ at Jozef Stefan Institut on October 11, 2015

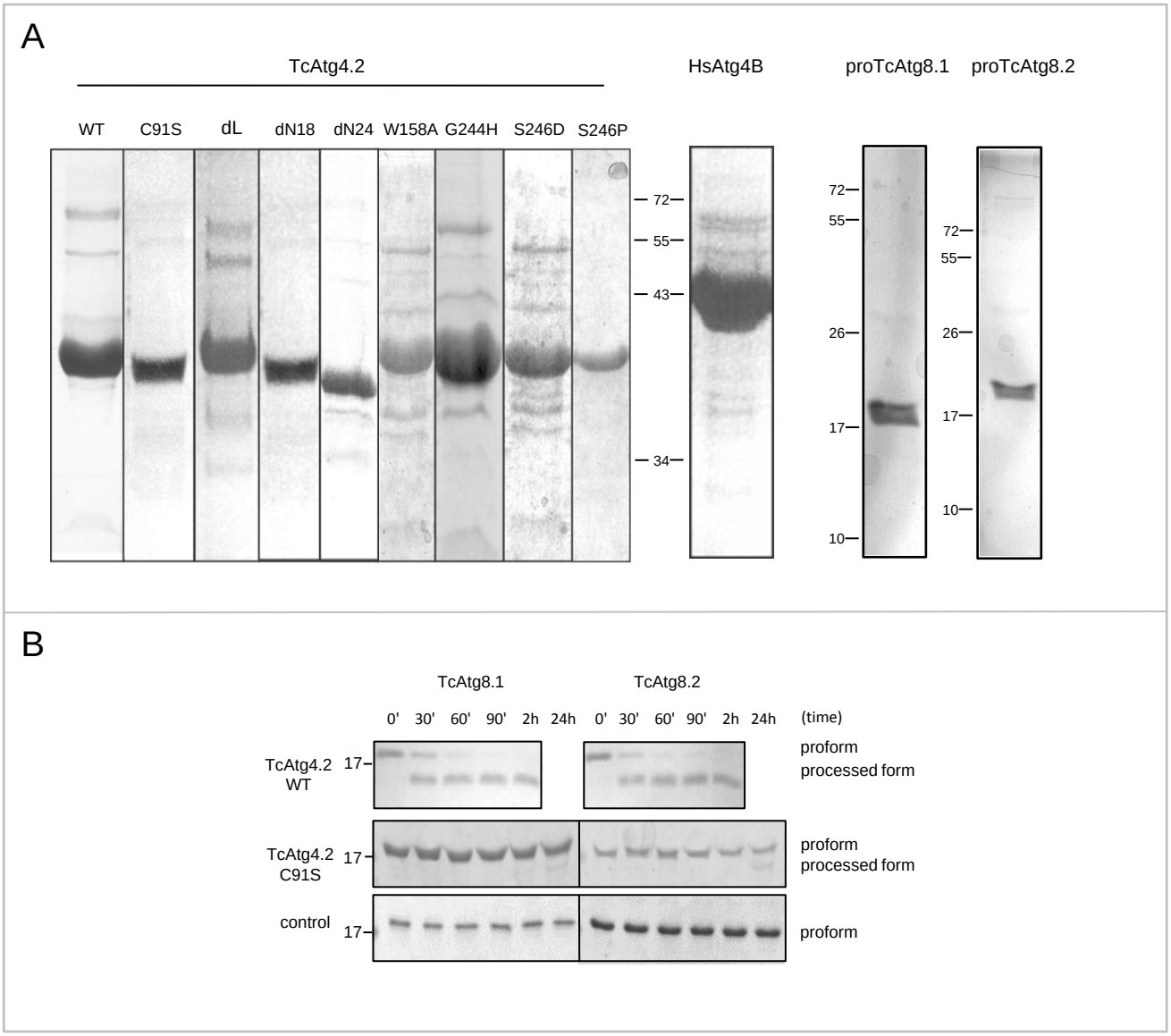

A
TcAtg4.2
HsAtg4B
proTcAtg8.1
proTcAtg8.2
WT
C91S
dL
dN18
dN24
W158A
G244H
S246D
S246P
72
55
43
34
26
17
10
B
TcAtg8.1
TcAtg8.2
0'
30'
60'
90'
2h
24h
(time)
TcAtg4.2 WT
TcAtg4.2 C91S
control
proform
processed form

Figure 1

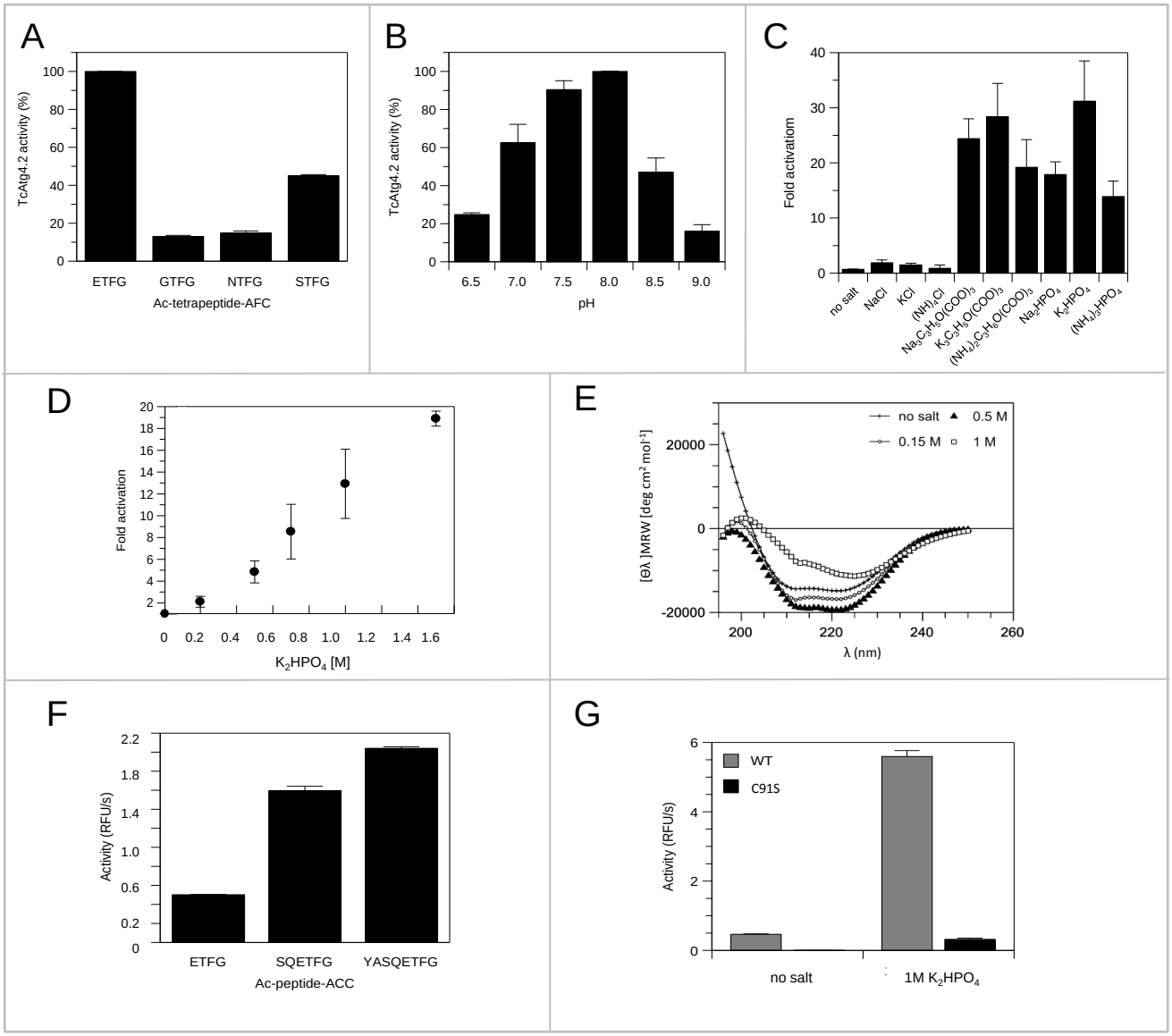
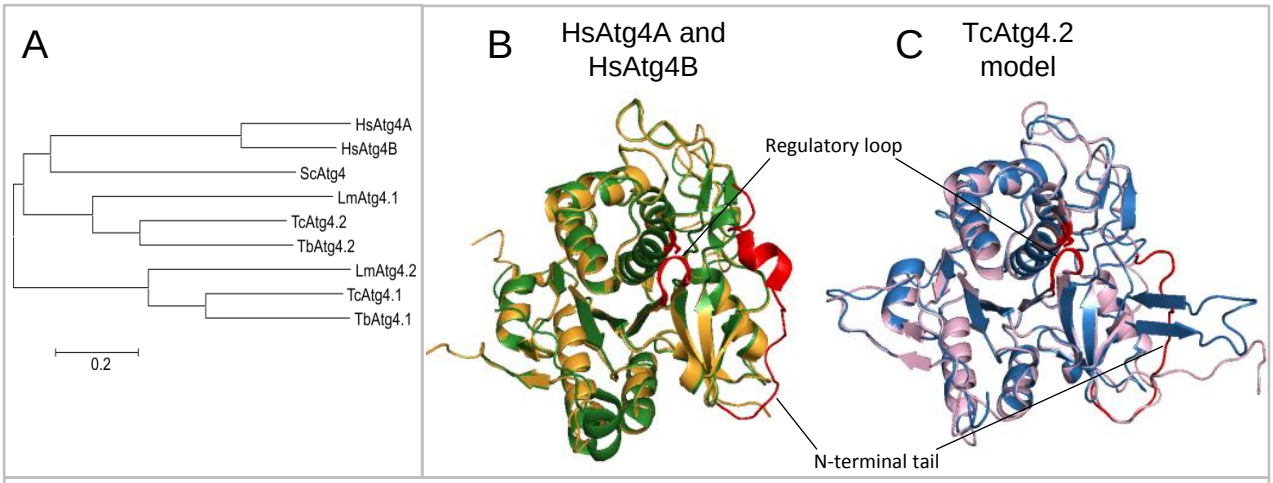

A
TcAtg4.2 activity (%)
ETFG
GTFG
NTFG
STFG
Ac-tetrapeptide-AFC
B
TcAtg4.2 activity (%)
pH
C
Fold activation
no salt
NaCl
KCl
$(NH_4)_2Cl$
$Na_3C_3H_5O(COO)_3$
$K_3C_3H_5O(COO)_3$
$(NH_4)_3C_3H_5O(COO)_3$
$Na_2HPO_4$
$K_2HPO_4$
$(NH_4)_3HPO_4$
D
Fold activation
$K_2HPO_4$ [M]
E
no salt
0.5 M
0.15 M
1 M
[Θλ ]MRW [deg cm$^2$ mol$^{-1}$]
λ (nm)
F
Activity (RFU/s)
ETFG
SQETFG
YASQETFG
Ac-peptide-ACC
G
WT
C91S
Activity (RFU/s)
no salt
1M $K_2HPO_4$

Fig. 2




D

```
                                                                                *
HsAtg4B   BVASRLWFTYRKNFPAIGGTGP----------------------------TSDTGWGCMLRCGQMIFAQA  85
HsAtg4A   AISARLWFTYRRKFSPIGGTGP----------------------------SSDAGWGCMLRCGQMMLAQA
TcAtg4.2  TEALLYFSYRNRIVPLM-NGA----------------------------TTDLFWGCMIRTGQMMLAHA
TbAtg4.2  ACKLLYFSYRCQFEPLR-NGS----------------------------TTDIGWGCTIRAGQMMLAHA
LmAtg4.1  TKKLLYFSYRNCFPPLP-SGS----------------------------TTDTHWGCLVRTTQMLVGTC
TcAtg4.1  RNGFFLLTYRMNFSPLPHSS----------------------------VTSDKGWGCLVRSSQMLLAHA
TbAtg4.1  ENSFYLFTYRRYFDPLPYST----------------------------LTSDKGWGCLARATQMLLACS
LmAtg4.2  TDTFLIFTYRDGFEAIPAVTRL--------------------------IETDQGWGCLLRTSQMLLAHF
yeast     VQSRVNFTYRTRFVPIARAPDGPSPLSLNLLVRTNPISTIEDYIANPDCFNTDIGWGCMIRTGQSLLGNA

HsAtg4B   LVCRHLGRDWRWTQRKRQPDSYFSVLNAFIDRKDSYYSIHQIAQMGVGE-GKSIGQWYGPNTVAQVLKKLA 156
HsAtg4A   LICRHLGRDWSWEKQKEQPKEYQRILQCFLDRKDCCYSIHQMAQMGVGE-GKSIGEWFGPNTVAQVLKKLA
TcAtg4.2  FMRYFNGGGPHIGS-ERLQELRARTQTLFCDVPSAPFGIHAVTSEGTKH-GVNCGEWFGPTPIAKTLS--A
TbAtg4.2  LMRYKNGGGASFED-SIVPSLKQATQHLFHDDPSAPFGIHAITNKGVQH-GAPCGSWFGPTHVAVVMG--A
LmAtg4.1  LLRYHCKGAYVLPE-ADNAELKERISRLFMDVPSAPLGIHKAEDEAHKN-SVKYASMLSPTEAGMAIA--A
TcAtg4.1  LWRYS------------ANDCRLDHFRDMDTEDSTPFSLHKMVRAVMKKADVFRPEYWTPSQGCEAIRCCV
TbAtg4.1  LRRHS------------AQDCKLQYFADLDDEQVAPFSLHCMVRHILKQGESLRPVYWAPSQGCEAISGCV
LmAtg4.2  LWVHG------------RPADRKLSLFFDHSAETAPFSIHNMIRSVWNR-RVFKAEYWSPSQGCEAIKRTV
yeast     LQILHLGRDFRVNG-NESLER ESKFVNWFNDTPEAPFSLHNFVSAGTELSDKRPGDWFGPAATARSIQS-

HsAtg4B   VFDTWSSLAVHIAMDNTVVMEEIRRLCRTSVPCAG-ATAFPADSDRHCNGFPAGAEVTNRPSPWRPLVLLI 226
HsAtg4A   LFDEWNSLAVYVSMDNTVVIEDIKKMCRVLPLSADTAGDRPPDSLTASN---QSKGTSAYCSAWKPLLLIV
TcAtg4.2  LMASYLAAGGEGPVVLAFPERQIFLEEVKELLRQS----------------------------THVVLLI
TbAtg4.2  LMEDYLRNGGQGPDVLVLRDRQVMEDEVRKILLLS----------------------------KHVLLLI
LmAtg4.1  ALIAFRAQGGDVPFTFCCESRHIDEPAVMAKLLEG----------------------------QHVVLII
TcAtg4.1  NNAVDRKLIP-PIRVVVCSQGCLLAREICSNLEFG----------------------------TVLILA
TbAtg4.1  KRATERGILSSPLSVVITVAGAVPAEEVSCHLKESR----------------------------NVLILA
LmAtg4.2  QGAVKTEQLQTRVMVVTSTNGCIYADEVQHTFKQGAD----------------------------VVLVLA
yeast     -LIYGFPECGIDDCIVSVSSGDIYENEVEKVFAENPN----------------------------SRILFLL
                                  Regulatory loop
HsAtg4B   PLRLGLT-DINEAYVETLKHCFMMPQSLGVIGGKPNSAHYFIGYVGEE-LIYLDPHTTQPAVEPTDGCFIP 294
HsAtg4A   PLRLGIN-QINPVYVDAFKECFKMPQSLGALGGKPNNAYYFIGFLGDE-LIFLDPHTTQTFVDTEENGTVN
TcAtg4.2  PVMLGIR-VISEKYSQLMKRCLEMESSIGILGGKSRSALFLFGHQDDD-VFFLDPHCVQPAFTSS------
TbAtg4.2  PVMLGPH-HISEGYAKLLKRCLRMESTVGAVGGKEGSAFFFMGYQGGN-LIVLDPHYAQSAFTCS------
LmAtg4.1  PVVLGIA-PMSDQYELVMLKILDVKACCGIAGGFKQASLYMFGHQGRS-VFFMDPHYVQNAYTSS------
TcAtg4.1  PMRCGASRRMTQMMFFSLEHLLHSSACIGVVGGVPQRSYYILGTSGQR-LLYLDPHCMTQEALVSSHAEKA
TbAtg4.1  PLRCGASRYMSQKMFLSLEHLLLAPESVGMVGGVPNRGYYIIGTGAQELLLYLDPHCKTQDALLSSEPGET
LmAtg4.2  SVRVSAAAQLTQESYLQIEKLMEQPQCLGVVGGVPGRSYYFFAHNQTQ-LFYLDPHQRTAAALLCEGLSAA
yeast     GVKLGIN-AVNESYRESICGILSSTQSVGIAGGRPSSSLYFFGYQGNE-FLHFDPHIPQ PAVEDS------

HsAtg4B   DESFHCQHPPCRMSIAELDPSIAVGFFCKTEDDFNDW 393
HsAtg4A   DQTFHCLQSPQRMNILNLDPSVALGFFCKEEKDFDNW
TcAtg4.2  GSPGELTCARRVLPTTSYDTSMTLGFYISSLDSLALF
TbAtg4.2  DTQGKISGEWYTLPLTSCSTSVLLGFYIHSPDSFSQF
LmAtg4.1  RTVGTLEGSRGELRARRFDPCMVLGFYLHTPEDYRVF
TcAtg4.1  GVVTVTASLVKSVRWDCVDTSCFLGFLVDSFAEWLEL
TbAtg4.1  GVVKPTSSNLRSVPYGQVDTSFFLGFFVDSQSRWESL
LmAtg4.2  ASVTPSVADVRCVHWSRVDTSLFLAFAVTTRDEWAAL
yeast     FVESCHTSKFGKLQLSEMDPSMLIGILIKGEKDWQQW
```

Figure 3

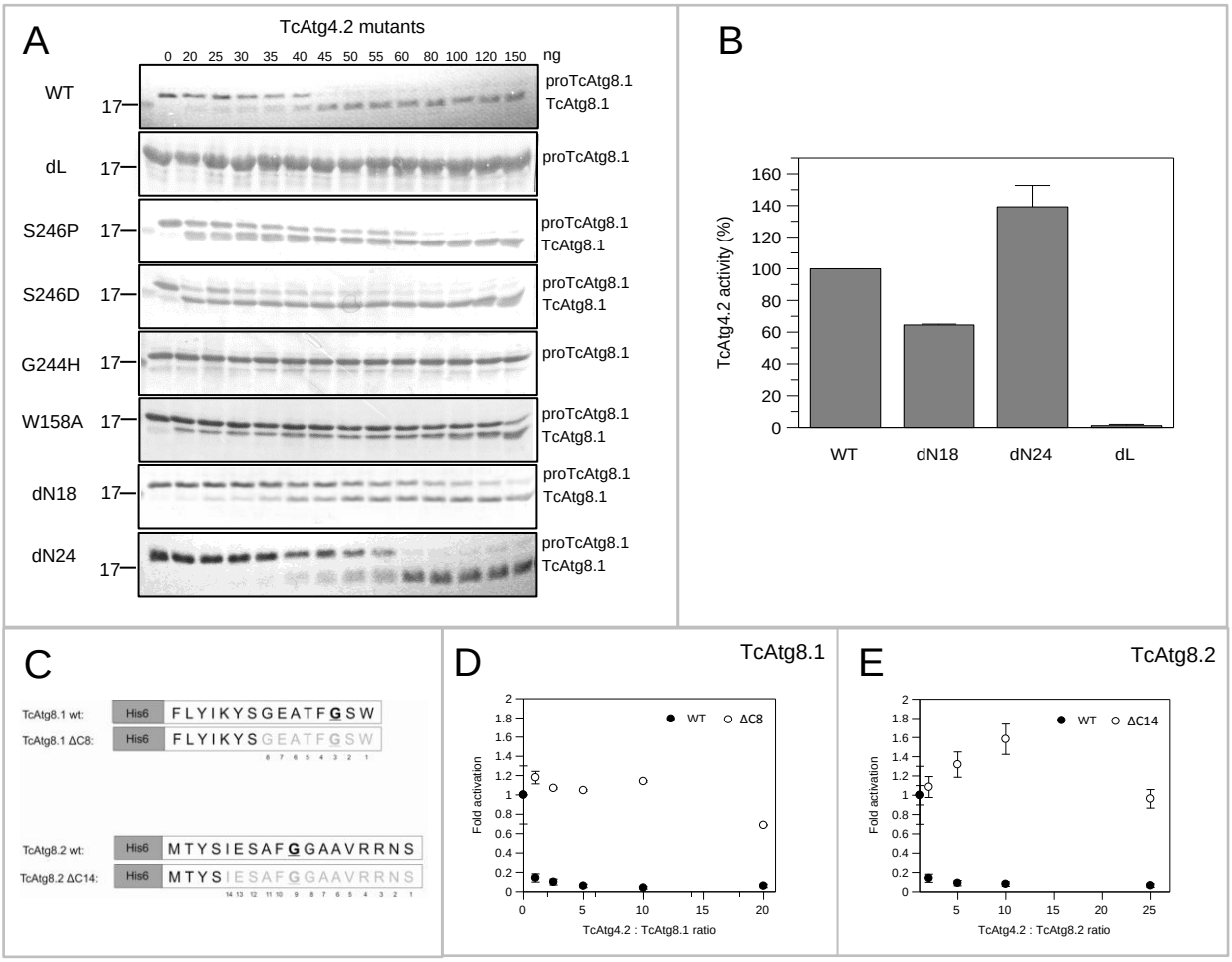

A
TcAtg4.2 mutants
0 20 25 30 35 40 45 50 55 60 80 100 120 150 ng
WT
dL
S246P
S246D
G244H
W158A
dN18
dN24
17
proTcAtg8.1
TcAtg8.1
B
TcAtg4.2 activity (%)
0 20 40 60 80 100 120 140 160
WT
dN18
dN24
dL
C
TcAtg8.1 wt: His6 FLYIKYSGEATFGSW
TcAtg8.1 ΔC8: His6 FLYIKYSGEATFGSW
TcAtg8.2 wt: His6 MTYSIESAFGGAAVRRNS
TcAtg8.2 ΔC14: His6 MTYSIESAFGGAAVRRNS
D
TcAtg8.1
WT
ΔC8
Fold activation
TcAtg4.2 : TcAtg8.1 ratio
E
TcAtg8.2
WT
ΔC14
Fold activation
TcAtg4.2 : TcAtg8.2 ratio

Figure 4

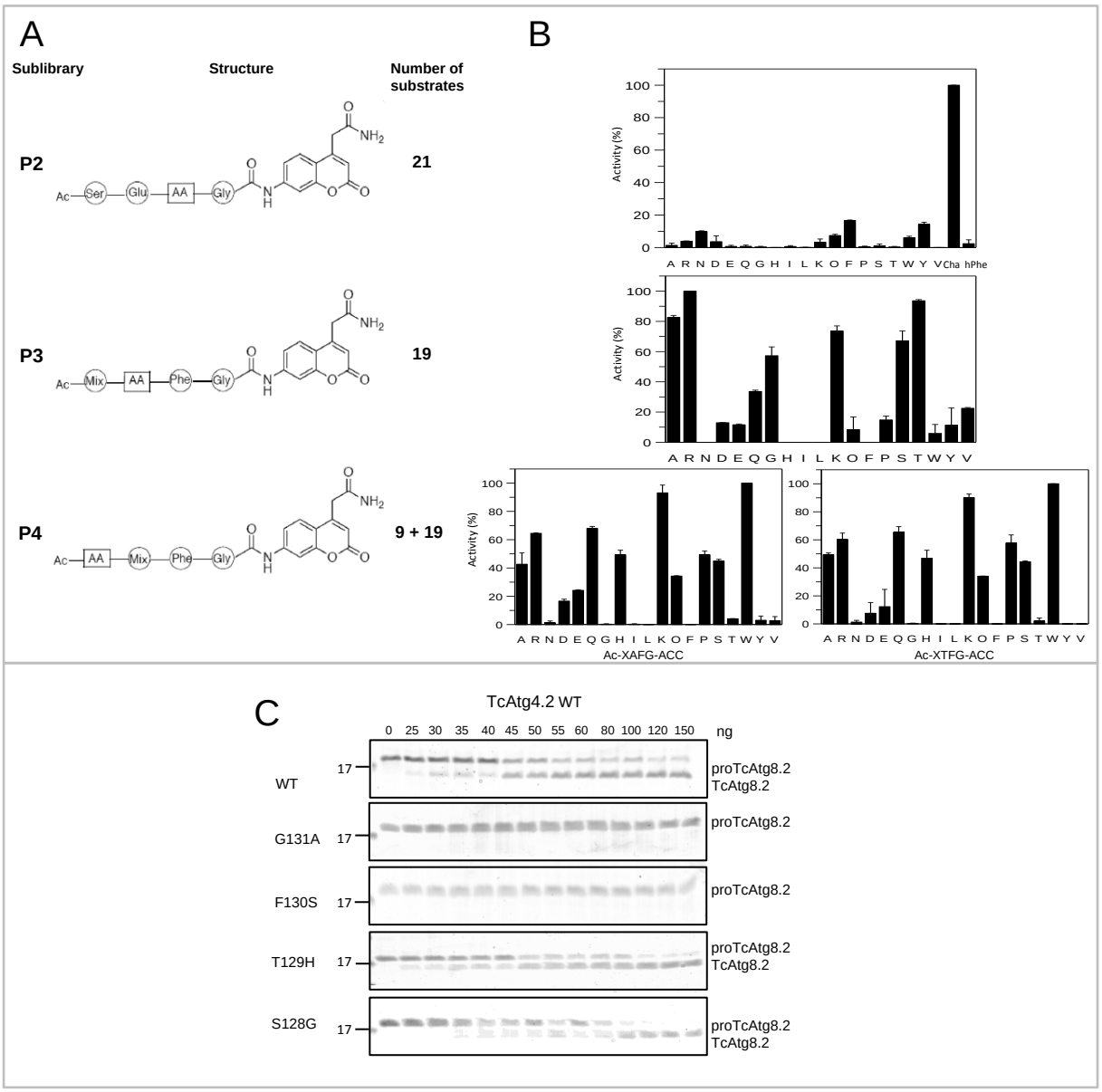

A
Sublibrary
Structure
Number of substrates
P2
21
P3
19
P4
9 + 19
B
Activity (%)
A R N D E Q G H I L K O F P S T W Y V Cha hPhe
Ac-XAFG-ACC
Ac-XTFG-ACC
C
TcAtg4.2 WT
0 25 30 35 40 45 50 55 60 80 100 120 150 ng
WT
G131A
F130S
T129H
S128G
17
proTcAtg8.2
TcAtg8.2

Figure 5

A

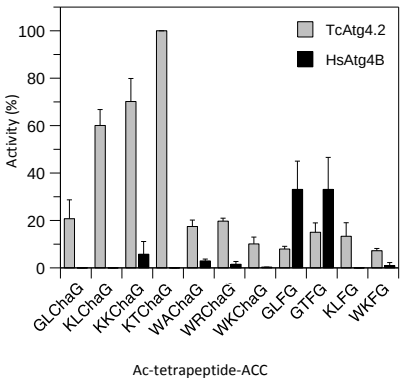
**Substrates (11)**

**Cha at P2:**

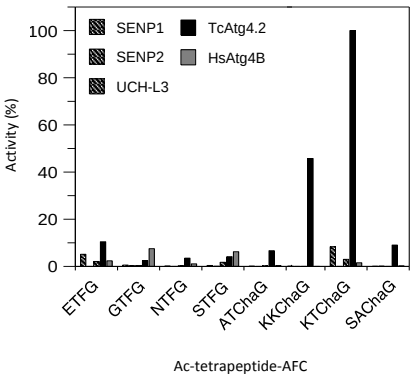
**Ac-GLChaG-ACC**
**Ac-KLChaG-ACC**
**Ac-KKChaG-ACC**
**Ac-KTChaG-ACC**
**Ac-WAChaG-ACC**
**Ac-WRChaG-ACC**
**Ac-WKChaG-ACC**

**Phe at P2:**

**Ac-GLFG-ACC**
**Ac-GTFG-ACC**
**Ac-KLFG-ACC**
**Ac-WKFG-ACC**

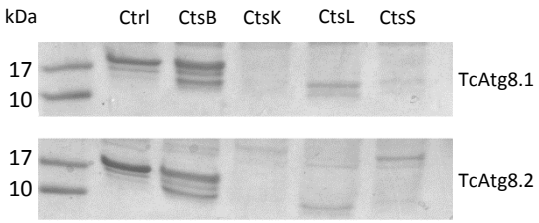



B

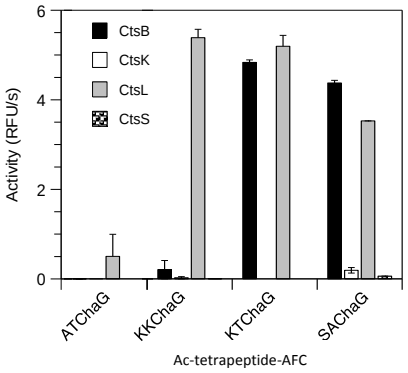



| Substrate | $k_{cat}/K_m$ [$M^{-1}$ $s^{-1}$] for TcAtg4.2 |
|---|---|
| Ac-ATChaG-AFC | 0.2 ± 0.03 |
| Ac-KKChaG-AFC | 137 ± 8 |
| Ac-KTChaG-AFC | 112 ± 7 |
| Ac-SAChaG-AFC | 1.4 ± 0.2 |

C




D



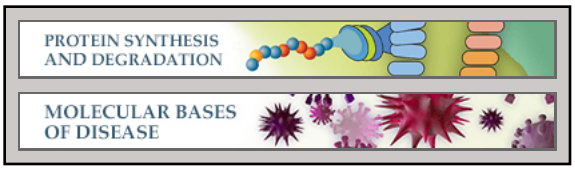

| | $k_{cat}/K_m$ [$M^{-1}$ $s^{-1}$] for Ac-KKChaG-AFC |
|---|---|
| **CtsL** | 5100 ± 530 |
| **TcAtg4.2** | 137 ± 8 |

Figure 6




Protein Synthesis and Degradation:

# Biochemical Characterization and Substrate Specificity of Autophagin-2 from the Parasite Trypanosoma cruzi




Jelena Rajkovic, Marcin Poreba, Dejan Caglic, Robert Vidmar, Aleksandra Wilk, Agata Borowik, Guy S. Salvesen, Vito Turk, Marcin Drag and Boris Turk

*J. Biol. Chem.* published online October 7, 2015

Access the most updated version of this article at doi: 10.1074/jbc.M115.687764

Find articles, minireviews, Reflections and Classics on similar topics on the JBC Affinity Sites.

Alerts:
- When this article is cited
- When a correction for this article is posted

Click here to choose from all of JBC's e-mail alerts

This article cites 0 references, 0 of which can be accessed free at
http://www.jbc.org/content/early/2015/10/07/jbc.M115.687764.full.html#ref-list-1

Downloaded from http://www.jbc.org/ at Jozef Stefan Institut on October 11, 2015

Oncogene (2013), 1–9
© 2013 Macmillan Publishers Limited All rights reserved 0950-9232/13
www.nature.com/onc

ORIGINAL ARTICLE

# Stefin B deficiency reduces tumor growth via sensitization of tumor cells to oxidative stress in a breast cancer model

M Butinar[1,2], MT Prebanda[1], J Rajković[1,2], B Jerič[1,2], V Stoka[1,2], C Peters[3], T Reinheckel[3], A Krüger[4], V Turk[1,2,5], B Turk[1,5,6] and O Vasiljeva[1,2,7]

Lysosomal cysteine cathepsins contribute to proteolytic events promoting tumor growth and metastasis. Their enzymatic activity, however, is tightly regulated by endogenous inhibitors. To investigate the role of cathepsin inhibitor stefin B (Stfb) in mammary cancer, *Stfb null* mice were crossed with transgenic polyoma virus middle T oncogene (PyMT) breast cancer mice. We show that ablation of Stfb resulted in reduced size of mammary tumors but did not affect their rate of metastasis. Importantly, decrease in tumor growth was correlated with an increased incidence of dead cell islands detected in tumors of Stfb-deficient mice. *Ex vivo* analysis of primary PyMT tumor cells revealed no significant effects of ablation of Stfb expression on proliferation, angiogenesis, migration and spontaneous cell death as compared with control cells. However, upon treatment with the lysosomotropic agent Leu-Leu-OMe, cancer cells lacking Stfb exhibited a significantly higher sensitivity to apoptosis. Moreover, Stfb-ablated tumor cells were significantly more prone to cell death under increased oxidative stress. These results indicate an *in vivo* role for Stfb in protecting cancer cells by promoting their resistance to oxidative stress and to apoptosis induced through the lysosomal pathway.

*Oncogene* advance online publication, 19 August 2013; doi:10.1038/onc.2013.314

**Keywords:** cathepsin inhibitor; stefin; breast cancer; mouse model; oxidative stress

## INTRODUCTION

Proteolysis has a crucial role in tumor invasion and metastasis. The roles of lysosomal cysteine proteinases, the cysteine cathepsins, in these processes have been confirmed by numerous clinical reports and evidence accumulated from experimental cancer models.[1–4] Cathepsins belong to the family of papain-like proteases (clan CA, family C1) and are localized primarily in endosomal and lysosomal compartments.[5,6] However, under several pathological conditions, these enzymes can escape from endosomal vesicles by being secreted to the extracellular milieu or, alternatively, translocated into the cytosol.[7] Cysteine cathepsins have been shown to have a clear role as tumor-promoting enzymes,[8–10] suggesting the possibility of anti-cathepsin therapy in cancer treatment.[11–15] On the other hand, cysteine cathepsins could participate in induction of tumor cell death through mediation of apoptosis,[16,17] which, however, requires cytosolic release of these enzymes from lysosomes.[18] An additional level of complexity is introduced by the fact that the proteolytic activity of cysteine cathepsins is regulated by their endogenous inhibitors called cystatins.[19]

The endogenous protein inhibitors of cysteine cathepsins, the cystatin superfamily, can be subdivided into three families, stefins (type I), cystatins (type II) and kininogens (type III).[20] In mammals, including human, rat, bovine, mouse and porcine, two members of the type I family, stefin A (cystatin A or α) and stefin B (Stfb; cystatin B or β), have been identified. Both inhibitors are single-chain polypeptides with ~100 amino acid residues (molecular mass, ~11 kDa) and are localized intracellularly.[21] In contrast to stefin A, which exhibits a restricted expression pattern with especially high levels in skin and some types of blood cells, Stfb is widely distributed in various cell types and tissues. Stfb is considered as a general cytosolic cysteine cathepsin inhibitor in mammalian cells, where it probably serves to protect the cell against inappropriate proteolysis due to cysteine cathepsin leakage from the lysosomes.[22] Moreover, it is one of the cystatins for which genetic evidence points to an important biological function. Loss-of-function alterations in the Stfb gene (either through a multiplied repeat unit in the promoter region or through point mutations in the structural gene) are present in both alleles of the gene in patients with a form of progressive myoclonus epilepsy.[23] Furthermore, because of the important role of cysteine cathepsins in cancer progression, the ratio of cystatins to cysteine cathepsins has been thoroughly investigated. As such, Stfb levels were correlated with diagnosis and prognosis for cancer patients with different malignancies.[24] Strikingly, increased concentrations of Stfb in the body fluids of carcinoma patients have been shown to correlate significantly with shorter survival.[25] Although a higher level of cathepsin inhibitors may counter-balance the upregulation of cysteine cathepsins, their role in cancer still remains poorly defined.

To elucidate the role of Stfb (also known as cystatin B) in cancer progression and metastasis, we have established a Stfb-ablated mouse mammary cancer model by crossing Stfb-deficient mice[26] with a strain of mice susceptible to mammary cancer (polyoma virus middle T oncogene (PyMT) mice), which express the PyMT under control of the mouse mammary tumor virus (MMTV) long-

[1]Department of Biochemistry and Molecular and Structural Biology, Jožef Stefan Institute, Ljubljana, Slovenia; [2]Jožef Stefan International Postgraduate School, Ljubljana, Slovenia; [3]Institute of Molecular Medicine and Cell Research, BIOSS Centre for Biological Signalling Studies, Albert-Ludwigs-University Freiburg, Freiburg, Germany; [4]Institut für Experimentelle Onkologie und Therapieforschung des Klinikums rechts der Isar, Technische Universität München, München, Germany; [5]Centre of Excellence for Integrated Approaches in Chemistry and Biology of Proteins, Ljubljana, Slovenia and [6]Faculty of Chemistry and Chemical Technology, University of Ljubljana, Ljubljana, Slovenia. Correspondence: Dr O Vasiljeva, The Department of Biochemistry and Molecular and Structural Biology, Jožef Stefan Institute, Jamova 39, Ljubljana 1000, Slovenia.
E-mail: olga.vasiljeva@ijs.si
[7]Current address: CytomX Therapeutics Inc., 650 Gateway Boulevard Suite 125, South San Francisco, CA 94080, USA.
Received 17 January 2013; revised 19 May 2013; accepted 17 June 2013

terminal repeat promoter.[27] Depletion of Stfb has been shown to result in reduced tumor growth, suggesting a novel function for Stfb in defending tumor cells against oxidative stress.

## RESULTS

### Progression of PyMT-induced mammary carcinomas

To examine the role of Stfb in the progression of PyMT-induced breast cancer, Stfb-deficient mice (*Stfb*$^{-/-}$) were backcrossed to the FVB/N genetic background for 10 generations. These mice did not show an abnormal behavioral or neurological phenotype at 14 weeks of age, similarly to original *Stfb*$^{-/-}$ inbred C57BL/6 strain.[26] These mice were further crossed with PyMT transgenic mice,[27] resulting in two groups of female mice, hemizygous for the PyMT transgene: *PyMT;Stfb*$^{+/+}$ and *PyMT;Stfb*$^{-/-}$. Western blot analyses of Stfb revealed overexpression of this inhibitor in mammary tumors of PyMT transgenic mice, relative to the non-transformed mammary glands (Figure 1a). Furthermore, immunohistochemical staining of primary PyMT tumors revealed that Stfb was predominantly localized in the tumor cells of *PyMT;Stfb*$^{+/+}$ tumors and not in the cells of tumor stroma (Figure 1b). To investigate the effect of Stfb deficiency in the context of breast cancer, we have compared *PyMT;Stfb*$^{+/+}$ and *PyMT;Stfb*$^{-/-}$ transgenic mice for tumor development, progression, proliferation and cell death. To assess the development of mammary tumors in both groups of mice, all 10 mammary glands of each mouse were palpated three times a week, starting on day 30 after birth in a genotype-blind fashion. To evaluate the genotype-dependent differences in the occurrence of the first palpable tumors, we determined the time point at which cancer-prone mice developed the first two tumors. In the *PyMT;Stfb*$^{-/-}$ group, the first two palpable mammary tumors were detected in all mice at the age of 59 days, which is 6 and 3 days later than in the control *PyMT;Stfb*$^{+/+}$ mice (Figure 1c). Despite the apparent shift of Kaplan–Meier plots for tumor-free mice between the two Stfb genotypes, no significant difference between these groups was detected. This data excludes major effects of Stfb in initiation of tumor in PyMT mammary cancer model induced by expression of the PyMT transgene. To analyze the effect of Stfb on the progression of established tumors, their diameter was measured 30 days after detection. Tumors were grouped by size into the

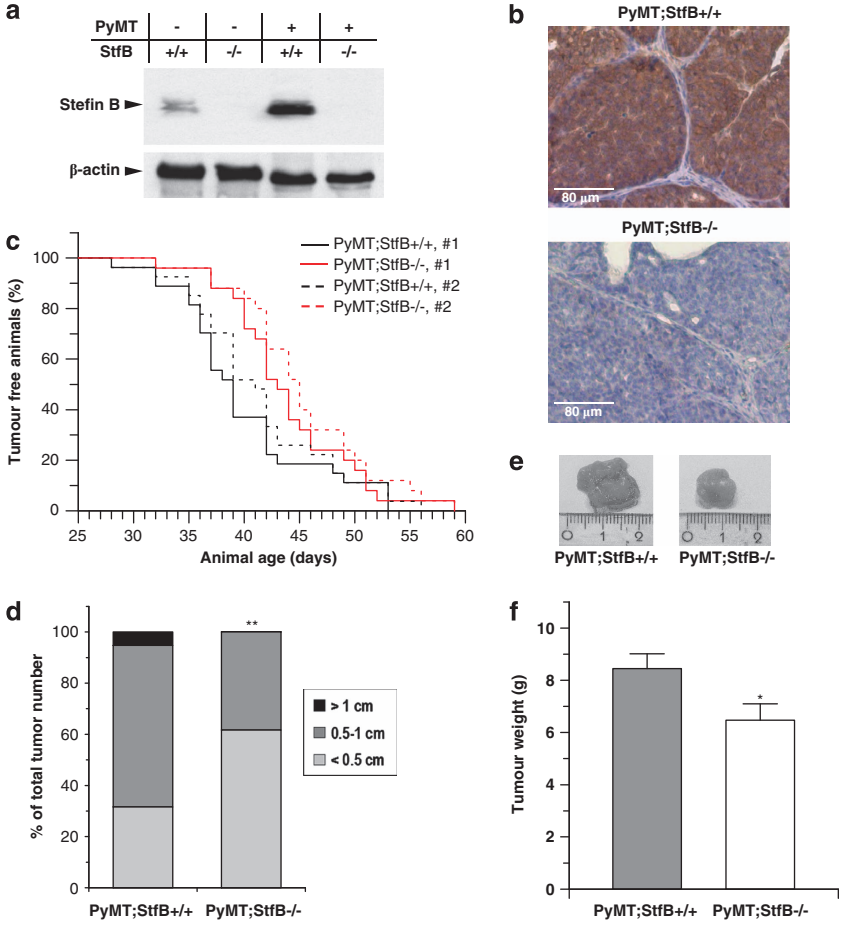



**Figure 1.** Suppression of PyMT-induced tumor growth in Stfb-deficient female mice. (**a**) Expression pattern of Stfb in mammary glands and PyMT-induced mammary carcinomas indicates a strong upregulation of Stfb in tumor tissue. Western blot analysis of *Stfb*$^{+/+}$, *Stfb*$^{-/-}$, *PyMT;Stfb*$^{+/+}$ and *PyMT;Stfb*$^{-/-}$ lysates are shown. β-actin served as a loading control. (**b**) Detection of Stfb by immunohistochemistry staining of *PyMT;Stfb*$^{+/+}$ and *PyMT;Stfb*$^{-/-}$ tumor sections. Scale bar, 80 μm. (**c**) Kaplan–Meier plots for tumor-free *PyMT;Stfb*$^{+/+}$ ($n=27$) and *PyMT;Stfb*$^{-/-}$ ($n=25$) female mice. First (no. 1) and second (no. 2) palpable mammary tumors were detected 6 and 3 days later in *PyMT;Stfb*$^{-/-}$ female mice as compared with *PyMT;Stfb*$^{+/+}$ female mice. Statistics were analyzed using log-rank test. (**d**) Size of mammary cancer nodes 30 days after first detection of the individual tumor node. The first 2–3 mammary tumors in each female mouse were analyzed in the *PyMT;Stfb*$^{+/+}$ ($n=38$) and *PyMT;Stfb*$^{-/-}$ ($n=47$) cohorts of mice. Proportions were compared statistically by $\chi^2$-test. $^{**}P<0.01$. (**e**) Representative images of the single tumors excised from *PyMT;Stfb*$^{+/+}$ and *PyMT;Stfb*$^{-/-}$ mice at 14 weeks of age. (**f**) The cumulative tumor weight per mouse for all mammary tumors was calculated for *PyMT;StB*$^{-/-}$ ($n=23$) and *PyMT;StB*$^{+/+}$ ($n=35$) mice at 14 weeks of age. Statistics were analyzed using Student's *t*-test. $^{*}P<0.05$.


© 2013 Macmillan Publishers Limited

three categories based on their diameters: small ($<0.5$ cm), medium (0.5–1 cm) and large ($>1$ cm) (Figure 1d). The proportion of those groups was compared between control *PyMT;Stfb*$^{+/+}$ and *PyMT;Stfb*$^{-/-}$ mice revealing significantly lower tumor burden in *PyMT;Stfb*$^{-/-}$ mice. Notably, although 70% of tumors in *PyMT;Stfb*$^{+/+}$ were larger $>0.5$ cm, only 40% of tumors in *PyMT;Stfb*$^{-/-}$ group were in the range of 0.5–1 cm, and no tumors $>1$ cm in diameter were detected. At 14 weeks of age, mice were killed and mammary tumors were excised. The finding of the reduced tumor size in *PyMT;Stfb*$^{-/-}$ mice was confirmed *ex vivo* (Figure 1e) and substantiated by the measure of a significant reduction of the cumulative weight of all tumors per mouse in *PyMT;Stfb*$^{-/-}$ cohort of mice, as compared with control *PyMT;Stfb*$^{+/+}$ mice (Figure 1f). Tumors in Stfb-deficient mice, with an average weight of 6.47 g, were 23% lighter than those in *PyMT;Stfb*$^{+/+}$ mice, with an average weight of 8.44 g. These results provide evidence for decreased tumor growth associated with depletion of Stfb in the breast cancer model.

### Effect of Stfb ablation on proliferation, cell death and angiogenesis of PyMT-induced mammary carcinomas

Given the substantial differences in growth of PyMT-induced tumors between *PyMT;Stfb*$^{-/-}$ and *PyMT;Stfb*$^{+/+}$ mice, we examined the effect of Stfb on hallmark processes of malignant growth, such as tumor proliferation, cell death and angiogenesis, in late-stage primary PyMT tumors. Cell proliferation in mammary tumors was quantified by immunohistochemical detection of the proliferation marker Ki67 (Figure 2a). The numbers of Ki67-positive cells did not differ significantly between tumors with different Stfb genotypes (Figure 2b). However, as Stfb is localized in the cytosol, its involvement in cell death-related processes could account for the smaller cancers in *PyMT;Stfb*$^{-/-}$ mice. The incidence of dead cells in primary PyMT tumors was determined by terminal dUTP nick-end labeling staining as a measure of DNA fragmentation associated with cell death. Large areas of dead cells were observed in *PyMT;Stfb*$^{-/-}$ mice, unlike in the control group ($P<0.05$) (Figure 2c). Necrotic areas in tumor samples were measured by computer-assisted histomorphometry. Although areas of dead cells comprised $<1.5\%$ of wild-type tumors, these areas comprised 7–8% of examined tumor tissue sections from *PyMT;Stfb*$^{-/-}$ mice (Figure 2d). This observation suggests a role for Stfb in tumor cell apoptosis *in vivo*, which was confirmed by immunohistochemical staining for active caspase-3 (Figure 2e and f). To investigate whether this process could be correlated with limited supply of tumors with oxygen and nutrients due to impaired vasculature formation in the growing tumors, we have assessed the effect of Stfb on tumor angiogenesis by immunofluorescence staining of the marker CD31. Ablation of Stfb had no significant effect on the vessel density in PyMT tumors (Figure 2g). Taken together, these data indicate a specific role for Stfb in regulating cell death events in mammary cancer and provide an explanation for the significant reduction of PyMT tumors in Stfb-deficient mice.

### PyMT tumor cell analysis

To address the role of Stfb in tumor cell proliferation and cell death, we examined primary PyMT cells prepared from 14-week-old *PyMT;Stfb*$^{+/+}$ and *PyMT;Stfb*$^{-/-}$ mice. No effect of the Stfb genotype on proliferation of primary tumor cells was detected *in vitro* by use of the BrdU assay (Supplementary Figure S1), corroborating the data on Ki67 immunohistochemistry analysis of the tumor tissue. Interestingly, no difference in cell death ratio was detected by measuring the viability of the tumor cells obtained from tumor cells of the two Stfb genotypes. However, given the predominant localization of Stfb in cytosolic cell compartment, where the lysosomal protease pathway of induction of apoptosis takes place,[28] we decided to investigate the role of Stfb in sensitivity of tumor cells to apoptosis induction. Initially, we have measured expression and activity of cysteine cathepsins in tumor lysates of *PyMT;Stfb*$^{+/+}$ and *PyMT;Stfb*$^{-/-}$ mice. Notably, although no difference in expression of cysteine cathepsins was determined by quantitative real-time PCR (Figure 3a), almost a two-fold increase in cathepsin activity was detected in *PyMT;Stfb*$^{-/-}$ tumors (Figure 3b), indicating an important role of this inhibitor in regulation of cathepsins activity. To induce the lysosomal pathway of apoptosis, destabilization of lysosomal membranes in tumor cells of both *Stfb* genotypes was stimulated by the lysosomotropic detergent Leu-Leu-OMe. Treatment of cells with Leu-Leu-OMe is known to induce cysteine cathepsin leakage into the cytosol, where they degrade the antiapoptotic Bcl-2 family members Bcl-2, Bcl-xL and Mcl-1, and process another Bcl-2 family member Bid into its pro-apoptotic form tBid,[16,17] leading to activation of the intrinsic apoptosis pathway and activation of caspases 3 and 7. Stfb-ablated primary tumor cells were significantly more sensitive to this apoptotic stimulus, resulting in an up to 85% increase in cell death in *PyMT;Stfb*$^{-/-}$ cells, as compared with the 30% of apoptotic cells in *PyMT;Stfb*$^{+/+}$ tumor cells at 1 mM Leu-Leu-OMe concentration (Figure 3c). This sensitivity of Stfb-depleted tumor cells to a cell death stimulus suggests a possible role of this inhibitor as a 'cell guard' against apoptosis induced by cathepsins. This hypothesis was confirmed by the use of the synthetic cysteine cathepsin inhibitor E64d, which almost completely protected tumor cells from apoptosis (Figure 3c), resulting in an almost fourfold reduction of the number of apoptotic cells. We next measured DEVDase activity of tumor cells after treatment with Leu-Leu-OMe, and found it to be threefold higher in Stfb-depleted tumor cells (Figure 3d), supporting the above idea. However, upon induction of apoptosis with an anti-CD95 (Fas/APO-1) monoclonal antibody, no significant difference was detected between *PyMT;Stfb*$^{+/+}$ and *PyMT;Stfb*$^{-/-}$ tumor cells as reflected by the number of annexin V-positive cells (Figure 3e). This supports the previous findings that cathepsin release from lysosomes is not a major event in Fas-induced apoptosis,[29] thereby providing evidence that the increased level of cell death in Stfb-deficient tumors could not be induced by the Fas/CD95 signaling pathway.

Oxidative stress was recently identified as one of the pivotal factors provoking cell death in Stfb-ablated neurons, which leads to progressive myoclonus epilepsy disorder.[30] Because malignant cells in general are under intrinsic oxidative stress, and are thus more vulnerable to damage by reactive oxygen species (ROS)-generating agents,[31] we have investigated the effect of Stfb deficiency on the sensitivity of tumor cells to induced oxidative stress. Primary tumor cells of both Stfb genotypes, *PyMT;Stfb*$^{+/+}$ and *PyMT;Stfb*$^{-/-}$, were exposed to hydrogen peroxide ($H_2O_2$), a representative ROS, and tumor cell death was assessed by annexin V staining (Figure 4a). Notably, a significant increase in the percentage of annexin V-positive cells was detected in *PyMT;Stfb*$^{-/-}$ primary tumor cells, as compared with wild-type *PyMT;Stfb*$^{+/+}$ cells (Figure 4b). Moreover, a fivefold increase of DEVDase activity was determined in *PyMT;Stfb*$^{-/-}$ primary tumor cells upon exposure to 1 mM $H_2O_2$, whereas no difference in caspase activity was detected in wild-type *PyMT;Stfb*$^{+/+}$ cells (Figure 4c). This data indicates an increased sensitivity of Stfb-depleted cells to oxidative stress, through induction of apoptotic cell death.

The lack of blood supply in the fast-growing tumors leads to deprivation of nutrients and growth factors that causes increased levels of intracellular ROS.[32] Thereby, we have cultured *PyMT;Stfb*$^{+/+}$ and *PyMT;Stfb*$^{-/-}$ cells in serum-free medium (also known as serum starvation) to mimic tumor cell oxidative stress in cell culture. Notably, an increase in tumor cell death was detected in *PyMT;Stfb*$^{-/-}$ tumor cells as compared with *PyMT;Stfb*$^{+/+}$ tumor cells (Supplementary Figure S2). Taken together, our results support the role of Stfb as an oxidative

© 2013 Macmillan Publishers Limited

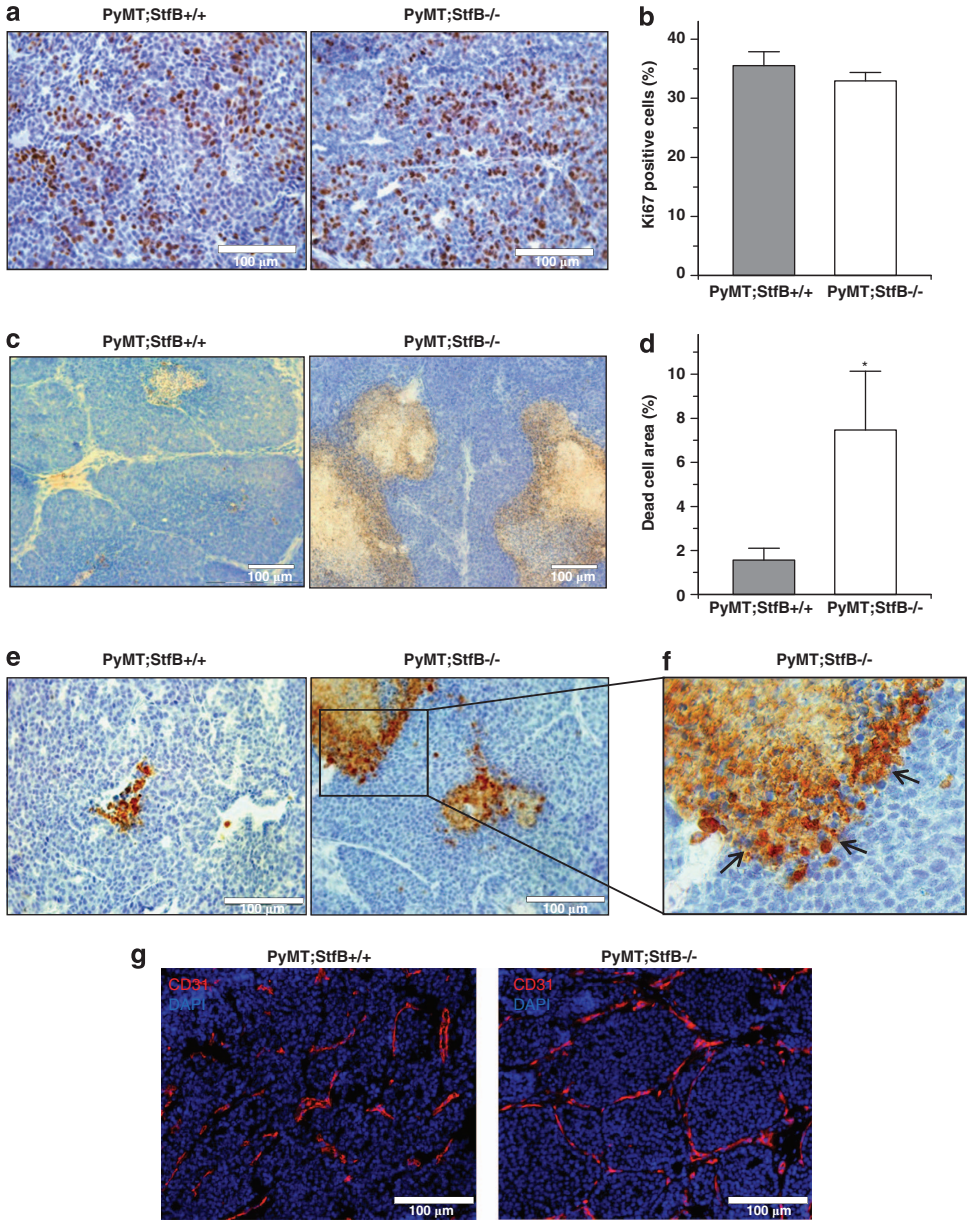



**Figure 2.** Proliferation, cell death and vessel density in late-stage mammary carcinomas. (**a**) Cell proliferation in primary tumors determined by immunodetection of Ki67 in *PyMT;Stfb*$^{+/+}$ and *PyMT;Stfb*$^{-/-}$ mice at 14 weeks of age. Representative images for each genotype are shown under $\times 40$ magnification. (**b**) Quantification of Ki67-positive cells as percentage of total cells in *PyMT;Stfb*$^{+/+}$ ($n=13$) and *PyMT;Stfb*$^{-/-}$ ($n=14$) tumors. Ki67 index was calculated from 20 high-power fields per animal by computer-assisted data analysis using the HistoQuest software (TissueGnostics). (**c**) Immunohistochemical detection of areas of dead cells in primary tumors of *PyMT;Stfb*$^{+/+}$ and *PyMT;Stfb*$^{-/-}$ mice at 14 weeks of age by terminal dUTP nick-end labeling staining. Representative images for each genotype are shown under $\times 40$ magnification. (**d**) The percentage of areas of dead cells was determined on high-power fields of *PyMT;Stfb*$^{+/+}$ ($n=13$) and *PyMT;Stfb*$^{-/-}$ ($n=12$) mice tumors by computer-assisted data analysis. Statistics were analyzed using Student's *t*-test. *$P<0.05$. (**e**) Representative pictures of cell death areas in primary tumors by immunodetection of active caspase-3 in *PyMT;Stfb*$^{+/+}$ and *PyMT;Stfb*$^{-/-}$ mice at 14 weeks of age. Scale bar, 100 μm. (**f**) Higher-magnification image of the selected area of **e** illustrating the specific caspase-3-positive staining in *PyMT;Stfb*$^{-/-}$ mice. (**g**) Representative images of immunofluorescence staining of the endothelial cell-specific marker CD31 (red staining) on *PyMT;Stfb*$^{+/+}$ and *PyMT;Stfb*$^{-/-}$ tumors.

stress-resistance factor, limiting the sensitivity of a tumor cell to hypoxia and nutrient restriction.

## DISCUSSION

Cysteine cathepsins have a dual role in cancer progression. First, they promote tumor invasion through (i) activation of the extracellular proteolytic cascade(s), (ii) degradation of the extracellular matrix and (iii) inactivation of adhesion molecules, for example, E-cadherin. Second, they participate in the apoptotic pathways. Although these two activities have apparently opposing functions, there is a clear physical separation of the processes in different cell compartments, allowing for the possibility of their selective targeting.[7] Although the proteolysis required for tumor invasion occurs mostly in the extracellular space,[1,2] the apoptotic pathway is clearly intracellular and dependent on translocation of cathepsins from the endosomal/lysosomal compartment into the cytosol.[5,18] In the present study, we have investigated the role of


© 2013 Macmillan Publishers Limited

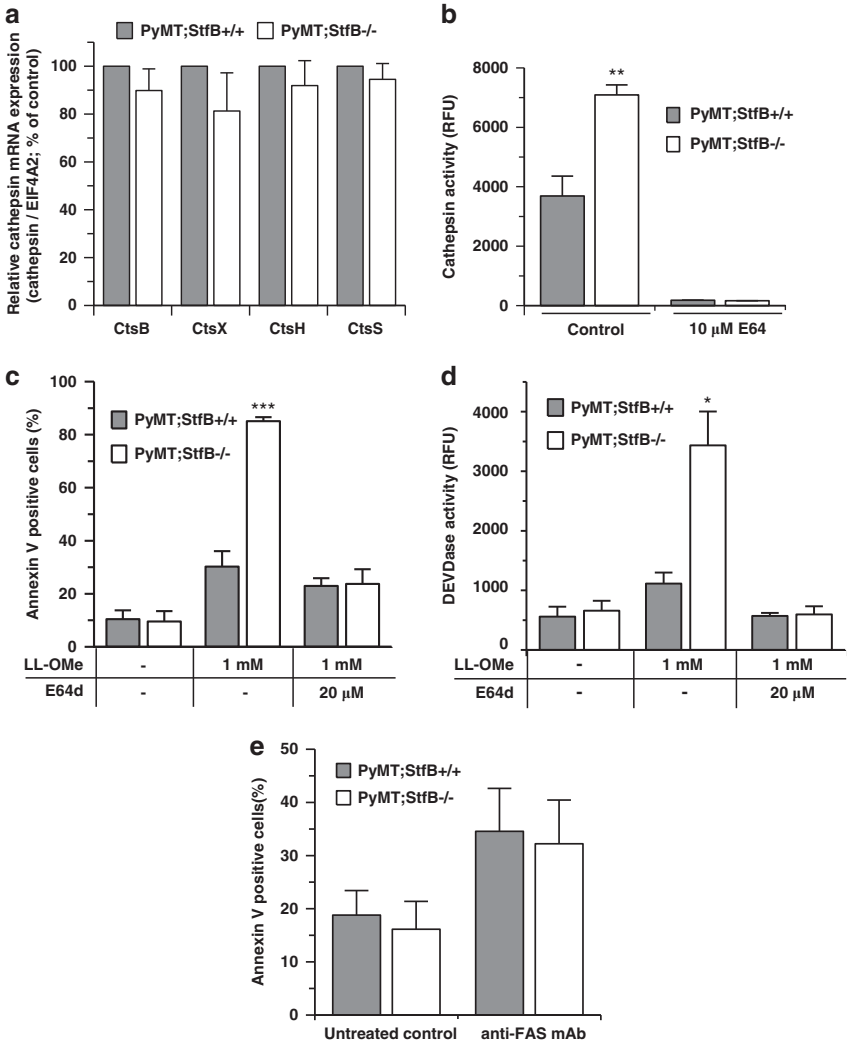



**Figure 3.** Ablation of Stfb leads to increased sensitivity of primary PyMT tumor cells to apoptosis induced with lysosomotropic agent. (**a**) Expression of cysteine cathepsins in *PyMT;Stfb*$^{+/+}$ ($n=4$) and *PyMT;Stfb*$^{-/-}$ ($n=4$) primary mammary tumors. Comparison of mRNA expression of cathepsin B (Ctsb), cathepsin X (Ctsz), cathepsin H (Ctsh) and cathepsin S (Ctss) in tumor samples was measured by quantitative real-time PCR. Data are presented as means and s.e., expressed as a percentage of the control (100%). (**b**) Activity of cysteine cathepsins in tumor tissue determined by hydrolysis of fluorogenic substrate Z-Phe-Arg-AMC on *PyMT;StB*$^{+/+}$ ($n=5$) and *PyMT;StB*$^{-/-}$ ($n=6$) mammary tumor lysates in the presence or absence of E64 inhibitor. Data are presented as means and s.e. Statistics were analyzed using Student's *t*-test. $^{**}P<0.01$. (**c**) Leu-Leu-OMe (LL-OMe) concentration-dependent cell death in *PyMT;Stfb*$^{+/+}$ ($n=4$) and *PyMT;Stfb*$^{-/-}$ ($n=4$) primary tumor cells. Cell death was measured by fluorescence-activated cell sorting analysis using annexin V–phycoerythrin. $^{***}P<0.001$. (**d**) DEVDase activity in Leu-Leu-OMe-treated *PyMT;Stfb*$^{+/+}$ ($n=4$) and *PyMT;Stfb*$^{-/-}$ ($n=4$) primary tumor cells. Data are presented as means and s.e. Statistics were analyzed using Student's *t*-test. $^{*}P<0.05$. (**e**) Fas dose-dependent cell death in *PyMT;Stfb*$^{+/+}$ ($n=4$) and *PyMT;Stfb*$^{-/-}$ ($n=4$) primary tumor cells was assessed after 18 h of stimulation in the presence of CHX (1 μg/ml).

the intracellular inhibitor of cysteine cathepsins, Stfb, which is localized predominantly in the cytosol,[22] where it serves to protect the cell against leakage of lysosomal enzymes. Consistent with that, depletion of Stfb had no effect on tumor invasion and metastasis-related processes (data not shown) that require translocation of cysteine cathepsins to the extracellular milieu. In contrast, significant reduction of tumor size and weight was observed in the *PyMT;Stfb*$^{-/-}$ group of mice, which correlated with the increased level of tumor cell death in tumors depleted of Stfb (Figure 2c–f). Surprisingly, given the well-substantiated role of cysteine cathepsins in various cell death pathways, no difference in spontaneous levels of apoptosis was detected between *PyMT;Stfb*$^{+/+}$ and *PyMT;Stfb*$^{-/-}$ primary tumor cells. However, according to current knowledge, cysteine cathepsins must be released into the cytosol in order to be involved in propagation of apoptosis.[33] To enable this, lysosomal membrane destabilization is required, which could be triggered by different lysosomotropic compounds, such as detergents, including the amino acid methyl ester Leu-Leu-OMe,[16,17,34,35] which are able to induce lysosomal membrane permeabilization. In agreement with that, a significant increase in apoptosis was observed in Stfb-depleted primary PyMT tumor cells as compared with the wild-type tumor cells (Figure 3c and d). Moreover, this result is consistent with the previous report on depletion of cysteine cathepsin B in the same tumor model, where primary tumor cells were significantly less sensitive to apoptosis induced by Leu-Leu-OMe.[36]

Furthermore, lysosomal membranes can be destabilized by low concentrations of $H_2O_2$,[37–40] which is a physiological mediator of cell death. Growing evidence suggests that cancer cells produce high levels of ROS and are constantly under oxidative stress.[31,41–43] Moreover, it is generally accepted that oxidative stress has an

© 2013 Macmillan Publishers Limited

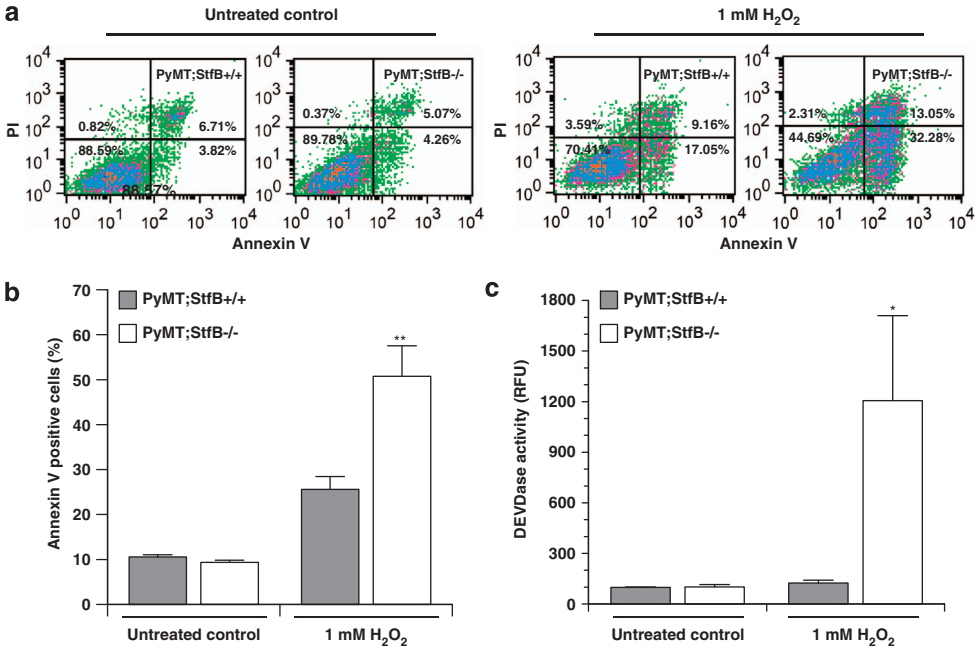



**Figure 4.** Stfb is associated with resistance of PyMT tumor cells to oxidative stress. (**a**) Fluorescence-activated cell sorting analysis of annexin V–phycoerythrin and propidium iodide (PI)-stained *PyMT;Stfb*$^{+/+}$ ($n=6$) and *PyMT;Stfb*$^{-/-}$ ($n=6$) primary tumor cells. Left two columns: untreated controls; right two columns: after treatment with 1 mM $H_2O_2$ for 18 h. (**b**) Ablation of Stfb leads to increase of $H_2O_2$-induced programmed cell death in PyMT tumor cells determined as a percentage of annexin V-positive cells after treatment with 1 mM $H_2O_2$ for 18 h. Data are presented as means and s.e. $^{**}P<0.01$. (**c**) DEVDase activity determined in the cell extracts of 1 mM $H_2O_2$-treated *PyMT;Stfb*$^{+/+}$ and *PyMT;Stfb*$^{-/-}$ primary tumor cells. Data are presented as means and s.e. Statistics were analyzed using Student's *t*-test. $^{*}P<0.05$.

important role in apoptosis in carcinomas. $H_2O_2$ is a ubiquitous ROS that is generated from nearly all sources of oxidative stress and can freely cross cell membranes. It has been widely used to model ROS-induced apoptosis in experimental situations.[44–46] Recently, $H_2O_2$-dependent lysosomal destabilization has been described in human prostate cancer PC-3 cells[47] and in human leukemia HL-60 cells.[38] Moreover, an involvement of lysosomal cysteine proteinases has been confirmed in the latter study by the use of E64d inhibitor. These data propose that in the absence of Stfb the protection of cells against ROS-induced apoptosis could be reduced. This hypothesis is supported by the results of Lehtinen *et al.*,[30] who have shown that knocking out Stfb or reducing its levels sensitizes cerebellar granule neurons to oxidative stress-induced cell death, resulting in neuronal death and degeneration.[30] This explains why the absence of this inhibitor triggers progressive degeneration of cerebellar granule neurons, leading to progressive myoclonus epilepsy (EPM1).[23] In our study, we have clearly demonstrated an increased sensitivity of breast tumor cells lacking Stfb to $H_2O_2$ and serum starvation-induced apoptosis compared with the wild-type tumor cells (Figure 4 and Supplementary Figure S2). This not only is in agreement with previous findings on cerebellar granule neurons but also suggests a novel function for Stfb in defending tumor cells from oxidative stress. Moreover, the recent findings on sensitization of thymocytes to staurosporin-induced apoptosis[48] and melanoma cells to tumor necrosis factor-related apoptosis-inducing ligand-induced apoptosis,[49] upon gene knockout or short hairpin RNA knockdown of Stfb, respectively, support the protective function of Stfb against apoptosis. Interestingly, a role of Stfb in stabilization of the FADD like IL beta converting enzyme (FLICE)-like inhibitory protein, which can interrupt apoptotic signaling at the death-inducing signaling complex (DISC) level by competing with caspase-8 for binding to Fas Associated protein with death domain (FADD), was recently discovered on melanoma cell lines,[49] thus proposing a cathepsin activity-independent function for Stfb. Furthermore, the results on the tumor-protective role of Stfb may explain the clinical data showing that higher levels of Stfb in tumor tissues and body fluids are associated with poor prognosis for patients with different types of cancer. These reports are also supported by the recent data on a proteome analysis of differentially expressed proteins by mass spectrometry, where Stfb was identified as a tissue and urinary biomarker of bladder cancer recurrence and progression.[50] Moreover, elevated Stfb level was also determined as the most significant variable predicting disease recurrence and grade/stage progression of transitional cell carcinoma.[50]

Interestingly, depletion of extracellular cysteine cathepsin inhibitor, cystatin C, results in a reduction of epithelial cell apoptosis and increase of proliferation and angiogenesis in a mouse model of multistage epithelial carcinogenesis.[51] Thus, collectively, the results of Yu *et al.*[51] and our data provide additional evidence for the importance of the subcellular localization of the disrupted protease–protease inhibitor counter-balance for the impact on tumor progression: extracellular for cystatin C and cytosolic for Stfb. Moreover, the data for another intracellular inhibitor of cysteine cathepsins, stefin A, corroborate this hypothesis revealing the association of stefin A expression with poor histological differentiation, high proliferative activity and increased risk of death in tumors of breast cancer patients.[52] Furthermore, similarly to our Stfb model, tumors positive for stefin A were larger than stefin A-negative tumors.[52]

Carcinoma cells synthesize ROS at a high rate, and many tumors thus appear to be under persistent oxidative stress.[41] However, many cancer cells become well adapted to such stress and develop resistance to oxidative stress and ROS-mediated apoptosis. Our results suggest an important role of Stfb for building up such resistance by protecting cells against apoptosis, thereby promoting tumor cell survival and cancer progression. This underlines the need for further research of the molecular signaling pathways regulated by the protease inhibitors[53] and the development of new strategies for cancer therapy to enhance therapeutic activity and selectivity.


© 2013 Macmillan Publishers Limited

## MATERIALS AND METHODS

### Animals

Mice were used in accordance with protocols approved by the Veterinary Administration of the Republic of Slovenia and the government Ethical Committee. Procedures for animal care and use were in accordance with the 'PHS Policy on Human Care and Use of Laboratory Animals' and the 'Guide for the Care and Use of Laboratory Animals'. The *Stfb*-deficient mouse strain was kindly provided by Dr Richard M. Myers.[26] *Stfb*$^{-/-}$ mice were backcrossed for eight generations to the transgenic mouse strain expressing PyMT under the control of MMTV long-terminal repeat promoter (FVB/N-TgN (MMTVPyVT)634-Mul).[27] After the intercross, wild-type and Stfb-deficient tumor bearing mice were named *PyMT;Stfb*$^{+/+}$ and *PyMT;Stfb*$^{-/-}$, respectively. Animals were bred and maintained in accordance with the Slovenian law for animal protection.

### Tumor progression study

Beginning at age 30 days, female mice were examined three times a week for the development of mammary tumors by finger palpation in a genotype-blinded fashion. Their diameters were measured 30 days after being first detected. At the age of 14 weeks, mice were killed and all 10 mammary tumors were excised and weighted.

### Histomorphometry

For volumetric measurement of total lung metastasis or disseminated tumor colonies in lungs, the paraffin-embedded lungs were cut into 5-μm thick slices from at least three different planes. Each section was stained with hematoxylin and eosin. The average metastasis size was determined by computer-assisted measurement using Cellquest software (Olympus, Tokyo, Japan).

### Immunohistochemistry and immunofluorescence

Histological measurement of proliferation by Ki67 staining, cell death and tumor vascularization rate by CD31 staining were done as described.[9,36] Right (thoracic) mammary glands were sectioned, and tissue sections for each tumor were taken from *PyMT;Stfb*$^{+/+}$ and *PyMT;Stfb*$^{-/-}$ mice. Rabbit anti-active caspase-3 antibody (Abcam ab2302, Cambridge, UK; 1:40 dilution) was used to detect apoptotic epithelial and cancer cells. Rabbit anti-mouse Stfb antibodies (Abcam, Cambridge, UK, ab53725; 1:1000 dilution) were used for immunohistochemical detection of Stfb. Detection of primary antibodies was done by Vectastain Elite ABC kit (Vector Laboratories, Burlingame, CA, USA) in accordance to the manufacturer's instructions, followed by incubation with 3,3-DAB (Sigma-Aldrich, Steinheim, Germany) and nuclear staining with hematoxylin. For Ki67 data assessment, 20 fields per tumor were selected at random, using a $\times 40$ objective, and quantified using TissueQuest software (TissueGnostics, Vienna, Austria). Areas of dead cells in tumor sections were determined using the ApoptTag Peroxidase In Situ apoptosis detection Kit (Millipore, Billerica, MA, USA) and an Olympus microscope (Olympus IX 81) with Imaging Software for Life Science Microscopy Cell. For vascularization, samples were co-stained and mounted in SlowFade Gold antifade reagent with DAPI (Invitrogen) and examined with an Olympus fluorescence microscope (Olympus IX 81) with Imaging Software for Life Science Microscopy Cell.

### Isolation of primary tumor cells from PyMT-induced mammary carcinomas

Primary MMTV-PyMT cells were isolated and cultured as described.[10] Only low-passage number cells ($<4$ passages total) were used for experiments. All primary cells were maintained in DMEM (Gibco, (Invitrogen), Paisley, Scotland, UK) supplemented with 10% fetal bovine serum (Sigma-Aldrich, St Louis, MO, USA), 2 mM L-glutamine (Invitrogen), 100 U of penicillin and 100 μg/ml streptomycin (Invitrogen). Cultured cells were maintained at 37 °C in a humidified 5% $CO_2$ atmosphere.

### Quantitative real-time PCR

Total RNA was isolated from flash-frozen PyMT mammary tumors with an Allprep DNA/RNA/Protein Mini kit (Qiagen, Valencia, CA, USA) and treated with TURBO DNA-free kit (Ambion, Life Technologies, Foster City, CA, USA) for genomic DNA elimination. RNA quality (A260/230 and A260/280 ratios) was assessed spectrophometrically, whereas RNA integrity was confirmed by 1.2% gel electrophoresis. RNA was further reverse transcribed into cDNA with a random nanomer primers using Precision nanoScript Reverse Transcription kit (Primerdesign Ltd, Southampton, UK). mRNA expression levels of cathepsin B, cathepsin S, cathepsin X and cathepsin H were detected by SYBR green detection chemistry using 2 × Precision MasterMix (Primerdesign Ltd). Eukaryotic translation initiation factor 4A2 was selected as the most stable expressed reference gene by GeNorm reference gene selection kit (Primerdesign Ltd), and normalized values were used to calculate the relative mRNA expression of individual genes. Quantitative real-time PCR reaction was run on Mx3005P Real-time PCR system (Agilent, Stratagene products, Waldbronn, Germany) using the following conditions: 95 °C for 10 min (an initial denaturation step) followed by 40 cycles of 95 °C for 15 s and 60 °C for 1 min (annealing and extension). In addition, melting curve (55–95 °C) was performed at the end of each run. Intron spanning gene-specific primers (Primerdesign Ltd) were as follows: cathepsin B, 5′-TACTTGCTGTGGTATCCAGTGTG-3′ (forward) and 5′-ATGGTGTATGGTAAGCAGCCTAC-3′ (reverse); cathepsin S, 5′-CTGTTCTTGACAAGCCAATATTTATTC-3′ (forward) and 5′-AGCCAGTAATC TTTGCCATCA-3′ (reverse); cathepsin X, 5′-CTATGCCAATGGTCCCATCAG-3′ (forward) and 5′-CCTGGTCCTGGTGCTCAG-3′ (reverse); and cathepsin H, 5′-TTTGATGTATAAAAGTGGCGTCTA-3′ (forward) and 5′-GAGTTTTTCAC AATCCAGTAGAGT-3′ (reverse). The relative expression ratios of target genes were calculated considering their real-time PCR efficiencies.

### Induction of apoptosis

Apoptosis was induced with anti-CD95 monoclonal antibody Jo-2 (BD Pharmingen, San Diego, CA, USA) at a final concentration of 0.2 μg/ml in the presence of cyclohexamide (CHX) for 18 h. The mediator of oxidative stress, $H_2O_2$, was applied at a final concentration of 1 mM for 18 h. The lysosomotropic agent Leu-Leu-OMe was applied at final concentration of 1 mM with or without 20 μM E64d for 18 h.[16] At indicated time points, cells were harvested and lysed (50 mM HEPES, 200 mM NaCl, 0.1% (w/v) CHAPS, 10% (w/v) sucrose, 5 mM $MgCl_2$, 0.02 (w/v) BSA, 1% (w/v) NP-40 and 0.5% (w/v) Triton X-100) on ice then centrifuged at 10000 *g* (10 min), and supernatants were separated. Total protein concentration was determined using the Bradford assay (Bio-Rad, München, Germany). Cells, untreated and treated with anti-CD95 monoclonal antibody, 1 mM $H_2O_2$ or 1 mM Leu-Leu-OMe, were labeled with annexin V–phycoerythrin/7AAD (BD Pharmingen). Exposure to phosphatidylserine and DNA fragmentation were measured by labeling cells with annexin V–phycoerythrin in the presence of propidium iodide according to the manufacturer's instructions. Cells were then subjected to flow cytometry (fluorescence-activated cell sorting) analysis using FACScalibur flow cytometer (Becton Dickinson, Franklin Lakes, NJ, USA).

### Cathepsin activity in mammary tumor lysates

Frozen tissues of primary tumors were disrupted in 200 μl of 0.1 M TRIS buffer pH 8.5, 5 mM EDTA, 200 mM sodium chloride and 0.2% SDS, using an Ultrathurrax (IKA, Staufen, Germany), and centrifuged at 1000 *g* for 10 min. Cysteine cathepsin activity was determined by hydrolysis of the general cathepsin substrate Z-Phe-Arg-4-methyl-coumarin-7-amide (Z-Phe-Arg-AMC, 10 μM; Bachem, Bubendorf, Switzerland) in 0.1 M phosphate buffer, pH 6.0, containing 1 mM EDTA, 0.1% (v/v) polyethylene glycol and 1 mM dithiothreitol, in the presence or absence of E64 cysteine cathepsin inhibitor at a final concentration of 10 μM. Kinetics of substrate hydrolysis were monitored continuously during 10 min by Tecan Infinite M1000 PRO (Tecan, Gröding, Austria) plate reader at excitation and emission wavelengths of 370 and 460 nm, respectively.

### DEVDase activity

Cell lysates (75 μg of protein) were transferred into a black 96-well plate. Caspase buffer (50 mM HEPES, 200 mM NaCl, 0.1% (w/v) CHAPS, 10% (w/v) sucrose, 5 mM MgCl2 and 0.02 (w/v) BSA) was added to a final volume of 90 μl and incubated for 15 min at 37 °C. A volume of 10 μl acetyl-DEVD-7-amino-4-trifluoromethylcoumarin (Bachem) was added to a final concentration of 100 μM, and DEVDase activity was measured by Tecan Infinite M1000 PRO (Tecan) plate reader at excitation and emission wavelengths of 400 and 505 nm, respectively.

### Immunoblotting

Equal amounts (100 μg) of protein were resolved on 12.5% SDS polyacrylamide gel electrophoresis gels and electrotransferred to polyvinylidene difluoride membranes. Blots were probed with rabbit anti-Stfb

© 2013 Macmillan Publishers Limited

antibodies (Abcam; ab53725, 1:1000 dilution) and rabbit anti-actin antibodies (Sigma-Aldrich) at 1:800 and 1:2000 dilutions, respectively. Secondary conjugated goat anti-rabbit antibodies were used at 1:5000 dilutions.

### Statistical analysis

Quantitative data are presented as means ± s.e. The differences were compared using Student's *t*-test. Proportions were compared using the $\chi^2$-test, and statistical analysis of Kaplan–Meier plots was done by log-rank test. When *P*-values were $\leqslant 0.05$, differences were considered statistically significant.

## CONFLICT OF INTEREST

The authors declare no conflict of interest.

## ACKNOWLEDGEMENTS

We thank Richard Myers and Len Pennacchio, formerly of Stanford University, for providing with Stfb knockout mouse strain, Georgy Mikhaylov and Matej Vizovisek for their technical and methodological assistance, Eva Zerovnik for valuable discussions and Roger H. Pain for critical reading of the manuscript. This work was supported by the European Commission FP7 grant 201279 (Microenvimet: CP, TR, AK, BT and OV), the Slovenian Research Agency (research grants no. J3-4267 to OV and P1-0140 to BT) and Deutsche Forschungsgemeinschaft SFB 850 project B7 (CP and TR).

## REFERENCES

1 Gocheva V, Joyce JA. Cysteine cathepsins and the cutting edge of cancer invasion. *Cell Cycle* 2007; **6**: 60–64.
2 Mohamed MM, Sloane BF. Cysteine cathepsins: multifunctional enzymes in cancer. *Nat Rev Cancer* 2006; **6**: 764–775.
3 Turk V, Kos J, Turk B. Cysteine cathepsins (proteases)--on the main stage of cancer? *Cancer Cell* 2004; **5**: 409–410.
4 Vasiljeva O, Reinheckel T, Peters C, Turk D, Turk V, Turk B. Emerging roles of cysteine cathepsins in disease and their potential as drug targets. *Curr Pharm Des* 2007; **13**: 387–403.
5 Turk B, Turk V. Lysosomes as 'suicide bags' in cell death: myth or reality? *J Biol Chem* 2009; **284**: 21783–21787.
6 Turk V, Stoka V, Vasiljeva O, Renko M, Sun T, Turk B *et al.* Cysteine cathepsins: from structure, function and regulation to new frontiers. *Biochim Biophys Acta* 2012; **1824**: 68–88.
7 Vasiljeva O, Turk B. Dual contrasting roles of cysteine cathepsins in cancer progression: Apoptosis versus tumour invasion. *Biochimie* 2008; **90**: 380–386.
8 Gocheva V, Zeng W, Ke D, Klimstra D, Reinheckel T, Peters C *et al.* Distinct roles for cysteine cathepsin genes in multistage tumorigenesis. *Genes Dev* 2006; **20**: 543–556.
9 Sevenich L, Schurigt U, Sachse K, Gajda M, Werner F, Muller S *et al.* Synergistic antitumor effects of combined cathepsin B and cathepsin Z deficiencies on breast cancer progression and metastasis in mice. *Proc Natl Acad Sci USA* 2010; **107**: 2497–2502.
10 Vasiljeva O, Papazoglou A, Kruger A, Brodoefel H, Korovin M, Deussing J *et al.* Tumor cell-derived and macrophage-derived cathepsin B promotes progression and lung metastasis of mammary cancer. *Cancer Res* 2006; **66**: 5242–5250.
11 Bell-McGuinn KM, Garfall AL, Bogyo M, Hanahan D, Joyce JA. Inhibition of cysteine cathepsin protease activity enhances chemotherapy regimens by decreasing tumor growth and invasiveness in a mouse model of multistage cancer. *Cancer Res* 2007; **67**: 7378–7385.
12 Gopinathan A, Denicola GM, Frese KK, Cook N, Karreth FA, Mayerle J *et al.* Cathepsin B promotes the progression of pancreatic ductal adenocarcinoma in mice. *Gut* 2012; **61**: 877–884.
13 Joyce JA, Baruch A, Chehade K, Meyer-Morse N, Giraudo E, Tsai FY *et al.* Cathepsin cysteine proteases are effectors of invasive growth and angiogenesis during multistage tumorigenesis. *Cancer Cell* 2004; **5**: 443–453.
14 Mikhaylov G, Mikac U, Magaeva AA, Itin VI, Naiden EP, Psakhye I *et al.* Ferri-liposomes as an MRI-visible drug-delivery system for targeting tumours and their microenvironment. *Nat Nanotechnol* 2011; **6**: 594–602.
15 Shree T, Olson OC, Elie BT, Kester JC, Garfall AL, Simpson K *et al.* Macrophages and cathepsin proteases blunt chemotherapeutic response in breast cancer. *Genes Dev* 2011; **25**: 2465–2479.
16 Cirman T, Oresic K, Mazovec GD, Turk V, Reed JC, Myers RM *et al.* Selective disruption of lysosomes in HeLa cells triggers apoptosis mediated by cleavage of Bid by multiple papain-like lysosomal cathepsins. *J Biol Chem* 2004; **279**: 3578–3587.
17 Droga-Mazovec G, Bojic L, Petelin A, Ivanova S, Romih R, Repnik U *et al.* Cysteine cathepsins trigger caspase-dependent cell death through cleavage of Bid and antiapoptotic Bcl-2 homologues. *J Biol Chem* 2008; **283**: 19140–19150.
18 Stoka V, Turk V, Turk B. Lysosomal cysteine cathepsins: signaling pathways in apoptosis. *Biol Chem* 2007; **388**: 555–560.
19 Turk B, Turk D, Salvesen GS. Regulating cysteine protease activity: essential role of protease inhibitors as guardians and regulators. *Curr Pharm Des* 2002; **8**: 1623–1637.
20 Turk V, Stoka V, Turk D. Cystatins: biochemical and structural properties, and medical relevance. *Front Biosci* 2008; **13**: 5406–5420.
21 Turk B, Turk V, Turk D. Structural and functional aspects of papain-like cysteine proteinases and their protein inhibitors. *Biol Chem* 1997; **378**: 141–150.
22 Alakurtti K, Weber E, Rinne R, Theil G, Haan G-Jd, Lindhout D *et al.* Loss of lysosomal association of cystatin B proteins representing progressive myoclonus epilepsy, EPM1, mutations. *Eur J Hum Genet* 2004; **13**: 208–215.
23 Pennacchio LA, Lehesjoki AE, Stone NE, Willour VL, Virtaneva K, Miao J *et al.* Mutations in the gene encoding cystatin B in progressive myoclonus epilepsy (EPM1). *Science* 1996; **271**: 1731–1734.
24 Jedeszko C, Sloane BF. Cysteine cathepsins in human cancer. *Biol Chem* 2004; **385**: 1017–1027.
25 Kos J, Krasovec M, Cimerman N, Nielsen HJ, Christensen IJ, Brunner N. Cysteine proteinase inhibitors stefin A, stefin B, and cystatin C in sera from patients with colorectal cancer: relation to prognosis. *Clin Cancer Res* 2000; **6**: 505–511.
26 Pennacchio LA, Bouley DM, Higgins KM, Scott MP, Noebels JL, Myers RM. Progressive ataxia, myoclonic epilepsy and cerebellar apoptosis in cystatin B-deficient mice. *Nat Genet* 1998; **20**: 251–258.
27 Guy CT, Cardiff RD, Muller WJ. Induction of mammary tumors by expression of polyomavirus middle T oncogene: a transgenic mouse model for metastatic disease. *Mol Cell Biol* 1992; **12**: 954–961.
28 Stoka V, Turk B, Schendel SL, Kim TH, Cirman T, Snipas SJ *et al.* Lysosomal protease pathways to apoptosis. Cleavage of bid, not pro-caspases, is the most likely route. *J Biol Chem* 2001; **276**: 3149–3157.
29 Bojič L, Petelin A, Stoka V, Reinheckel T, Peters C, Turk V *et al.* Cysteine cathepsins are not involved in Fas/CD95 signalling in primary skin fibroblasts. *FEBS Lett* 2007; **581**: 5185–5190.
30 Lehtinen MK, Tegelberg S, Schipper H, Su H, Zukor H, Manninen O *et al.* Cystatin B deficiency sensitizes neurons to oxidative stress in progressive myoclonus epilepsy, EPM1. *J Neurosci* 2009; **29**: 5910–5915.
31 Hileman EO, Liu J, Albitar M, Keating MJ, Huang P. Intrinsic oxidative stress in cancer cells: a biochemical basis for therapeutic selectivity. *Cancer Chemother Pharmacol* 2004; **53**: 209–219.
32 Rygiel TP, Mertens AE, Strumane K, van der Kammen R, Collard JG. The Rac activator Tiam1 prevents keratinocyte apoptosis by controlling ROS-mediated ERK phosphorylation. *J Cell Sci* 2008; **121**: 1183–1192.
33 Repnik U, Turk B. Lysosomal-mitochondrial cross-talk during cell death. *Mitochondrion* 2010; **10**: 662–669.
34 Goldman R, Kaplan A. Rupture of rat liver lysosomes mediated by L-amino acid esters. *Biochim Biophys Acta* 1973; **318**: 205–216.
35 Uchimoto T, Nohara H, Kamehara R, Iwamura M, Watanabe N, Kobayashi Y. Mechanism of apoptosis induced by a lysosomotropic agent, L-Leucyl-L-Leucine methyl ester. *Apoptosis* 1999; **4**: 357–362.
36 Vasiljeva O, Korovin M, Gajda M, Brodoefel H, Bojič L, Krüger A *et al.* Reduced tumour cell proliferation and delayed development of high-grade mammary carcinomas in cathepsin B-deficient mice. *Oncogene* 2008; **27**: 4191–4199.
37 Antunes F, Cadenas E, Brunk UT. Apoptosis induced by exposure to a low steady-state concentration of H2O2 is a consequence of lysosomal rupture. *Biochem J* 2001; **356**: 549–555.
38 Ishisaka R, Utsumi K, Utsumi T. Involvement of lysosomal cysteine proteases in hydrogen peroxide-induced apoptosis in HL-60 cells. *Biosci Biotechnol Biochem* 2002; **66**: 1865–1872.
39 Takahashi T, Kitaoka K, Ogawa Y, Kobayashi T, Seguchi H, Tani T *et al.* Lysosomal dysfunction on hydrogen peroxide-induced apoptosis of osteoarthritic chondrocytes. *Int J Mol Med* 2004; **14**: 197–200.
40 Yin L, Stearns R, Gonzalez-Flecha B. Lysosomal and mitochondrial pathways in H2O2-induced apoptosis of alveolar type II cells. *J Cell Biochem* 2005; **94**: 433–445.
41 Brown NS, Bicknell R. Hypoxia and oxidative stress in breast cancer. Oxidative stress: its effects on the growth, metastatic potential and response to therapy of breast cancer. *Breast Cancer Res* 2001; **3**: 323–327.
42 Szatrowski TP, Nathan CF. Production of large amounts of hydrogen peroxide by human tumor cells. *Cancer Res* 1991; **51**: 794–798.
43 Toyokuni S, Okamoto K, Yodoi J, Hiai H. Persistent oxidative stress in cancer. *FEBS Lett* 1995; **358**: 1–3.


© 2013 Macmillan Publishers Limited

44 Datta K, Babbar P, Srivastava T, Sinha S, Chattopadhyay P. p53 dependent apoptosis in glioma cell lines in response to hydrogen peroxide induced oxidative stress. *Int J Biochem Cell Biol* 2002; **34**: 148–157.
45 Mao Y, Song G, Cai Q, Liu M, Luo H, Shi M *et al.* Hydrogen peroxide-induced apoptosis in human gastric carcinoma MGC803 cells. *Cell Biol Int* 2006; **30**: 332–337.
46 Zuliani T, Denis V, Noblesse E, Schnebert S, Andre P, Dumas M *et al.* Hydrogen peroxide-induced cell death in normal human keratinocytes is differentiation dependent. *Free Radic Biol Med* 2005; **38**: 307–316.
47 Kariya S, Sawada K, Kobayashi T, Karashima T, Shuin T, Nishioka A *et al.* Combination treatment of hydrogen peroxide and X-rays induces apoptosis in human prostate cancer PC-3 cells. *Int J Radiat Oncol Biol Phys* 2009; **75**: 449–454.
48 Kopitar-Jerala N, Schweiger A, Myers RM, Turk V, Turk B. Sensitization of stefin B-deficient thymocytes towards staurosporin-induced apoptosis is independent of cysteine cathepsins. *FEBS Lett* 2005; **579**: 2149–2155.
49 Yang F, Tay KH, Dong L, Thorne RF, Jiang CC, Yang E *et al.* Cystatin B inhibition of TRAIL-induced apoptosis is associated with the protection of FLIP(L) from degradation by the E3 ligase itch in human melanoma cells. *Cell Death Differ* 2010; **17**: 1354–1367.
50 Feldman AS, Banyard J, Wu CL, McDougal WS, Zetter BR. Cystatin B as a tissue and urinary biomarker of bladder cancer recurrence and disease progression. *Clin Cancer Res* 2009; **15**: 1024–1031.
51 Yu W, Liu J, Shi MA, Wang J, Xiang M, Kitamoto S *et al.* Cystatin C deficiency promotes epidermal dysplasia in K14-HPV16 transgenic mice. *PLoS ONE* 2010; **5**: e13973.
52 Kuopio T, Kankaanranta A, Jalava P, Kronqvist P, Kotkansalo T, Weber E *et al.* Cysteine proteinase inhibitor cystatin A in breast cancer. *Cancer Res* 1998; **58**: 432–436.
53 Turk B, Turk D, Turk V. Protease signalling: the cutting edge. *EMBO J* 2012; **31**: 1630–1643.

Supplementary Information accompanies this paper on the Oncogene website (http://www.nature.com/onc)

© 2013 Macmillan Publishers Limited